

2014

Elucidating the Anti-Inflammatory Roles of Heparin and Shear Stress in Atherosclerosis

Joshua B. Slee
Lehigh University

Follow this and additional works at: <http://preserve.lehigh.edu/etd>



Part of the [Molecular Biology Commons](#)

Recommended Citation

Slee, Joshua B., "Elucidating the Anti-Inflammatory Roles of Heparin and Shear Stress in Atherosclerosis" (2014). *Theses and Dissertations*. Paper 1629.

This Dissertation is brought to you for free and open access by Lehigh Preserve. It has been accepted for inclusion in Theses and Dissertations by an authorized administrator of Lehigh Preserve. For more information, please contact preserve@lehigh.edu.

**Elucidating the Anti-Inflammatory Roles of Heparin and Shear Stress in
Atherosclerosis**

by

Joshua B. Slee

A Dissertation

Presented to the Graduate and Research Committee

of Lehigh University

in Candidacy for the Degree of

Doctor of Philosophy

in

Cell and Molecular Biology

Lehigh University

August 20, 2013

© 2013 Copyright
Joshua B. Slee

Approved and recommended for acceptance as a dissertation in partial fulfillment of the requirements for the degree of Doctor of Philosophy

Joshua B. Slee

Elucidating the Anti-Inflammatory Roles of Heparin and Shear Stress in Atherosclerosis

August 20, 2013

Defense Date

August 20, 2013

Approved Date

Linda Lowe-Krentz, Ph.D.
(Must Sign with Blue Ink)

Committee Members:

Michael Kuchka, Ph.D.

M. Katherine Iovine, Ph.D.

Bryan Berger, Ph.D.

Acknowledgements

First and foremost, I would like to extend my gratitude to Dr. Lowe-Krentz. Nearly six years ago, she saw something in me that was worth her investment. The summer before I officially started at Lehigh, she invited me to join her BSDI summer project to which I excitedly accepted. Looking back, this was one of the best decisions during my graduate career. It allowed me to “get my feet wet” in the lab and get a jump start on my project. I hate to admit it, but without her contacting me to join her lab for the summer; I may not have ever considered her lab in the first place. So I guess she knew more about me at the time than I did. Looking back, it was a no-brainer type of decision, because I immediately fell in love with the research and the lab. Dr. Lowe-Krentz has been a true inspiration and an excellent mentor. I don’t think there has been one time when I went to her and she didn’t have an answer to my question or problem. Admittedly, it usually wasn’t the answer that I wanted to hear, but it was always the answer I needed to hear. She is an example of a professor who as devoted her career to top notch research, educating both graduate and undergraduate students, and developing the next generation of scientists and teachers. She has always been there when I needed her, even as far as proof reading this document while on her family vacation. She is the best advisor and mentor that a graduate student could ask for.

Secondly, I would like to thank my committee members for their unwavering support and endless help in my many times of need. Aside from their intellectual and scientific support, they have been invaluable in terms of making life biggest choices. Dr. Michael Kuchka for providing me with excellent seats to Iron Pigs baseball games. Dr. Cassimeris for always volunteering to sample my pulled pork and relentlessly arguing with me over Duke Athletics. Dr. Bryan Berger for introducing me his lab members, especially those who are just as unique as me. On more serious note, I thank Dr. Iovine

for stepping in at the last minute and serving on my committee; she truly is a life saver. Dr. Cassimeris for making a microscopist and cell biologist out of me. Dr. Bryan Berger for technical help with electroporation. Lastly, I extend my deepest gratitude to Dr. Michael Kuchka for serving as a great example of a dedicated teacher and for the opportunity to guest lecture in his class. I will carry the concepts that I've learned watching him teach with me into my own career.

I would be amiss if I did not thank my wife, Kyle, who stood by my side through every long night in the lab, studying, writing, reading or whining about failed experiments. I doubt whether I would have been able to complete this program without her support. She rode the roller coaster that a doctoral program is with me. She enjoyed the peaks and suffered through the valleys with me all the while finishing her Master's degree in Athletic Training, starting a new job, and planning our wedding. No matter how bad of a day that I had, she always found a way to make things better. She was instrumental in my preparation for my qualifying exam. She would sit with me for hours as I described apoptosis, the cell cycle, vesicular transport, etc. Sometimes, I think she might have known it better than me. She truly is the cornerstone of the foundation of our family.

I would also like to thank my parents, James and Kathy, for always believing in me. Throughout my life, they have always been right behind me to catch me when I fell and hold me on their shoulders when I succeeded. As true parents, they always put their needs behind mine, so I could pursue my dreams of getting a doctorate degree. They always have and still continue to jump into action whenever I need anything and I appreciate it more than they could ever know. I would also like to thank my step mother Dana for stepping into my life and immediately having a positive influence on me and my father. Another person who deserves my gratitude is Gary for coming into my

mother's and my lives and serving as a role model and friend. Lastly, I would like to thank my father- and mother-in-law, Bob and Val, for their continued support of Kyle and me.

The entire faculty and staff of the Department of Biological Sciences made my time here at Lehigh much more enjoyable and seamless. There are too many names to list, but there have been times when I've walked into someone's office or lab and needed something to which they immediately provided their assistance. The one person that stands out in particular who needs mentioning is Maria Brace. Although she swears that she isn't very mother-like to her own children, she served as an excellent mother-substitute to me. I will truly miss our discussions about food, barbeque in particular, politics, current events, and anything we felt like talking about. Maria truly is the lifeblood of the department and helped me out of numerous sticky situations. I am saddened by the thought of no longer being able to walk past her office in the morning to a "good morning, how are you doing?" I am forever grateful for her willingness to fix everything, and I literally mean everything.

Throughout my time at Lehigh I've met many people who have been instrumental to my success. I've made colleagues for life and build lasting friendships. Although everyone was extremely helpful, a few people stand out in my mind as being exceedingly wonderful. Dr. Michael Kearsse was truly the epitome of the perfect graduate student, always willing to share his knowledge and experience. Dr. Raymond Pugh provided scientific insight, daily kindergarten humor, friendly political debates, and endless conversation. Trista Barthol for literally doing whatever I asked her to in the lab, discussing Northampton High School, blaring country music in the lab with me, and her endless drive to complete lab work. Walter Joseph, Natalie Krane, Amanda Dilger, Annie Suh, and Theresa Collins for making me feel young and hip again. Dr. Wutigri

Nimlamool for helping me with ECL development and fluorescent microscopy. Lee Graham for never saying “no” when I needed to borrow something from the core or teaching labs and tirelessly working to keep the cell culture hoods operation in our lab.

I would also like to thank my mentors from my undergraduate and master’s career, without them I might have mistakenly ended up with an M.D. instead of a Ph.D. I extend my gratitude to: Dr. Deborah Hokien for being the first person to introduce me to research outside of the classroom. Dr. Peter Eden for instilling in me the need to question everything, to not take things at face value, and for being the best teacher I’ve ever had. Lastly, Dr. Kenneth Rundell for giving me the opportunity to do world class research which ultimately had a large part to do with me getting into Lehigh’s Ph.D. program, professional guidance, and a lasting friendship. I’m sure that I am forgetting important people, so I apologize if your name was omitted, but please know that I am thankful in my heart.

In closing, I would again like to thank Dr. Lowe-Krentz, my committee, past and current labmates and classmates, Margorie Nemes for establishing the fellowship which supported my work for a semester, the Howard Hughes Medical Institute BDSI program which support my first summer’s research, and the Department of Biological Sciences for their endless support during my time as a Ph.D. student at Lehigh University.

Table of Contents

Acknowledgements	iv
Table of Contents	viii
List of Figures	xiii
List of Tables	xv
List of Abbreviations	xvi
Abstract	1
Chapter 1: Introduction	3
Chapter 2: General Methods	26
2.1: Cell Culture	27
2.2: Immunofluorescence Staining	28
2.3: SDS-Polyacrylamide Gel Electrophoresis (SDS-PAGE) and Western Blotting	28
2.4: Confocal Microscopy	30
2.5: Fluorescent Microscopy	30
2.6: DNA Plasmid Sub-Cloning	30
2.7: Heparin Preparation and Treatment	32
Chapter 3: Actin realignment and cofilin regulation are essential for barrier integrity during shear stress	33
3.1: Induction	34
3.2: Methods	39
3.2.1: Cell Culture	39
3.2.2: JNK and p38 Inhibitor Treatments	39
3.2.3: FSS Experiments	40
3.2.4: Immunofluorescence Staining	40
3.2.5: Cofilin Mutant Transfection Protocol	41
3.2.6: SDS-PAGE and Western Blotting	41
3.2.7: Confocal Microscopy Image Analysis	42

3.3: Results	43
3.3.1: FSS-induced changes in cofilin phosphorylation	43
3.3.2: Cofilin activity is required for FSS-induced actin realignment	44
3.3.3: JNK and p38 involvement in FSS-induced cofilin phosphorylation	46
3.3.4: FSS-induced increased LIMK phosphorylation	47
3.3.5: Slingshot (serine-978) phosphorylation is not FSS-dependent	48
3.3.6: FSS-Induced VE-Cadherin and β -Catenin Localization at Cell-Cell Junctions	49
3.5: Discussion	40
3.6: Figures	58
Chapter 4: Heparin blocks TNF α -induced stress responses in vascular endothelium	69
4.1: Introduction	70
4.2: Methods	74
4.2.1: Cell Culture	74
4.2.2: TNF α and Heparin Treatment	74
4.2.3: Immunofluorescence Staining	74
4.2.4: Fluorescent Microscopy	75
4.3: Results	75
4.4: Discussion	76
4.5: Figure	79
Chapter 5: Identification of the heparin receptor: building the case for TMEM184A	80
5.1: Introduction	81
5.2: Methods	87
5.2.1: Cell Culture	87

5.2.2: Immunofluorescence Staining	87
5.2.3: TMEM184A siRNA Electroporation Protocol	88
5.2.4: Heparin Assay in TMEM184A siRNA-treated Cells	88
5.2.5: TMEM184A shRNA Electroporation Protocol	89
5.2.6: Fluorescent Heparin Uptake	89
5.2.7: GFP-tagged TMEM184A (GFP-TMEM184A) co-localization with Rhodamine-Heparin	90
5.2.8: Fluorescent Microscopy	90
5.2.9: Confocal Microscopy	90
5.2.10: SDS-PAGE and Western Blotting	90
5.2.11: Heparin Receptor Immunoprecipitation	91
5.3: Results	92
5.3.1: TMEM184A is detectable in vascular cells by Western Blotting and IF Microscopy	92
5.3.2: TMEM184A is expressed in a variety of cells	93
5.3.3: TMEM184A co-localizes with VAMP	95
5.3.4: TMEM184A co-localizes with CAV-1 and eNOS in vascular cells	96
5.3.5: TMEM184A is present in HeLa cells	97
5.3.6: All Cells Investigated Internalize Rhodamine-Heparin	98
5.3.7: Immunoprecipitation of the Heparin Receptor Detects TMEM184A	99
5.3.8: GFP-Tagged TMEM184A co-localizes with Rhodamine-heparin	101
5.3.9: siRNA-mediated knockdown of TMEM184A decreases heparin sensitivity in A7r5s	102

5.3.10: shRNA-mediated knockdown of TMEM184A in A7r5s	105
5.4: Discussion	105
5.5: Figures	115
Chapter 6: Heparin regulates specific genes in VSMCs	130
6.1: Introduction	131
6.2: Methods	136
6.2.1: Cell Culture	136
6.2.2: Heparin Treatment for PCR Arrays	136
6.2.3: Heparin and Serum Treatment for Short-Term RT-PCR	136
6.2.4: Heparin Treatment for Long-Term Microarray Analysis	136
6.2.5: SDS-PAGE and Western Blotting	137
6.2.6: RNA Isolation and Processing	137
6.2.7: RT-PCR Data Analysis ($2^{-\Delta\Delta CT}$ Method)	138
6.2.8: Microarray Analysis	138
6.3: Results	139
6.3.1: PCR Array data suggests that only a few of the selected genes are regulated by heparin	139
6.3.2: PCR Array data and targeted RT-PCR data suggest that heparin does not regulate MKP-1 by control of mRNA levels	140
6.3.3: Microarray data agrees with PCR Array and targeted RT-PCR analyses of DUSP1, CDKN1B (p27 ^{kip1}), and CDKN1C (p57 ^{kip2})	141
6.3.4: Microarray data suggest heparin up-regulates gene expression	143
6.4: Discussion	146

6.5: Figures	157
Chapter 7: Heparin responses in VSMCs involved PKG	168
7.1: Introduction	169
7.2: Methods	173
7.2.1: Cell Culture	173
7.2.2: PKG siRNA Transfection	173
7.2.3: Heparin Assay in PKG siRNA- Transfected Cells	173
7.2.4: Immunofluorescence Staining	173
7.2.5: Fluorescence Microscopy	173
7.2.6: SDS-PAGE and Western Blotting	173
7.3: Results	173
7.4: Discussion	174
7.5: Figure	178
Chapter 8: Conclusions and future directions	180
Chapter 9: References	190
Chapter 10: Appendices	226
Vita	238

List of Figures

Figure 1.1: The cost of treating cardiovascular disease	4
Figure 1.2: Risk factors for atherosclerosis	5
Figure 1.3: Heparin's effect on the MAPK pathway in VSMCs	9
Figure 1.4: The relationship between FSS and atherosclerosis	20
Figure 1.5: The three phases of actin microfilament rearrangement in response to high fluid shear stress	22
Figure 1.6: Regulation of cofilin	23
Figure 3.1: Proposed mechanosensing complex	35
Figure 3.2: Cofilin structure, with Serine-3 phosphorylation site circled	37
Figure 3.3: FFS-induced changes in cofilin phosphorylation	58
Figure 3.4: The effect of cofilin activity on FFS-induced actin realignment	59
Figure 3.5: The roles of JNK and p38 in FFS-induced cofilin phosphorylation	61
Figure 3.6: FFS-induced changes in LIMK phosphorylation	62
Figure 3.7: FFS-induced changes in SSH phosphorylation	63
Figure 3.8: The role of cofilin in FFS-induced barrier staining	65
Figure 3.9: The role of JNK and p38 activity in FFS-induced barrier staining	67
Figure 4.1: Heparin attenuates TNF α -induced stress fibers and nuclear stress kinase activity	79
Figure 5.1: TMEM184A is expressed in vascular endothelial and smooth muscle cells	115
Figure 5.2: TMEM184A is expressed in CHO, MDCK, and MEF cells	116
Figure 5.3: TMEM184A co-localizes with VAMP	117
Figure 5.4: TMEM184A co-localizes with caveolin-1	118
Figure 5.5: TMEM184A co-localizes with eNOS in vascular cells	119

Figure 5.6: HeLa cells express TMEM184A	120
Figure 5.7: All cells investigated internalize Rhodamine-Heparin	121
Figure 5.8: Immunoprecipitation of the heparin receptor detects TMEM184A	122
Figure 5.9: GFP-tagged TMEM184A co-localization with Rhodamine-heparin	123
Figure 5.10: Validation of FITC-control siRNA uptake and decreased TMEM184A surface staining in cells exposed to TMEM184A siRNA	125
Figure 5.11: siRNA-mediated knockdown of TMEM184A in A7r5s	126
Figure 5.12: shRNA-mediated knockdown of TMEM184A in A7r5s	129
Figure 6.1: Regulation of the G ₁ to S cell cycle transition	132
Figure 6.2: Data from the literature indicate that exogenous heparin and endogenous heparan sulfates are anti-proliferative in VSMCs	135
Figure 6.3: MAPK PCR array data highlights	157
Figure 6.4: EGF/PDGF PCR array data highlights	158
Figure 6.5: Short-term heparin treatment does not alter MKP-1 gene expression	159
Figure 6.6: Flow chart diagramming pathways with a significant number of heparin regulated genes (either fold increase or fold decrease)	160
Figure 7.1: Knockdown of PKG decreases heparin effects on ERK activity and pElk	178

List of Tables

Table 1.1: The anti-inflammatory effects of heparin	18
Table 6.1: Microarray results organized by number of genes regulated by heparin broken down by signaling pathway	163
Table 6.2: Genes with a fold change ≥ 1.5	165
Table AI.1: Reverse Transcription Reaction Step 1	228
Table AI.2: Reverse Transcription Reaction Step 2	229
Table AI.3: RT-PCR Reaction Set-up	229
Table AI.4: RotorGene Cycling Conditions	230
Table AI.5: SABiosciences RT ² Genomic DNA Elimination Reaction Mix	230
Table AI.6: SABiosciences RT Reaction Mix	231
Table AI.7: SABiosciences PCR Reaction Mix	231
Table AI.8 SABioscience PCR Array Cycling Parameters	232
Appendix II: MAPK PCR Array Genes	233
Appendix III: EGF/PDGF PCR Array Genes	234
Appendix IV: Microarray Results showing genes with significant fold changes	234

List of Abbreviations

12B1/18E9/18B6/18H6	Anti-Heparin Receptor Monoclonal Antibodies
A7r5s	Cloned Rat Vascular Smooth Muscle Cells
ADF	Actin Depolymerizing Factor
AGE	Advanced Glycation End Products
ANF/P	Atrial Natriuretic Factor/Protein
AT	Antithrombin
BAOECs	Bovine Aortic Endothelial Cells
BAOSMCs	Bovine Aortic Smooth Muscle Cells
BCIP	5-Bromo-4-Chloro-3-Indolyl Phosphate
Cav-1	Caveolin-1
CDK	Cyclic-Dependent Kinase
CDKI	Cyclic-Dependent Kinase Inhibitor
CHO	Chinese Hamster Ovary Cells
cGMP	cyclic Guanosine Monophosphate
DMEM	Dulbecco's Modified Eagle's Medium
DUSP1	Dual-Specificity Phosphatase-1 (MKP-1)
ECL	Enhanced Chemiluminescence
EGF	Epidermal Growth Factor
Ena/VASP	Enabled/Vasodilator-Stimulated Phosphoprotein
eNOS	Endothelial Nitric Oxide Synthase
ERK	Extracellular Signal-Related Kinase
FAK	Focal Adhesion Kinase
FITC	Fluorescein Isothiocyanate
FGF	Fibroblast Growth Factor
FSS	Fluid Shear Stress or shear stress
GAG	Glycoasaminoglycan

GFP	Green Fluorescent Protein
GUCY1B3	guanylate cyclase 1, soluble, beta 3
HeBS	Hepes-Buffered Saline
hiFBS	Heat-Inactivated Fetal Bovine Serum
HUVECs	Human Umbilical Vein Endothelial Cells
IFN- γ	Interferon- γ
IGF	Insulin-Related Growth Factor
I κ B	Inhibitor of NF κ B
IL-1 β	Interleukin-1 β
iNOS	Inducible Nitric Oxide Synthase
IRS-1	Insulin Receptor Substrate-1
JIP	JNK-Interacting Protein
JNK	<i>c-jun</i> NH ₂ -terminal Kinase
LDL	Low-Density Lipoprotein
LIMK	Lin-11/Isl-1/Mec-3 domain-containing protein kinase
LOX-1	Oxidized Low Density Lipoprotein (Lectin-Like) Receptor 1
MALDI-TOF	Matrix-Assisted Laser Desorption/Ionization – Time of Flight
MAPK	Mitogen-Activated Protein Kinase
MAPKAP	Mitogen-Activated Protein Kinase-Activated Protein Kinase
MDCKs	Madin-Darby Canine Kidney Epithelial cells
MEFs	Mouse Embryonic Fibroblasts
MEM	Minimum Essential Media
MKK	MAP Kinase Kinase
MKKK	MAP Kinase Kinase Kinase
MKP-1	MAPK Phosphatase-1 (DUSP1)
NBT	Nitro-Blue Tetrazolium Chloride
NF- κ B	Nuclear Factor κ B

NO	Nitric Oxide
NOS	Nitric Oxide Synthase
ODSH	<i>O</i> -desulfated heparin
PBS	Phosphate-Buffered Saline
PDGF	Platelet-Derived Growth Factor
PFA	Paraformaldehyde
PKA	cAMP-Dependent Protein Kinase
PKG	cGMP-Dependent Protein Kinase
PMN	Polymorphonuclear
RAGE	Receptor for Advanced Glycation End Products
RAOSMCs	Rat Aortic Smooth Muscle Cells
Rb	Retinoblastoma Protein
RIPA	Radioimmunoprecipitation
S3A	Serine-3-Alanine (cofilin mutant)
S3D	Serine-3-Aspartic Acid (cofilin mutant)
SAPK	Stress-Activated Protein Kinase
Sdmg1	Sexually Dimorphic Expressed in Male Gonads (TMEM184A)
SDS	Sodium Dodecyl Sulfate
SDS-PAGE	SDS-Polyacrylamide Gel Electrophoresis
Serpin	Serine (or cysteine) Protease Inhibitor
sGC	Soluble Guanylyl Cyclase
SNARE	Soluble N-Ethylmaleimide-Sensitive Factor-Attachment Protein Receptor
SSH	Slingshot Phosphatase
TESK	Testicular Protein Kinase
TMEM184A	Transmembrane Protein 184A
TNF α	Tumor Necrosis Factor α
TRITC	Tetramethyl Rhodamine Isothiocyanate

VAMP	Vesicle-Associated Membrane Protein
VEGF	Vascular Endothelial Growth Factor
VSMCs	Vascular Smooth Muscle Cells

Abstract

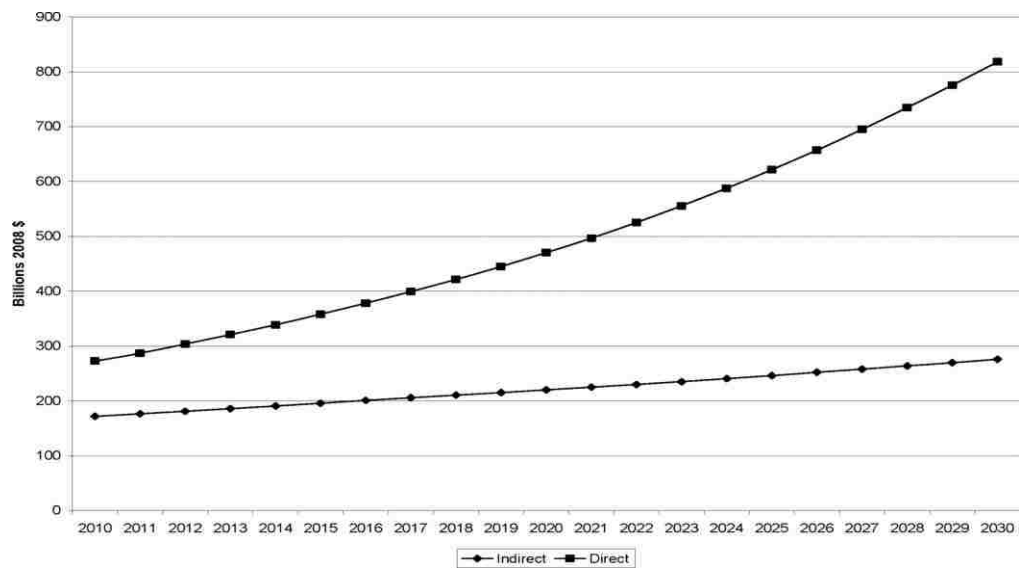
Atherosclerosis, an inflammatory disease characterized by the hardening of the arteries and often attributed to poor life style choices, is the leading cause of death in the United States, Europe, and most of Asia. This disease is caused by injury to the arterial wall, causing an inflammatory response which can become misregulated, and over the lifetime of an individual can lead to plaque formation. Hallmarks of atherosclerotic plaque formation include the proliferation and migration of vascular smooth muscle cells (VSMCs) to the injured site in the arterial wall and endothelial cell dysfunction, both of which contribute to plaque formation. In an attempt to control this unwarranted inflammation and cellular proliferation, heparin has been studied because of its anti-inflammatory and anti-proliferative effects. Unfortunately, the mechanisms by which heparin induces these effects are not well understood. In this study, experiments aimed at identification of a receptor for heparin furthered the understanding of the signaling mechanisms underlying heparin's anti-inflammatory and anti-proliferative effects. To gain a better understanding of the underlying signaling cascade induced by heparin, various gene expression analyses were performed in heparin-treated VSMCs. While heparin is one of the major signals opposing vascular disease progression, other signals including laminar shear stress also provide similar opposing actions. Along with investigation of heparin signaling, experiments demonstrating a role for cofilin in actin remodeling during laminar shear stress have been completed. Cofilin, a member of the Actin Depolymerizing Factor family of proteins, is an actin severing protein which promotes actin depolymerization from the actin minus end when cofilin is unphosphorylated. This work also underscored the importance of cofilin and actin

realignment in shear stress-induced endothelial barrier integrity. The culmination of this work has unveiled a deeper understanding of the molecular mechanisms underlying atherosclerosis and the anti-inflammatory effects of heparin and laminar shear stress.

Chapter 1: Introduction

Atherosclerosis and its complications claim more lives than any other single disease, and together they are the leading cause of death in Western societies and Japan (Fan J and Watanabe T 2003 and Rudijanto A 2007). Not only is vascular disease a health concern, it is also a financial issue because it has been predicted that in the United States alone, treatment of patients with vascular disease accounted for health care spending of over \$300 billion in 2010 (Heidenreich PA et al. 2009). The cost of treatment of patients with vascular disease is predicted to increase for the foreseeable future with the cost predicted to be well over \$800 billion by 2030, not accounting for inflation (Figure 1.1) (Heidenreich PA et al. 2009).

*Figure 1.1: The cost of treating cardiovascular disease
(Adapted from Heidenreich PA et al. 2009)*

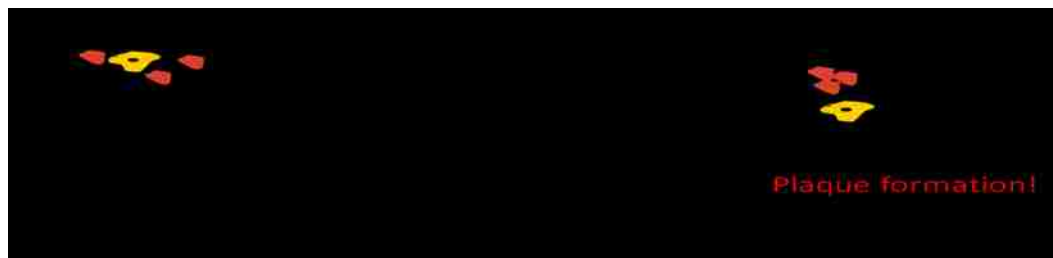


The cost of treating patients with cardiovascular disease correlates with the percentage of the population classified as obese. In a study conducted in 2009-2010, nearly one-third of the United States adult population and almost 17% of the adolescent population were considered obese (Ogden CL et al. 2012). These values have been

steadily increasing since 1999 and are predicted to increase at the same or a more rapid rate in the future (Ogden CL et al. 2012). These statistics emphasize the importance of furthering our understanding of the underlying causes of atherosclerosis and potential ways treat it.

Atherosclerosis is an inflammatory disease which occurs in response to an injury to the arterial wall, resulting in endothelial cell dysfunction (Ross R 1999, Rudijanto A 2007, and Libby P, Ridker PM, and Maseri A 2002). The endothelial cell dysfunction can be caused by a variety of factors, but most often it is attributed to elevated Low-Density Lipoprotein (LDL)/high cholesterol, diabetes mellitus, abnormally high radicals due to cigarette smoking, high blood pressure, certain genetic alterations, obesity, and pathogens such as Chlamydia pneumonia (Fan J and Watanabe T 2003) (Figure 1.2). Although these factors are known to predispose an individual to the development of atherosclerosis, they do not cause atherosclerosis. Many individuals may have one or multiple of these risk factors and never develop cardiovascular disease. It is also true that some patients do not have any of these risk factors and have advanced cardiovascular disease. The mechanistic relationships between these risk factors and atherosclerosis are still largely unclear.

Figure 1.2: Risk factors for atherosclerosis



Atherosclerosis begins with an injury to the endothelial cell layer in medium and large sized arteries (Ross R 1999, Rudijanto A 2007, and Libby P, Ridker PM, and Maseri A 2002), and the risk factors detailed above are in some way related to this injury. This initial lesion is called a fatty streak and can be found in infants and young children as well as adults (Napoli C et al. 1997). Fatty streaks are pure inflammatory lesions consisting of monocyte-derived macrophages and T lymphocytes (Stary HC et al. 1994). In most cases these inflammatory fatty streaks are resolved, and there is no further build up in these areas.

Regardless of the cause of the injury to the arterial wall, endothelial cell dysfunction follows, leading to excessive, chronic inflammation and phenotypic changes in the endothelial cell layer. These changes alter the normal anticoagulant nature of the endothelial layer and change it to a pro-coagulant nature. This pro-coagulant nature triggers the release of inflammatory cytokines and growth factors, triggering the surrounding vascular smooth muscle cells (VSMCs) to become proliferative and migratory (Ross R 1993 and Ross R 1999). This change in the VSMC layer causes the cells to exit their normal non-proliferative, quiescent, and well-differentiated state and enter the cell cycle, proliferate, and lose their differentiated phenotype. This VSMC proliferation leads to thickening of the arterial wall, often referred to as arterial wall remodeling (Ross R 1993 and Ross R 1999).

Continued inflammation leads to specific gene expression programs resulting in transcription of pro- and anti-inflammatory proteins which affect the attraction of leukocytes and platelets, vascular permeability, coagulation, and ultimately control the

course and outcome of the inflammatory reactions (Viemann D et al. 2006, Libby P, Ridker PM, and Maseri A 2002, and reviewed in Libby P 2012). The recruitment of macrophages and lymphocytes causes the release of additional inflammatory molecules such as hydrolytic enzymes, cytokines, chemokines, and growth factors leading to more wall damage and the development of a fibrous plaque (Ross R 1999, Viemann D et al. 2006, Libby P, Ridker PM, and Maseri A 2002, and reviewed in Libby P 2012). Fibrous plaques are the most advanced and dangerous, in that they are generally unstable and do not have a well-defined structure. These characteristics often predispose the clot to rupture which can lead to devastating ischemia of the heart (heart attack), brain (stroke), or extremities (gangrene) (Ross R 1993 and Ross R 1999).

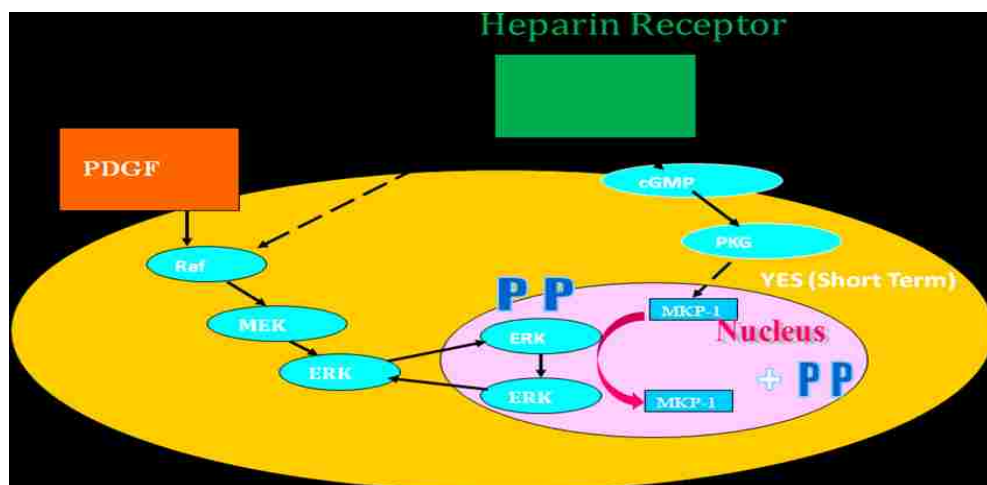
Endothelial cells lining all blood vessels play an important role during systemic inflammation because of their position and immediate exposure to inflammatory mediators. The two major inflammatory mediators (cytokines) that are elevated during systemic inflammation are Interleukin-1 β (IL-1 β) and tumor necrosis factor-alpha (TNF α) (Kishikawa H, Shimokama T, and Watanabe T 1993, Rus HG, Niculescu F, and Vlaicu R 1991, Moyer CF et al. 1991, and Galea J et al. 1996). Studies have documented that endothelial cells respond to various external stimuli, in part by altering gene expression for cytokines, adhesion molecules, pro-coagulation factors, and other proteins (Paleolog EM et al. 1994, Dixit VM et al. 1990, Ross R 1997, and Ross R 1999). Therefore, the response of endothelial cells to IL-1 β and TNF α treatment will likely provide necessary information that may help to explain some of the dysfunction that occurs (Zhao B et al. 2003).

As previously mentioned, one of the major hallmarks of atherosclerosis is the proliferation of VSMCs induced by inflammatory signaling. Therefore, a logical treatment for atherosclerosis would include a molecule or drug capable of attenuating VSMC proliferation and thereby inhibiting fibrous plaque development. The glycosaminoglycan (GAG) heparin has those capabilities. It has been shown to elicit a cell cycle block in VSMCs at the G₁ phase (Reilly CF et al. 1989 and Fasciano S et al. 2005) and has not been shown to trigger resistance in VSMCs (Mrabat H et al. 2009). Heparin is a naturally occurring complex carbohydrate which is well-known for its anti-coagulant properties, but has been widely studied for potential use in attenuating or reversing the atherogenic process (Edelberg JM et al. 1991 and Fasciano S et al. 2005). The anti-proliferative effects of heparin *in vivo* and *in vitro* have been well-documented throughout the literature as well as from previous members of the Lowe-Krentz laboratory (Clowes AW and Karnowsky MJ 1977, Mrabat H et al. 2009, Kazi M et al. 2002, Savage JM et al. 2001, and Blaukovitch CI et al. 2010). Despite the wealth of information regarding the anti-proliferative effects of heparin on VSMCs in the literature, relatively little is known about the actual mechanism(s) of action for heparin.

Evidence in the literature suggests that heparin exerts its anti-proliferative effects via at least two mechanisms. One mechanism includes the regulation of Mitogen-Activated Protein Kinase (MAPK) cascade intermediates (Yu L et al. 2006, Blaukovitch CI et al. 2012, Dickinson RJ and Keyse SM 2006, Pukac LA et al. 1997, and Dhillon AS et al. 2007), which are involved in cell growth and proliferation and by imposing a cell cycle block at the G₁ phase through upregulation or down regulation of specific genes

necessary for the transition from the G₁ to the S phase (Reilly CF et al. 1989, Fasciano S et al. 2005, Vadivello PK et al. 1997, Mishra-Gorur K and Castellot JJ 1999, Ottlinger ME, Pukac LA, and Karnovsky MJ 1993, and Pukac LA et al. 1997). Previous work in the lab and work done within this dissertation have built the case that heparin binding to a putative heparin receptor induced the synthesis of cGMP (cyclic Guanosine Monophosphate), leading to PKG (cGMP-dependent protein kinase) activation, and MKP-1 (MAPK phosphatase-1) upregulation (Figure 1.3) (Blaukovitch CI et al. 2012). MKP-1 localizes to the nucleus, functions as a dual-specificity phosphatase (DUSP), and removes both activating phosphorylations from ERK, thereby inactivating ERK (Rohan PJ et al. 1993). Sustained activation of ERK results in Elk-1 phosphorylation in the nucleus (Shin HS et al. 2003). This MKP-1-mediated loss of active ERK in the nucleus results in decreased Elk-1 activity as well (Shin HS et al. 2003). MKP-1 new protein synthesis as a result of heparin treatment can be seen as early as 10 min (Blaukovitch CI et al. 2010).

Figure 1.3: Heparin's effect on the MAPK pathway in VSMCs (Adapted from Pugh R. Dissertation Lecture 2010)



The case for PKG involvement in heparin-induced MKP-1 mediated dephosphorylation of ERK draws parallels from insulin and insulin-related growth factor (IGF) signaling. Both insulin and IGF induce the expression of inducible nitrous oxide synthase (iNOS), leading to increased cGMP in response to NO-activated soluble guanylyl cyclase (sGC) (Begum N et al. 1998 and Jacob A et al. 2002). This increase in cGMP was shown to be sufficient to induce MKP-1 and decrease ERK activity. Atrial natriuretic factor or peptide (ANF or ANP) has also been shown to elevate cGMP levels in VSMCs (Baldini PM et al. 2002 and Tantini B et al. 2005). ANP activates intracellular guanylyl cyclase and thereby elevates cGMP (Baldini PM et al. 2002 and Tantini B et al. 2005). Aside from their known roles in vasorelaxation, ANP and cGMP have been shown to decrease VSMC proliferation (Baldini PM et al. 2002); building the possibility that heparin's effects could be mediated by cGMP and PKG signaling. Aside from inducing MKP-1 protein synthesis, heparin also down-regulates Raf activity. Since Raf is an upstream kinase of ERK, decreased Raf activity leads to decreased ERK activity (Pukac LA et al. 1997 and Slee JB, Pugh R, and Lowe-Krentz LJ 2012) (Figure 1.3). Since Raf activity is down-regulated in response to heparin treatment, it is clear that down-regulation of ERK activity would follow. It has been shown in the literature that heparin treatment causes a rapid downregulation of mRNA levels of genes involved in the regulation of cell proliferation, including *c-fos*, *c-jun*, *myb*, and *myc*, again decreasing proliferation (Mishra-Gorur K and Castellot JJ 1999).

It was established in the mid-nineties that endothelial nitric oxide synthase (eNOS) interacts with caveolin, the structural component of caveolae (reviewed in: Rath

G, Dessy C, and Feron O 2009). Caveolae are flask-like invaginations of membranes which occur at different densities in most cell types and are prominent in vascular endothelial cells, adipocytes, fibroblasts, and epithelial cells (reviewd in: Childow JG Jr and Sessa WC 2010), where they form stable membrane domains often referred to as lipid rafts. Caveolae have also been shown to regulate vesicle transport by serving as carriers in exocytic and endocytic pathways (Parton RG and Simons K 2007 and Childow JG Jr and Sessa WC 2010). Caveolins (1, 2, and 3) have cytoplasmic N- and C- termini, sites for post translational modifications, and a scaffolding domain, all of which are involved in forming an organized hub for signal transduction (reviewed in: Patel HH, Murray F, and Insel PA 2008). Caveolins have been shown to group together upstream signaling components (including G-protein coupled receptors and receptor tyrosine kinases) and downstream components (including G-protein coupled receptor subunits, effector enzymes, and ion channels) to centralize and enhance signal processing and transduction. Caveolin-1 (cav-1) is of particular importance in the vasculature, predominantly vascular endothelial cells, due to its regulation of eNOS within caveolae. Endothelial cav-1 is involved in caveolae formation throughout the endothelium of the entire vascular system where it regulates endothelial nitric oxide (NO) production, vascular permeability, and vascular remodeling (Parton RG and Simons K 2007, Childow JG Jr and Sessa WC 2010, and Patel HH, Murray F, and Insel PA 2008).

The second way in which heparin exerts its anti-proliferative affects in VSMCs is by imposing a cell cycle block at the G₁ phase (Fasciano S et al. 2005, Vadivello PK et al. 1997, Reilly CF et al. 1989, Mishra-Gorur K and Castellot JJ 1999, Ottlinger ME

1993, and Pukac LA et al. 1997). Cellular proliferation is regulated primarily by control of the cell cycle, which consists of four distinct sequential phases (G_0/G_1 , S, G_2 , and M). Most smooth muscle cells in the adult vascular system are in a quiescent state, typically arrested in the G_0 or G_1 phases of the cell cycle. Research has shown that heparin strongly down-regulates the levels of cyclin D1 mRNA and protein, cdk2 mRNA, and cdc2 protein leading to cell cycle block at the G_1 phase (Vadivello PK et al. 1997). One cyclin-dependent kinase inhibitor (CDKI) upregulated by heparin treatment is p27^{kip1}. This stable accumulated p27^{kip1} protein level in G_1 is essential for the heparin-induced decreases in VSMC proliferation because p27^{kip1} prevents the activation of cyclin-dependent kinase 2 (Cdk2) (Fasciano S et al. 2005). It has also been shown by other groups that p27^{kip1} is upregulated in response to heparin treatment, again blocking cellular proliferation at G_1 (Yu L et al. 2006 and Fouty BW et al. 2001). It is also suggested in the literature that heparin blocks progression through G_1 by inhibition of the PKC-dependent pathway of cell cycle progression (Pukac LA et al. 1990). This PKC inhibition results in the blocking of second messengers required for *fos* expression (Pukac LA et al. 1992) and decreased ERK activation (Mishra-Gorur K and Castellot JJ 1999, Ottlinger ME et al. 1993, and Pukac LA et al 1997).

It is becoming clearer in the literature that heparin and low (or non-) anticoagulant heparin derivatives exhibit strong anti-inflammatory properties. These anti-inflammatory properties could be harnessed to improve the treatment of vascular diseases such as atherosclerosis and graft arteriosclerosis which can be caused by excessive inflammation and innate and adaptive immune responses (Hansson GK et al. 2002). Heparin and low

anticoagulant heparin have been shown to inhibit inflammation by disrupting multiple levels of the inflammatory cascade (Thourani VH et al. 2000). Heparin treatment inhibits complement activation *in vivo* (Weiler JM et al. 1992), adhesion molecules P- and L-selectin binding to thrombin-activated human lung microvascular endothelial cells (Wang L et al. 2001), Polymorphonuclear (PMN) elastase and cathepsin G activities *in vitro* and *in vivo* (Fryer A et al. 1997), and nuclear factor κ B (NF κ B) nuclear translocation (Thourani VH et al. 2000). Additionally, heparin treatment inhibits interferon- γ (IFN- γ) responses, competes for binding with IP-10, I-TAC, and Mig on endothelial cells, and prevents transendothelial migration and arterial recruitment of memory T cells (Ranjbaran H et al. 2006).

The NF κ B pathway is involved in a variety of cellular processes including immune responses, cell survival, stress responses, and is mis-regulated in chronic inflammation and other diseases (reviewed in: Shih VF et al. 2011). In non-stimulated cells, NF κ B is bound in the cytoplasm by its inhibitor, I κ B, preventing nuclear translocation and DNA binding. In response to specific stimuli, I κ B kinase phosphorylates I κ B resulting in I κ B degradation and NF κ B release and activation. Active NF κ B migrates to the nucleus, binds DNA and induces the transcription of pro-inflammatory genes (Shih VF et al. 2011), such as TNF α , propagating the inflammatory response (reviewed in: Thourani VH et al. 2000). It has also been documented that inhibiting NF κ B reduces level of circulating TNF α (Cain BS et al. 1999). Heparin has been reported to block this pathway in at least two ways. First, heparin treatment of cultured human umbilical vein endothelial cells (HUVECs) prevents NF κ B nuclear

translocation and heparin inclusion in DNA binding assays inhibited NF κ B binding to DNA (Thourani VH et al. 2000). If this anti-inflammatory mechanism is true, it would require heparin to be released in the cytoplasm, something for which a mechanism has yet to be elucidated. Heparin also decreases the activity of NF κ B by inhibiting the interaction of RAGE (Receptor for Advanced Glycation End Products) with its ligands AGEs (Advanced Glycation End Products). The RAGE system is one mechanism known to elicit pro-inflammatory cascades in vascular endothelium and smooth muscle (Basta G et al. 2002, Goldin A et al. 2006, and Lander HM et al. 1997). Rao NV et al. (2010) reported that both heparin and low anti-coagulant 2-O, 3-O-desulfated heparin (ODSH) prevented inflammatory cells from utilizing RAGE as a vascular adhesion molecule. The overall importance of their work is that heparin and ODSH can disrupt several steps in leukocyte-mediated inflammation. However, the role of RAGE in heparin signaling was outside the scope of this dissertation.

It has been well established in the literature that many cells, including cells of the vasculature, such as endothelial and smooth muscle, bind and internalize heparin via receptor-mediated endocytosis shown using radiolabeled or fluorescent heparin (eg. Bârzu T et al. 1985 and Castellot JJ et al. 1985). Thourani VH et al. (2000) reported that pre-treatment of HUVECs with 200 μ g/ml heparin or OSDH inhibited TNF α -induced translocation of NF κ B from the cytoplasm to the nucleus. The authors employed immunohistochemistry for p65 nuclear staining and *in vitro* electrophoretic mobility shift assays showing that heparins reduce NF κ B-DNA binding. The explanation given by Thourani VH et al., suggests that heparin is bound and internalized by vascular

endothelium and smooth muscle (Bârzu T et al. 1985 and Castellot JJ et al. 1985), allowing the negatively charged heparin molecule to bind to the positively charged nuclear localization sequence of NF κ B thereby blocking its association with the nuclear pore complex (Thourani VH et al. 2000).

Although Thourani VH et al. postulated this mechanism, they did not address how heparin was internalized or how it was released into the cytoplasm and did not rule out possible heparin-receptor binding and signaling. Other work performed by Penc SF et al. (1999) found that the GAG dermatan sulfate, which possesses different sugars and sulfate locations, actually induced the activation of NF κ B and its downstream responses in cultured human dermal microvascular endothelium, but the authors were unable to confirm whether this was due to a direct or indirect response. These results suggest that that different GAGs can mediate different responses based on their differing chemistries (Lindahl U et al. 1998); although it is supported that exogenous heparin mediates similar responses to certain heparan sulfates given their similar chemistries (Gitay-Goren H et al. 1992, Spivak-Kroizman T et al. 1994, Ono K et al. 1999, and Mamluk R et al. 2002).

Both heparin and ODSH block the adhesion of P-selectin to P-selectin glycoprotein ligand-1 expressing U937 cells and disrupt leukocyte arrest by Mac-1/RAGE inhibition (Rao NV et al. 2010). Again, both heparin and ODSH were shown to inhibit Mac-1-mediated binding of AMJ2-C11 mouse alveolar macrophages, to immobilized RAGE, and both prevented U937 cells from binding to RAGE. They were also able to show that heparin and ODSH disrupt diapedesis through the inhibition of the binding of azurocidin to heparin-BSA-coated wells. Lastly, their work indicated that

heparin and ODSH disrupted the secretion of pro-inflammatory granular contents. Heparin and ODSH inhibited Human Leukocyte Elastase and cathepsin G enzyme activity with synthetic chromogenic substrates. It was also determined that both blocked RAGE from binding to S100 calgranulins, which are also secreted by leukocytes (Rao NV et al. 2010). The Rao study not only strengthens our understanding of the anti-inflammatory aspects of heparin, it also provides evidence that the anti-coagulant functions of heparin can be removed, specifically, by 2-O and 3-O desulfation, while the important anti-inflammatory capabilities are retained (Rao NV et al. 2010).

A model that is well-established and well-supported in the literature is that heparin can compete for binding with pro-inflammatory molecules and thus exert its anti-inflammatory effects (Ali S et al. 2003, Ranjbaran H et al. 2006, and Hatakeyama M et al. 2004). This model is supported by evidence that heparin or heparin-like molecules bind various growth factors, cytokines, and chemokines including fibroblast growth factor (FGF) (Mongiat M et al. 2000), vascular endothelial growth factor (VEGF) (Gitay-Goren H et al. 1992), interleukins 1-8 (Ramsden L and Rider CC 1992, Roberts R et al. 1988, Lortat-Jacob H et al. 1997, Clarke D et al. 1995, and Webb LM et al. 1993), and interferon-gamma (IFN- γ) (Ranjbaran H et al. 2006 and Hatakeyama M et al. 2004). The last of which, IFN- γ , has received much attention due to the discovery that heparin can inhibit certain IFN- γ -inducible cytokine profiles (Ranjbaran H et al. 2006 and Hatakeyama M et al. 2004). These findings are intriguing, because of the role of IFN- γ as a pro-inflammatory cytokine, and because analyses of atherosclerotic lesions in clinical specimens indicate that they possess T-cell infiltrate with IFN- γ -secreting cytokine

profiles and up-regulated IFN- γ -inducible molecules (Frostedgård J et al. 1999, van Besouw NM et al. 1997, and Mach F et al. 1999). These findings suggest that in vascular disease there is an aberrant up-regulation of the IFN- γ responses which could be therapeutically attenuated with heparin or heparin-like molecules.

The IFN- γ response is initiated by CD4+ helper T cells (Th) or CD8+ cytotoxic T cells (Tc) which produce IFN- γ , whose maturity is regulated by IL-12 and promoted by IL-18 (Salgame P et al. 1991). IFN- γ strongly induces IFN- γ -inducible protein of 10 kDa (IP-10)/CXCL10, IFN-inducible T cell α chemoattractant (I-TAC)/CXCL11, and monokine induced by IFN- γ (Mig)/CXCL9 (Bonecchi R et al. 1998) in vascular cells which are important for T cell behavior (Ranjbaran H et al. 2006). It has been determined that heparin is a competitive inhibitor of ligands, including IP-10, I-TAC, and Mig, for the IFN- γ receptor. Clinical doses (3 mg/kg) of heparin increase plasma levels of all three in patients with coronary atherosclerosis undergoing coronary artery bypass graft surgery (Ranjbaran H et al. 2006). Exposing EDTA-mobilized HUVECs pre-incubated with IP-10 to heparin resulted in an increase in IP-10 in the supernatant. This suggests a competitive binding model in which heparin displaces bound IP-10 from HUVECs (Ranjbaran H et al. 2006). Control experiments with trypsin did not result in the release of IP-10, further suggesting the release of surface-bound IP-10 (Ranjbaran H et al. 2006).

The Ranjbaran study also indicated that at relatively high doses, heparin may inhibit the production of these chemokines in atherosclerotic coronary arteries of patients undergoing coronary artery bypass graft surgery (Ranjbaran H et al. 2006).

Corresponding to the lack of receptor bound IP-10; heparin was also able to inhibit IP-10-

dependent transendothelial migration of T cells (Ranjbaran H et al. 2006). A related study performed by Hatakeyama M et al. in 2004 suggested that heparin can inhibit IFN- γ -induced fractalkine (CX3CL1) expression in HUVECs, preventing chemoattraction of mononuclear cells and their eventual adhesion. Using ELISA binding assays, the authors determined that heparin decreased the amount of IFN- γ bound to wells coated with IFN- γ Receptor 1 (Hatakeyama M et al. 2004). Western blotting using native gels showed that pre-incubation of HUVECs with heparin resulted in a shift in the molecular weight of IFN- γ , suggesting that heparin can bind directly to IFN- γ (Hatakeyama M et al. 2004). The results of these assays indicate a plausible mechanism in which heparin binds IFN- γ and blocks it from binding to its receptor (Hatakeyama M et al. 2004). The authors also concluded from Western blot data that heparin was capable of inhibiting the IFN- γ -induced phosphorylation of STAT-1 (Hatakeyama M et al. 2004). These two articles suggest that the IFN- γ arm of the inflammatory pathway may be a preferential target of heparin. The anti-inflammatory effects of heparin are summarized in Table 1.1.

Exogenous Heparin	
Complement System	Inhibition of complement activation (Weiler JM et al. 1992)
Leukocyte Tethering and Rolling	Inhibition of P- and L-Selectin (Wang L et al. 2001)
NF κ B Signaling	Inhibition of NF κ B nuclear translocation (Thourani VH et al. 2000)
	Inhibition of AGE-RAGE binding (Rao NV et al. 2010)
IFN- γ Responses	Competitive inhibition of IP-10, I-TAC, and Mig for the IFN- γ receptor (Ranjbaran H et al. 2006)
	Inhibition of STAT-1 phosphorylation (Hatakeyama M et al. 2004)

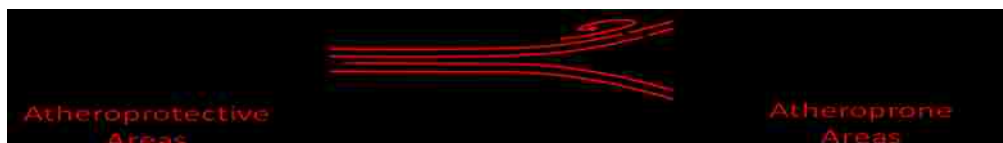
The anti-inflammatory mechanisms of heparin and heparan sulfates discussed herein only represent a small subset of the known anti-inflammatory capabilities of this class of molecules. Ongoing research suggests that heparin can be experimentally modified to reduce the anti-coagulant properties while maintaining the anti-inflammatory properties. In addition, it has been shown that heparin treatment induces endothelial cells to produce additional heparan sulfates (Morrison P and Lowe-Krentz LJ 1989), suggesting that triggering this pathway, even without heparin as the signal, could increase the anti-inflammatory nature of the vasculature. It is likely that our understanding of the anti-inflammatory properties of heparin and heparan sulfates is still in its infancy. Since it has been established that heparin can be internalized by cells of the vasculature (Bârzu T et al. 1985 and Castellot JJ et al. 1985), one can speculate that many of the anti-inflammatory behaviors of heparin could be receptor-mediated. Heparin internalization suggests receptor involvement, supporting the possibility of receptor-based signaling, which has yet to be identified in the literature.

It has been widely documented in the literature and by previous members of the Lowe-Krentz laboratory that heparin mediates a portion of its effects through a cell surface receptor, suggesting that a putative heparin receptor exists on the surface of VSMCs (Savage JM et al. 2001) and vascular endothelial cells (Patton WA et al. 1995). It has also been documented by previous members of the Lowe-Krentz lab that treatment with monoclonal antibodies that block heparin binding to endothelial cells also mimics the effects of heparin in vascular smooth muscle cells (Blaukovitch CI et al. 2010 and Savage JM et al. 2001) and vascular endothelial cells (Patton WA et al. 1995). Although

it is well-documented that the heparin receptor exists, there has not been published evidence reporting the isolation and characterization of the receptor. Due to this fact, there is not much known about the receptor itself. However, given the highly charged nature of heparin chains, the most likely mechanism for transport across the membrane would be through a receptor. Therefore our lab set out to identify a receptor for heparin.

Along with heparin as an anti-inflammatory agent, shear stress plays an important role in maintaining vascular homeostasis. The hypothesis that shear stress was a causative agent in atherosclerosis was originally proposed in the late 1960s (reviewed in Caro CG, Fitz-Gerald JM, and Schroter RC 1969). Atheroprotective conditions are found in regions of the vasculature where blood flow is continuous and undisturbed (laminar), which can be mimicked in a laboratory setting using 15 dynes/cm² shear stress (high fluid shear stress – FSS) (Birukov KG et al. 2002, Dewey C et al. 1981, Mott RE and Helmke BP 2007). Atheroprone regions of the vascular system occur in areas of turbulent blood flow (i.e. artery bifurcations), which can be mimicked in the lab using 4 dynes/cm² shear stress (low FSS) (Siasos G et al. 2007 and Kadohama H et al. 2006) (Figures 1.2 and 1.4).

Figure 1.4: The relationship between FSS and atherosclerosis



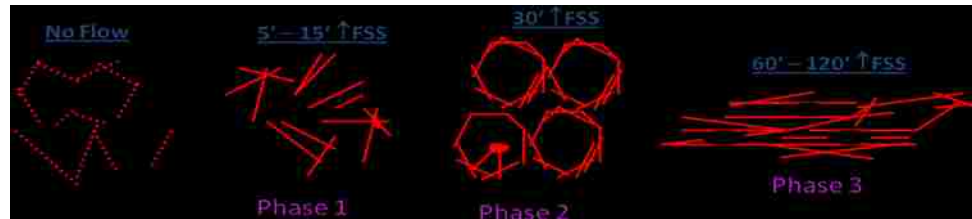
In vivo and *in vitro* evidence indicates that laminar shear stress causes endothelial cell, nuclei, and actin microfilament alignment in the direction of FSS (Birukov KG et al. 2002, Dewey C et al. 1981, Mott RE and Helmke BP 2007, and Mengistu M et al. 2011). It has been well-documented in the Lowe-Krentz lab and in the literature that under high

FSS (15 dynes/cm²), endothelial cells undergo a series of morphological changes, culminating in the alignment of the whole cell, actin microfilaments, microtubules, and intermediate filaments in the direction of FSS (Figure 1.5) (Flitney FW et al. 1996, Franke R et al. 1984, Galbraith CG, Shalak R, Chien S 1998, Helmke BP et al. 2001, Malek AM and Izumo S 1996, Sato M, Levesque M, and Nerem R 1987, Wechezak A, Viggers R, and Sauvage L 1985, Mengistu M et al. 2011, and Azuma N et al. 2001), but the molecular mechanisms underlying this remodeling are unclear.

As shown in Figure 1.5, at approximately 5 to 15 min, an upregulation in actin microfilaments is seen in response to high FSS, which has been termed Phase 1. The formation of stress fibers can be seen as early as 5 min of high FSS. Stress fibers are actomyosin bundles composed of 10-30 actin filaments held together by cross-linking proteins such as alpha-actinin and filamin, and non-muscle myosin and tropomyosin (Cramer L, Siebert M, and Mitchinson T 1997, Lazarides E and Burridge K 1975, Wang K, Ash J, and Singer S 1975, Weber K and Groeschel-Steward U 1974). Stress fiber formation is a conserved adaptation of eukaryotic cells, but its assembly is not well understood. Phase 2 is marked by the formation of a dense cortical actin band around 30 min of high FSS. This dense contractile endothelial actin ring not only helps maintain cell-cell junctions, but also gives these cells the capability to contract and regulate the permeability of the endothelium (Schnittler H 1998 and Schnittler H et al. 2001). Lastly, Phase 3 is marked by the alignment of the whole cell and actin microfilaments in the direction of shear stress at time points greater than 60 minutes of high FSS (Mengistu M et al. 2011 and reviewed in Mengistu M, Slee JB, and Lowe-Krentz LJ 2012). The

alignment in the direction of FSS allows ECs to reduce their height in order to decrease the magnitude of the strain they experience from hemodynamic forces (Barbee K, Davies P, and Lal R 1994, Hu S et al. 2003, Karcher H 2003, Pellegrin S and Mellor H 2007).

Figure 1.5: The three phases of actin microfilament rearrangement in response to high fluid shear stress
(Adapted from Mengistu M et al. 2011 and Mengistu M, Slee JB, Lowe-Krentz LJ 2012)

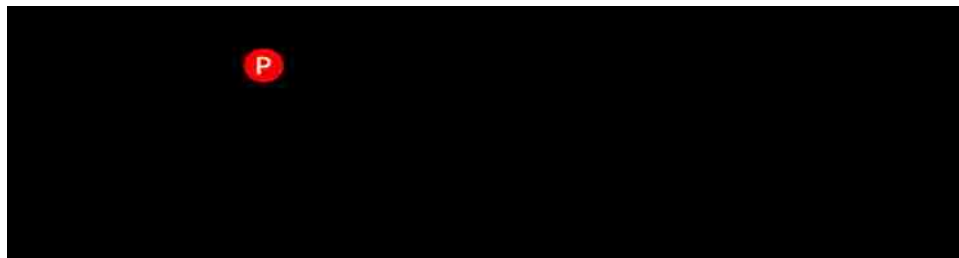


Several mechanisms have been proposed for sensing, transducing, and responding to FSS. The cytoskeleton has been shown to be responsible for the transmission of stresses from the cell surface to various intracellular locations such as cell-cell adhesion sites, focal adhesion sites, and the nucleus (reviewed in: Barakat A and Davies P 1998). It has also been suggested that a mechanosensing complex is found in endothelial cells to elicit mechanical signals to the actin cytoskeleton, which is discussed further in Chapter 3 (Conway D and Schwartz MA 2012). A role for cell-cell junctions in this process is also emerging and plays a large role in the mechanosensing complex (Tzima E et al. 2005). Although much is known about responses to FSS in vascular endothelium, a detailed mechanism has yet to be determined.

Regulation of actin microfilament dynamics depends in part upon the Actin Depolymerizing Factor (ADF) family of proteins, of which cofilin is a prominent player (reviewed in: Lin M-C et al. 2010, Suurna MV et al. 2006, Chen Q and Pollard TD 2013, and Nishida E et al. 1987). It is well-documented that phospho-cofilin is

dephosphorylated by cofilin phosphatases, including chronophin and the slingshot (SSH) family of protein phosphatases and therefore activated by various external stimuli (Suurna MV et al. 2006, Won KJ et al. 2008, Keezer SM et al. 2003, and Cote M et al. 2010). Once dephosphorylated, cofilin is involved in the regulation of actin dynamics (Suurna MV et al. 2006, Won KJ et al. 2008, Keezer SM et al. 2003, and Cote M et al. 2010). To inactivate cofilin various extracellular signals trigger its phosphorylation via the Lin-11/Isl-1/Mec-3 domain-containing protein kinase (LIM Kinase) family (reviewed in: Bernard O 2007, Moriyama K, Iida K, and Yahara I 1996) or by the related testicular protein kinase (TESK) (Suurna MV et al. 2006, Won KJ et al. 2008, Keezer SM et al. 2003, and Cote M et al. 2010), inducing the inhibition of actin dynamics leading to actin stress fiber accumulation (Suurna MV et al. 2006, Won KJ et al. 2008, Keezer SM et al. 2003, and Cote M et al. 2010). As shown in Figure 1.6, cofilin regulation is opposite of traditional phosphorylation control mechanisms, in that phosphorylation of cofilin is required to, in essence, inactivate the protein, inducing the inhibition of actin dynamics (Suurna MV et al. 2006, Won KJ et al. 2008, Keezer SM et al. 2003, and Cote M et al. 2010).

Figure 1.6: Regulation of cofilin



Published evidence indicates that c-Jun N-terminal kinase (JNK) and p38, both members of sub-groups of the larger MAPK family, associate with actin microfilaments and mediate shear stress-induced endothelial cell and actin filament realignment (Azuma N et al. 2001, Hamel M et al. 2006, Wang J et al. 2005, and Mengistu M et al. 2011). MAPKs are a ubiquitous group of serine/threonine kinases which play a role in transmitting extracellular signals required for various cellular functions. All MAPKs are activated by specific kinases (MAPKKs) that phosphorylate a threonine and tyrosine residue in a conserved TEY (Threonine-Glutamic Acid-Tyrosine) motif for ERKs, TPY (Threonine-Proline-Tyrosine) motif for stress-activated protein kinases (SAPKs)/JNKs, and TGY (Threonine-Glycine-Tyrosine) motif for p38 (Nishida E and Gotoh Y 1993, Ruderman JV 1993, Seger R and Krebs EG 1995, Cano E and Mahadevan LC 1995, Davis RJ 1994, and Kyriakis JM et al. 1994).

The MAPKs are a family of protein kinases involved in of three pathways which are defined as follows. First, the “classical” MAPKs or extracellular signal regulated kinases (ERKs) is involved in proliferation and differentiation (Nishida E and Gotoh Y 1993, Ruderman JV 1993, Seger R and Krebs EG 1995, Cano E and Mahadevan LC 1995, Davis RJ 1994, and Kyriakis JM et al. 1994). The second pathway is the JNK or stress-activated protein kinases (SAPK) which is involved in inflammation and stress-induced signaling (reviewed in: Kyriakis JM et al. 1994). Lastly the p38 pathway was originally thought to be involved mainly in cellular signaling in response to osmotic shock. But it is becoming clear that this pathway is involved in much more than previously thought (reviewed in: Zarubin T and Han J 2005, Daum G et al. 1997, and

Thornton TM and Rincon M et al. 2009). A recent review article highlights evidence in the literature suggesting that p38 MAPK is involved in the regulation of the G₁-S and G₂-M phase transitions of the cell cycle (reviewed in: Thornton TM and Rincon M 2009).

The work collected within this dissertation advances our understanding of the anti-inflammatory capabilities of heparin and shear stress in the vasculature. The heparin signaling cascade, heparin-induced gene expression changes, and the relationship between FSS and actin realignment in vascular endothelium were investigated. It was shown that TMEM184A is a cell surface receptor for heparin and that TMEM184A is involved in vesicular trafficking and signal transduction, fitting with it being a receptor for heparin. It was determined that heparin signaling involves cGMP and PKG; presenting the possibility that heparin signaling depends on eNOS (endothelial nitric oxide synthase) which also co-localizes with TMEM184A. An anti-inflammatory quality of heparin was determined by showing that it attenuates stress responses induced by TNF α as assayed by stress fiber induction and nuclear stress kinase (pJNK and pp38) activity in sub-confluent vascular endothelial cells. Along with investigating the anti-inflammatory qualities of heparin, microarray data reveal that heparin regulates a large number of genes in vascular smooth muscle cells, which cluster in groups related to integrin interactions, receptor signaling, proteoglycans, and proteolysis pathways to highlight a few. Lastly, the anti-inflammatory nature of shear stress involves cofilin which is required for FSS-induced actin realignment and barrier integrity, emphasizing the importance of the actin cytoskeleton in the atheroprotective regions of the vasculature.

Chapter 2: General Methods

2.1: Cell Culture

Bovine aortic endothelial cells (BAOECs) were obtained from Cell Applications (San Diego, CA) and cultured using Cell Applications BAOEC media according to their recommendations or gradually exchanged to supplemented MEM media (described below) for large volume experiments. Briefly, BAOECs were initially cultured in Cell Applications media for 2-3 passages, after which supplemented MEM media was blended in each passage until the Cell Applications media was completely removed. This was typically performed over 2-3 passages. A7r5s (rat aortic smooth muscle cells) obtained from ATTC, Manassas, VA, primary rat aortic smooth muscles cells (RAOSMCs) and primary bovine aortic endothelial cells (BAOSMCs) obtained from Cell Applications, San Diego, CA were cultured according to the manufacturer's recommended instructions using minimum essential eagle's medium (MEM) (Sigma, St. Louis, MO) supplemented with pre-tested 10% heat inactivated fetal bovine serum (hiFBS) (Gibco, Grand Island, NY or Biowest, Miami, FL), 5% L-glutamine (Sigma), 1% sodium pyruvate (Sigma, #S8636), 1% minimum non-essential amino acids (Sigma, #M7145), and 1% penicillin/streptomycin antibiotics (Sigma, #P0781). Chinese Hamster Ovary (CHO) cells obtained from Dr. Bryan Berger and Mouse Embryonic Fibroblast (MEF) cells obtained from Dr. Matthias Falk were cultured using Dulbecco's Modified Eagle's Media (DMEM) supplemented identical to the MEM media. Madin-Darby Canine Kidney Epithelial (MDCK) cells obtained from Dr. Anastasia Thevenin/Dr. Matthias Falk were cultured in low glucose DMEM supplemented (Sigma) with 10% hiFBS, 5% L-glutamine, and 1% penicillin/streptomycin antibiotics. Cells were cultured at 37 °C and

5% CO₂ with humidity. Culture plates were pre-treated with 0.2% porcine gelatin for 1 hr prior to cell seeding. Typically, vascular cells were between passages 5 and 20 for experiments, except A7r5s, CHOs, and MDCKs which are cloned lines and last much longer in cell culture.

2.2: Immunofluorescence Staining

For cofilin staining and select TMEM184A staining, cells were washed with phosphate buffered saline (PBS), fixed, and permeabilized with ice-cold methanol for 5 min at -20 °C and washed again with PBS. The cover slips were incubated with primary antibodies overnight at 4 °C. Cells were then washed with PBS and incubated with secondary antibodies conjugated to FITC/AlexaFluor488® or TRITC (Jackson ImmunoResearch, West Grove, PA) overnight at 4 °C. In all other experiments, cells were fixed with 2.0% formaldehyde (Sigma) or 4.0% paraformaldehyde (Sigma) for 15 min at room temperature with shaking and permeabilized with 0.2% or 0.3% Triton-X-100 (Sigma) for 5 min at room temperature with shaking. Coverslips were incubated with primary antibodies overnight at 4 °C and secondary antibodies for 2 hr at room temperature. Both primary and secondary antibodies were used at dilutions recommended by the suppliers. Cover slips were mounted in mowoil (Calbiochem, Darmstadt, Germany) to minimize photobleaching.

2.3: SDS-Polyacrylamide Gel Electrophoresis (SDS-PAGE) and Western Blotting

100 mm plates of cultured cells were harvested with SDS sample buffer as previously described (Hamel M et al. 2006). Proteins were resolved by SDS-PAGE and electrophoretically transferred onto nitrocellulose and blots were probed with primary

antibodies specific for the protein of interest and secondary antibodies conjugated to biotin (Jackson ImmunoResearch). Blots were developed using ExtraAvidin™ alkaline phosphatase, BCIP, and NBT (Sigma). Bands of interest were identified by comparison with lanes using only secondary antibodies and by molecular weight based on migration of pre-stained Rainbow™ molecular weight markers (GE Healthcare Biosciences, Piscataway, NJ). R_f values for the molecular weight markers were used to generate a standard curve which was used to calculate the molecular weight of the bands of interest. Acylamide solutions were obtained from Amresco (Solon, OH).

For select TMEM184A work, blots were developed using ECL reagents for enhanced clarity. Briefly, membranes were washed 3X with TBST following biotin-conjugated secondary antibody incubation and placed into pre-mixed ABC (Avidin-Biotin Complex, Thermo Scientific) reagent for 30 min with shaking at room temperature. Following ABC reagent incubation, membranes were washed 3X with TBST. In the dark room, membranes were incubated with pre-mixed ECL (Enhanced Chemiluminescence, Thermo Scientific) reagent for 3 min, followed by film exposure. Film exposures varied from 1 – 15 min depending on signal intensity. Once film was exposed it was developed manually using Kodak D-76 Film Developer and fixed with Sprint Record Speed Fixer (Dan's Camera City, Allentown, PA). Development time averaged around 5 min, but varied with signal intensity. Once developed, films were fixed for 1 min. ABC and ECL reagents were used at concentrations recommended by the manufacturer.

2.4: Confocal Microscopy

Fluorescent labels were visualized using the Zeiss© LSM 510 Meta with a 63X oil-immersion lens at room temperature. All images were taken at approximately the same Z-plane of the cell where intensity was the greatest. Gain intensity was set just below saturating levels for the control [or static (and no inhibitor in some cases) for cofilin experiments] slide and those settings were used to image the remaining slides within a replicate for each protein of interest. The images shown are representative of the mean integrated fluorescence density for the protein indicated at each time point tested.

2.5: Fluorescent Microscopy

Fluorescent microscopy was used to obtain whole cell levels of various proteins. Fluorescent labels were visualized using a Nikon eclipse TE 2000-U fluorescence microscope with a 60X oil-immersion lens (Nikon, Tokyo Japan) at room temperature. Micrographs were captured with a SPOT RT KE camera. All images were taken at the same gain intensity and exposure time to allow for comparison across images. Gain intensity and exposure time were set just below saturating levels for the control slide and those settings were used to image the remaining slides in a replicate.

2.6: DNA Plasmid Sub-Cloning

To propagate DNA plasmids (GFP-vinculin (Kenneth Yamada, National Institute of Dental and Craniofacial Research, Bethesda, MD), cofilin mutant constructs (Theo Rein, Max Plank Institute of Psychiatry, Munich, Germany), TMEM184A shRNA constructs, and GFP-tagged TMEM184A (OriGene, Rockville, MD) standard microbiology techniques and Qiagen QIAprep mini-prep kits (Cat. No. 27104) (Valencia,

CA) were used. LB broth (Lennox) and LB agar (Lennox) (Difco Labs, Detroit, MI) were prepared by adding 25 g or 40 g (respectively) to 1 L of Millipore water and autoclaved for 30 min. Once autoclaved, solutions were allowed to cool to room temperature and 100 µg/ml antibiotic was added (typically kanamycin or ampicillin (Sigma) depending on the resistance gene on the plasmid). Plates were poured and once solidified were placed in the refrigerator. LB broth was kept in the refrigerator until needed.

The JM109 (Promega, Madison, WI) *E. coli* strain was used to propagate most plasmids, and the DH5α (Invitrogen, Grand Island, NY) *E. coli* strain was used to propagate GFP-Tagged TMEM184A and TMEM184A shRNA constructs. *E. coli* were transformed with ~50 ng of plasmid using the following protocol. Briefly, 100 µl of JM109s/DH5αs were mixed with 50 ng of plasmid and incubated on ice for 10 min and were then heat shocked at 42 °C for 2 min. Following heat shock, they were placed on ice and 500 µl of LB (no antibiotic) was added. The mixture was then incubated at 37 °C for 1 hr with shaking. Bacteria were then spun down for 15 min to pellet and the pellet was re-suspended with the liquid in the tube. 100 µl of transformed bacteria solution was added to 1 LB + antibiotic plate. Each transformation yields 5 plates. Plates were incubated at room temperature for 10 min and then flipped upside down and placed in an incubator overnight at 37 °C.

After overnight incubation, 1 colony was placed into a tube containing 5 ml of LB broth + antibiotic and incubated for ~ 16 hr at 37 °C with shaking. After the 16 hour incubation, Qiagen's miniprep plasmid isolation protocol was followed. Briefly, the bacteria were pelleted and supernatant removed. The pellet was re-suspended in 250 µl of

Buffer P1 and transferred to a microcentrifuge tube. 250 μ l of Buffer P2 was then added and the tube was inverted 4-6 times to mix. 350 μ l of Buffer N3 was added and the tube was mixed by inversion 4-6 times. Tubes were centrifuged for 10 min at 13,000 rpm. The supernatant was then applied to a QIAprep spin column and centrifuged for 1 min. Flow-through was discarded and the column was washed with 500 μ l of Buffer PB and centrifuged for 1 min. Flow-through was discarded and 750 μ l of Buffer PE was added and centrifuged for 1 min. Flow-through was discarded and centrifuged for an additional 1 min to remove any residual wash buffer. The QIAprep column was then placed in a clean 1.5 ml tube. DNA was eluted by adding 50 μ l of Buffer EB directly to the center of the QIAprep spin column, and letting stand for 1 min. Tubes were centrifuged for 1 min to elute DNA. Nanodrop analysis was performed to obtain DNA concentration and purity based on $A_{260/280\text{nm}}$. $A_{260/280\text{nm}}$ values of ~ 1.8 were considered suitable to further use. Purified plasmids were stored at $-20\text{ }^{\circ}\text{C}$ until needed.

2.7: Heparin Preparation and Treatment

In all experiments requiring heparin treatment, a 20 mg/ml stock was made fresh daily and diluted to 200 μ g/ml in complete culture medium or starvation medium (media without hiFBS). Throughout all experiments, heparin pretreatment was held constant at 20 min prior to other stimulation. Heparin from porcine skin was obtained from Sigma.

Chapter 3:

**Actin realignment and cofilin regulation are essential for barrier integrity during
shear stress**

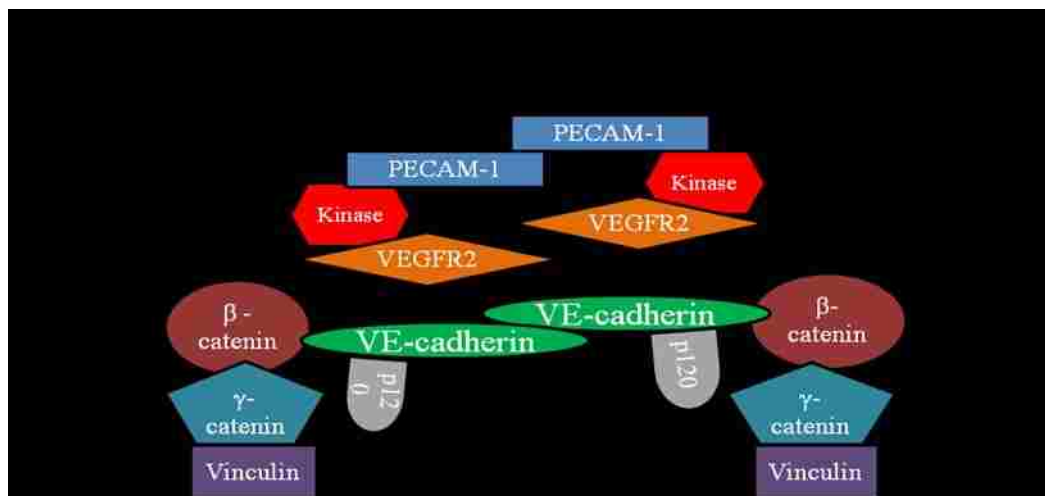
3.1: Induction

Fluid shear stress (FSS) plays important roles in embryonic morphogenesis of the vasculature, regulation of vessel diameter in adulthood, maintaining vascular homeostasis, and is implicated in the development of atherosclerosis (reviewed in Hahn C and Schwartz MA 2009). Vascular endothelial cells (ECs) respond to sustained laminar FSS by increasing their anti-thrombotic activity, decreasing reactive oxygen species, increasing antioxidant enzymes, and altering growth factor signaling (reviewed in Yamamoto K and Ando J 2011). It has been estimated that more than 600 EC genes respond to FSS (Ohura N et al. 2003). FSS has been shown to activate a variety of signaling pathways in ECs, but it is still unclear how the cell initially senses this mechanical stress. The signaling pathways which have been shown to be activated by FSS include: ion channels leading to Ca^{2+} influx, tyrosine kinase receptors leading to JNK activation, G-protein coupled receptors, and various adhesion proteins (reviewed in Yamamoto K and Ando J 2011).

There have been recent advances in understanding the mechanotransduction induced by FSS, such as the importance of cell-cell junctions (Tzima E et al. 2005) and involvement of the actin cytoskeleton (Osborn EA et al. 2006). It is becoming clear that at least one mechanosensing mechanism involves a complex of PECAM-1 (platelet endothelial cell adhesion molecule-1), VE-cadherin (vascular-endothelial cadherin), and VEGFR2 (vascular endothelial growth factor receptor 2) (Figure 3.1) (Conway D and Schwartz MA 2012). Within this complex, PECAM-1 and VEGFR2 are responsible for downstream signaling, while VE-cadherin functions as an adaptor (Tzima E et al. 2005).

VE-cadherin is an endothelial cell specific component of adherens junctions and is essential for maintaining endothelial barrier integrity (Vincent PA et al. 2004). The cytoplasmic domain of VE-cadherin associates with p120-, β -, γ -, and α -catenin in endothelial cell-cell junctions to mediate downstream signaling (Dejana E, Orsenigo F, and Lampugnani MG 2008), with VE-cadherin connecting to the actin cytoskeleton via β -catenin (Tharakan B et al. 2012). Given the importance of the endothelial barrier for vascular permeability, it is imperative that the endothelial barrier remain intact during FSS. ECs exposed to FSS exhibit a marked increase in transendothelial resistance, illustrating a strengthening of the barrier compared to static cells (DePaola N et al. 2001, Seebach J et al. 2000). Given that the VE-cadherin/ β -catenin adhesions are linked to actin, we predicted that disruptions to the actin realignment process during FSS would disrupt endothelial barrier integrity.

*Figure 3.1: Proposed mechanosensing complex
(Adapted from Conway D and Schwartz, MA 2012 with established links to actin added)*



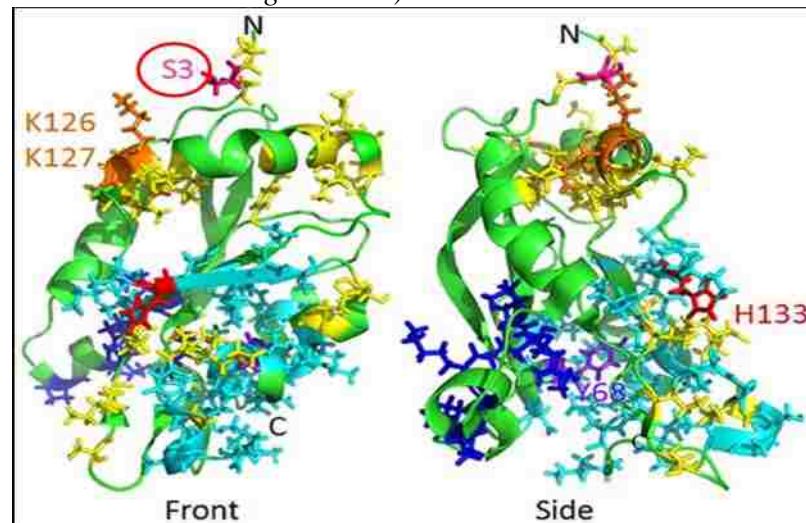
In vivo and in vitro evidence indicates that laminar FSS (15 dynes/cm^2) causes endothelial cell and actin microfilament alignment in the direction of FSS (Mengistu M et

al. 2011, Kadohama T et al. 2006, Noria S et al. 2004, Malek AM and Izumo S 1996) (see Figure 3.2), but the molecular mechanisms underlying this remodeling remain unclear. JNK and p38 are critically important during FSS-induced actin realignment. Studies investigating the role of JNK during FSS indicate that the JNK signaling pathway mediates, at least in part, FSS-induced actin realignment (Mengistu M et al. 2011, Hahn C et al. 2011). It has also been demonstrated that p38 activity is required for complete FSS-induced actin remodeling (Azuma N et al. 2001 and Mengistu M, Slee JB, and Lowe-Krentz LJ 2012). There is a large amount of data detailing the roles of JNK and p38 in migrating cells during wound healing (Reviewed in: Mengistu M, Slee JB, and Lowe-Krentz LJ 2012), as well as evidence for association with cytoskeletal structures in proliferating ECs (Hamel M et al. 2006).

Regulation of actin microfilaments depends in part upon the Actin Depolymerizing Factor (ADF)/cofilin family of proteins, of which cofilin-1 is the most prominent in non-muscle tissue (Lin MC et al. 2010, Suurna MV et al. 2006, Berstein BW and Bambrug JR 2010). The ADF/Cofilin proteins are expressed in all eukaryotes and can, for the most part, rescue deletions of other family members (Berstein BW and Bambrug JR 2010). However, cofilin-1 cannot be rescued by other family members and knockout is embryonically lethal in mice (Gurniak CB, Perlas E, and Witke W 2005). One of the major regulatory mechanisms controlling cofilin (from this point forward refers to cofilin-1) activity is phosphorylation at serine-3 (Figure 3.2) (reviewed in: Bernard O 2007, Moriyama K, Iida K, and Yahara I 1996, and Nagaoka R, Abe H, Obinata T 1996). Phospho-cofilin (serine-3) (p-cofilin) is dephosphorylated by cofilin

phosphatases, including chronophin and the slingshot (SSH) family of protein phosphatases and therefore activated. Once dephosphorylated, cofilin binds to both G-actin and F-actin in a 1:1 molar ratio and promotes F-actin depolymerization (Nishida E, Maekawa S, and Sakai H 1984). Cofilin is inactivated by phosphorylation at serine-3 via the Lin-11/Isl-1/Mec-3 domain-containing protein kinase (LIMK) family, resulting in the formation of actin stress fibers (Suurna MW et al. 2006, Won KJ et al. 2008, Keezer SM et al. 2003, Côté MC et al. 2010, and Bernard O 2007).

Figure 3.2: Cofilin structure, with Serine-3 phosphorylation site circled (Bernstein BW & Bamburg JR 2010)



It is becoming clear in the literature that actin is essential not only in the cytoplasm, but also in the nucleus, for regulation of transcription and gene expression (Zheng B et al. 2009 and Pederson T 2008). Actin alone is incapable of entering the nucleus, as it lacks a nuclear localization sequence, requiring it to associate with other proteins to facilitate nuclear entry. One of the leading hypotheses is that cofilin is responsible for localizing actin to the nucleus (Bernstein BW and Bamburg JR, 2010, Mengistu M, Slee JB, Lowe-Krentz LJ 2012). Cofilin has a nuclear localization sequence

(KKRKK) similar to that of SV40 large T antigen (Iida K, Matsumoto S, and Yahara I 1992 and Kardon D et al. 1984), and dephosphorylated cofilin has been reported to localize to the nucleus after various cell stresses, such as heat shock, latrunculin B treatment, or ATP depletion (Pendleton A et al. 2003 and Iida K, Matsumoto S, and Yahara I 1992). LIMK-1 possesses two leucine-rich nuclear export signals within its PDZ domain and one NLS-like sequence responsible for nuclear localization (Yang N and Mizuno K 1999 and Matsuzaki F et al. 1988), suggesting that LIMK-1 could phosphorylate cofilin in the nucleus. Definitive roles for cofilin in the nucleus have yet to be elucidated, but it has been predicted to facilitate nuclear actin depolymerization, as it does in the cytoplasm.

In this study, we exposed vascular ECs to 15 dynes/cm² FSS to determine the role of cofilin in FSS-induced actin realignment, further our understanding of the role of stress kinases in this process, and assess the effect of FSS-induced actin realignment on EC barrier integrity. The results indicate that FSS induces accumulation of p-cofilin in the nucleus, likely phosphorylated by pLIMK1/2, whose activity in the nucleus is also responsive to FSS. Our results indicate that proper FSS-induced regulation of cofilin and actin are essential for FSS-induced realignment and barrier maintenance and enhancement. This work has been published in its entirety as *J. Cell. Biochem.* 114: 782–795, 2013.

3.2: Methods

3.2.1: Cell Culture

BAOECs were cultured onto 30 mm diameter, 0.17 mm thick glass cover slips coated with 30 µg/ml bovine collagen type I (BD, San Jose, CA) in phosphate-buffered saline, placed in six-well culture plates, and grown for approximately 18 hours until they formed a confluent monolayer. BAOECs were incubated for 1 hr in shear media (MEM containing HEPES (Sigma-Aldrich, St. Louis, MO), supplemented with 0.5% heat-inactivated FBS (Biowest, Miami, FL or Invitrogen, Grand Island, NY)) prior to shear exposure to maintain pH and to minimize bubble formation. The cover slips were assembled into a modified POC-mini-plate flow chamber (Yalcin HC, Perry SF, and Ghadiali SN 2007) for exposure to FSS conditions. Typically, BAOECs between passages 5 and 20 were used for these experiments.

3.2.2: JNK and p38 Inhibitor Treatments

JNK activity was inhibited using SP600125 (Calbiochem-EMD Millipore Chemicals, Billerica, MA), a competitive inhibitor for JNK (Bogoyevitch MA et al. 2004). p38 activity was inhibited using SB203580 (Calbiochem) which binds to the ATP-binding pocket inhibiting its catalytic activity, but not p38 phosphorylation (Kumar S et al., 1999). BAOECs were cultured as described above and were then incubated with 10µM of either the JNK or the p38 inhibitor in shear media for 1 hour prior to FSS exposure. FSS exposure was carried out as described below.

3.2.3: FSS Experiments

A POC mini chamber from Hemogenix (Colorado Springs, CO) was modified by adding a gasket with a rectangular flow channel to create an adjustable-height parallel-plate flow chamber as previously described (Yalcin HC, Perry SF, and Ghadiali SN 2007). FSS was calculated using the following equation: $\tau_w = \frac{6\mu Q}{WH^2}$ where τ_w is the wall shear stress, μ is the viscosity (0.007 dynes/cm² at 37 °C), Q is the flow speed, and W and H are the width and height of the gasket, respectively. BAOECs were exposed to 15 dynes/cm² shear stress (τ_w) according to the following parameters: W = 1 cm, H = 0.01 cm and Q = 2.14 ml/min. A constant flow of shear media was supplied to the POC mini parallel-plate flow chamber using a REGLO Digital continuous flow pump from ISMATEC International (IDEX Health & Science, Wertheim-Mondfeld, Germany). The FSS experiments were carried out at 37 °C.

3.2.4: Immunofluorescence Staining

Primary antibodies against p-Cofilin (serine-3), pLIMK1/2 (threonine-508/505), VE-cadherin, β -catenin (Santa Cruz Biotechnology, Santa Cruz, CA), total Cofilin (Santa Cruz Biotechnology and Cell Signaling, Boston, MA), pLIMK (serine-323), or pSSH (serine-978) (ECM Biosciences, Versailles, KY) were used as described in Chapter 2. Sample preparation for immunofluorescence staining is described in the Chapter 2.

In experiments in which actin stress fibers were detected, TRITC-phalloidin (Sigma-Aldrich, St. Louis, MO) was used. For these samples, the cells were fixed with 2.0% formaldehyde (Sigma-Aldrich) and permeabilized with 0.2% Triton-X-100 (Sigma-Aldrich). Cover slips were washed with PBS and incubated with TRITC-phalloidin at the

supplier's recommended dilution overnight at 4°C. Following incubation, cover slips were mounted as described in Chapter 2.

3.2.5: Cofilin Mutant Transfection Protocol

A constitutively active, phosphorylation defective cofilin (serine-3-alanine – S3A) mutant construct and a constitutively inactive, phosphomimic cofilin (serine-3-aspartic acid – S3D) mutant were used (Mutants provided by Theo Rein, Max Planck Institute of Psychiatry, München, Germany) (Rüegg J et al. 2004). BAOECs were electroporated with 20 µg/ml of one cofilin construct and GFP-vinculin (GFP-vinc - provided by Kenneth Yamada, National Institute of Dental and Craniofacial Research, Bethesda, MD) as a fluorescent control using the Bio-Rad Gene Pulser X-Cell System (Hercules, CA) and the manufacturer's recommended protocol modified to achieve a confluent monolayer of BAOECs. Briefly, 100 mm confluent plates of cells were trypsinized, rinsed with PBS, suspended in HEPES-buffered saline (HeBS), electroporated, and re-plated. The BAOECs were electroporated with a single 15.0 ms pulse of 160 V. Once confluent, the cells were split onto glass cover slips as described above, grown to confluency (approximately 18 hr), and exposed to FSS as described above. GFP-vinc is readily taken up and expressed by BAOECs, but in our experiments did not associate appreciably with focal adhesions in the time between seeding and FSS experiments. Transfection efficiencies close to 100% were consistently obtained based on GFP-vinc transfection.

3.2.6: SDS-PAGE and Western Blotting

Confluent BAOECs expressing GFP-vinc, S3A cofilin, or S3D cofilin were harvested and a Western Blot was performed as described in Chapter 2, with antibodies

for p-cofilin or total-cofilin and secondary antibodies conjugated to biotin (Jackson ImmunoResearch). Blots were developed using ExtraAvidin™ alkaline phosphatase system.

3.2.7: Confocal Microscopy Image Analysis

Confocal microscopy performed as described in Chapter 2. ImageJ software was used to determine the integrated fluorescence density of the nucleus and cytoplasm of 10 to 15 cells per replicate. A single replicate consisted of a static, 15 min, 30 min, and in some cases a 60 min time point. Given that gain intensity differs between replicates, a normalization protocol was developed to allow for comparison across replicates with regard to a specific protein. Within a replicate, the changes in integrated fluorescence density values were determined relative to the mean integrated fluorescence density of the static (and no inhibitor in some cases) time point. Cell values for each time point within a replicate were averaged, yielding a single mean for each time point within the replicate. These time point mean values were then averaged across replicates and a statistical analysis was performed. For image presentation, the brightness and contrast of all p-cofilin and total cofilin images were increased by a value of 10 in the Zeiss software after analysis to enhance visual clarity. All images are orientated with the direction of FSS from the bottom to the top of the page.

3.3: Results

3.3.1: FSS-induced changes in cofilin phosphorylation

To address the question of cofilin involvement in early actin realignment, FSS-induced changes in cofilin activity were tracked by fluorescently labeling p-cofilin (serine-3) in confluent BAOECs exposed to 15 dynes/cm² FSS for 15 and 30 min. The intensity and spatial distribution of p-cofilin were different depending on the duration of FSS exposure (Figure 3.3). Under static conditions, p-cofilin was distributed throughout the cytoplasm and the nucleus, with nuclear staining being more intense, signifying a slightly higher concentration of cofilin phosphorylation (inactive) in the nucleus. Cytoplasmic p-cofilin decreased in response to FSS by 43.56% at 15 min (n=9, p<0.0001) and by 31.68% at 30 min (n=5, p=0.0036) relative to static conditions. Nuclear p-cofilin increased in response to FSS by 39.00% at 15 min (n=9, p=0.0011) and by 28.00% at 30 min (n=4, p=0.0253) relative to static conditions, suggesting that FSS may induce cofilin phosphorylation (inactivation) in the nucleus. By 60 min, p-cofilin had returned closer to control levels and differences were no longer significant. These results indicate that cofilin is responsive to FSS as illustrated by FSS-dependent changes in p-cofilin intensity and spatial distribution. Similar experiments to evaluate total cofilin with two different cofilin antibodies showed no FSS-induced differences relative to static conditions (Figure 3.3), indicating that cofilin is phosphorylated and inactivated in a particular location rather than FSS-inducing significant changes in p-cofilin movement or protein degradation. Secondary antibody only controls for both p-cofilin and total cofilin indicate that non-specific detection does not account for the staining patterns seen in both

cases (data not shown). Similar results for p-cofilin and total-cofilin were also obtained with formaldehyde and Triton-X-100 fixed and permeabilized cells (data not shown). Because cofilin staining patterns of other cell types reported in the literature are different than what we observed in confluent endothelial cells, cofilin localization in sub-confluent BAOECs was also determined. Total cofilin localization in sub-confluent BAOECs was primarily cytoplasmic with little nuclear staining. Cytoplasmic total cofilin in sub-confluent BAOECs was slightly elevated compared to confluent BAOECs (data not shown). The staining pattern for p-cofilin in sub-confluent cells largely resembled p-cofilin staining in confluent endothelial cells (data not shown). These results suggest that confluent endothelial layers have different cofilin distributions than sub-confluent cells of many types.

3.3.2: Cofilin activity is required for FSS-induced actin realignment

In order to determine whether cofilin activity was required for FSS-induced actin realignment, two cofilin mutants were employed (Figure 3.4A). GFP-vinc was used as a transfection control and had no effect on FSS-induced actin realignment in the direction of FSS (Figure 3.4A, top panel). BAOECs expressing the phosphorylation defective, constitutively active, serine-3-alanine (S3A) cofilin mutant formed atypical cortical actin bands at 30 min, but failed to start elongating in the direction of FSS at 60 min (Figure 3.4A, middle panel). BAOECs expressing the phospho-mimic, constitutively inactive, serine-3-aspartic acid (S3D) cofilin mutant failed to form cortical actin bands at 30 min and did not start elongating in the direction of FSS at 60 min (Figure 3.4A, bottom panel). BAOECs expressing either of the mutants have disorganized actin networks prior

to the onset of FSS which persist through FSS, with the S3D mutant resulting in highly atypical actin networks (Figure 3.4A). Both S3A and S3D-expressing BAOECs had increased stress fibers relative to GFP-vinc expressing BAOECs, with BAOECs expressing S3D cofilin exhibiting the highest amount of stress fibers (Figure 3.4A). Western blots to detect p-cofilin (Figure 3.4B) and total cofilin (Figure 3.4C) in BAOECs expressing S3A and S3D cofilin show similar cofilin levels in BAOECs expressing the mutants as compared to GFP-vinc only cells. As shown in Figure 3.4B, specific p-cofilin bands were detected around 20.3 kD corresponding to the approximate molecular weight of cofilin, and around 27.9 kD corresponding to the approximate molecular weight of cofilin plus one ubiquitin. A large specific p-cofilin band around 12.5 kD was also detected, indicative of cofilin degradation (Figure 3.4B). Consistent with the total cofilin immunofluorescence data, total cofilin western blotting yielded very faint banding patterns similar to those detected in the p-cofilin blot (Figure 3.4C). Control cells and cells expressing either cofilin mutant exhibit specific banding patterns consistent with up to four ubiquitin chains indicative of increased targeting for protein degradation in cofilin mutant transfected BAOECs (data not shown). Staining with a different total cofilin antibody resulted in darker staining of the 12.5 kD bands, but not darker staining of the intact or high molecular weight specific bands. Taken together, the results indicate that proper cofilin regulation is necessary for FSS-induced actin realignment and that cofilin is significantly degraded in confluent BAOECs.

3.3.3: JNK and p38 involvement in FSS-induced cofilin phosphorylation

It has previously been reported that chemically inhibiting JNK with SP600125 and p38 with SB203580 blocked FSS-induced actin realignment in the direction of FSS (Mengistu M et al. 2011, Azuma N et al. 2001, Mengistu M, Slee JB, and Lowe-Krentz LJ 2012). Under static and FSS conditions, the roles of JNK and p38 in modulating cofilin phosphorylation were determined (Figure 3.5). Pretreatment of BAOECs with SP600125 prior to FSS exposure resulted in significantly decreased cytoplasmic and nuclear p-cofilin. Cytoplasmic p-cofilin was decreased by 42.57% (n=4, p=0.0004) and nuclear p-cofilin was decreased by 45.00% (n=4, p=0.0012) relative to uninhibited BAOECs at static conditions (Figure 3.4, middle panel). Upon FSS, SP600125-treated BAOECs exhibited a 50.36% decrease in nuclear p-cofilin at 15 min (n=3, p=0.0264) and a non-significant nuclear p-cofilin decrease of 40.63% (n=3, p=0.0745) at 30 min (Figure 3.5, middle panel) relative to uninhibited BAOECs exposed to FSS for the same duration. BAOECs treated with SP600125 and SB203580 vehicle did not differ from untreated cells at static conditions (data not shown). Pretreatment of BAOECs with SB203580 prior to FSS exposure resulted in significantly decreased p-cofilin in the cytoplasm and the nucleus. Cytoplasmic p-cofilin decreased 38.61% (n=5, p=0.0009) and nuclear p-cofilin decreased 30.00% (n=5, p=0.0213) relative to uninhibited BAOECs (Figure 3.5, bottom panel). p-cofilin levels in SB203580 pretreated cells were not significantly different from untreated cells after 15 and 30 min of FSS (Figure 3.5, bottom panel). Continual exposure of BAOECs to SP600125 during FSS did not differ from pre-treatment prior to FSS exposure (data not shown). Similar experiments investigating the affect of SP600125 on

total cofilin localization showed no difference from untreated cells at the same time points (data not shown). Together these results imply that JNK and to a lesser extent p38 are involved in modulating cofilin activity in BAOECs before and during FSS.

3.3.4: FSS-induced increased LIMK phosphorylation

Given that the majority of cofilin literature indicates that only dephosphorylated cofilin is capable of nuclear import under various cellular stressors (i.e. Pendleton A et al. 2003 and Iida K, Matsumoto S, and Yahara I 1992), it is unlikely that p-cofilin is able to translocate to the nucleus. Therefore the major cofilin kinases, LIMK1/2, were analyzed for their roles in FSS-induced phosphorylation of cofilin in the nucleus. Under static conditions, pLIMK1/2 (threonine-508/505 – active) was distributed throughout the cytoplasm and the nucleus, with nuclear staining being slightly more intense (Figure 3.6A). Cytoplasmic pLIMK1/2 increased 46.00% (n=5, p=0.0003) at 15 min and 54.00% (n=5, p=0.0348) at 30 min of FSS relative to static conditions. Nuclear pLIMK1/2 increased 22.00% (n=5, p=0.0407) at 15 min and 47.00% (n=5, p=0.0338) at 30 min of FSS relative to static conditions. SP600125 was used to inhibit JNK and determine the role of JNK in mediating the effects on LIMK1/2 phosphorylation. Cells treated with SP600125 showed no significant differences in pLIMK1/2 relative to cells not treated with inhibitor at the same time point, suggesting that JNK is not upstream of pLIMK1/2 (Thr-508/505) (Figure 3.6A). These results indicate that pLIMK1/2 (Thr-508/505) is FSS responsive, providing a potential mechanism for the FSS-induced increase of p-cofilin in the nucleus, but this process does not appear to be mediated by JNK.

A second phosphorylation site on LIMK1L (serine-323), shown to be a p38-mediated phosphorylation site (Kobayashi M et al. 2006), was also probed for FSS-induced activity changes. Under static conditions, pLIMK1L exhibited cytoplasmic and nuclear distribution (Figure 3.6B). Upon exposure to 15 dynes/cm² FSS for 15 and 30 min, there were no apparent changes in pLIMK1L activity and spatial distribution (Figure 3.6B), suggesting that this phosphorylated form of LIMK1L is not responsive to FSS. These results, taken together with the p38 inhibitor results, indicate that p38 is likely not a major player in FSS-induced cofilin changes. Together with the pLIMK1/2 results, these results imply that only the conserved Thr-508/205 phosphorylation sites on LIMK1/2 are responsive to FSS.

3.3.5: Slingshot (serine-978) phosphorylation is not FSS-dependent

Because the changes seen in pLIMK1/2 localization cannot completely explain the changes in p-cofilin, FSS-induced localization changes in the major cofilin phosphatase, slingshot, were determined using antibodies specific for phosphorylation at serine-978 (pSSH), an established inhibitory phosphorylation site (Soosairajah J et al. 2005). Prior to FSS exposure, pSSH is distributed fairly evenly throughout the nucleus and cytoplasm. Upon exposure to 15 dynes/cm² FSS for 15 and 30 min, pSSH intensity did not significantly change in the nucleus or the cytoplasm, suggesting that slingshot activity is not responsive to FSS. In addition, when JNK was inhibited with SP600125 or p38 with SB203580, no significant differences were seen relative to the same time point without corresponding inhibitor (Figure 3.7A and B). In some cases, independent of FSS exposure or inhibitor treatment, a small subset of pSSH was localized to puncta along the

cell membrane. Together these results indicate that slingshot phosphorylation at serine-978 is not responsive to FSS and that JNK and/or p38 is not involved in phosphorylating and inactivating slingshot under these conditions.

3.3.6: FSS-Induced VE-Cadherin and β -Catenin Localization at Cell-Cell Junctions

It has previously been shown that FSS decreases endothelial barrier permeability and strengthens the endothelial barrier (DePaola N et al. 2001, Seebach J et al. 2000). Therefore, we sought to determine the effects of actin realignment on barrier integrity by determining VE-cadherin, and β -catenin localization using the cofilin mutants and stress kinase inhibitors. Under static conditions, VE-cadherin staining was localized primarily to cell-cell contacts (Figure 3.6a, top panel – BAOECs expressing GFP-vinc as a transfection control). Upon exposure to FSS, VE-cadherin staining became more regular at cell-cell contacts with fewer small gaps or breaks in the staining (Figure 3.8A, top panel), indicating an increase in apparent barrier integrity. This FSS-induced barrier tightening was absent from BAOECs expressing either S3A (Figure 3.8A, middle panel) or S3D (Figure 3.8A, bottom panel) cofilin mutants as illustrated by large gaps (Figure 3.8A, arrowheads) or small breaks (Figure 3.8A, arrows) in VE-cadherin staining at cell-cell contacts. The gaps present in barrier staining were noticeably larger in BAOECs expressing either cofilin mutant compared to GFP-Vinc. Similar results were obtained when cells were stained for β -catenin (Figure 3.8B). Taken together, these results imply that proper cofilin activity and actin alignment is required for enhancing cell-cell junctions during FSS.

In similar experiments, BAOECs were treated with SP600125 (JNK inhibitor) or SB203580 (p38 inhibitor), exposed to 15 dynes/cm² FSS, and VE-cadherin was fluorescently stained. Again, under control conditions, VE-cadherin was localized to cell-cell contacts and apparent barrier integrity increased after FSS exposure (Figure 3.9A, top panel). BAOECs treated with either SP600125 or SB203580 failed to exhibit the FSS-induced endothelial barrier tightening seen in the control experiments (Figure 3.9A, bottom panels), as evidenced by large gaps (Figure 3.9A, arrowheads) or small breaks (Figure 3.9A, arrows) in VE-cadherin staining. The gaps present in barrier staining were noticeably larger in BAOECs treated with either inhibitor compared to uninhibited cells. Similar results were obtained when stained for β -catenin (Figure 3.9B). BAOECs treated with SP600125 and SB203580 vehicle did not differ from untreated cells at static conditions (data not shown). Together, these results suggest that JNK and p38 are required to enhance endothelial barrier integrity during FSS.

3.5: Discussion

To my knowledge, this is the first report documenting that elevated FSS causes a significant decrease in active cofilin in the nucleus and an increase in active cofilin in the cytoplasm without affecting total cofilin levels in either compartment. The lack of change in total cofilin indicates that FSS likely does not cause expression changes or alter protein degradation during FSS exposure up to 30 min, but rather induces phosphorylation (activity) changes. The increase in active cofilin in the cytoplasm would allow for increased actin polymerization needed for cortical actin band formation and realignment

of stress fibers in the direction of FSS. The increase in p-cofilin in the nucleus may be necessary to prevent cofilin from being exported back to the cytoplasm. These results help further our understanding of the atheroprotective nature of regions in the vasculature where blood flow is laminar with ECs exhibiting an elongated shape aligned in the direction of FSS (Langille BL and Adamson SL 1981, Nerem RM, Levesque MJ, and Cornhill JF 1981). My data also indicate that total cofilin in confluent BAOECs is predominantly nuclear, whereas in sub-confluent BAOECs total cofilin is predominantly cytoplasmic, suggesting that confluent cells require more nuclear cofilin than sub-confluent cells, but the reason for this difference unknown.

BAOECs expressing either S3A or S3D cofilin failed to start elongating in the direction of FSS at 60 min, and exhibited highly disorganized actin structures prior to the onset of FSS, suggesting that cofilin is essential for the process of FSS-induced actin realignment. The importance of cofilin activity regulation during FSS-induced actin realignment is illustrated in the fact that both cofilin mutants disrupt proper FSS-induced actin realignment. The increased stress fiber accumulation in the BAOECs expressing S3D cofilin coincides with what would be more p-cofilin (inactive) leading to more stress fiber accumulation. S3A-expressing BAOECs still form impaired cortical actin bands, again stressing the need for proper cofilin activity regulation during FSS. All cells (control or cofilin mutant) show high levels of cofilin degradation as assayed by western blotting, suggesting that confluent BAOECs significantly degrade cofilin. Banding consistent with ubiquitination was observed in control and cofilin mutant cells, consistent with published evidence suggesting cofilin ubiquitination and proteosomal degradation

(Yoo Y et al. 2010). Western blotting data for total cofilin was consistent with immunofluorescent imaging suggesting that cofilin is predominantly phosphorylated in BAOECs.

Having established that the cofilin activity changes are regulated in part by FSS, the roles of stress kinases in this process were determined. Inhibition of JNK with SP600125 and inhibition of p38 with SB203580 significantly reduced the levels of p-cofilin in both the nucleus and the cytoplasm prior to the onset of FSS, establishing a role for JNK and p38 in modulating cofilin phosphorylation under static conditions. After the onset of FSS, we observed no additional effects of p38 inhibition, while JNK inhibition had significant continuing effects on nuclear p-cofilin but not cytoplasmic p-cofilin or nuclear or cytoplasmic total cofilin during FSS. An established p38-mediated phosphorylation site on LIMK1L (serine-323) (Kobayashi M et al. 2006) was not FSS-responsive, suggesting that while p38 mediates FSS-induced actin remodeling, it is not due to LIMK1L phosphorylation at serine-323.

pLIMK1/2 (threonine-508/505) increased in the nucleus in response to 15 dynes/cm² FSS, ultimately leading to cofilin phosphorylation in the nucleus. Evidence from the literature supports the notion that both LIMK1 and LIMK2 possess a NLS and are capable of nuclear import and export (Yang N and Mizuno K 1999, Goyal P et al. 2005). These results suggest that cofilin can be phosphorylated in the nucleus, likely by pLIMK1/2. Despite the responsiveness of pLIMK1/2 to FSS, no effects of inhibiting JNK were seen. Although JNK and p38 have established roles in FSS-induced actin realignment and effects on cofilin phosphorylation, it appears that neither is acting

through LIMK to facilitate these changes. The increase in cytoplasmic pLIMK1/2 in response to FSS is opposite to what we would expect given our data showing decreased cytoplasmic p-cofilin. Evidence from the literature indicates that FSS activates Rho/ROCK, leading to LIMK activation, as shown by *in vitro* cofilin phosphorylation, without distinguishing between nuclear and cytoplasmic compartments (Lin T et al., 2003).

To examine the pattern of FSS-induced decrease of p-cofilin in the cytoplasm, the responsiveness of the phosphatase slingshot to FSS was determined. Looking specifically at pSSH (serine-978), an established inhibitory phosphorylation site known to cause sequestration via 14-3-3 (Soosairajah J et al. 2005), it was noted that overall pSSH levels do not change in response to FSS. Despite no FSS-induced pSSH protein level changes, puncta were evident in numerous cells. If SSH is the phosphatase responsible for cofilin dephosphorylation during FSS, JNK or p38 modulation of SSH activity is not mediated through serine-978 phosphorylation. It is also possible that these stress kinases do not modulate SSH activity. Other phosphatases may be necessary for transducing FSS stimuli. The exact mechanism leading to decreased cytoplasmic cofilin phosphorylation remains unclear.

Having determined that common cofilin kinases and phosphatases do not appear to be controlled by JNK or p38, we suspect that inhibiting JNK and p38 does not directly alter cofilin phosphorylation. Rather the effects of JNK and p38 on changes in cofilin phosphorylation may be due to altered cofilin accessibility instead of altered LIMK or SSH activity. Thus, the p-cofilin product would change, but not the covalent

modifications that activate/inactivate the upstream kinases and/or phosphatases. One potential pathway known to regulate cofilin which has also been linked to FSS is the Rho/ROCK pathway, which leads to LIMK activation (Lin T et al. 2003). Expression of dominant negative mutants of both Rho and ROCK disrupt FSS-induced actin realignment in BAOECs (Li S et al. 1999). Although this could explain the cofilin phosphorylation under FSS conditions, it does not appear to explain why blocking JNK or p38 decreases cofilin phosphorylation under control conditions. The cofilin regulation system is highly complex making it difficult to map out the signaling events downstream of FSS. It has been shown that SSH not only dephosphorylates (activates) cofilin, but is also capable of dephosphorylating (inactivating) LIMK, furthering the cell's ability to activate cofilin (Soosairajah J et al. 2005 and reviewed in Huang TY, DerMardirossian C, and Bokoch GM 2006). An additional layer of complexity exists in that SSH is also enhanced by F-actin binding to enhance cofilin activation (Nagata-Ohashi K et al. 2004, Soosairajah J et al. 2005, and reviewed in Huang TY, DerMardirossian C, and Bokoch GM 2006). It is possible that the effect of inhibiting JNK and p38 is decreased during FSS, because of enhanced activation of SSH due to increased F-actin induced by the FSS, accompanied by SSH-induced LIMK inactivation and cofilin activation.

Since the cofilin mutants and stress kinase inhibitors disrupt FSS-induced actin realignment, they were used to determine how FSS-induced actin realignment affects barrier integrity. Cells expressing either S3A or S3D show numerous gaps and breaks in VE-cadherin or β -catenin staining at cell-cell junctions which were noticeably larger than GFP-vinc only cells, as do cells treated with stress kinase inhibitors. These results

suggest that proper cofilin regulation and actin realignment are required to maintain and enhance cell-cell junctions during FSS, which is important for maintaining vascular barrier integrity. These results agree with published data showing that FSS decreases endothelial barrier permeability, preventing the transport of unwanted molecules across the endothelial layer (DePaola N et al. 2001, Seebach J et al. 2000).

Although we were unable to determine the link between cofilin and JNK or p38, it is clear that proper cofilin regulation, JNK activity, and p38 activity are required to maintain and enhance endothelial cell junctions. It is reasonable to hypothesize that the central link is the actin cytoskeleton. Improper realignment of the actin cytoskeleton during FSS caused either by mutated cofilin or stress kinase inhibitors results in decreased barrier integrity. Actin associates with adherens junctions via β -catenin, which associates with the cytoplasmic domain of VE-cadherin (Tharakan B et al. 2012). Therefore disrupting actin realignment during FSS has severe physiological outcomes in preventing FSS-induced barrier integrity, which would allow improper transport across the endothelial layer. These results emphasize the importance of FSS-induced actin realignment and maintenance of barrier integrity. Further support for the actin cytoskeleton in maintaining endothelial cell-cell junctions, was reported by Furman C et al. (2007), where they showed that enabled/vasodilator-stimulated phosphoprotein (Ena/VASP) protein activity is required for normal stress fiber accumulation and cell-cell junction integrity (Furman C et al. 2007).

In summary, this work documents that FSS mediates changes in cofilin phosphorylation. FSS-induced increased p-cofilin in the nucleus is likely due to the need

for actin function in the nucleus for elongation of the nucleus in the direction of FSS. pLIMK1/2 also increased in the nucleus after FSS exposure suggesting cofilin phosphorylation in the nucleus. Phosphorylation in the nucleus likely blocks export and could be a mechanism to retain cofilin in the nucleus. It is also clear that JNK activity induces cofilin phosphorylation in the nucleus, but this affect does not seem to be due to phosphorylation of LIMK1/2 or SSH, which did not change with SP600125 treatment. This suggests that JNK in some way enhances cofilin phosphorylation, but not through directly altering LIMK or SSH activity. Cofilin mutants were used to mimic specific states of cofilin phosphorylation, resulting in decreased correct actin realignment, regardless of whether there was a high level of inactive or of active cofilin. The cofilin mutants and stress kinase inhibitors decrease barrier integrity, illustrating the importance of correct actin realignment in endothelial barrier integrity during FSS.

It is becoming clearer that endothelial cells of an artery are constantly exposed to mechanical signals from the shear stress of blood flow. As our understanding of this process continues to expand, a role for shear stress in atherosclerosis is being discovered. For reasons which are still being elucidated, elevated shear stress helps to protect against the development of atherosclerosis. Atherosclerosis, as an inflammatory disease, averts most traditional anti-inflammatory mechanisms controlling the development of arterial lesions and plaques. Elevated shear stress has been shown to be anti-inflammatory in the vasculature protecting against the development of atherosclerosis by promoting an intact endothelium. An intact endothelium has anti-inflammatory qualities preventing unwarranted inflammation, whereas “leaky” endothelium is primed for inflammation

secreting pro-inflammatory molecules (4-8). The work done within this chapter demonstrates that through the action of cofilin, FSS-mediated actin realignment is required for maintaining an intact endothelium which is necessary to keep the vasculature in an anti-inflammatory state.

3.6: Figures

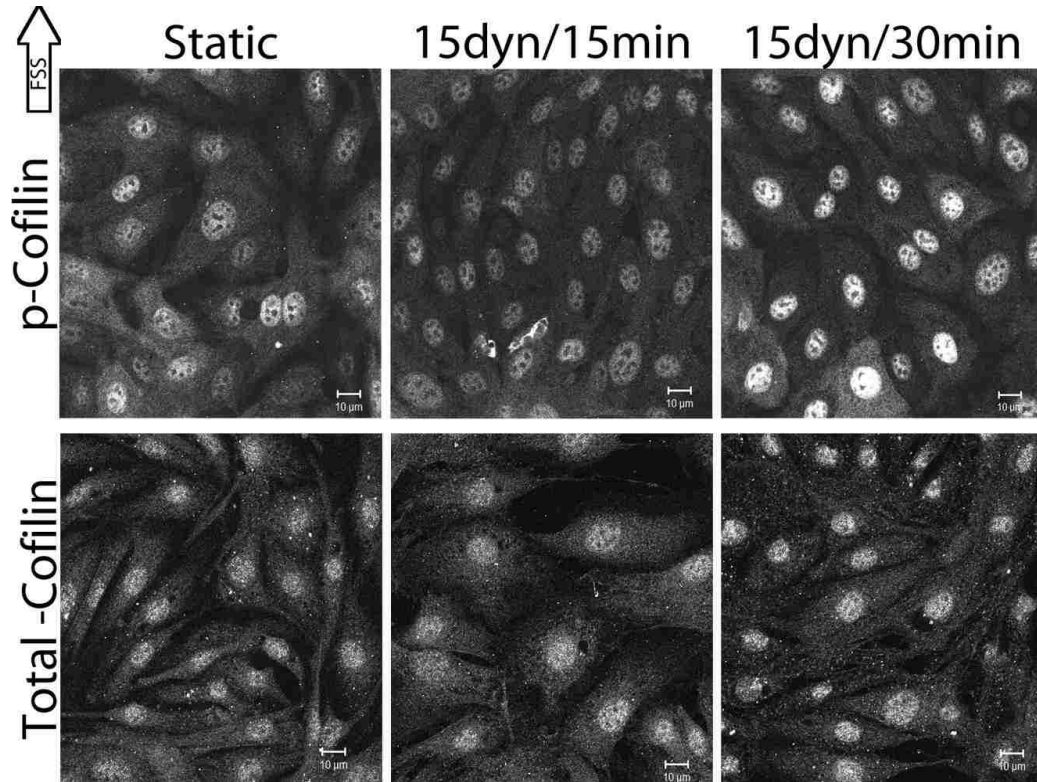


Figure 3.3: FFS-induced changes in cofilin phosphorylation

Confluent monolayers of BAOECs were exposed to 15 dynes/cm² FFS for 15 and 30min. BAOECs were labeled with antibodies against p-cofilin (top panel) or total cofilin (bottom panel; Santa Cruz Biotechnology). Gain intensity was set just below saturating levels for the static p-cofilin and total cofilin separately and those settings were used to image the remaining slides within the replicate for each protein. Image analysis was performed as described in the methods. Images shown are representative of at least three replicates. Scale bars=10 µm. (Slee JB and Lowe-Krentz LJ. 2013)

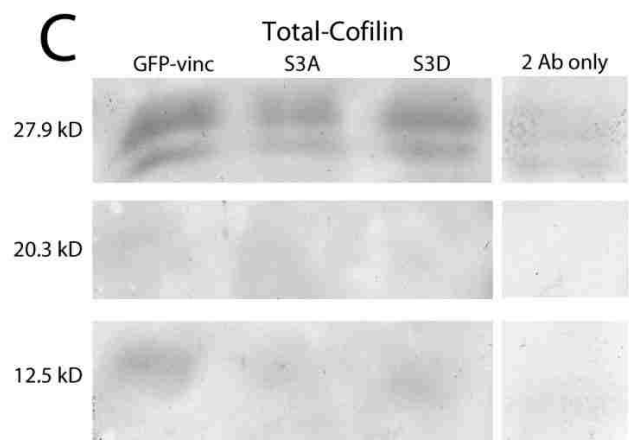
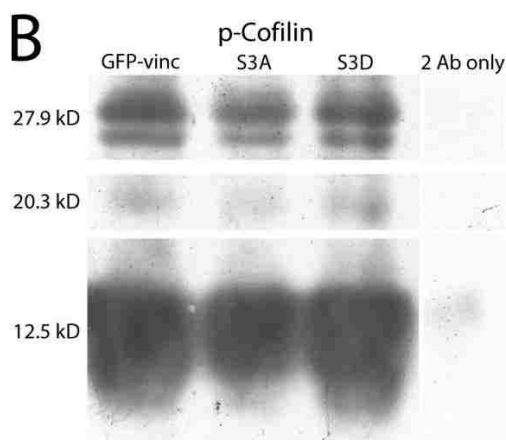
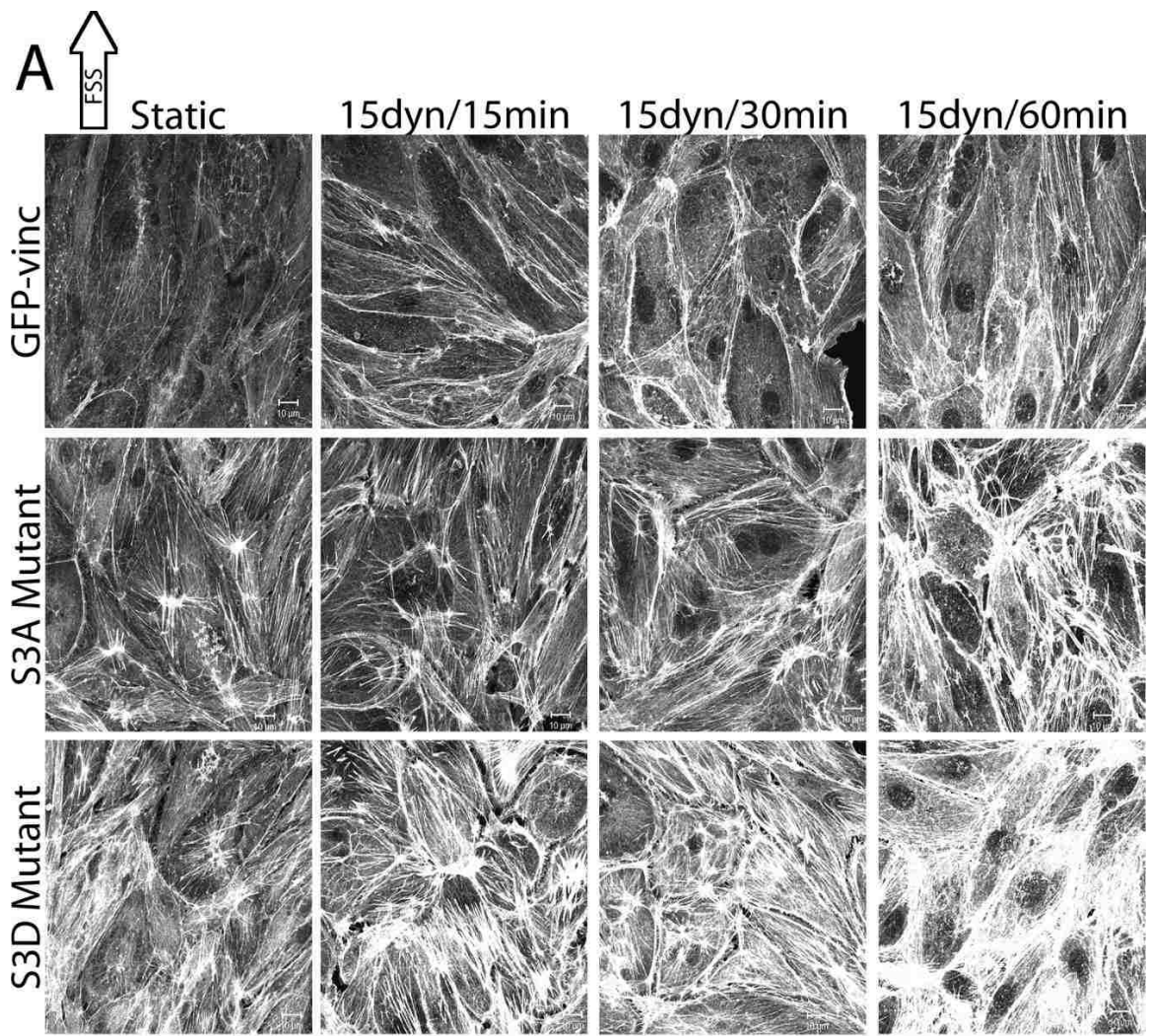


Figure 3.4: The effect of cofilin activity on FSS-induced actin realignment
BAOECs were electroporated with 20 mg/ml of either S3A or S3D cofilin constructs in combination with GFP-vinc as a fluorescent marker of transfection efficiency as described in the methods. BAOECs expressing the mutant constructs were exposed to 15 dynes/cm² FSS for 15, 30, and 60min and labeled for actin stress fibers using TRITC-phalloidin. The images shown are representative of 10 repeats. A: Top panel, BAOECs expressing GFP-vinc alone showing FSS-induced actin realignment. Middle panel, BAOECs expressing S3A cofilin showing impaired actin realignment during FSS. Bottom panel, BAOECs expressing S3D cofilin showing impaired actin realignment during FSS. Scale bars=10 mm. B,C: BAOECs were electroporated with GFP-vinc, S3A cofilin, or S3D cofilin as indicated. Whole cell lysates harvested 24–48 h post-transfection were immunoblotted with anti-p-cofilin (B) or anti-total cofilin (C) antibodies. Corresponding secondary antibody only controls (2 Ab only) were also performed for both p-cofilin (B) and total cofilin (C). Molecular weights of the bands were calculated based on Rf values created from the markers are indicated on the left. (Slee JB and Lowe-Krentz LJ. 2013)

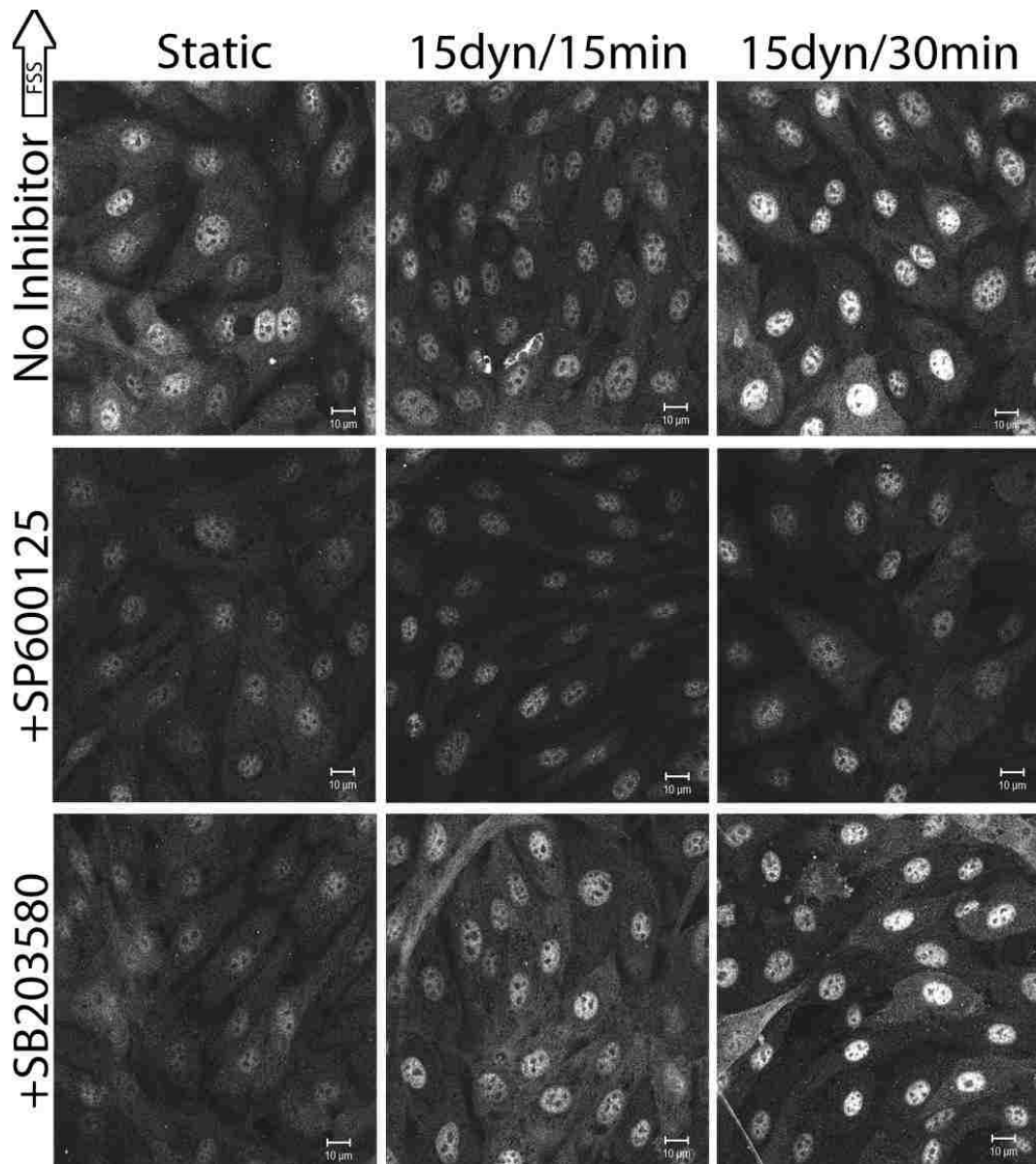


Figure 3.5: The roles of JNK and p38 in FSS-induced cofilin phosphorylation
 Confluent monolayers of BAOECs were treated with SP600125 (JNK inhibitor) or SB203580 (p38 inhibitor) for 1 h prior to FSS exposure. Following inhibitor incubation, BAOECs were exposed to 15 dynes/cm² FSS for 15 and 30 min and labeled with antibodies against p-cofilin. Image analysis was performed as described in Materials and Methods Section. The images shown are representative of at least three replicates. Top panel, uninhibited BAOECs. Middle panel, SP600125-treated BAOECs. Bottom panel, SB203580-treated BAOECs. Scale bars=10 μm. (Slee JB and Lowe-Krentz LJ. 2013)

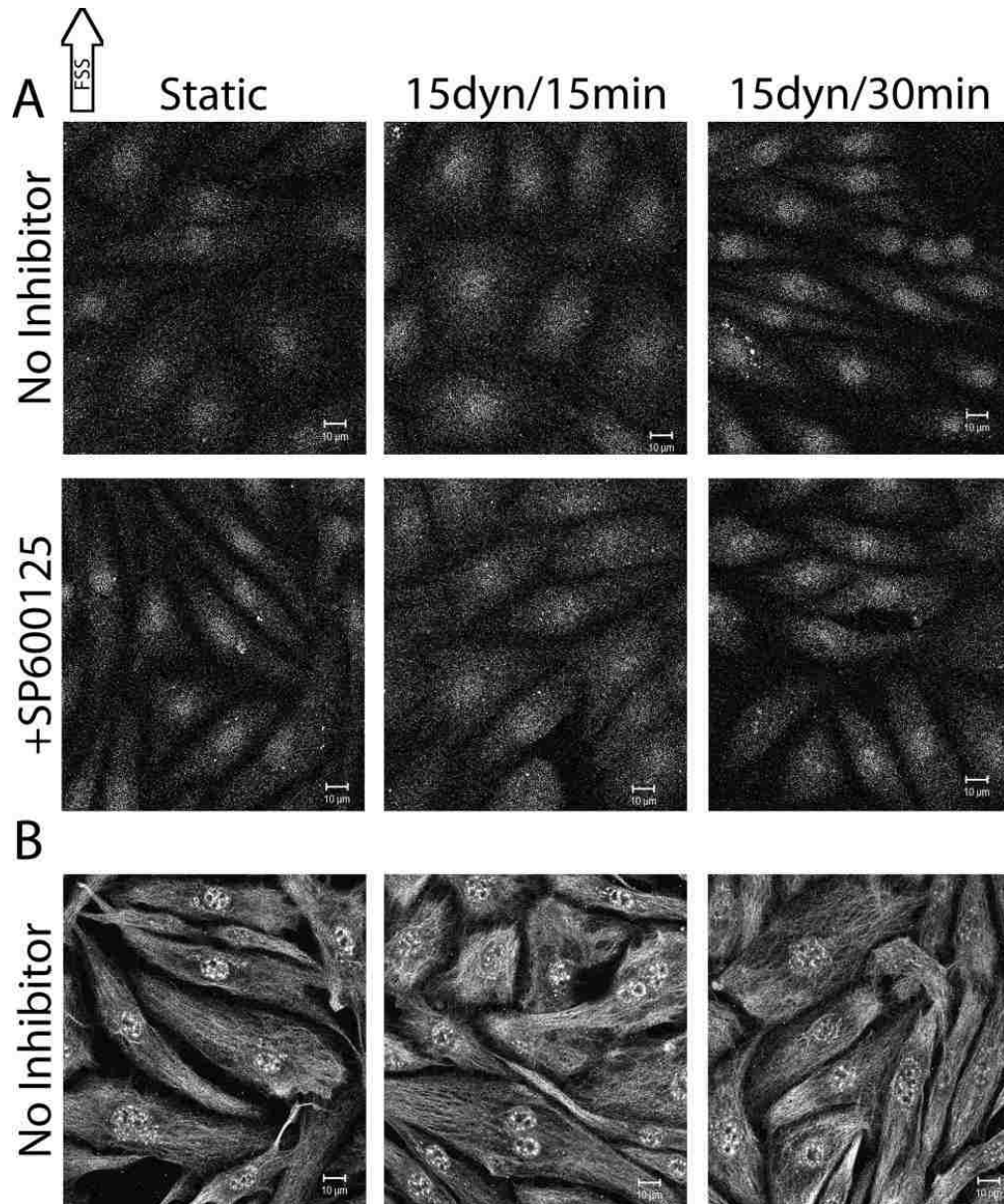


Figure 3.6: FFS-induced changes in LIMK phosphorylation

Confluent monolayers of BAOECs were exposed to 15 dynes/cm² FFS for 15 and 30 min and labeled with antibodies against pLIMK1/2 (threonine-508/505; A) or pLIMK1L (serine-323; B). Image analysis was performed as described in Materials and Methods Section. The images shown are representative of at least four replicates. A: Top panel, uninhibited BAOECs. Bottom panel, SP600125-treated BAOECs. B: Uninhibited BAOECs. Scale bars=10 μm. (Slee JB and Lowe-Krentz LJ. 2013)

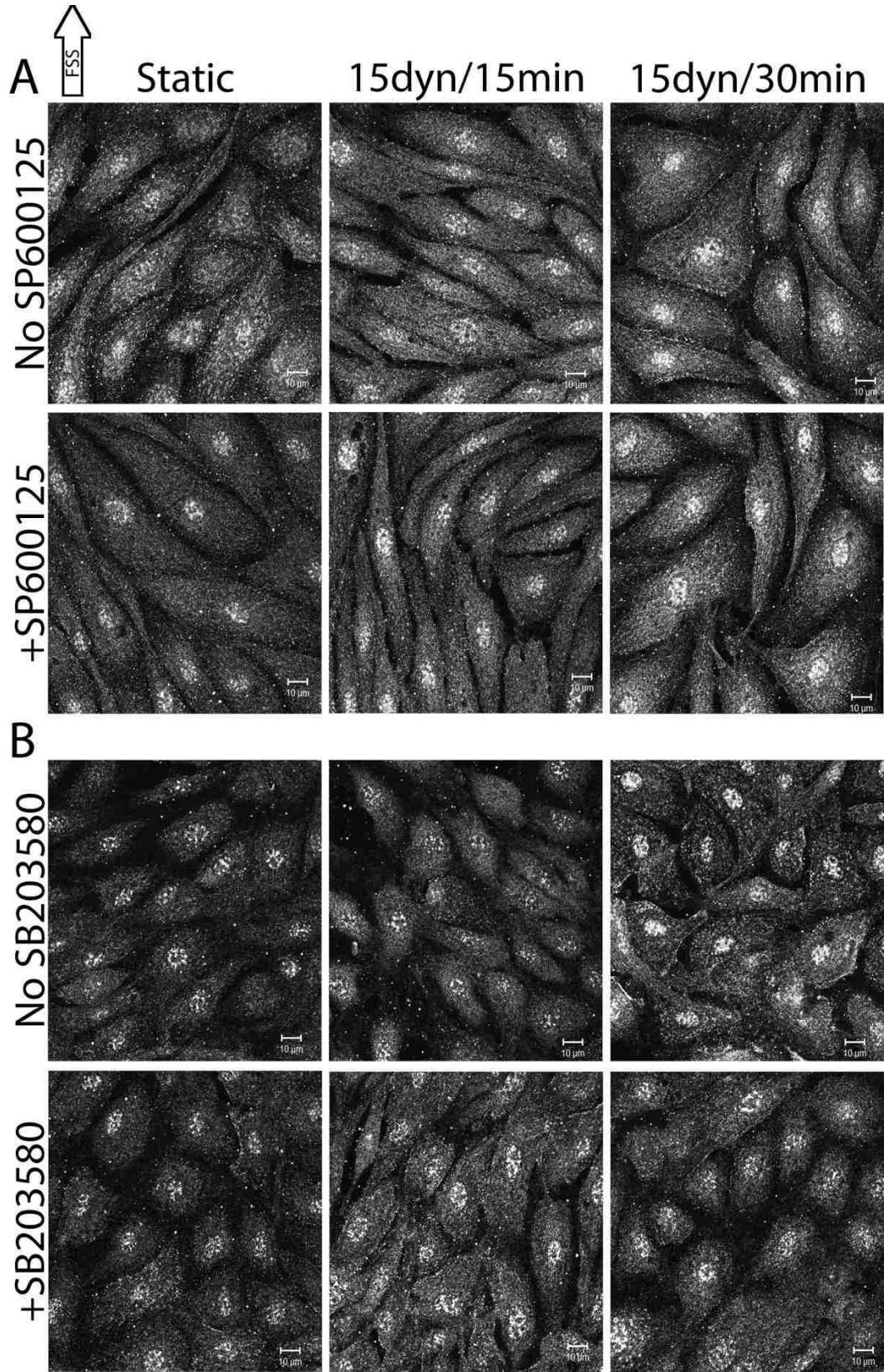


Figure 3.7: FSS-induced changes in SSH phosphorylation

Confluent monolayers of BAOECs were exposed to 15 dynes/cm² FSS for 15 and 30 min and labeled with antibodies against pSSH (serine 978). Image analysis was performed as described in Materials and Methods Section. The images shown are representative of at least three repeats. A: SP600126-treated BAOECs. B: SB203580-treated BAOECs. Scale bars=10 μ m. (Slee JB and Lowe-Krentz LJ. 2013)

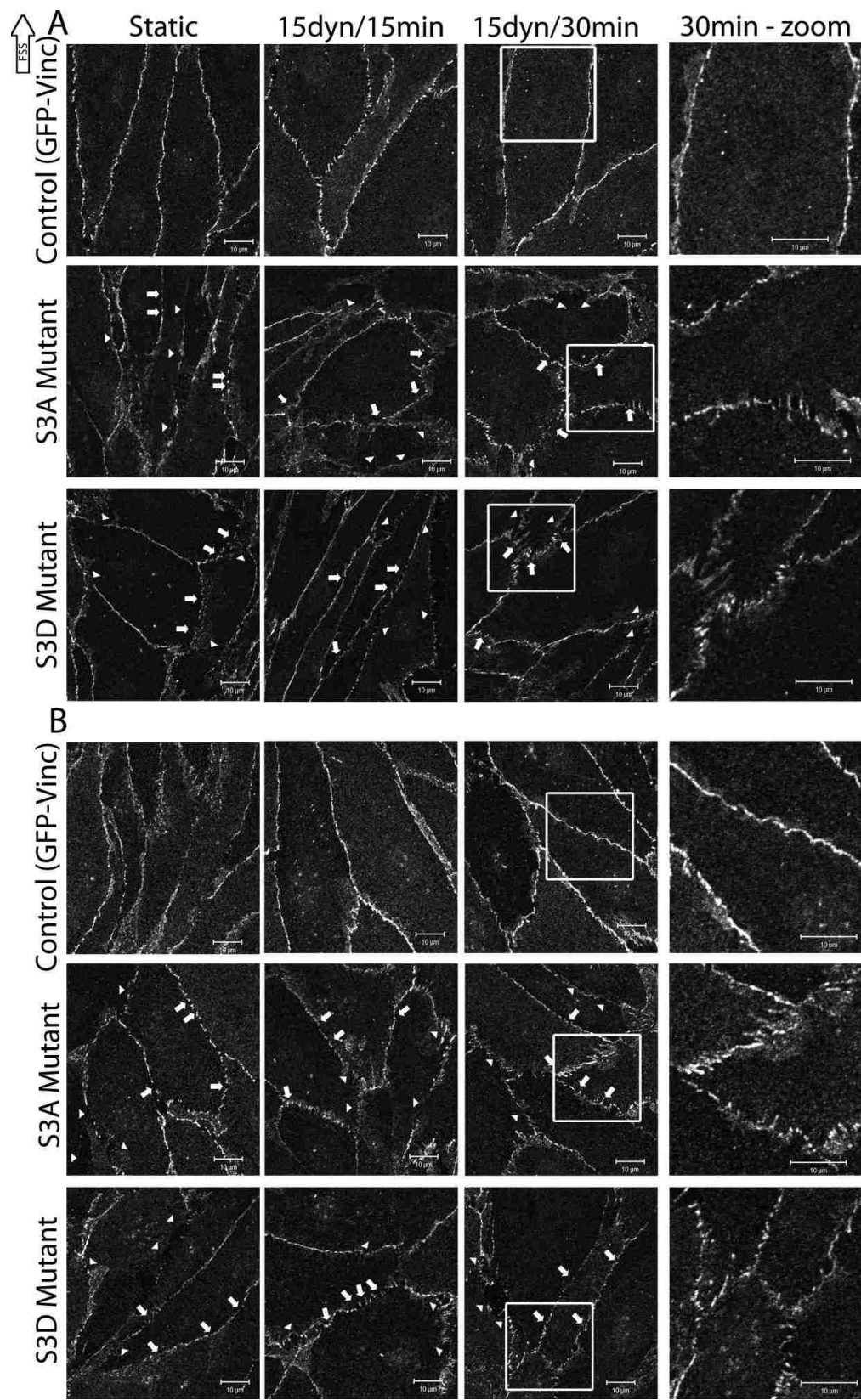


Figure 3.8: The role of cofilin in FSS-induced barrier staining
BAOECs were electroporated with 20 mg/ml of either S3A or S3D cofilin constructs in combination with GFP-vinc as a fluorescent marker of transfection efficiency as described in Materials and Methods Section. BAOECs expressing the mutant constructs were exposed to 15 dynes/cm² FSS for 15 and 30min and labeled using antibodies against VE-cadherin (A) or β -catenin (B). The images shown are representative of three repeats. In both A and B, the top panel images are expressing GFP-vinc alone, the middle panel images are BAOECs expressing S3A and GFP-Vinc, and the bottom panel images are BAOECs expressing S3D and GFP-vinc. The three left columns are magnified 2X the original. The rightmost column is magnified 4X the original and highlights the boxed area in the column immediately to the left. Arrows point to small breaks in staining. Arrowheads point to large gaps in staining. Scale bars=10 mm. (Slee JB and Lowe-Krentz LJ. 2013)

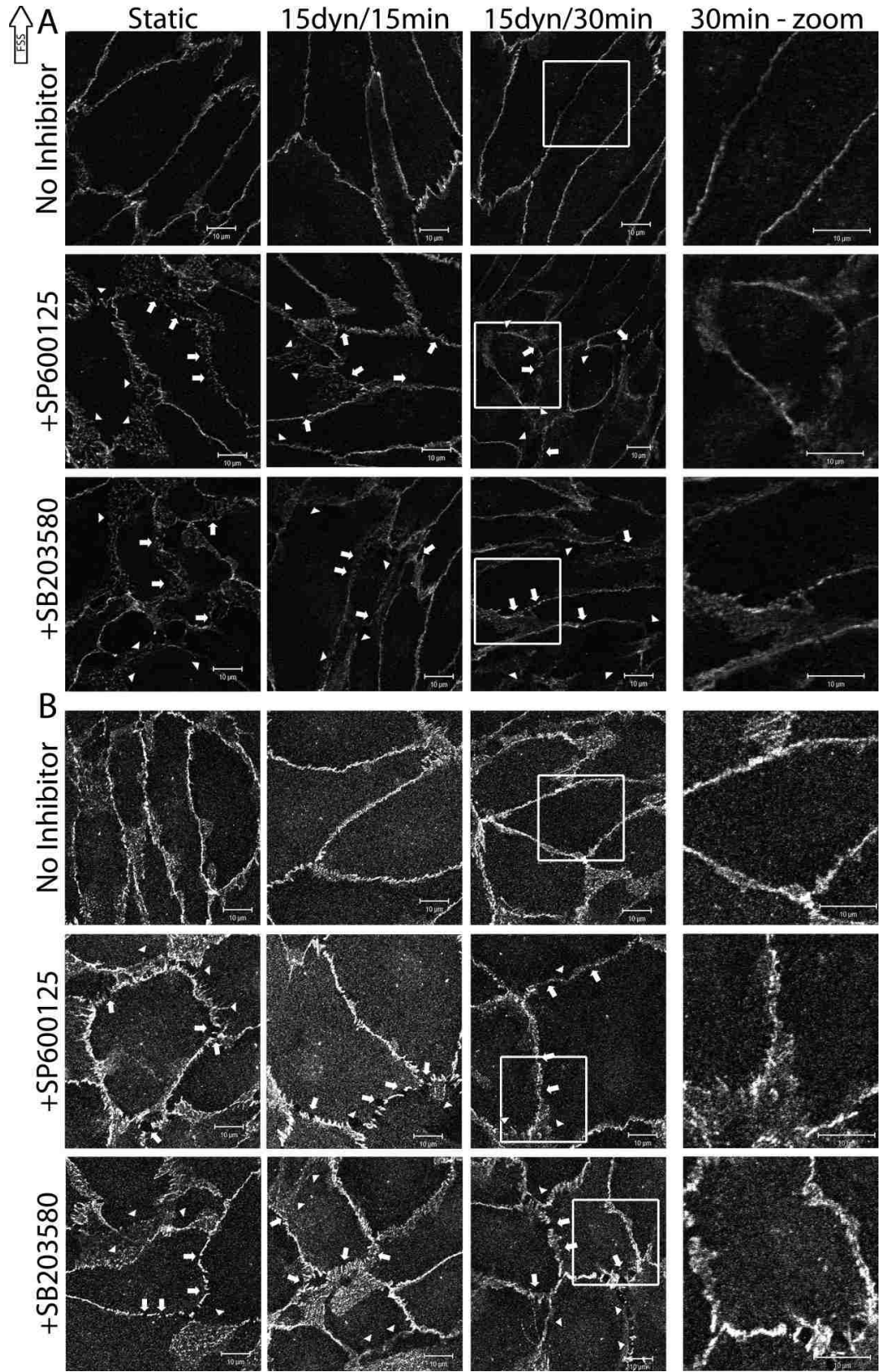


Figure 3.9: The role of JNK and p38 activity in FSS-induced barrier staining
Confluent monolayers of BAOECs were treated with SP600125 (JNK inhibitor) or SB203580 (p38 inhibitor) for 1 h prior to FSS exposure. Following inhibitor incubation, BAOECs were exposed to 15 dynes/cm² FSS for 15 and 30 min and labeled with antibodies for VE-cadherin (A) or β -catenin (B). The images shown are representative of the trends which have been identified through at least two repeats. In both A and B, the top panel images are expressing GFP-vinc alone, the middle panel images are BAOECs expressing S3A and GFP-vinc, and the bottom panel images are BAOECs expressing S3D and GFP-vinc. The three left columns are magnified 2X the original. The rightmost column is magnified 4X the original and highlights the boxed area in the column immediately to the left. Arrows point to small breaks in staining. Arrowheads point to large gaps in staining. Scale bars=10 μ m. (Slee JB and Lowe-Krentz LJ. 2013)

Chapter 4: Heparin blocks TNF-induced stress responses in vascular endothelium

4.1: Introduction

The endothelium serves an important role in maintaining the integrity of the vascular system. The endothelium of healthy vasculature is non-thromogenic and anti-inflammatory preventing coagulation and inflammation. Any type of damage to this endothelial layer causes local inflammatory and mitogenic changes in an attempt to repair the wound. These changes cause the endothelial cells to become proliferative to heal the wound in the endothelial layer (Ross R 1999). If the damage is not properly repaired continued inflammation occurs resulting in increased connective tissue, VSMC proliferation, and eventual atherosclerotic plaque development. The changes noted above in the endothelial layer also result in the cells becoming “sticky” promoting clotting and the recruitment of inflammatory mediators and immune cells (Spronk H, van der Voort D, and ten Cate H 2004).

Endothelial cells lining all blood vessels play an important role during systemic inflammation because of their position and immediate exposure to inflammatory mediators (Zhao B et al 2003). The two major inflammatory mediators (cytokines) that are elevated during systemic inflammation are Interleukin-1 β (IL-1 β) and TNF α (Zhao B et al 2003). Studies have documented that endothelial cells respond to various external stimuli, in part by altering gene expression for cytokines, adhesion molecules, pro-coagulation factors, and other proteins (Zhao B et al 2003). Therefore, the response elicited by endothelial cells to IL-1 β and TNF α treatment will likely provide necessary information that may help to explain some of the dysfunction that occurs (Zhao B et al 2003).

Stress-activated protein kinase (SAPK) enzymes are activated in response to various stressors such as cytokines and inflammatory agents. Activation of JNK occurs in response to select cytokines (TNF α and IL-1 β), various diseases, heat, UV light, hyperosmolarity (reviewed in Bogoyevitch M and Kobe B 2006). The best characterized responses to JNK activation are changes in transcription occurring as the result of JNK phosphorylation of transcription factors including *c-jun*, ATF-2, Elk-1 and heat shock factor 1 (reviewed in Bogoyevitch M and Kobe B 2006). JNK has also been shown to be important in the cytoplasm, having established roles in epithelial and endothelial cell migration and wound repair (David L et al. 2007, Shen J and DiCorleto P 2008, Volin M et al. 2010, and Zhang L et al. 2005). Some of the substrates of JNK have known links to the actin cytoskeleton, suggesting that JNK may be involved, at least in part, in the regulation of the actin. It has also been shown by members of our lab that JNK associates with the actin cytoskeleton and is important for actin remodeling in vascular endothelial cells (Hamel M et al. 2006, Mengistu M et al. 2011, and reviewed in Mengistu M, Slee JB, and Lowe-Krentz LJ 2012).

The p38 family is a second major stress kinase family important in the vasculature system. Inflammatory signals, including TNF α , result in the activation of p38 enzymes (reviewed in Cuadrado A and Nebreda A 2010). Like JNK, p38 activity is involved in TNF α , VEGF, and hypoxia-induced microfilament remodeling (Kayyali US et al. 2002, Kiemer A et al. 2002, and Liao W, Feng L, Zheng J, DB C 2010). Related to Chapter 1, shear stress activates p38 to help facilitate FSS-induced actin cytoskeletal remodeling (Azuma N et al. 2001, Wang J et al. 2005, Mengistu M et al. 2011, and reviewed in

Mengistu M, Slee JB, and Lowe-Krentz LJ 2012). p38 also has well-established transcription factor targets such as ATF (reviewed in Cuadrado A and Nebreda A 2010). The p38 enzymes also phosphorylate and activate other kinases including MAPKAP-2, MSK-1, and MNK1 (Cuadrado A and Nebreda A 2010). p38 also has indirect roles in the cytoplasm through MAPKAP-2. p38 activity results in phosphorylation of the Arp 2/3 complex protein p16-Arc (Singh S et al. 2003), HSP27 (An SS et al. 2005 and McMullen ME et al. 2005), LIMK (Côté MC et a. 2010 and Kobayashi M et al. 2006), and capZIP (Eyers CE et al. 2005). Active p38 in shear-stressed endothelial cells grown on collagen has been found in focal adhesions (Hamel M et al. 2006 and Orr AW et al. 2005) and is associated with integrins in cells grown on collagen and laminin (Wang J et al. 2005). Many of the p38 targets have the ability to modulate the actin cytoskeleton, linking stress activity to cytoskeletal changes.

Given the well established role for SAPKs in mediating vascular endothelial cell stress responses, much research has been focused on finding inhibitors of JNK and p38. Since both JNK and p38 are heavily involved in the inflammatory process, a number of well established anti-inflammatory treatments have been shown to affect the JNK and/or p38 pathways. Two of the better characterized anti-inflammatory treatments that decrease JNK activity include curcumin and aspirin (Cho J-W et al. 2005 and Jiang G et al. 2003). The same is true for the immunosuppressant FK506 which blocks both p38 and JNK activation (Kaminska B 2005). Glucocorticoids are natural inhibitors of inflammation and stress signaling, which can decrease SAPKs through the synthesis of MKP-1 (Kassel O et al. 2001 and Lasa M et al. 2002). Although effective at reducing inflammation and stress

kinase activity, glucocorticoids have many systemic effects which make them unlikely candidates for long-term treatment (Rhen T and Cidlowski J 2005). Whereas small molecule inhibitors are more specific than glucocorticoids they still target systemic SAPKs as well.

As discussed in Chapter 1, heparin exhibits anti-inflammatory properties that could be of promise for potential therapy (for review see Slee JB, Pugh R, and Lowe-Krentz 2012). Data collected in the Lowe-Krentz lab indicate that endothelial cell signaling through stress/inflammatory pathways is altered by heparin treatment. We have shown that treatment of vascular endothelial cells with heparin results in decreased p38 activation and decreased p38 target phosphorylation out to 15 min (Hamel M diss 2001 and Kanyi D diss 2006). The JNK pathway is also affected by heparin treatment. Data suggest that heparin and anti-heparin receptor antibody treatment of endothelial cells results in less JNK activation after treatment with TNF α , and c-jun transcription factor phosphorylation is also decreased (Hamel M diss 2001 and Kanyi D diss 2006). As is the case with vascular smooth muscle cells, the activation of Hsp27 is also decreased and heparin treatment of vascular endothelial cells results in MKP-1 synthesis (Hamel M diss 2001 and Kanyi D diss 2006).

The experiments in this chapter were designed to help complete the story initiated by Daniela Kanyi and Marianne Hamel. The purpose of these experiments was to elucidate a physiological endpoint for stress responses in endothelial cells. To do so, I investigated the role of heparin in attenuating TNF α -induced stress kinase activity and actin stress fiber formation. Data collected within this dissertation align well with the

previously collected data. Taken together, the collection of data document that heparin alters signal transduction to the actin cytoskeleton through JNK and p38, and further, that such heparin effects on SAPK activity are dependent on heparin binding to a cell surface receptor as shown for Erk effects in VSMCs (Savage JM et al. 2001).

4.2: Methods

4.2.1: Cell Culture

BAOECs were maintained in Cell Applications media and cultured on glass coverslips as described in Chapter 2 for immunofluorescent staining. Cells were seeded at a density that would allow them to be between 50-70% confluent to mimic “wounded” cells in the vasculature.

4.2.2: TNF α and Heparin Treatment

BAOECs were treated with 50 ng/ml TNF α for 120 min to analyze changes in actin stress fibers and for 10 min to analyze changes in stress kinase (pJNK and pp38) activity. Some cells were pretreated with 200 μ g/ml heparin 20 min prior to TNF α stimulation to determine heparin’s affect on these outcomes. Control cells were left untreated and other cells were treated with heparin for 20 min.

4.2.3: Immunofluorescence Staining

Primary antibodies against pJNK (Santa Cruz) and pp38 (Cell Signaling), were used as described in Chapter 2. Sample preparation for immunofluorescence staining is described in the Chapter 2, using 4% PFA and 0.3% Triton. AlexaFlour488®-phalloidin

was used to detect actin stress fibers and was included with secondary antibody incubation.

4.2.4: Fluorescent Microscopy

Fluorescent microscopy was performed as described in Chapter 2.

4.3: Results

As shown in Figure 4.1, 50 ng/ml TNF α causes significantly increased stress fibers and nuclear stress kinase activity in BAOECs. Control cells exhibit very few stress fibers and a 20 min heparin (200 μ g/ml) treatment seems to reduce their levels even further (Figure 4.1A). A 50 ng/ml TNF α treatment for 120 min significantly increased actin stress fiber intensity and number, which is significantly attenuated by a 20 min heparin pretreatment (Figure 4.1A). The 20 min heparin pretreatment reduces stress fiber intensity and number to a level comparable to untreated control cells (Figure 4.1A). These results suggest that heparin represses TNF α -induced stress fiber formation in vascular endothelial cells.

Shorter treatments of TNF α were necessary to identify visible changes in nuclear stress kinase activity (pJNK and pp38). As shown in Figure 4.1B, BAOECs have a basal level of nuclear stress kinase activity, which is reduced by a 20 min heparin treatment. Following a brief 10 min TNF α (50 ng/ml) treatment, both pJNK and pp38 in the nucleus are significantly increased compared to untreated control (Figure 4.1B). Nuclear p38 activity increases more than nuclear JNK activity at this treatment time of TNF α , however pJNK increases have been noted after 120 min TNF α treatment (data not

shown). As was the case for stress fiber induction, a 20 min pretreatment with heparin markedly reduces both pJNK and pp38 relative to TNF α -treated cells (Figure 4.1B). The cells treated with heparin prior to TNF α stimulation exhibit nuclear pJNK and pp38 levels comparable to control cells. These data suggest that heparin attenuates TNF α -induced nuclear stress kinase activity.

4.4: Discussion

The actin cytoskeleton reorganizes in response to extracellular conditions. TNF α -induced actin polymerization involves p38 (Kierner A et al. 2002) which is required for hypoxia-induced actin redistribution to stress fibers (Kayyali US et al. 2002). p38 and JNK are also involved in smooth muscle cell actin expression and remodeling (Tock J et al. 2003 and Wang J et al. 2005). Finally, the addition of growth factors to endothelial cells causes both cytoskeletal rearrangement and the activation of SAPK pathway constituents (Xia Y et al. 2000).

Focal adhesions link the internal cytoskeleton to the extracellular matrix. Signaling through integrins from the extracellular matrix outside causes the rearrangement of the cytoskeletal architecture (Applin AE et al. 1998). Stress-activated protein kinases have been shown to be activated in response to signaling through the focal adhesions (Oktay M et al. 1999). In endothelial cells, stress fibers align parallel to the direction of blood flow; and the ends of stress fibers become associated with focal adhesions during flow-induced reorganization (Girard PR and Nerem RM 1995). When endothelial cells are subjected to shear stress, actin fibers become realigned in a manner

which depends on p38 (Azuma N et al. 2001 and Wang J et al. 2005) and JNK (Mengistu M et al. 2011). Adhesion-induced focal adhesion kinase (FAK) activation causes the activation of JNK and p38 (Almeida E et al. 2000, Jo H et al. 1997, and Li S et al. 1997).

As discussed in Chapter 1, heparin has been shown to decrease inflammation, and research from our laboratory and others indicates that heparin causes decreases in vascular smooth muscle cell ERK activation through binding to a receptor. Our original identification of the heparin receptor was in endothelial cells, suggesting that vascular endothelium could be a target for the anti-inflammatory nature of heparin. Therefore, I examined the possibility that heparin would induce decreases in endothelial stress kinase activity and thereby alter stress kinase-based cytoskeletal rearrangements. Heparin treatment of endothelial cells did result in blocking TNF- α induced stress fiber changes (Figure 4.1A). This is consistent with heparin having anti-inflammatory effects beyond those of interfering directly with selectin-dependent cell adhesion in the vasculature. Heparin treatment also caused decreases in JNK and p38 activity at shorter TNF α treatment times (Figure 4.1B). This suggests that heparin has potential as an anti-inflammatory molecule to reverse the damage to the endothelial layer caused by excessive TNF α -induced inflammation in atherosclerotic vasculature. Combining my data with the work performed by Marianne Hamel and Daniela Kanyi showed that not only does heparin attenuate TNF α -induced stress fibers and nuclear stress kinase activity; it also has inhibitory roles on TNF α -induced c-jun transcription factor phosphorylation, Hsp27 activation, and Erk activation through the action of MKP-1. Given that heparin induces nuclear stress kinase activity changes, this presents the possibility that heparin

could also be inducing transcriptional changes. The culmination of this work will be a publication furthering our understanding of heparin as an anti-inflammatory molecule in vascular endothelium.

4.5: Figure

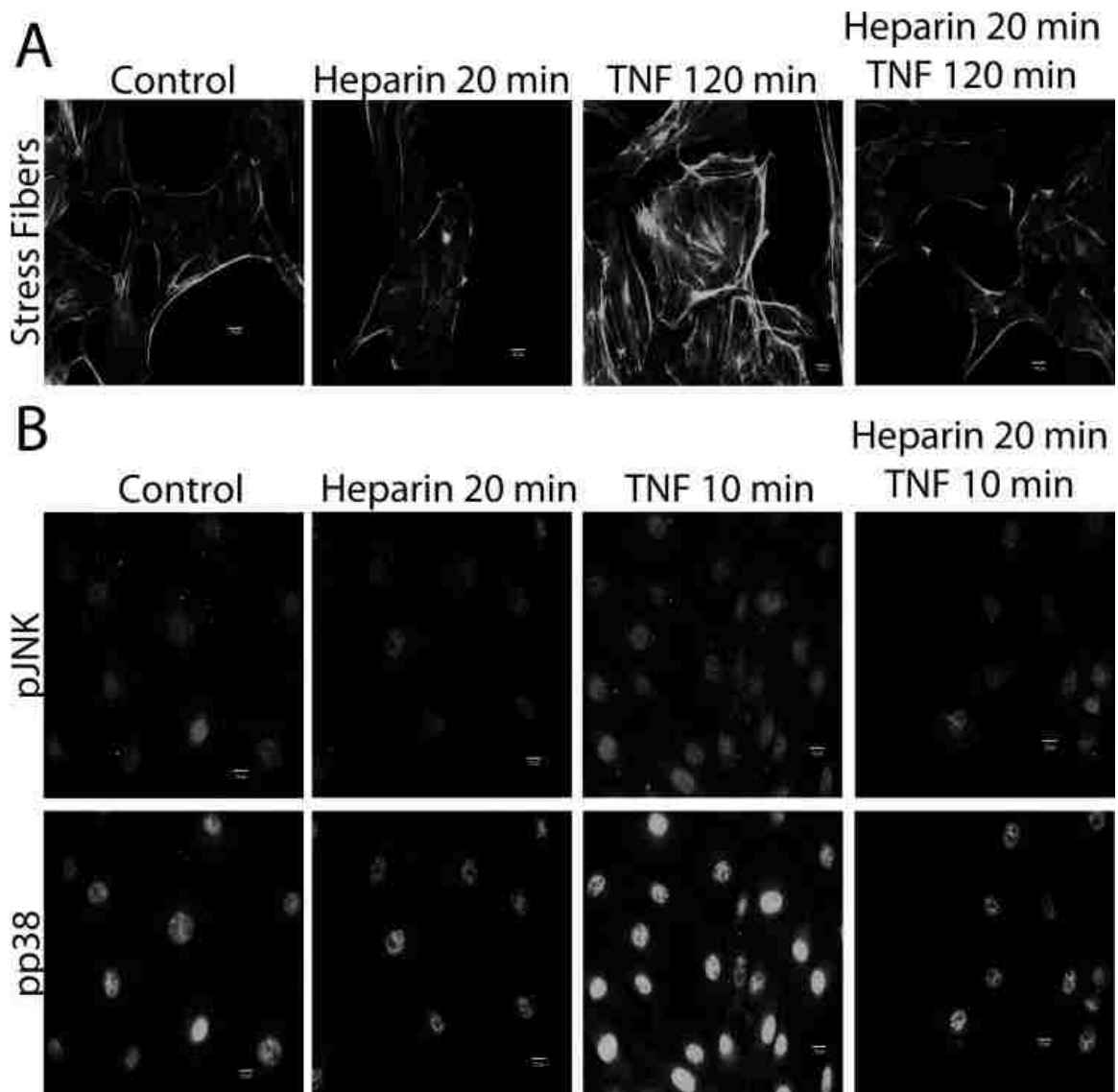


Figure 4.1: Heparin attenuates TNF α -induced stress fibers and nuclear stress kinase activity

(A) BAOECs stained for actin stress fibers with AlexaFluor $\text{\textcircled{R}}$ 488-Phalloidin. Cells were treated with 50 ng/ml TNF α for 120 min with or without a 20 min heparin pretreatment. (B) BAOECs stained for stress kinases pJNK (top panel) or pp38 (bottom panel). Cells were treated with 50 ng/ml TNF α for 10 min with or without a 20 min heparin pretreatment. For comparison, untreated control cells and cells treated with 20 min of heparin were included. Cells in both (A) and (B) were fixed with 4% PFA and permeabilized with 0.3% Triton. Images are representative of three experiments. Scale bars = 10 μ m.

Chapter 5: Identification of the heparin receptor: building the case for TMEM184A

5.1: Introduction

It has been well established that many cells including vascular cells, such as endothelial and smooth muscle, bind and internalize heparin (egs. Bârzu T et al. 1985 and Castellot JJ et al. 1985) and have well-established responses to heparin (egs. Reilly CF et al. 1989, Fasciano S et al. 2005, Vadivello PK et al. 1997, and Blaukovitch CI et al. 2010). The same is true for cells that are not known to be heparin sensitive or possess known heparin signaling pathways, such as HeLa cells, which have been shown to internalize heparin which has been reported to end up in the nucleus (Busch SJ et al. 1992). The fact that cells bind/internalize heparin but are not heparin sensitive raises the possibility that most or all cells bind/internalize heparin but lack the downstream signaling molecules involved in transducing the signal. This suggests that most or all cells have a receptor for heparin, but may or may not be sensitive to heparin.

Along with tagged heparin uptake, it has also been widely documented in the literature and by previous members of the Lowe-Krentz laboratory that heparin mediates a portion of its effects through a cell surface receptor, suggesting that a putative heparin receptor exists on the surface of vascular smooth muscle cells (Savage JM et al. 2001 and Castellot JJ et al. 1984) and vascular endothelial cells (Patton WA et al. 1995 and Barzu T et al. 1986). It has also been documented by previous members of our lab that treatments with monoclonal antibodies that block heparin binding to endothelial cells also mimic the effects of heparin in vascular smooth muscle cells (Blaukovitch CI et al. 2010 and Savage JM et al. 2001) and vascular endothelial cells (Patton WA et al. 1995). The results from studies using the monoclonal antibodies against the heparin receptor are the

most convincing results suggesting that heparin acts via a receptor. Using the monoclonal antibodies in place of heparin in cell proliferation or stress assays removes any potential for heparin to act via electrostatic interactions or based solely on sequestering growth factor and cytokines. However, it is clear that heparin does also act via electrostatic interactions and sequestrations of certain molecules; therefore, heparin may act through multiple ways to influence cell behavior (Ali S et al. 2003; Ranjbaran H et al. 2006; Hatakeyama M et al. 2004, Blaukovitch CI et al. 2010, Savage JM et al. 2001, Patton WA et al. 1995, and reviewed in: Slee JB, Pugh R, Lowe-Krentz LJ. 2012).

Given the complexity of regulation that heparin and heparin-like molecules have over proliferation of vascular cells, the fact that heparin-induced decreases in ERK activity are effective whether growth factors are inducing the activity or phorbol esters are employed (Mishra-Gorur K and Castellot JJ 1999, Ottlinger ME, Pukac LA, and Karnovsky MJ 1993, Pukac LA et al. 1997), and the fact that antibodies to a putative heparin receptor are equally functional (Savage JM et al. 2001, Blaukovitch CI et al. 2010), it is unlikely that these anti-proliferative affects are due to heparin-like molecules blocking growth factor binding. This presents a situation in which heparin could be acting through a receptor to mediate its downstream signaling. Heparin is a very negatively charged molecule and is considerably larger than most biological molecules, making it virtually impossible for simple diffusion across the membrane. The size and highly charged nature of heparin chains makes receptor-mediated endocytosis the most likely mechanism for transport across the membrane.

Although it is well-documented that the heparin receptor exists, there has not been published evidence reporting the isolation and characterization of the receptor. Therefore our lab set out to identify a receptor for heparin. Unpublished data collected by Raymond Pugh Ph.D. for his doctoral dissertation suggest that he was able to isolate and purify the heparin receptor from BAOECs using the monoclonal anti-heparin receptor antibodies (Pugh R. Diss 2010). Through a collaboration with Walter Patton Ph.D. (Lebanon Valley College, former Lowe-Krentz lab member), Pugh was able to obtain a limited amount of protein sequence data. To obtain this sequence data, ladder sequencing of the receptor was performed using MALDI-TOF (Matrix-Assisted Laser Desorption/Ionization – Time of Flight) Mass Spectrometry. This technique has been outlined in the literature, demonstrating the use of carboxypeptidase Y to generate C-terminal cleavage products (ladders) of a peptide (or peptides) followed by MALDI-TOF analysis to first identify peptides (Patton WA 2004). Briefly, the receptor protein was cleaved first with trypsin or chymotrypsin to generate short peptides, followed by carboxypeptidase Y digestion, producing the amino acids or ladders. The mass lost from each cleavage corresponds to a specific amino acid, which allows for the sequencing of peptide fragments. Bioinformatic searches can then used to find sequence similarities to known proteins/genes.

This technique yielded several hits to Transmembrane Protein 184A (TMEM184A), which is an uncharacterized transmembrane protein. These results suggest but do not confirm that Raymond Pugh had isolated and purified what could be the putative heparin receptor. Having identified TMEM184A as a potential heparin receptor presents the opportunity for further research aimed at validating TMEM184A as

the heparin receptor. Also, given the fact that TMEM184A is still largely uncharacterized, the opportunity exists to explore its sub-cellular distribution and conservation across cell types. Virtually any findings regarding TMEM184A conservation, localization, and function are novel and important. Therefore, concurrent with linking TMEM184A function to the heparin receptor, work aimed at characterizing TMEM184A was also completed.

The sequencing of the human and other genomes has identified a host of genes with unknown functions. TMEM184A or sexually dimorphic expressed in male gonads (Sdmg1) is one protein identified through genome sequencing which still does not have a clearly defined function. TMEM184A is predicted to be a multi-pass transmembrane protein and contains a potential C-terminal dileucine targeting motif for endosome/lysosome targeting (Best D et al. 2008 and Bonifacino JS and Traub LM 2003). A few studies document roles in germ cell sex differentiation (Best D et al. 2008), membrane trafficking in SK11 Sertoli cells, and expression in secretory exocrine cells (Best D and Adams IR 2009). Other than these published reports, there is very little information about TMEM184 expression patterns in other cell types or evidence for a specific function of TMEM184A.

In SK11 Sertoli cells, TMEM184A is localized to endosomes and knock down leads to defects in membrane trafficking (Best D et al. 2008). TMEM184A was found to co-localize with two distinct endosomal populations in SK11 Sertoli cells: vesicle-associated membrane protein (VAMP)-7-containing perinuclear endosomes, and VAMP3/8-containing peripheral endosomes (Best D et al. 2008). It has also been shown

in pancreatic acinar cells that TMEM184A co-localizes with VAMP2 in secretory granules (Best D and Adams IR 2009). VAMPs (synaptobrevins) are a family of SNARE (soluble N-ethylmaleimide-sensitive factor-attachment protein receptor) proteins anchored in the membrane by a carboxy-terminal transmembrane domain and involved in membrane transport primarily by mediating vesicle fusion (Chen YA and Scheller RH 2001, Reinhard J and Scheller SH 2006, Fasshauer D et al. 1998, and Laage R et al. 2000). It has been suggested that TMEM184A could facilitate intra-lumenal cargo interaction with lipid microdomains or cytosolic membrane trafficking proteins (Best D et al. 2008).

Caveolae (lipid rafts) are non-clathrin-coated invaginations of the plasma membrane and are present in most mammalian cell types and particularly prominent in endothelial cells (Sowa G 2012). Caveolins act as scaffolds in caveolae which concentrate numerous receptors and signaling molecules involved in transport and signal transduction (Parton and Simmons 2007, Patel HH, Murray F, and Insel PA 2008, and Rath G, Dessy C, and Feron O 2009). Caveolin-1 (cav-1) is expressed in most cell types and is essential for caveolae formation (Sowa G 2012). Lipid rafts containing cav-1 are important in vascular endothelial cells, where they have been linked to the regulation of eNOS (endothelial nitric oxide synthase) which is involved in the control of vascular reactivity and inflammation (Chidlow JH and Sessa WC 2010 and Rath G, Dessy C, and Feron O 2009).

TMEM184A may have a functional role in vascular cells, given the large amount of intracellular transport these cells perform. In fact, all cells transport proteins to and

from the plasma membrane and would likely have this protein if it is involved in vesicle trafficking. Therefore, I aimed to determine the presence of TMEM184A in vascular cells and a range of other cell types and to begin elucidation of the function of TMEM184A in these cells. To our knowledge, this is the first report documenting the presence of TMEM184A in a broad range of cells types. Using western blotting and immunofluorescent microscopy, we have identified TMEM184A as more widely expressed than previously thought, where it co-localizes with VAMP-1, 2, and/or 3, cav-1, and eNOS. Given these findings, it is likely that TMEM184A is conserved across many cell types where it may play a role in membrane trafficking and/or signal transduction.

The goals of this chapter were to confirm the identification of the heparin receptor and to characterize TMEM184A as the probable receptor for heparin. The first aim of this chapter was to characterize TMEM184A in vascular cells (BAOECs, BAOSMCs, and RAOSMCs) as well as two cell lines (CHOs and MDCKs) and a fourth primary cell type MEFs. The second aim was to functionally identify TMEM184A as the heparin receptor using immunoprecipitations and siRNA/shRNA-mediated knockdown of TMEM184A coupled to functional assays. It is important to note that although these experiments were treated independently, they overlap significantly. The results from characterizing TMEM184A in different cell types support the notion that TMEM184A functions as a receptor for heparin. The siRNA/shRNA experiments do not in any way conflict with data characterizing TMEM184A in the cells investigated. Therefore, this collection of

seemingly independent studies is actually quite interrelated and helps to further our understanding of TMEM184A as a receptor for heparin.

The portions of this work relating to the presence of TMEM184A in BAOECs, BAOSMCs, RAOSMCs, CHOs, MDCKs, and MEFs and co-localization with VAMP, cav-1, and eNOS has been submitted to FEBS Letters Open Access for publication. Data collected with the HeLa cell line was not submitted for publication with the other cell lines.

5.2: Methods

5.2.1: Cell Culture

BAOECs, BAOSMCs, RAOSMCS, CHOs, MEFs, MDCKs, and HeLas were maintained and cultured on glass coverslips as described in Chapter 2 for immunofluorescent staining.

5.2.2: Immunofluorescence Staining

Primary antibodies against TMEM184A-NTD, TMEM184A-INT, VAMP1/2/3, cav-1 (Santa Cruz Biotechnology, Santa Cruz, CA), and TMEM184A-CTD (ProSci Inc. Poway, CA) were used as described in Chapter 2.

The TMEM184A-NTD primary antibody is specific for a stretch of amino acids (11-63) near the N-terminus of human TMEM184A. The TMEM184A-CTD primary antibody specific for the C-terminal region was developed against a 16 amino acid region near the C-terminus of TMEM184A. The TMEM184A-INT primary antibody specific for an internal region of TMEM184A is developed for 20 amino acids between 250 and 300.

This is not meant to imply an intracellular region of TMEM184A, rather a stretch of amino acids in the middle of the protein.

5.2.3: TMEM184A siRNA Electroporation Protocol

A7r5s were the cells used for electroporation with TMEM184A siRNA. A single 100 mm plate of cells was trypsinized and pelleted. The cell pellet was resuspended in 1X PBS and pelleted again. The cell pellet was resuspended in 1 ml of HeBS electroporation buffer and divided into the following three samples (335 μ l each):

1. Negative control – not electroporated
2. Control siRNA – electroporated with 5 μ M control siRNA (in some cases FITC-siRNA)
3. TMEM184A siRNA – electroporated with 5 μ M TMEM184A siRNA

Cells were electroporated using the BioRad electroporator with the HeLa protocol modified to 170 V. After electroporation, the three samples were divided equally onto coverslips in 6 well culture dishes, providing a 6 well dish for each condition (negative control, control siRNA, and TMEM184A siRNA). Cells were fed supplemented media the next day to remove any HeBS electroporation buffer and were allowed to proliferate for approximately 72 hours prior to experimentation.

5.2.4: Heparin Assay in TMEM184A siRNA-treated Cells

Within each of the three groups described in the previous section, two coverslips served as controls, two were treated with PDGF for 15 min, and two were treated with 200 μ g/ml heparin for 20 min prior to PDGF treatment for 15 min. One control coverslip from each treatment was fixed with 4.0% PFA, but not permeabilized, and stained for

TMEM184A-INT and pERK (Santa Cruz Biotech) to visualize surface staining on the confocal microscope. One PDGF 15min and Heparin 20 min/PDGF 15min set was TMEM184A-INT and pElk-1 (Santa Cruz Biotech). The three remaining coverslips (control, PDGF 15 min, and Heparin 20 min/PDGF 15 min) were stained for TMEM184A-INT and pElk-1. Antibody treatment was described in Chapter 2.

5.2.5: TMEM184A shRNA Electroporation Protocol

A7r5s were electroporated with 20 µg/ml plasmids containing sequences for expression of short hairpin RNA (shRNA) as described above for TMEM184A siRNA. Four plasmids bearing four different shRNA sequences and a GFP tag were obtained from Origene along with a GFP-tagged scrambled non-specific control shRNA plasmid. Initially all four TMEM184A shRNA constructs were tested for transfection and knockdown efficiencies by looking for GFP expression and decreased TMEM184A expression/staining. Once a strong decrease in TMEM184A was evident, the two shRNA constructs that consistently provided the most significant knockdown were chosen for further study.

5.2.6: Fluorescent Heparin Uptake

BAOECs, BAOSMCs, MDCKs, and MEFs were treated with 100 µg/ml Rhodamine-conjugated heparin (Creative PEG Works, Winston-Salem, NC) for 1, 5, and 7 min. After Rhodamine-heparin incubation, cells were fixed with 4% PFA but not permeabilized, as described in Chapter 2. Cells were not permeabilized, because doing so results in some of the Rhodamine-heparin leaking out of cells.

5.2.7: GFP-tagged TMEM184A (GFP-TMEM184A) co-localization with Rhodamine-Heparin

A7r5s were transfected with 20 µg/ml GFP-TMEM184A using the electroporation settings used for siRNA/shRNA described above. After 24-48 hr, cells were treated with 100 µg/ml Rhodamine-heparin for 1-10 min and fixed with 4% PFA without permeabilization to allow for better retention of Rhodamine-heparin. Slides were processed for confocal microscopy as described in Chapter 2.

5.2.8: Fluorescent Microscopy

Fluorescent microscopy was used to determine whole cell expression levels of TMEM184A, relative knockdown of TMEM184A in siRNA/shRNA-treated cells, and the PDGF/Heparin-induced responses in pERK and pElk-1 levels. Performed as described in Chapter 2.

5.2.9: Confocal Microscopy

Confocal microscopy was used to visualize sub-cellular structure, localization of TMEM184A and co-localization with VAMP1/2/3, caveolin-1, or eNOS, surface staining of TMEM184A, GFP-TMEM184A, and Rhodamine-heparin uptake. Performed as described in Chapter 2.

5.2.10: SDS-PAGE and Western Blotting

Confluent BAOECs, BAOSMCs, CHOs, MDCKs, and MEFs were harvested, and a Western Blot was performed as described in Chapter 2. Primary antibodies described in the immunofluorescence microscopy section of this chapter were used for Western

Blotting. Blots were developed using ExtraAvidin™ alkaline phosphatase, BCIP, and NBT or the ECL system as described in Chapter 2.

5.2.11: Heparin Receptor Immunoprecipitation

Confluent 150 mm dishes of BAOECs and BAOSMCs were harvested in radioimmunoprecipitation (RIPA) buffer (150 mM NaCl, 10 μ M Tris pH 7.2, 0.1% SDS, 0.1% Triton-X-100, and 0.5% deoxycholate) (Sigma), supplemented with two protease inhibitor cocktails (Sigma, P8340 and P2714) used at the manufacturer's recommended concentrations. Briefly, 150 mm dishes were rinsed with cold PBS twice and incubated with 1 ml of RIPA buffer for 30 min at 4 °C with rocking. Following this incubation, cells were scraped off the plates and placed in a microcentrifuge tube and centrifuged for 10 min at 10,000 xg. The supernatant was mixed with 2 μ g/ml of anti-heparin receptor monoclonal antibodies and incubated overnight at 4 °C on a rocker. After antibody incubation, 75 μ l of equilibrated EZview red protein G affinity gel beads (Sigma) were added and incubated overnight at 4 °C on a rocker. After bead incubation, the beads were rinsed with RIPA buffer three times and protein was isolated by boiling the beads in SDS sample buffer for 5 min. Western Blots were performed as described above with antibodies specific for TMEM184A-NTD.

5.3: Results

5.3.1: TMEM184A is detectable in vascular cells by Western Blotting and IF microscopy

To determine if TMEM184A is present in vascular endothelial and smooth muscle cells, whole cell western blots were carried out for BAOECs and BAOSMCs. As shown in Figure 5.1A, distinct bands are present in the predicted molecular weight range of TMEM184A that are absent from secondary antibody only controls. The doublet bands could be due to post translational modifications (glycosylation) which have been suggested in other reports (Best D et al. 2008). These results suggest that TMEM184A is present in vascular cells at levels high enough to be detected by Western Blotting.

To gain a better understanding of TMEM184A sub-cellular localization, BAOECs, BAOSMCs, and RAOSMCs were stained with three separate TMEM184A primary antibodies described in the methods section. As shown in Figure 5.1B, TMEM184A is detectable by confocal microscopy in the three vascular cell types investigated, and each of the three antibodies recognizes a specific subset of TMEM184A. The N-Terminal antibody highlights TMEM184A peri-nuclear staining in vascular endothelial and smooth muscle cells (Figure 5.1B – NTD). The C-Terminal antibody detects TMEM184A that is localized to cytoplasmic vesicles and a subset associated with the membrane (Figure 5.1B – CTD). Although the peri-nuclear staining is not completely clear, the CTD detection is more intense in peri-nuclear regions agreeing with the data from the NTD detection showing peri-nuclear staining. The internal TMEM184A antibody recognizes a mixture of both NTD and CTD staining, showing

both peri-nuclear staining and a small amount of cytoplasmic staining (Figure 5.1B – INT), further indicative of peri-nuclear localization of TMEM184A. To ensure that this staining pattern was not a bovine cell type specific phenomenon, rat primary cells (RAOSMCs) were also examined and show the same patterns as the bovine cells. Since TMEM184A is predicted to be a transmembrane protein, we investigated whether it was detectable on the surface of vascular cells. As shown in Figure 5.1B, cells that were fixed with 4% PFA and not permeabilized show specific staining patterns on the surface of cells, suggesting that TMEM184A does, in fact, localize to the membrane (Figure 5.1B – right column). These results confirm that TMEM184A is not just limited to germ cells and secretory exocrine cells as previously published.

I hypothesize that each antibody recognizes a slightly different sub-cellular location of TMEM184A due to antigen accessibility in the different locations. TMEM184A is predicted to be a multi-pass transmembrane protein therefore certain regions of the protein may not be easily accessible for antibody recognition under these fixation conditions. Given these results, it is clear that TMEM184A is localized to peri-nuclear and cytoplasmic regions of vascular cells as well as at the cell surface. These data agree with published evidence documenting peri-nuclear localization of TMEM184A in SK11 sertoli cells lines (Best D et al. 2008) and extend known locations to the cell surface.

5.3.2: TMEM184A is expressed in a variety of cells

Having identified TMEM184A in vascular cells, we hypothesized that this protein may be expressed in a wider range of cell types than germ cells and certain secretory

exocrine cells (Best D et al. 2008 and Best D and Adams IR 2009), given published data suggesting a role for TMEM184A in membrane transport. Therefore, Western Blot analysis was performed to determine if TMEM184A was expressed in CHO, MEF, and MDCK cells. As shown in Figure 5.2A, specific proteins are seen in the predicted molecular weight region of TMEM184A that are absent from secondary antibody only controls, suggesting that TMEM184A is also present in cells outside of the vascular system.

Having documented that TMEM184A is expressed in CHO, MEF, and MDCK cells via Western Blotting, sub-cellular distribution was determined by IF microscopy. The staining pattern seen with the CHOs is peri-nuclear and cytoplasmic (Figure 5.2B – CHO), as with the vascular cells. The MEFs show the most similar staining patterns to the vascular cells having large amounts of peri-nuclear TMEM184A seen with all three antibodies (Figure 5.2B – MEF). MDCKs exhibited less well-defined peri-nuclear staining with all three antibodies and more well-defined membrane localization when stained with the NTD and Internal TMEM184A antibodies (Figure 5.2B – MDCK). The three different TMEM184A antibodies recognize slightly different sub-cellular localizations of the protein, which is consistent across all cell types investigated. Determining that peri-nuclear staining is detected across all cells investigated, suggests that TMEM184A could be serving similar purposes in multiple cell types as to what has been documented in the SK11 sertoli cell line (Best D et al. 2008).

5.3.3: TMEM184A co-localizes with VAMP

Because vascular cells serve as a highly selective barrier and perform large amounts of intracellular vesicle transport, we hypothesized that TMEM184A also plays a role in membrane transport universally. To examine this hypothesis, co-localization with an antibody that recognizes VAMP-1, 2, and 3 (VAMP) was investigated. The antibody used to detect VAMP was specific for isoforms 1, 2, and 3 of VAMP, because TMEM184A has been shown to co-localize with VAMP2 and 3 containing endosomes in SK11 Sertoli cells and pancreatic acinar cells (Best D et al. 2008 and Best D and Adams IR 2009). As shown in Figure 5.3A, vascular cells express a large amount of VAMP, which is diffuse through the cytoplasm with intense clusters in defined peri-nuclear regions where it co-localizes with TMEM184A. RAOSMCs and BAOECs show a large amount of co-localization at peri-nuclear regions (Figure 5.3A). These data are consistent with the results shown in germ cells and exocrine cells (Best D et al. 2008 and Best D and Adams IR 2009), suggesting that TMEM184A also functions in exocytosis and/or vesicular trafficking in vascular cells.

To determine if this co-localization with VAMP was conserved across multiple cells lines, similar experiments were carried out in CHO, MEF, and MDCK cells. The staining in the MEF cells most closely resembles the data from the vascular cells showing TMEM184A co-localization with VAMP at peri-nuclear regions (Figure 5.3B – MEF), again suggesting a role in membrane transport. The data from the CHO and MDCK cells are slightly different from vascular cells and MEF cells. As shown in Figure 5.3B, the staining pattern in CHO cells indicates that TMEM184A and VAMP co-localize at

defined membrane patches and around cytoplasmic vesicles more so than in peri-nuclear regions. The CTD antibody was used to detect TMEM184A in the CHO cell line because the NTD antibody gave diffuse staining without specific localization. The MDCK cell line showed the least amount of TMEM184A co-localization with VAMP, but still exhibited a small amount of co-localization at membrane regions (Figure 5.3B – MDCK).

Taken together, these results suggest that TMEM184A may play a role in membrane trafficking in all cells investigated, highlighting the importance of this protein. Given the conservation of TMEM184A expression and similarities in staining patterns and co-localization with VAMP to previously published work (Best D et al. 2008 and Best D and Adams IR 2009), it is likely that TMEM184A is involved in membrane transport in a variety of cell types.

5.3.4: TMEM184A co-localizes with CAV-1 and eNOS in vascular cells

Cav-1 is considered to be a cell signaling hub and has been linked to the regulation of vesicle transport in most cells and especially cells of the vasculature (Chidlow JH and Sessa WC 2010). Based on the importance of cav-1 in vascular cells, we investigated the hypothesis that TMEM184A co-localizes with cav-1. As shown in Figure 5.4A, cav-1 staining is localized primarily to patches of membrane, where a subset co-localizes with TMEM184A staining, further suggesting that TMEM184A is playing a role in membrane transport and potentially in cell signaling mediated through lipid rafts. The other three cell types investigated, CHO, MDCK, and MEF cells express cav-1 to lesser degrees than vascular smooth muscle and endothelial cells (Figure 5.4B). These cells exhibit co-localization with cav-1 at membrane patches, even though they express

lower levels of cav-1 (Figure 5B). The co-localization in all three cell lines occurs primarily at membrane patches of some but not all cells, typically on the exterior of clusters of cells (Figure 5.4B). These data suggest that TMEM184A is localized to cav-1-containing lipid rafts where it may influence lipid raft-based cell signaling events and/or in vesicle trafficking.

Given that TMEM184A and cav-1 co-localize in vascular cells, we hypothesized that TMEM184A would also co-localize with eNOS given its prominent role in mediating signaling events downstream of lipid rafts in vascular cells. As shown in Figure 5.5, TMEM184A-INT co-localizes with eNOS in the characteristic peri-nuclear regions in the three vascular cells investigated. These data raise the possibility that TMEM184A could be an important player in mediating lipid raft signal transduction through its co-localization with cav-1 and eNOS, two of the more well-defined lipid raft molecules. Suggested cav-1 interaction sequences are common among many transmembrane proteins and appear to be found in putative transmembrane segments of TMEM184A. These segments may or may not be critical for cav-1 interactions with other proteins but if they are, it appears that TMEM184A has these sequences available for interaction with cav-1 (Byrne DP, Dart C, and Rigden DJ 2012). Despite the probability of interaction, immunoprecipitation with TMEM184A-NTD did not appear to pull down cav-1 along with the TMEM184A (data not shown).

5.3.5: TMEM184A is present in HeLa cells

In addition to the cells reported above, the presence of TMEM184A in HeLa cells was investigated. HeLa cells have a significant amount of TMEM184A as determined by

IF microscopy (Figure 5.6). TMEM184A staining in HeLa cells is similar to the staining seen in the other cell lines investigated. TMEM184A is concentrated in peri-nuclear regions, with faint localization throughout the cytoplasm (Figure 5.6). Specific detection of TMEM184A was also seen on the surface of cells that were fixed with 4% PFA but not permeabilized (Figure 5.6). It is expected that TMEM184A would co-localize with VAMP in the peri-nuclear region given that in all cells tested this was the case (Figure 5.3). The presence of TMEM184A suggests that HeLa cells could internalize heparin. HeLa cells have been previously shown to internalize FITC-heparin which ultimately ends up in the nucleus (Busch SJ et al. 1992). Therefore expression of TMEM184A correlates with previously published reports documenting heparin internalization in HeLa cells.

5.3.6: All Cells Investigated Internalize Rhodamine-Heparin

To investigate whether a heparin binding protein exists on most cells, despite the lack of evidence for heparin signaling, Rhodamine-heparin uptake assays were performed in BAOECs, BAOSMCs, MDCKs, and MEFs. As shown in Figure 5.7, all cells investigated internalize Rhodamine-heparin to varying degrees. Control cells were not treated with Rhodamine-heparin and exhibit a small amount of auto-fluorescence seen in most cultured cells (Figure 5.7). In general, the trend seen in Rhodamine-heparin uptake is that more heparin is internalized by cells up to 7 min, as shown by increased puncta and overall cytoplasmic staining (Figure 5.7), where it leveled off and remained relatively unchanged (data not shown). Beyond 7 min, it was difficult to determine new Rhodamine-heparin uptake versus old Rhodamine-heparin recycling/degradation.

Therefore timing was kept fairly short to ensure that most new Rhodamine-heparin uptake was observed. These results suggest that cells which have been shown to possess TMEM184A (Figures 5.1 and 5.2) functioning in vesicle trafficking and cell signaling (Figures 5.3, 5.4, and 5.5) also internalize heparin. These results support our hypothesis that TMEM184A is a receptor for heparin, because TMEM184A expression and labeled heparin uptake occur in the same cells.

5.3.7: Immunoprecipitation of the Heparin Receptor Detects TMEM184A

To determine if the heparin receptor could be immunoprecipitated from BAOECs, the monoclonal antibodies against the heparin receptor were used to IP the heparin receptor and were then Western Blotted with the TMEM184A-NTD and CTD antibodies. The data suggest that TMEM184A was specifically detected when the heparin receptor antibodies were used. The results of the IP are oriented so that the antibodies listed at the top are the Western Blot antibodies and the antibodies below them (shown on an angle) are the IP antibodies. As shown in the far right two columns of Figure 5.8, VE-cadherin was used as an IP control demonstrating that the IP process was successful. There is a distinct band at ~140 kDa in the VE-cadherin IP and VE-cadherin Western Blot lane (second from right) that is absent from the goat secondary antibody only control (far right) lane, suggesting that VE-cadherin immunoprecipitation was successful. This result confirms that the conditions used to immunoprecipitate VE-cadherin were sufficient to see a specific band on the Western Blot. Unfortunately, since the same antibody was used at the IP and Western Blot antibody, there is detection of the heavy and light (not shown) chains of the antibody as seen in the two far right lanes of Figure 5.8. Given that VE-

cadherin is a high molecular weight protein, these bands do not interfere with the specific banding of VE-cadherin. Bead only IP controls were performed and do not result in any protein when either of the TMEM184A polyclonal antibodies were used (data not shown).

Two separate monoclonal antibodies against the heparin receptor were used (12B1 and 18E9), both of which have been shown to be successful in mimicking the effects of heparin and blocking radiolabelled heparin binding (Savage JM et al. 2001 and Patton WA et al. 1995). As shown in Figure 5.8 (left two columns), when 12B1 and 18E9 are used to IP the heparin receptor from BAOECs, specific bands are seen around the predicted molecular weight region (~52 kDa) which are absent from secondary antibody only controls (2 Ab only – TMEM184A (Rabbit) lane), when the IP products were probed with commercial antibodies against TMEM184A-NTD and CTD. The intensity of the signal vary depending on which TMEM184A antibody was used, likely based on the specificity of the antibody under these conditions. The two polyclonal TMEM184A or secondary antibodies recognize a protein complex in the 52 kDa region of the VE-cadherin IP control (left lanes of two left columns). This detection may be TMEM184A specifically, since VE-cadherin has well-defined links to actin, which could theoretically be involved in TMEM184A movement throughout the cytoplasm. However, it is clear that the monoclonal heparin receptor antibodies pulldown a protein which is then subsequently recognized by the TMEM184A antibodies, suggesting that TMEM184A could be the heparin receptor or, at the very least, complex with a protein that the monoclonal antibodies recognize.

Similar experiments were carried out with the BAOSMCs. In these experiments, insulin receptor substrate-1 (IRS-1) was used as a control in place of VE-cadherin. In these experiments, the control (IRS-1) IP antibody and the Western Blot antibodies were both rabbit, so the heavy and light chains of the antibody were detected in the control lanes (Figure 5.8B – left lanes of each column). However, the heparin receptor monoclonal antibodies are of mouse origin, so the protein seen in the 18B6 and 18H6 lanes is due to specific interaction with the IP product (Figure 5.9 – right two lanes of each column), suggesting that TMEM184A recognizes the protein that is pulled down by the heparin receptor antibodies. The secondary only control lanes show the antibody heavy chain, the IRS-1 lane, and a slight non-specific band in the 18B6 lane, suggesting that some of the detection may be due to non-specific secondary antibody recognition (Figure 5.8B – far left column). Although there is a small amount of non-specific interaction, the specific detection is considerably more intense, suggesting that TMEM184A antibodies recognize immunoprecipitated heparin receptor.

5.3.8: GFP-Tagged TMEM184A co-localizes with Rhodamine-heparin

To further suggest that specific detection of TMEM184A is obtained through antibody staining and that TMEM184A is a receptor for heparin, GFP-TMEM184A was transfected into A7r5s and imaged in fixed cells. As shown in Figure 5.9A, GFP-TMEM184A localizes predominantly to two domains in A7r5s. GFP-TMEM184A clusters intensely at peri-nuclear regions and membrane patches (Figure 5.9A). These locations agree with the patterns seen with antibody staining (Figure 5.1), strengthening the conclusions drawn from the antibody staining experiments. In order to support the

hypothesis that TMEM184A is a receptor for heparin, cells expressing GFP-TMEM184A were treated with Rhodamine-heparin. Extensive co-localization was evident between GFP-TMEM184A and Rhodamine-heparin at puncta throughout the cytoplasm (Figure 5.9B). Co-localization is shown in A7r5s treated with Rhodamine-heparin up to 5 min in Figure 5.9B, however similar co-localization can be seen up to at least 10 min and potentially even longer, though longer times have not been investigated (data not shown). It also appears that cells which have internalized Rhodamine-heparin exhibit less characteristic surface staining, suggesting that TMEM184A on the surface was internalized with the labeled heparin (Figure 5.9B). A7r5s expressing GFP-TMEM184A but not treated with Rhodamine-heparin were used as control and showed insignificant levels of red autofluorescence (data not shown). Taken together, these results confirm the sub-cellular localization of TMEM184A in vascular smooth muscle cells and also provide another line of evidence supporting TMEM184A as a receptor for heparin.

5.3.9: siRNA-mediated knockdown of TMEM184A decreases heparin sensitivity in A7r5s

To further the IP data and the co-localization work showing that GFP-tagged TMEM184A co-localizes with Rhodamine-heparin, siRNA specific for rat TMEM184A was obtained from Santa Cruz Biotechnology. Following the electroporation protocol described in the methods section of this chapter, transfection efficiencies of ~75% were consistently obtained in the A7r5 cell line (Figure 5.10A). As shown in Figure 5.10A, most cells exhibit fairly low levels of FITC-tagged scrambled control siRNA, suggesting that the electroporation protocol results in siRNA uptake by the cells. Even with the low

level of siRNA uptake, there does seem to be a significant effect on TMEM184A expression. As shown in Figure 5.10B, surface staining of TMEM184A is significantly decreased in TMEM184A siRNA-transfected cells relative to scrambled control siRNA-transfected cells. These data suggest that the TMEM184A siRNA decreases the amount of TMEM184A on the surface of cells, presumably decreasing a cell's ability to bind and internalize heparin.

In agreement with the surface decreases in TMEM184A siRNA-transfected cells, the internal staining of TMEM184A also seems to decrease relative to control siRNA-transfected cells that have been fixed and permeabilized (Figure 5.10 and 5.11). Because knockdown varied from experiment to experiment, knockdown levels are shown for each experimental sample along with staining for pERK or pElk-1. As shown in Figure 5.11A, TMEM184A staining is significantly reduced in TMEM184A siRNA-transfected cells relative to the same treatment in control siRNA-transfected cells. Control siRNA-transfected cells show a strong PDGF-induced increase in pElk-1 relative to control, which is robustly attenuated by a 20 min heparin pretreatment prior to the 15 min PDGF treatment. (Figure 5.11A – Control siRNA rows). PDGF induces a similar response in the TMEM184A siRNA-transfected cells, inducing a modest increase in pElk-1 staining intensity (Figure 5.11A – TMEM184A siRNA rows). When TMEM184A levels are decreased due to siRNA transfection, the heparin-induced attenuation of PDGF-induced pElk-1 staining intensity is lost (Figure 5.11A – TMEM184A siRNA rows). Stated differently, when TMEM184A levels are decreased, the cells are no longer as sensitive to heparin. These results suggest that TMEM184A is involved in mediating the heparin

responses in vascular smooth muscle cells potentially by serving as a receptor for heparin.

In similar experiments, the effect of TMEM184A knockdown on PDGF-induced and heparin attenuation of ERK was investigated. Due to the experimental design and the need for unpermeabilized surface only staining controls (Figure 5.10), there are not untreated controls for the pERK studies (Figure 5.11B). PDGF-induced ERK activity at 15 min is high, a finding which has been noted elsewhere (Gilotti AC diss. 2000 and Savage JM et al. 2001) As shown in Figure 5.11B (Control siRNA rows), a 20 min heparin treatment prior to a 15 min PDGF stimulation, greatly reduces active ERK in both the cytoplasm and the nucleus. The effect of heparin is again decreased in cells which have been transfected with TMEM184A siRNA (Figure 5.11B – TMEM184A siRNA rows), suggesting that TMEM184A is needed for cells to be heparin sensitive. Taken together, the data indicate that decreasing TMEM184A expression results in decreased heparin sensitivity. In and of itself, these data do not prove that TMEM184A is a receptor for heparin; but it does indicate that TMEM184A is involved in mediating heparin responses, presumably by acting as a receptor for heparin.

To ensure that the electroporation/transfection process did not significantly affect protein expression in A7r5s; scrambled Control siRNA-treated cells were also compared to cells which were not electroporated/transfected. These “untransfected” cells showed the same results as the control siRNA. The control siRNA had no effect on TMEM184A, pERK, or pElk-1 overall expression or localization relative to untransfected cells.

5.3.10: shRNA-mediated knockdown of TMEM184A in A7r5s

As shown in Figure 5.12, A7r5s were effectively electroporated with GFP-tagged control shRNA constructs and TMEM184A-specific shRNA constructs (shRNA-B and C). In cells which expressed the GFP-tagged constructs, there was a significant reduction in TMEM184A-NTD staining on the surface of A7r5s that were not permeabilized, suggesting that the shRNA significantly decreased TMEM184A on the surface of cells (Figure 5.12). Although significant knock down was determined for surface TMEM184A, the differential levels of internal TMEM184A were not as great as the surface knock down.

5.4: Discussion

TMEM184A is a largely uncharacterized protein, identified through genome sequencing, which was thought to be limited in its expression to the germ line and exocrine cells, based on previous investigations (Best D et al. 2008 and Best D and Adams IR 2009). In order to gain a better understanding of TMEM184A and to potentially find a cell line in which I could overexpress TMEM184A, I sought to further characterize TMEM184A in a variety of cell types. I have shown that TMEM184A is present in vascular cells and a variety of primary and cloned cell lines, suggesting that it is expressed in a wider range of cells. In an attempt to examine TMEM184A function in vascular cells, co-localization with VAMP, cav-1, and eNOS was performed. TMEM184A co-localizes at peri-nuclear regions with VAMP, suggesting emerging roles in vesicle transport modulation in these cells types which is consistent with previous

findings in exocrine cells (Best D and Adams IR 2009). I also determined that TMEM184A is present at cav-1-enriched lipid rafts, presenting the possibility that TMEM184A may be involved in cell signaling events mediated by lipid rafts. In the case of vascular endothelial lipid rafts, cav-1 is an important player in eNOS-mediated signaling events, and given TMEM184A presence, it may play a role in these signaling events as well. To this end, TMEM184A was also determined to co-localize with eNOS in vascular smooth muscle and endothelial cells.

The fact that TMEM184A co-localizes with both eNOS and cav-1 is not surprising given that eNOS and cav-1 physically interact via the scaffolding domain of cav-1 (Garcia-Cardena G et al. 1997 and Ju H et al. 1997). In this context cav-1 has been shown to have an inhibitory role in preventing NO release because cav-1 negatively regulates eNOS (Michel JB et al. 1997 and Bucci M et al. 2000). There have also been a large number of other proteins which have been established to localize to endothelial cell caveolae. These include receptor tyrosine kinases, G-protein coupled receptors and their subunits, TGF β receptors, and calcium channels (reviewed in: Sowa G 2012). This suggests that TMEM184A, if proven to be the heparin receptor, could preferentially localize to caveolae in order to participate in the signaling hub located at caveolae lipid rafts. TMEM184A co-localization with eNOS further suggests that it utilizes the caveolae network. The co-localization of TMEM184A and VAMP is likely due to VAMP serving as a vesicle marker to assist in determining the final destination of the vesicle.

Although physical interactions were not determined within the context of this dissertation, co-localization analysis suggests that TMEM184A could physically interact

with VAMP, cav-1, and/or eNOS or that they could be held in close proximity by a common protein complex. Suggested cav-1 interaction sequences are common among many transmembrane proteins and appear to be found in putative transmembrane segments of TMEM184A. These segments may or may not be critical for cav-1 interactions with other proteins but if they are, it appears that TMEM184A has these sequences available for interaction with cav-1 (Byrne DP, Dart C, and Rigden DJ 2012). Despite the probability of interaction, immunoprecipitation of TMEM184A-NTD did not appear to pull down cav-1 (data not shown).

To gain an understanding of whether TMEM184A localizes to the membrane for a period of time, cells were fixed with 4% PFA but not permeabilized with Triton-X-100. Admittedly, this method of looking at cell surface staining is imperfect, because cells are permeabilized slightly in the process, even though the PFA did not contain methanol. In most cases, an antibody for a cytoplasmic protein was included in the cell surface staining experiments, to show that the cells were not permeabilized enough for significant cytoplasmic staining. In a large percentage of the experiments, staining of the cytoplasmic protein was faint and altered from its traditional staining pattern, providing convincing evidence that the cells were not permeabilized significantly (data not shown). In agreement with these results, the staining pattern of TMEM184A was altered in a way which no longer showed peri-nuclear staining, suggesting that the cells were not appreciably permeabilized. Secondary antibody only controls were also done to confirm that the TMEM184A surface staining was specific. Despite the imperfections in the technique, it was the only technique readily available to look at cell surface staining, and

did provide a consistent representation of TMEM184A on the cell surface. These data suggest that TMEM184A does remain on the cell surface for a period of time as well as localizing to peri-nuclear regions, again supporting the hypothesis that TMEM184A could function as a receptor for heparin.

It has also been shown that cells which possess TMEM184A also internalize labeled heparin. Unfortunately, the Rhodamine-heparin uptake assays require cells to not be permeabilized making co-localization studies of Rhodamine-heparin and native TMEM184A virtually impossible. Co-localization of surface TMEM184A (staining in unpermeabilized cells) and Rhodamine-heparin can be done, but typically does not yield appreciable co-localization likely due to washing off of Rhodamine-heparin from surface interactions during rinsing and fixation. This hypothesis is supported by the fact that most Rhodamine-heparin is seen in small to large puncta in the cytoplasm and does not resemble surface staining seen with TMEM184A. Comparing TMEM184A staining seen in Figure 5.1B and 5.2B with Rhodamine-heparin uptake in Figure 5.7, there is potential that TMEM184A and Rhodamine-heparin would co-localize in the cells investigated. The clearest example of this is the MEF cell line which noticeably exhibits Rhodamine-heparin signal near nuclei, which is where TMEM184A-NTD is predominantly localized. Although not entirely convincing, these data support and do not disprove TMEM184A as the heparin receptor. Due to the above experimental limitations of staining for TMEM184A and looking for co-localization with Rhodamine-heparin, a GFP-tagged construct was obtained for these experiments. Although, it is debatable whether or not the

GFP tag will disrupt the orientation of TMEM184A in the membrane, it can still be used to determine sub-cellular localization and co-localization with Rhodamine-heparin.

GFP-TMEM184A is expressed at fairly high levels in A7r5s where it localizes to peri-nuclear regions and membrane patches (Figure 5.9A). Given that the TMEM184A antibodies were polyclonal antibodies which have the potential to detect proteins of similar sequence to TMEM184A, it was determined that exogenous expression of TMEM184A would only strengthen the conclusions drawn from antibody staining. The GFP-TMEM184A was found at intense peri-nuclear regions with virtually no staining in what appears to be the nuclei, something that was occasionally an artifact seen with antibody staining. GFP-TMEM184A also localized to patches at the membrane, further supporting the role of TMEM184A as a transmembrane protein, which could be accessible on the surface of the cells for heparin binding. Cells expressing GFP-TMEM184A were also treated with Rhodamine-heparin to investigate if the two co-localize. Internalized Rhodamine-heparin in A7r5s typically occurs as intense puncta throughout the cytoplasm, presumably representing internalized vesicles. Co-localization between GFP-TMEM184A and Rhodamine-heparin is evident in most cells as far out in time as I've investigated. The co-localization experiments provide yet another line of evidence that TMEM184A functions as a receptor for heparin. However, it is possible that TMEM184A is involved in intracellular transport and that is why co-localization is seen. Albeit plausible, considering all of the data indicating that TMEM184A functions as a receptor for heparin, it seems more likely that TMEM184A is functioning as a receptor for heparin.

To initially characterize TMEM184A as the heparin receptor, immunoprecipitations were performed using the lab's monoclonal heparin receptor antibodies, which mimic the effects of heparin and block radiolabelled heparin binding (Savage JM et al. 2001, Patton WA et al. 1995). Under the IP conditions described in the methods section of this chapter, the monoclonal antibodies were able to IP a protein which was recognized by the TMEM184A antibodies in both BAOECs and BAOSMCs. These data suggest that either TMEM184A is the heparin receptor or that TMEM184A interacts with a protein that is the heparin receptor. Although the IP data suggest that TMEM184A recognizes immunoprecipitated heparin receptor, the controls for these experiments are not as clean as desired. This is likely due to a variety of factors including the polyclonal nature of the TMEM184A antibodies and a small degree of non-specific secondary antibody interaction. Taking into consideration the mass spec data collected by Raymond Pugh, there is fairly convincing evidence that TMEM184A is the heparin receptor. Raymond's data showed that he was able to isolate protein using the same monoclonal antibodies for sequence analysis, demonstrating that the isolated protein shared significant sequence similarity with TMEM184A. Combining the proteomic data with the IP data discussed in this chapter, provides convincing evidence that TMEM184A is the heparin receptor or at least part of a heparin receptor complex. However, other members of the Lowe-Krentz have documented that other proteins do not co-IP with the heparin receptor (Patton WA et al. 1995 and Savage JM et al. 2001).

In order to further suggest that TMEM184A is the heparin receptor, functional assays need to be completed. To do this, there are two options. The first option is to

exogenously over-express TMEM184A in cells which do not possess or possess significantly less TMEM184A and determine increased heparin sensitivity. The second option is to knock down the levels of endogenous TMEM184A using siRNA or shRNA in a cell line known to possess TMEM184A and determine sensitivity to heparin. I have decided that the first option (exogenous over-expression) is not a feasible route to provide a functional link between heparin sensitivity and TMEM184A. This conclusion is based on the fact that all cells that have been investigated possess TMEM184A at high levels and bind/internalize labeled heparin, even though the cells have not been documented in the literature to be heparin sensitive. These facts suggest that all cells have TMEM184A and/or a receptor for heparin allowing them to internalize labeled heparin but lack the downstream signaling components necessary for heparin signaling to occur. Therefore my hypothesis is that over-expressing exogenous TMEM184A in these cells which already have the protein will not make them heparin sensitive in any way that has been documented or can be measured experimentally. However, the GFP-tagged TMEM184A did partly fulfill this line of evidence detailed above.

Again, the second method to functionally link TMEM184A to heparin sensitivity is to knock down TMEM184A using siRNA or shRNA and look for altered heparin sensitivity. It is my belief that this is the most effective way to link TMEM184A to heparin sensitivity, given the issues discussed with exogenous over-expression. The data collected using targeted siRNA suggests that a modest decrease of TMEM184A has been consistently achieved in the A7r5 cell line. The decrease in TMEM184A staining is very modest, but is sufficient to alter the cells' response to heparin as shown by pERK and

pElk-1 staining. Under normal conditions, both pERK and pElk-1 are strongly induced by 15 min of PDGF stimulation and a 20 min pre-treatment of heparin is sufficient to decrease this response by about half. When TMEM184A siRNA is incorporated and the cells have been verified to show moderately decreased TMEM184A staining, the cells are less responsive to heparin pre-treatment. In siRNA-treated cells, the heparin-induced decreases are absent or significantly less than seen with control cells. The degree to which cells lose their heparin sensitivity is in line with the efficacy of TMEM184A knockdown. These data suggest that TMEM184A functionally acts as a receptor for heparin, because when TMEM184A levels are even moderately decreased, heparin sensitivity is decreased.

The trends seen in the siRNA experiments agree with the hypothesis that TMEM184A is a receptor for heparin. However, I believe that only modest decreases are going to be obtainable using siRNA, due to the fact that the cells need to be exposed to siRNA for a minimum of 72 hours to even see a decrease in TMEM184A staining. It is likely that during this long time frame, the siRNA is degraded and loses its potency. Since TMEM184A is a membrane protein, presumably with fairly slow turnover, long exposure to siRNA is required to achieve any decreases in TMEM184A levels. For these reasons and to obtain better knockdown of TMEM184A, shRNA constructs were obtained. The shRNA constructs should be more effective over longer periods of time in knocking down TMEM184A protein levels, allowing a more clear interpretation of lost heparin sensitivity in cells expressing less TMEM184A.

In an attempt to achieve better knock down of TMEM184A in the A7r5 cell line and to support the siRNA data, shRNA constructs specific for TMEM184A were obtained. The results from these experiments suggest that two of the five constructs (shRNA-B and C) were significantly better at decreasing the level of TMEM184A on the surface of cells. However, only surface TMEM184A was significantly reduced by the shRNA constructs. Internal staining for TMEM184A was only marginally decreased by the specific shRNA compared to untransfected cells or control shRNA transfected cells. This along with the GFP-TMEM184A localization primarily to the membrane suggests that newly synthesized TMEM184A is transported to the membrane and remains there. Both shRNA and siRNA decrease the amount of newly synthesized protein which would likely be the TMEM184A associated with the membrane. Since both silencing mechanisms only decrease internal staining modestly, this suggests that TMEM184A is not readily recycled, although the mechanism and meaning behind this lack of recycling is unclear. In the future these shRNA construct can be used to create stable cell lines which constitutively express decreased TMEM184A. This could potentially increase the success of long-term decreases in TMEM184A which may be necessary to decrease both surface and internal levels.

The fact that GFP-tagged TMEM184A co-localizes with Rhodamine-heparin and the TMEM184A siRNA data do not prove that TMEM184A functions as a receptor for heparin, rather they suggest that TMEM184A is involved in mediating heparin signaling. The culmination of work completed by Raymond Pugh, using protein biochemistry and mass spec analysis suggested that TMEM184A shared significant sequence similarity to

the protein isolated using monoclonal antibodies against the heparin receptor. Combining Raymond's data with the IP data, co-localization data, and the siRNA data strongly supports the hypothesis that TMEM184A does, in fact, function as a receptor for heparin.

5.5: Figures

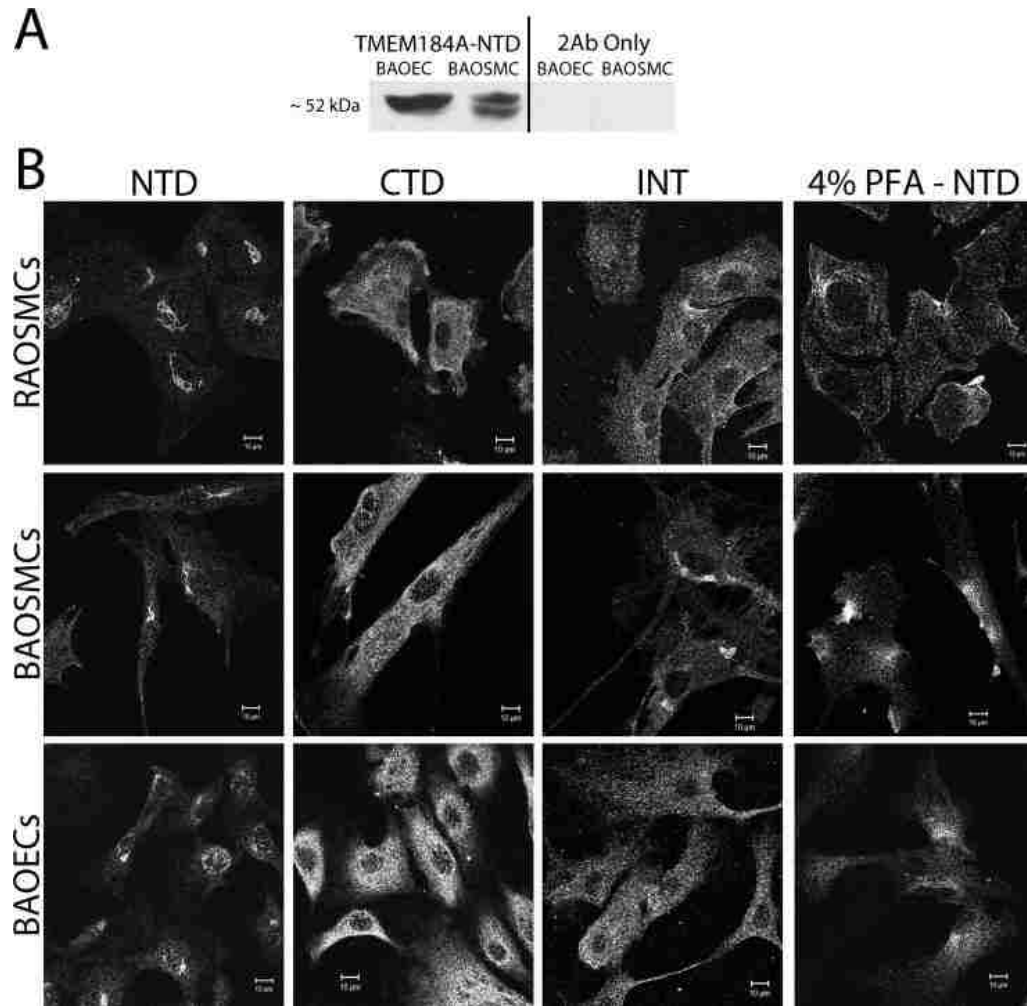


Figure 5.1: TMEM184A is expressed in vascular endothelial and smooth muscle cells

(A) Whole cell lysates were harvested in sample buffer, immunoblotted for TMEM184A-NTD, compared to corresponding secondary antibody only controls, and migration of colored molecular weight markers. Blots were developed using ECL reagents. (B) Cells were fixed and permeabilized with ice cold methanol (left three columns) and treated with antibodies specific for TMEM184A-NTD, CTD, or INT to determine sub-cellular localization. Cells in the far right column were fixed with 4% PFA without permeabilization to see mostly cell surface staining with the TMEM184A-NTD antibody. Images are representative of a least three repeats. Scale bars = 10 μ m.

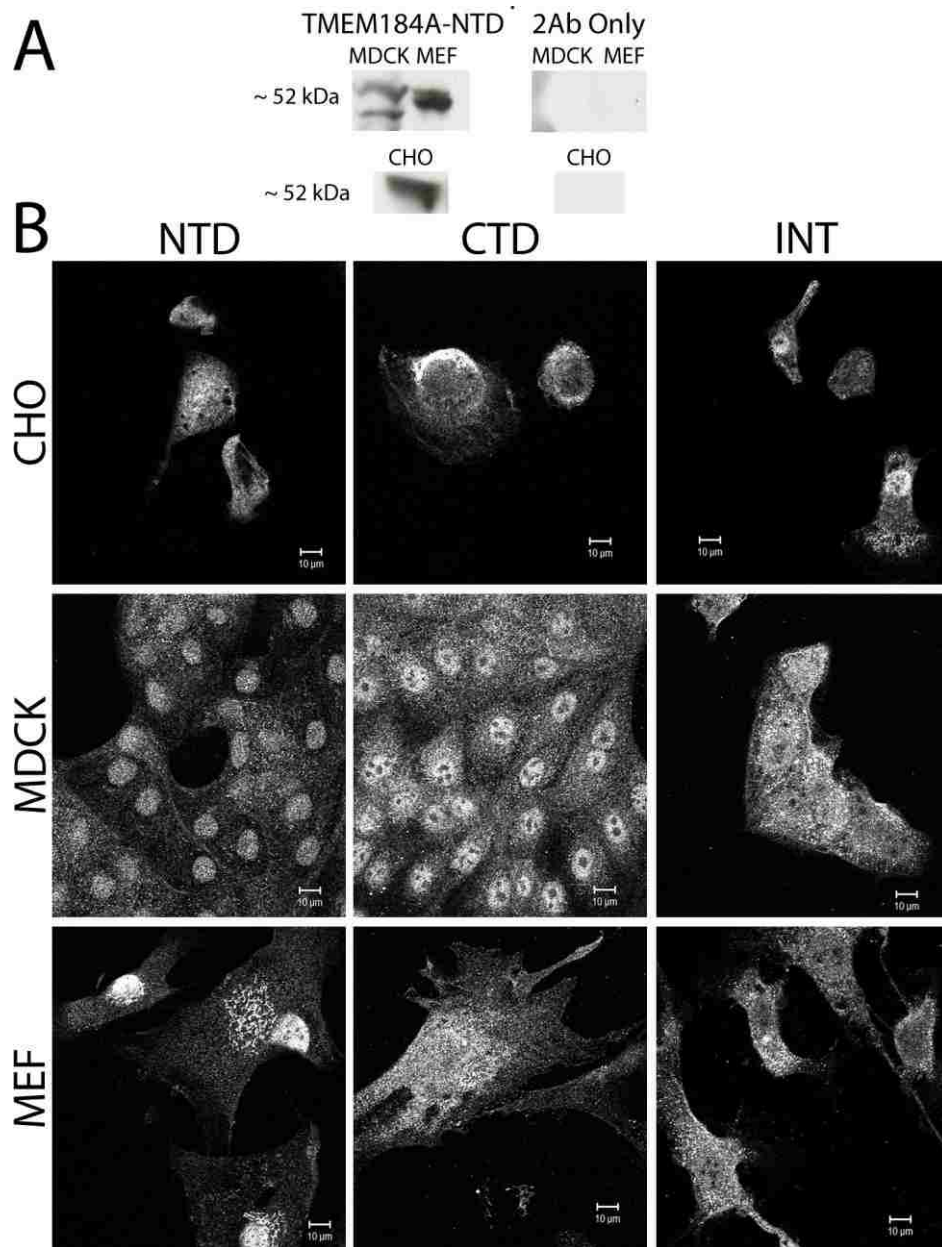


Figure 5.2: TMEM184A is expressed in CHO, MDCK, and MEF cells
 (A) Whole cell lysates were harvested in sample buffer, immunoblotted for TMEM184A-NTD, compared to corresponding secondary antibody only controls, and migration of molecular weight markers. Blots were developed using ECL reagents. (B) Cells were fixed and permeabilized with 4% PFA and 0.3% Triton and treated with antibodies specific for TMEM184A-NTD, CTD, or INT to determine sub-cellular localization. Images are representative of a least three repeats. Scale bars = 10 μ m.

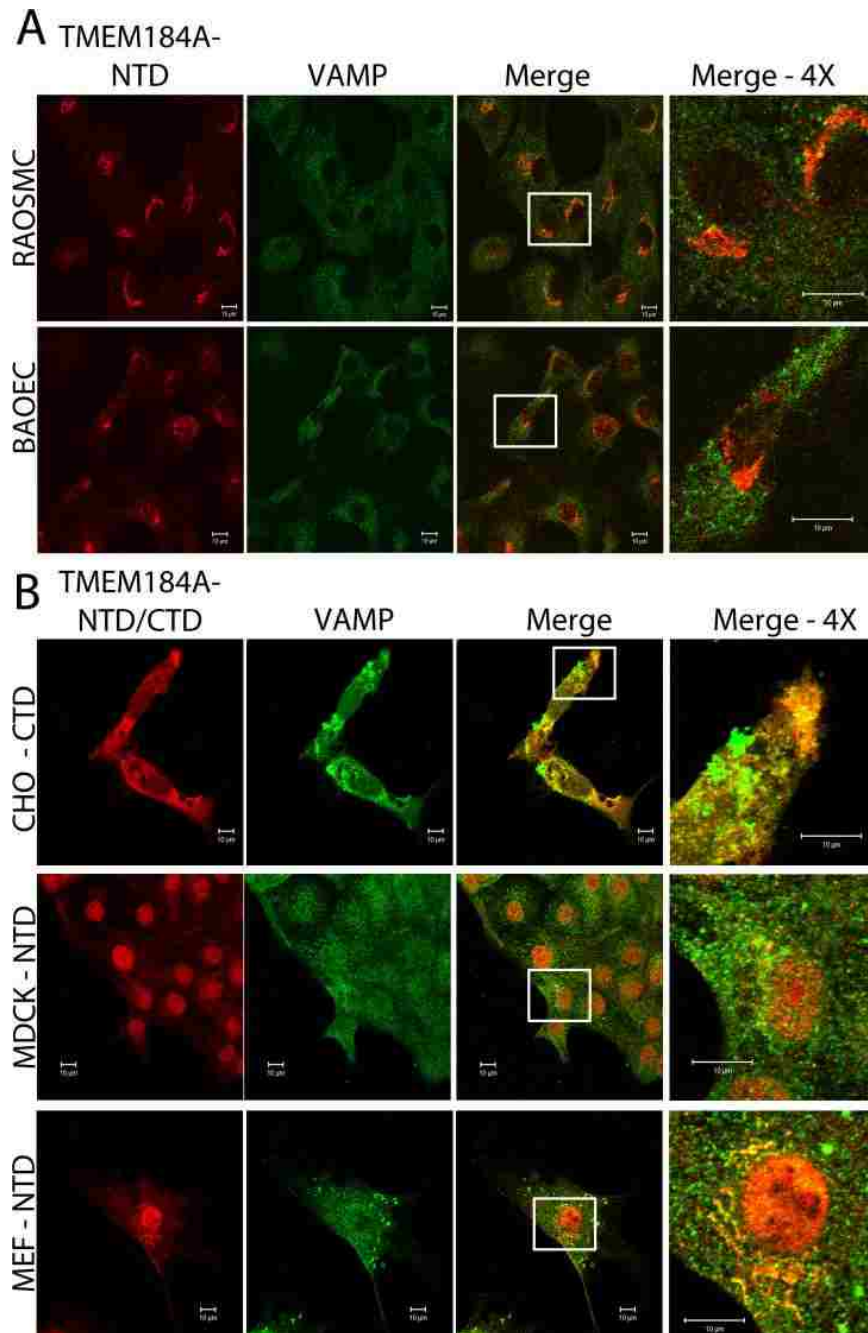


Figure 5.3: TMEM184A co-localizes with VAMP

(A) RAOSMCs and BAOECs were fixed and permeabilized with ice cold methanol and (B) CHOs, MDCKs, and MEFs were fixed and permeabilized with 4% PFA and 0.3% Triton. Cells were treated with antibodies specific for TMEM184A-NTD or CTD (Red) and VAMP1-3 (Green). Far right column is magnified 4X the original boxed area in the panel immediately to the left. Images are representative of a least three repeats. Scale bars = 10 μ m.

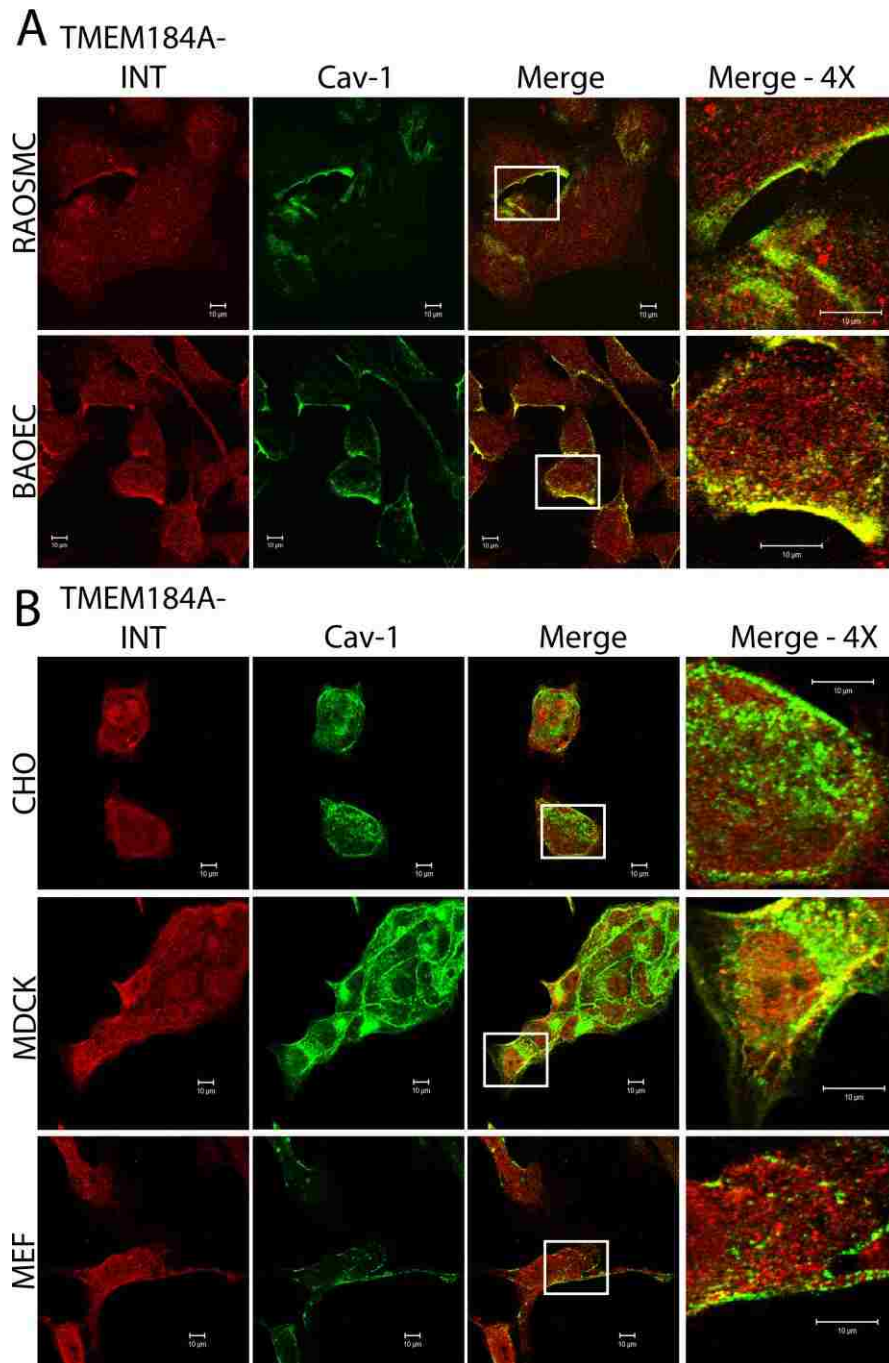


Figure 5.4: TMEM184A co-localizes with caveolin-1
 (A) RAOSMCs and BAOECs (B) CHO, MDCKs, and MEFs were fixed and permeabilized with 4% PFA and 0.3% Triton. Cells were treated with antibodies specific for TMEM184A-INT (Red) and cav-1 (Green). Far right column is magnified 4X the original boxed area in the panel immediately to the left. Images are representative of a least three repeats. Scale bars = 10 μ m.

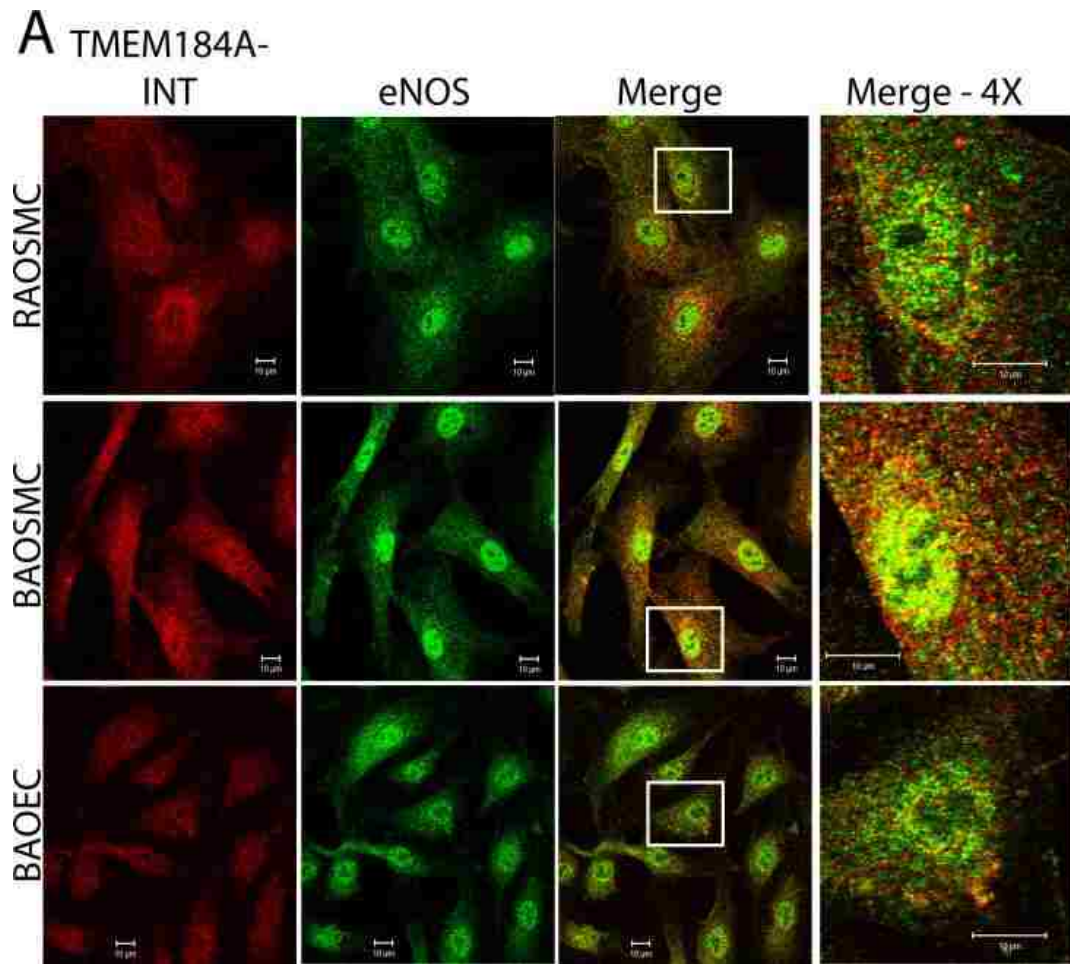


Figure 5.5: TMEM184A co-localizes with eNOS in vascular cells

BAOECs, BAOSMCs, and RAOSMCs were fixed and permeabilized with 4% PFA and 0.3% Triton. Cells were treated with antibodies specific for TMEM184A-INT (Red) and eNOS (Green). Far right column is magnified 4X the original boxed area in the panel immediately to the left. Images are representative of a least three repeats. Scale bars = 10 μ m.

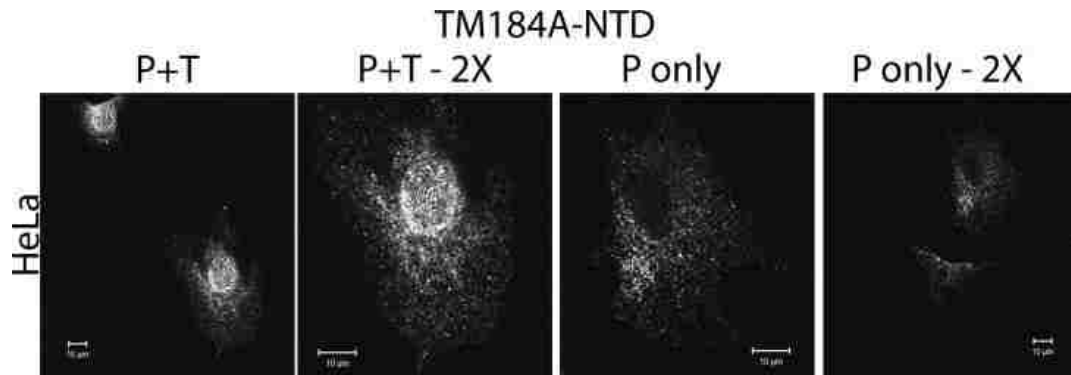


Figure 5.6: HeLa cells express TMEM184A

HeLa cells were fixed with 4% PFA or fixed with 4% PFA and permeabilized with 0.3% Triton as described in Chapter 2. Cells were labeled with antibodies specific for TMEM184A-NTD. Column 1 and 4 are magnified 2X the original immediately to the left. Images are representative of two repeats. Scale bars = 10 μ m.

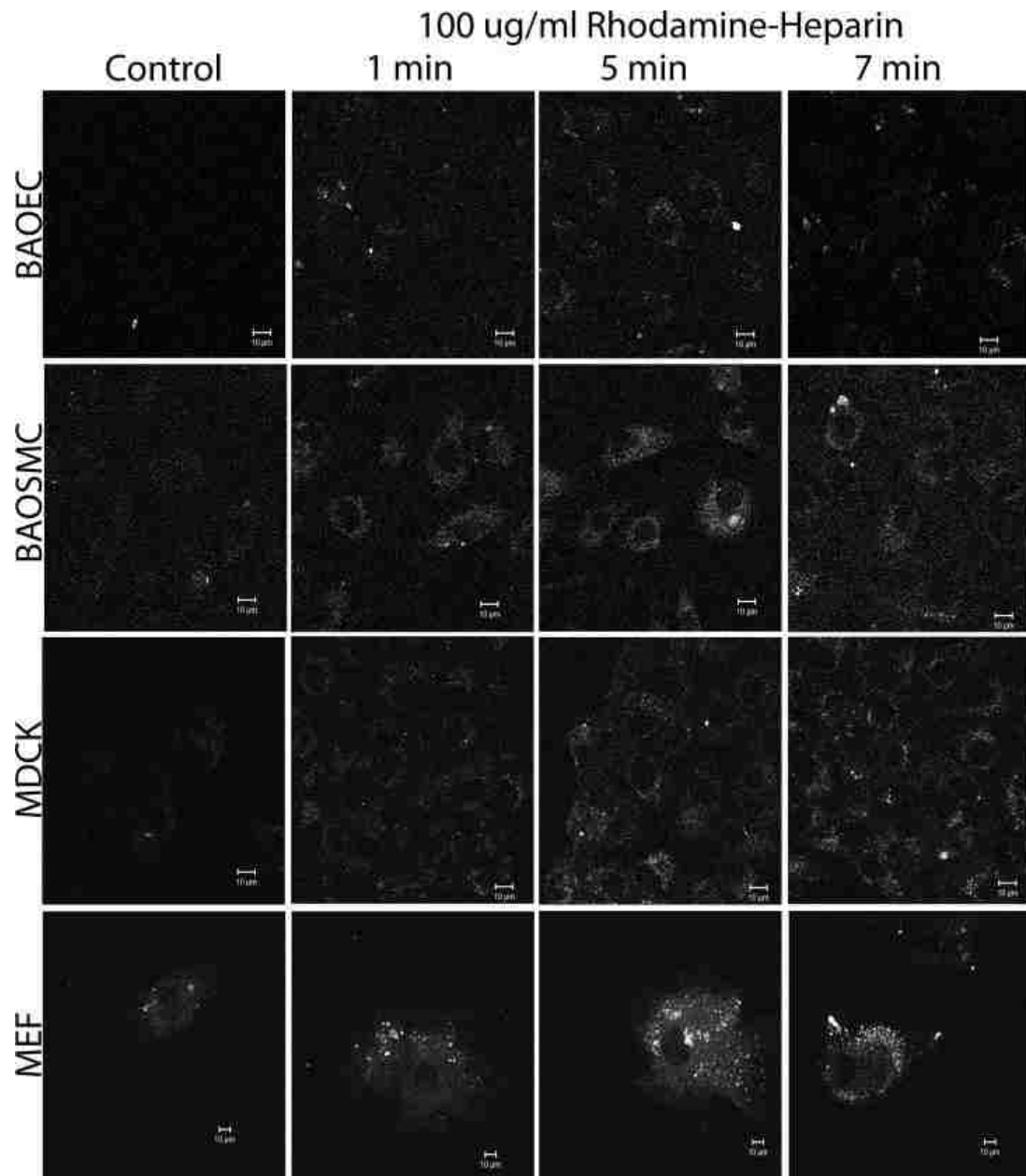


Figure 5.7: All cells investigated internalize Rhodamine-heparin
BAOECs, BAOSMCs, MDCKs, and MEFs were treated with 100 μ g/ml
Rhodamine-Heparin for 1, 5, and 7 min, following which they were fixed with 4%
PFA and not permeabilized. Control cells are untreated and represent low levels
of autofluorescence. BAOECs, BAOSMCs, and MDCKs were imaged at 63X
whereas the MEFs were imaged at 40X. Images are representative of two repeats.
Scale bars = 10 μ m.

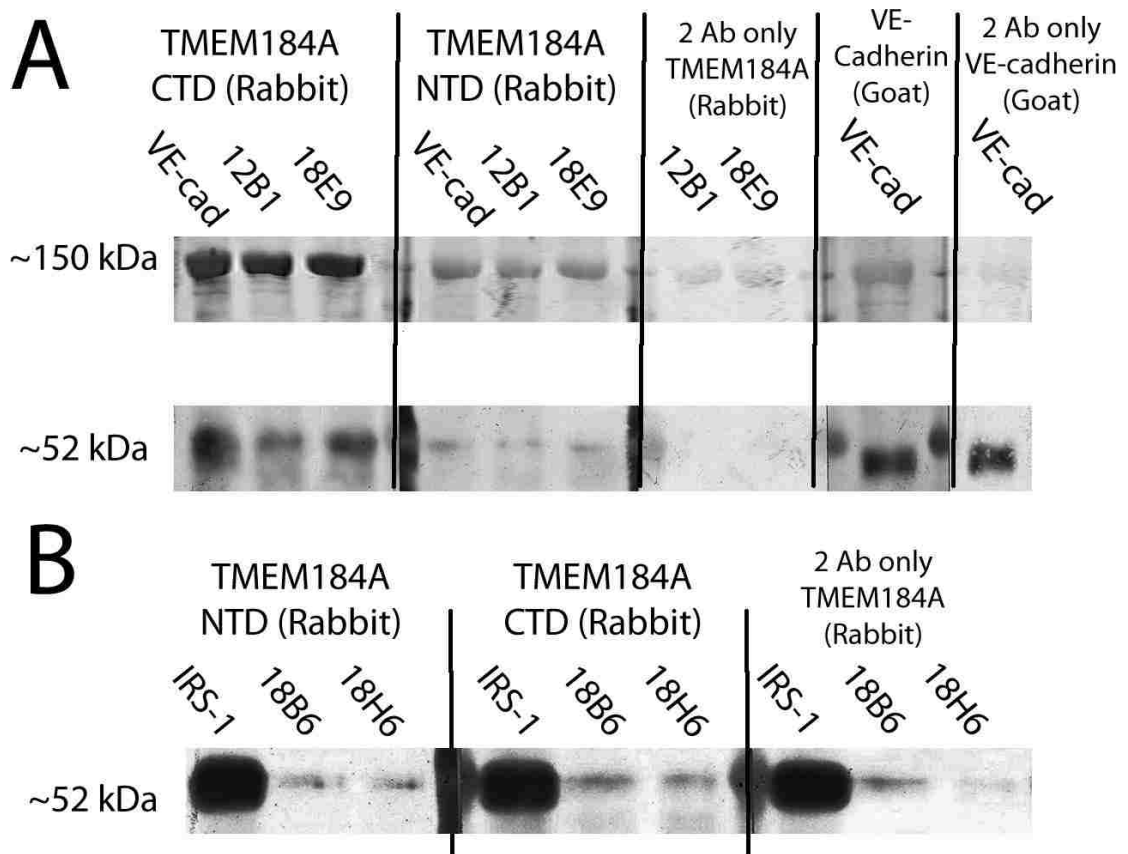


Figure 5.8: Immunoprecipitation of the heparin receptor detects TMEM184A
 150 mm dishes of (A) BAOECs and (B) BAOSMCs were harvested for immunoprecipitation as described in methods section. Cell lysates were incubated with (A) VE-cadherin or (B) IRS-1 antibodies as IP controls or monoclonal antibodies developed against the heparin receptor ((A) 12B1 and 18E9 or (B) 18B6 and 18H6) and purified using EZview affinity beads. The antibodies listed at the top are the antibodies used for the Western Blot, while the antibodies (shown on an angle) below that are the antibodies used for the IP. The VE-cadherin antibody is goat, the IRS-1 antibody is rabbit, and the heparin receptor antibodies are mouse monoclonals. One-fourth of the final sample was run on a single lane of an SDS-PAGE. Blots were developed using ExtraAvidin™ alkaline phosphatase, BCIP, and NBT, and converted to grayscale for post-hoc analysis.

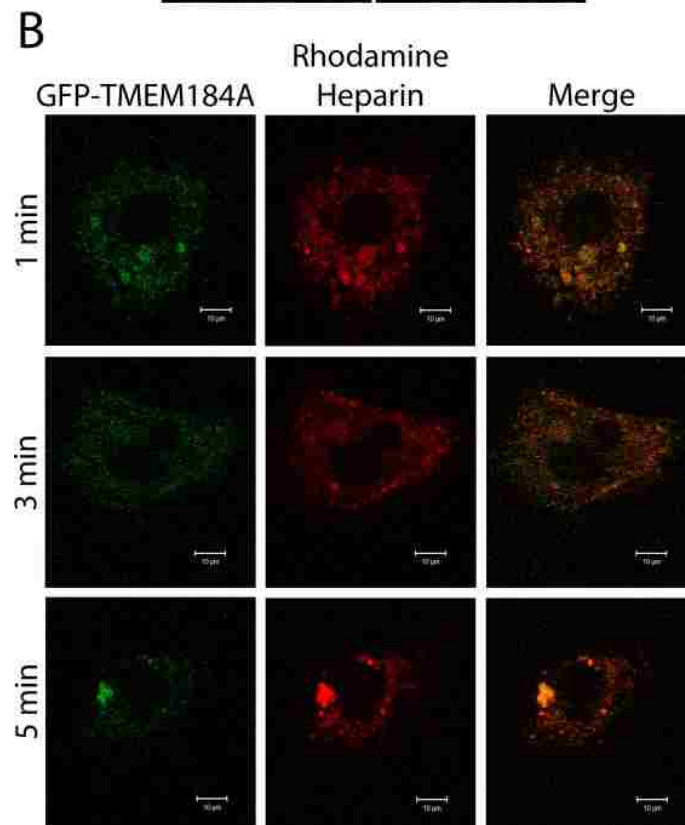
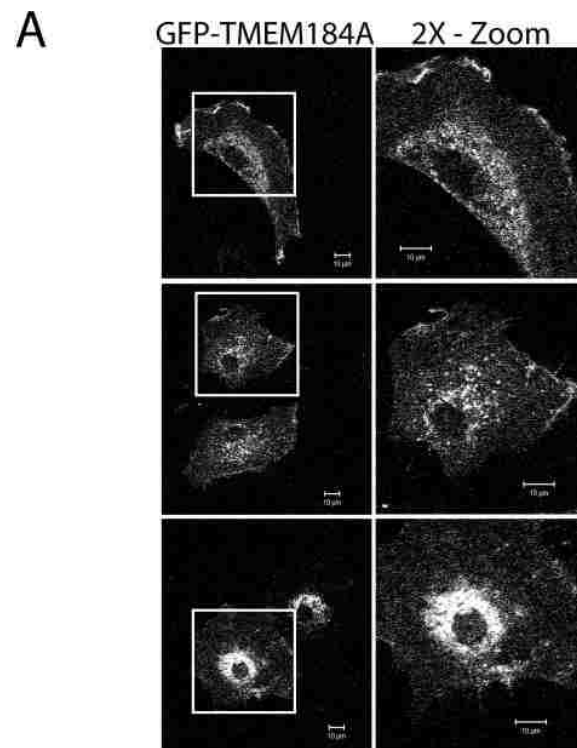


Figure 5.9: GFP-Tagged TMEM184A co-localization with Rhodamine-Heparin
(A) A7r5s were electroporated with 20 $\mu\text{g/ml}$ of GFP-TMEM184A and allowed to proliferate for 48 hr, following which they were fixed with 4% PFA and not permeabilized. Right column is magnified 2X the original boxed area on the left.
(B) A7r5s electroporated with GFP-TMEM184A as in (A) were treated with 100 $\mu\text{g/ml}$ Rhodamine-Heparin for the times indicated, following which they were fixed with 4% PFA and not permeabilized. All images are magnified 2X the original for clarity. Images are representative of two repeats. Scale bars = 10 μm .

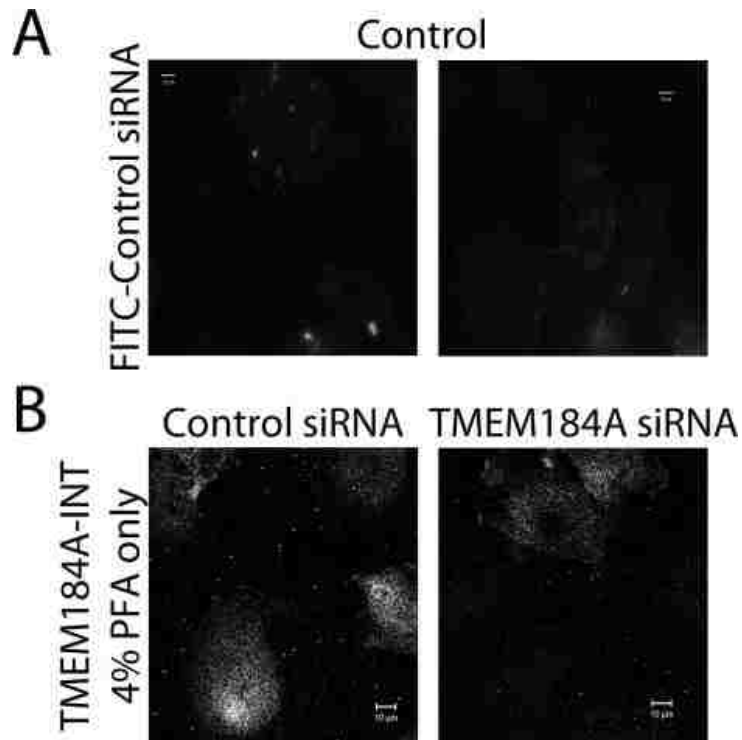
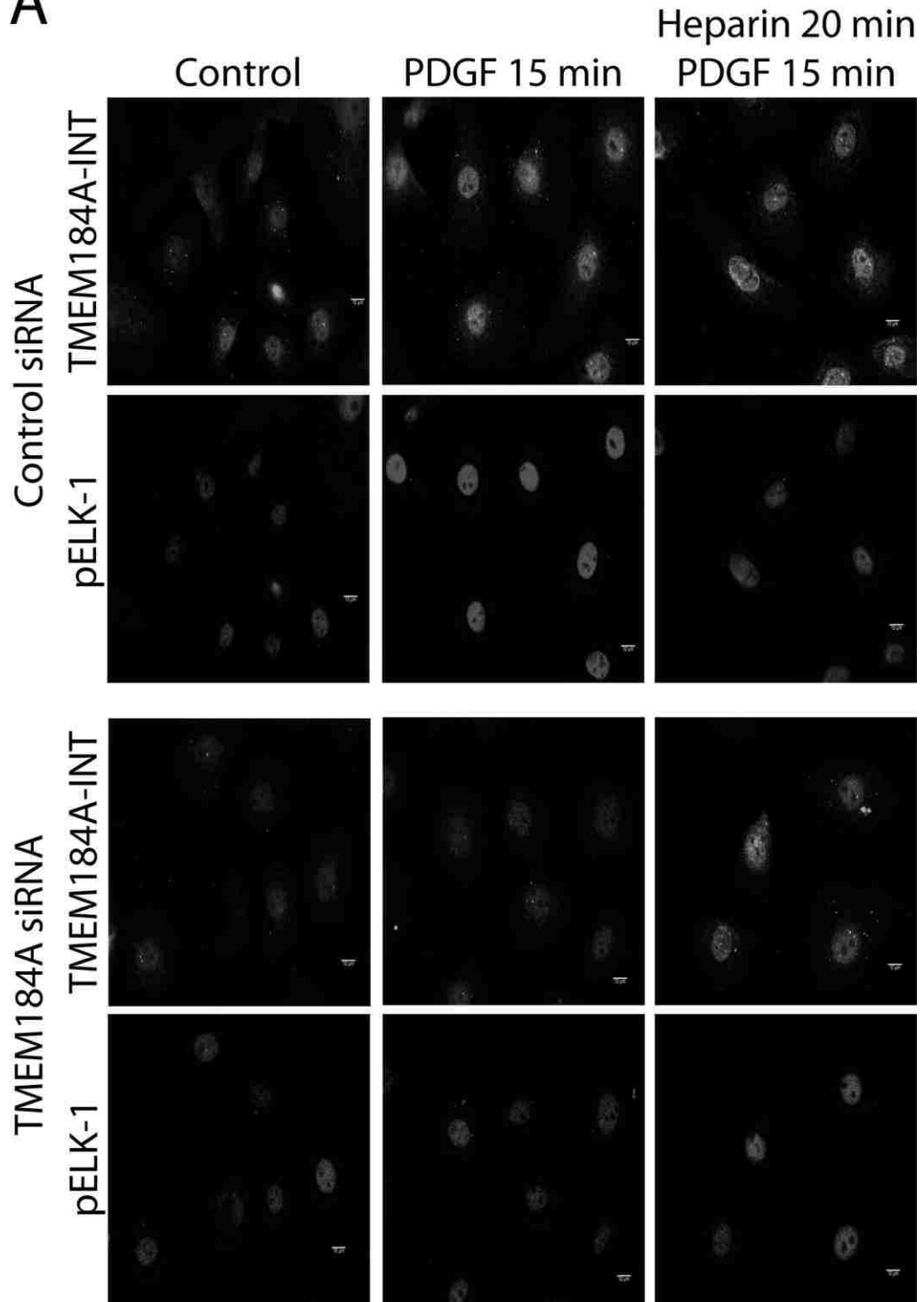


Figure 5.10: Validation of FITC-Control siRNA uptake and decreased TMEM184A surface staining in cells exposed to TMEM184A siRNA
A7r5s were electroporated with 20 $\mu\text{g/ml}$ FITC-control siRNA as described in the methods section (A). A7r5s were electroporated with untagged control siRNA or TMEM184A siRNA and cells were fixed with 4% PFA but not permeabilized and stained for TMEM184A-INT on the surface of cells (B). Images are representative of two repeats. Scale bars = 10 μm .

A



B

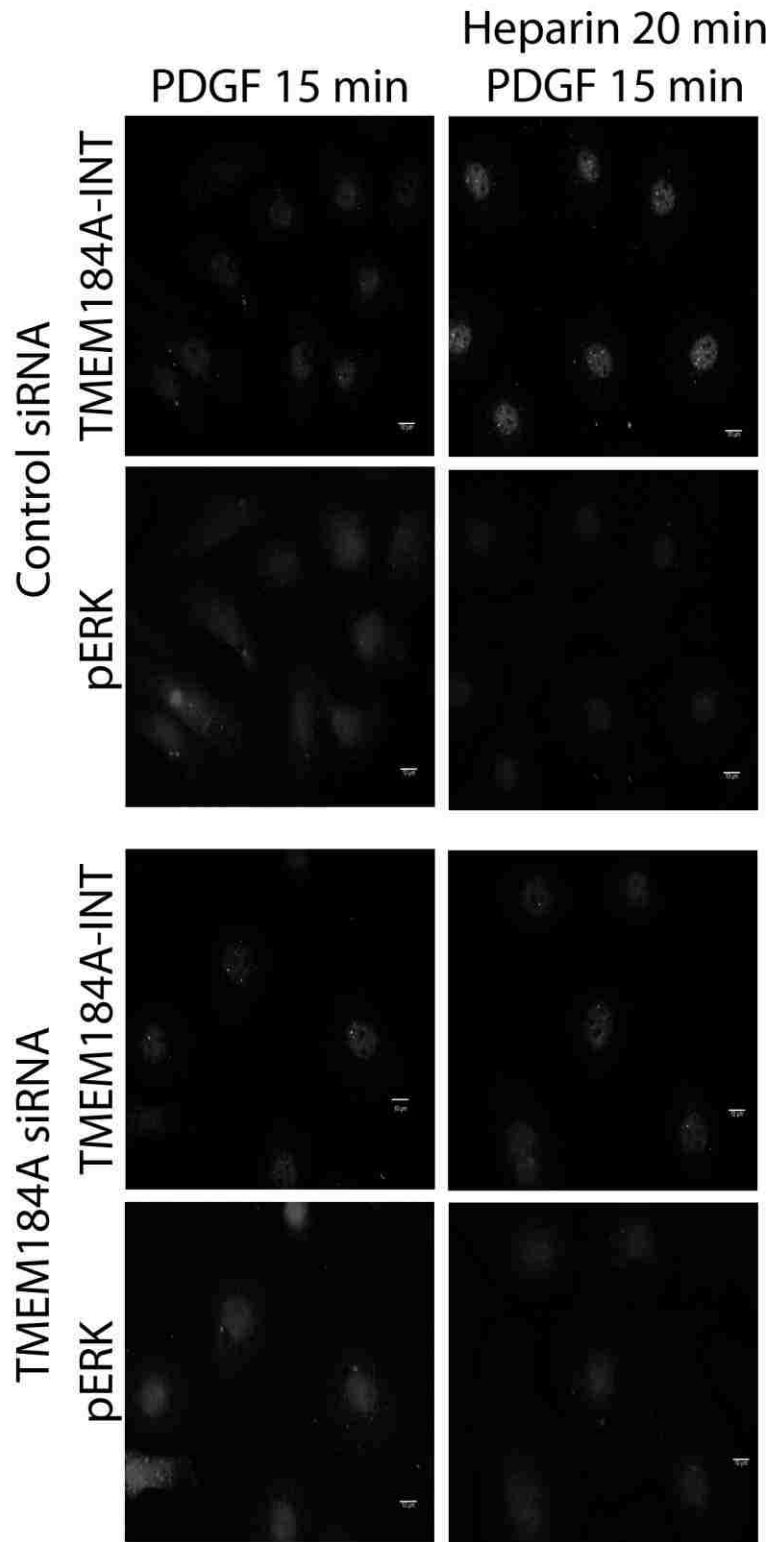


Figure 5.11: siRNA-mediated knockdown of TMEM184A in A7r5s
A7r5s were electroporated with control siRNA or TMEM184A siRNA as described in the methods section. Cells were fixed with 4% PFA and permeabilized with 0.3% Triton and stained for pElk-1 (A) and pERK (B) along with TMEM184A to judge knock down efficacy. Images are representative of three repeats. Scale bars = 10 μ m.

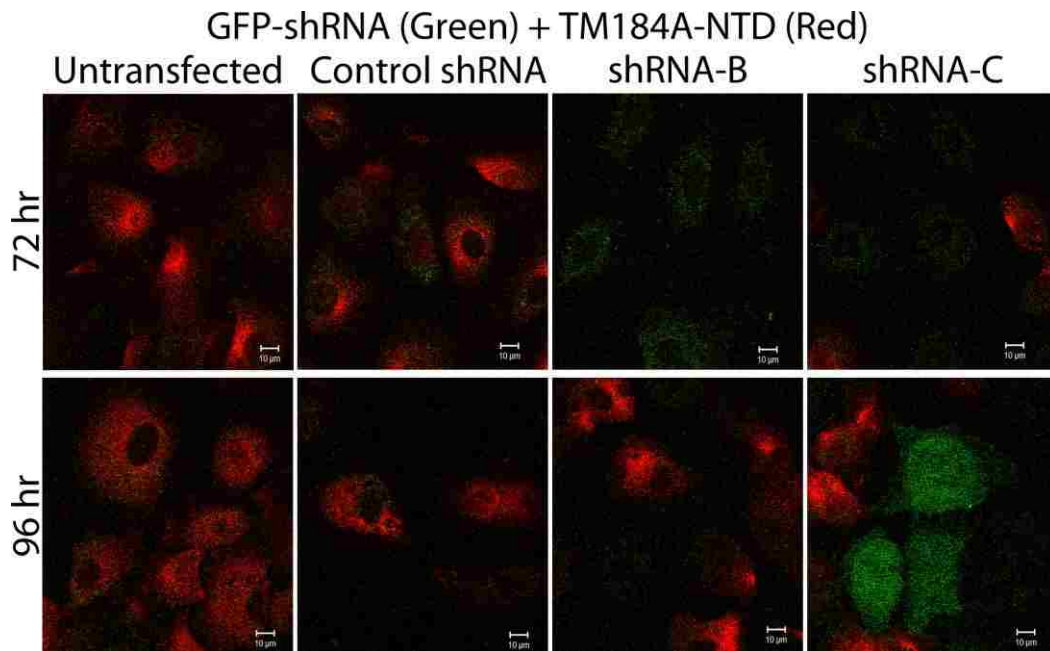


Figure 5.12: shRNA-mediated knockdown of TMEM184A in A7r5s
A7r5s were electroporated with 20 µg/ml of GFP-tagged constructs containing shRNA expression sequences (scrambled control shRNA, shRNA-B, or shRNA-C) and allowed to proliferate for 72 hr or 96 hr. Cells were fixed with 4% PFA but not permeabilized and stained for TMEM184A-NTD (red) mostly on the cell surface. Untransfected control cells were included for comparison. Images are representative of three repeats for 72 hr and one repeat for 96 hr. Scale bars = 10 µm

Chapter 6: Heparin regulates specific genes in vascular smooth muscle cells

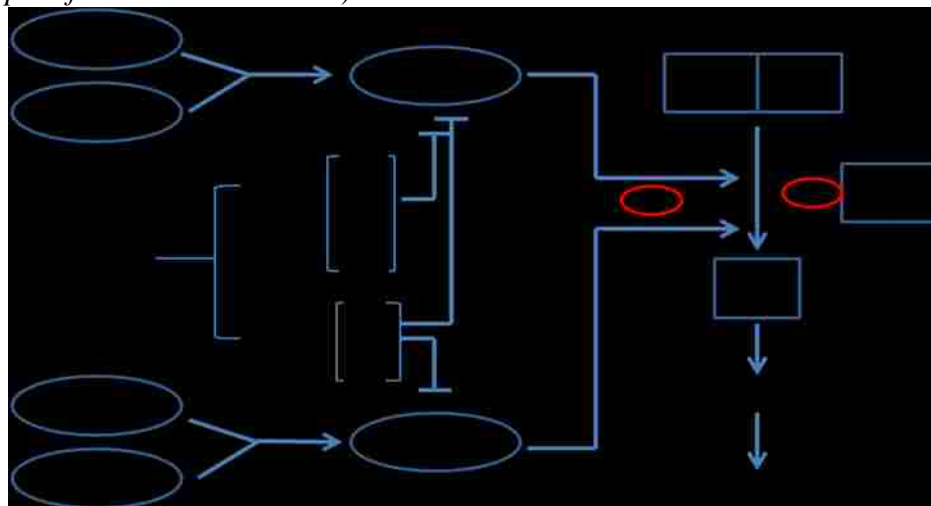
6.1: Introduction

Most smooth muscle cells in the adult vascular system are in a quiescent state, typically arrested in the G_0 or G_1 phases of the cell cycle. As mentioned previously, smooth muscle cells in atherosclerotic vasculature exit their quiescent state and enter a proliferative state. Progression through the cell cycle is driven primarily by the interaction of cyclin-dependent kinases (CDKs) and their regulatory subunits, the cyclins. Cyclin-CDK complexes induce the activation of transcription factors, ultimately resulting in progression through the cell cycle, cell growth, and cell proliferation (Fouty BW et al. 2001). Looking specifically at the G_1 -S transition, important cyclin-CDK complexes include cyclin D-CDK4/6 and cyclin E-CDK2, which are involved in phosphorylating and inactivating the Rb (retinoblastoma) protein, an inhibitor of E2F (Yu L et al. 2006 and Fouty BW et al. 2001). Once phosphorylated Rb dissociates from E2F, allowing E2F to carry out its function of inducing transcription of genes responsible for cell proliferation (Figure 6.1) (Yu L et al. 2006 and Fouty BW et al. 2001).

There are multiple levels of regulation over the cell cycle, including the expression of phase-specific cyclins, which are degraded when no longer necessary. An additional level of regulation is a class of negative regulators of cyclin-CDK complexes, CDK inhibitors (CKIs), which inhibit the phosphorylation of specific cyclin-CDK complexes (Yu L et al. 2006 and Fouty BW et al. 2001). By inhibiting cyclin-CDK complexes, CKIs can be considered anti-proliferative, because they block progression through the cell cycle. CKIs are broken into two families, the INK4 family (p15, p16, p18, p19) and the Cip/Kip family (p21, p27, and p57) (Yu L et al. 2006). The INK4

family of CDKIs is known to inhibit cyclin D-CDK4/6 complexes, while the Cip/Kip family of CDKIs is known to inhibit cyclin E-CDK2 and cyclin D-CDK4/6 complexes (Yu L et al. 2006). Regardless of cyclin-CDK complex inhibited, both families block the phosphorylation of Rb, maintaining E2F bound Rb, and preventing cell cycle progression and subsequent growth and proliferation (Figure 6.1) (Yu L et al. 2006 and Fouty BW et al. 2001).

Figure 6.1: Regulation of the G₁ to S cell cycle transition
(Adapted from Yu L et al. 2006)



As discussed previously, heparin has been shown to have anti-inflammatory characteristics in cells of the vasculature. In VSMCs, heparin exerts an anti-proliferative effect via at least two mechanisms. The two primary mechanisms include the regulation of MAPK cascade intermediates (Yu L et al. 2006), which are involved in cell growth and proliferation and by imposing a cell cycle block at the G₁ phase through up-regulation or down regulation of specific genes and proteins necessary for the transition from the G₁ to S phase (Reilly CF et al. 1989, Fasciano S et al. 2005, Vadiveloo, PK et al. 1997). This cell cycle block can be at least partially explained by an increase in heparin-

induced MKP-1 increase resulting in less active ERK and decreased cell proliferation (Blaukovitch CI et al. 2010 and Dickinson RJ and Keyse SM 2006). Along with inducing MKP-1 protein synthesis, heparin also down-regulates Raf activity, a kinase upstream of ERK, by inhibiting its phosphorylation (Pukac LA et al. 1997, Dhillon AS et al. 2007, and Slee JB, Pugh R, Lowe-Krentz LJ 2012). Along with regulation of MAPK kinase cascade intermediates, it has been reported that heparin treatment causes rapid down-regulation of mRNA levels of genes involved in the regulation of cell proliferation, including *c-fos*, *c-jun*, *myb*, and *myc*, again decreasing cellular proliferation in VSMCs (Mishra-Gorur K and Castellot JJ, 1999). The second mechanism through which heparin exerts its anti-proliferative effects in VSMCs is by imposing a cell cycle block at the G₁ phase (Fasciano S et al. 2005, Vadiveloo PK et al. 1997, Reilly CF et al. 1989). Most smooth muscle cells in the adult vascular system are in a quiescent state, typically arrested in the G₀ or G₁ phases of the cell cycle. VSMCs in atherosclerotic plaques are highly proliferative and migratory, accounting for large portion of the plaque mass (Ross R 1993 and Ross R 1999).

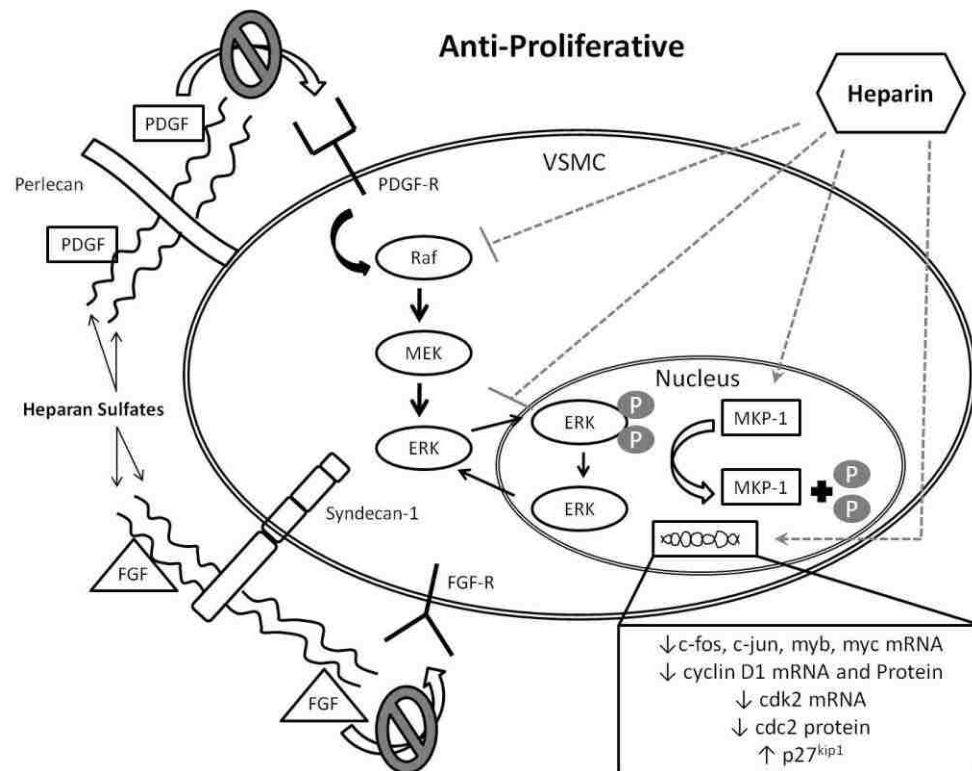
Research has shown that heparin strongly down-regulates the levels of cyclin D1 mRNA and protein, cdk2 mRNA, and cdc2 protein to achieve this cell cycle block (Vadiveloo PK et al. 1997). One CDKI up-regulated by heparin treatment is p27^{kip1}. This accumulated p27^{kip1} protein level prevents the activation of Cdk2, blocking S phase entry (Fasciano S et al. 2005, Yu L et al. 2006, and Fouty BW et al. 2001). Fasciano S and colleagues (2005) noted that heparin treatment did not affect p27^{kip1} mRNA levels at 12 and 18 hr of treatment, suggesting that heparin is mediating this affect post-

transcriptionally by stabilizing p27^{kip1} protein. The post-transcriptional regulation of p27^{kip1} raises the possibility that heparin could be regulating other genes in this manner rather than solely regulating gene expression.

MKP-1 activity has been shown by our lab to be up-regulated by heparin treatment leading to decreased ERK activity and thereby decreased cell proliferation (Blaukovitch CI et al. 2010). Additional unpublished data from our lab suggests that MKP-1 gene transcription occurs in response to heparin treatment. Treatment of smooth muscle cells with actinomyosin D and /or doxorubicin both of which block transcription, block MKP-1 synthesis. Other unpublished data suggest that blocking translation blocks the heparin-induced MKP-1 increase. These observations suggest that both transcription and translation are necessary to get the increase in MKP-1 in response to heparin treatment, but do not rule out transcript stability or sequestration. Therefore, the targeted RT-PCR, PCR arrays, and microarray analyses all included MKP-1 to determine if heparin up-regulated DUSP1/MKP-1 gene expression

Although much of the literature focuses on exogenous heparin treatment for therapeutic benefit, endogenous heparan sulfates also possess anti-proliferative properties in VSMCs. Along with exogenous heparin; certain endogenous heparan sulfates are anti-proliferative. Both endogenous perlecan and syndecan-1 inhibit VSMC proliferation (Kinsella MG et al. 2003 and Fukai N et al. 2009), and perlecan has been shown to sequester FGF2 from binding to its receptor (Tran PK et al. 2004). The anti-proliferative effects of heparin/heparin sulfates are summarized in Figure 6.2 (reviewed in: Slee JB, Pugh R, and Lowe-Krentz LJ 2012).

Figure 6.2: Data from the literature indicate that exogenous heparin and endogenous heparan sulfates are anti-proliferative in VSMCs (Adapted from: Slee JB, Pugh R, Lowe-Krentz LJ 2012)



Given the trend for potential heparin-induced gene expression changes, I aimed to investigate global gene expression (microarray), pathway specific gene expression (PCR arrays) and targeted gene expression (RT-PCR). Using these three techniques, I have identified many genes which are regulated by heparin, expanded our understanding of heparin-induced MKP-1 activity, and determined that two CDKI genes are not regulated by heparin treatment. The PCR arrays and targeted RT-PCR analyses also served to validate three genes from the microarray.

6.2: Methods

6.2.1: Cell Culture

A7r5s and RAOSMCs were used for gene expression analyses. For RT-PCR, PCR Arrays, and microarray analysis cells were grown to approximately 70-80% confluency, to ensure that cells were still in a proliferative state. In some experiments cells were synchronized via serum starvation for 2 days prior to experimentation. In these cases, cells were rinsed with EDTA prior to serum starvation to remove any remaining serum from the culture medium and fresh serum-free media was added.

6.2.2: Heparin Treatment for PCR Arrays

100 mm dishes of proliferative A7r5s (not synchronized via starvation) were used as starting material for PCR array analysis. Cells were treated with 200 µg/ml heparin for a single time point of 30 min and harvested according to the RNA isolation protocol outlined in Appendix I.

6.2.3: Heparin and Serum Treatment for Short-Term RT-PCR

100 mm dishes of A7r5s were synchronized via starvation for 2 – 3 days and used as starting material for RT-PCR analysis. Cells were treated with 200 µg/ml heparin for 20 min prior to 10% serum addition. Serum incubation varied from 10, 15, 20, and 30 min durations to optimize serum induction. RNA was isolated using the isolation protocol outlined in Appendix I.

6.2.4: Heparin Treatment for Long-Term Microarray Analysis

100 mm dishes of RAOSMCs were used as starting material for microarray analysis. RAOSMCs were kept in fully supplemented MEM media to allow for

microarray analysis of the effects of heparin in proliferative cells. Once the cells reached ~70-80% confluency, cells were treated with 200 µg/ml heparin for 24 hr and RNA was isolated using the protocol outlined in Appendix I.

6.2.5: SDS-PAGE and Western Blotting

In many cases, a Western Blot experiment was run in parallel to gene expression analysis to ensure the cells were heparin sensitive. In these instances, the experimental design was identical up to isolation of total RNA or protein. If the cells demonstrated heparin sensitivity, as indicated by heparin-induced decreases in pERK band intensity relative to control and serum only bands, then the experiment was allowed to proceed. SDS-PAGE and Western blotting were performed as described in Chapter 2 using the alkaline phosphatase detection method.

6.2.6: RNA Isolation and Processing

The methodology for RNA isolation, reverse transcription, RNA quality control, RT-PCR experimental set-up, cycling conditions, and PCR array analysis are described in Appendix I. In all cases (RT-PCR analysis, PCR arrays, and microarray) RNA was isolated from 100 mm dishes of A7r5s or RAOSMCs using the Qiagen RNeasy total RNA isolation kit with the optional on-column DNase digestion according to the manufacturer's recommended protocol. For the RT-PCR and microarray analysis, reverse transcription was carried out using Invitrogen's SuperScript III First-Strand Synthesis Super Mix according to Invitrogen's recommended protocol. For PCR arrays, reverse transcription was done using SABiosciences reverse transcription reagents according to their protocol.

6.2.7: RT-PCR Data Analysis ($2^{-\Delta\Delta C_T}$)

RT-PCR data was analyzed using fold change relative to GAPDH control. To calculate fold change: First calculate ΔC_T from raw C_T within a time point and replicate ($C_{T \text{ DUSP1}} - C_{T \text{ GAPDH}}$). Average ΔC_T value of control (DUSP1) across replicates, then calculate $\Delta\Delta C_T$ using this average control ΔC_T of DUSP1 ($\Delta C_{T \text{ DUSP1 EXPERIMENTAL}} - \Delta C_{T \text{ DUSP1 CONTROL}}$). Use this value to calculate fold change ($2^{-\Delta\Delta C_T}$). Fold change values were averaged and statistics were run across triplicates.

6.2.8: Microarray Analysis

Total RNA was isolated from RAOSMCs and quality was determined as described in Appendix I. Once total RNA was determined to be of high quality and yield, it was sent to Genome Explorations (Memphis, TN), an authorized service provider of Affymetrix microarrays. The Affymetrix GeneChip® Rat Gene 1.0 ST Array was used to determine heparin-induced gene expression in proliferative RAOSMCs treated with heparin for 24 hr relative to untreated control. Additional quality control measures were completed by Genome Explorations prior to RNA amplification, tagging, and hybridization. Genome Explorations performed all data analysis and provided a data package including significant gene changes, clusters of regulated genes, regulated pathways, as well as all of the raw data.

6.3: Results

6.3.1: PCR Array data suggests that only a few of the selected genes are regulated by heparin

All genes investigated in the PCR arrays are listed in Appendices II and III. Two separate PCR arrays were performed, one representing genes from the MAPK signaling cascade (Figure 6.3) and one representing genes from the epidermal growth factor (EGF) and platelet-derived growth factor (PDGF) signaling cascades (Figure 6.4). The PCR arrays were formatted for gene expression analysis in 96 well plates. Necessary controls account for six of those wells, leaving 90 genes for analysis. Since two PCR arrays were used, this allowed for the analysis of 180 genes that were picked based largely on known heparin signaling pathways. The results of both microarrays seem to suggest that heparin treatment for 30 min does not regulate a significant number of genes, since only 8 of the 180 (~4.4%) genes tested were heparin sensitive. These genes include MAPK10 (JNK3) – increased 2.07 and 1.63 fold, KCNH8 – decreased 2.54 fold, PDGFRA – decreased 5.94 fold, EGF – decreased 2.54 fold (Figure 6.1), MAP4K1 (kinase upstream of ERK) – increased 2.31 fold, MAPK13 (p38 Δ) – increased 3.61 fold, CDKN1C (p57^{kip2}) – increased 2.29 fold, and MAPK8ip2 (JIP1) – increased 3.07 fold (Figures 6.3 and 6.4).

More importantly than what the PCR array data showed as regulated by heparin was what they showed that was not regulated by heparin. These two arrays were chosen because they contained a number of cell cycle regulatory proteins. The data suggest that very few of the cell cycle regulatory proteins (cyclins, CDKs, and CDKIs) were regulated by heparin under these conditions. These results suggest that at shorter time points (less

than 30 min), heparin does not regulate mRNA level changes but possibly protein stability as seen with p27^{kip1} (Fasciano S et al. 2005).

6.3.2: PCR Array data and targeted RT-PCR data suggest that heparin does not regulate MKP-1 by control of mRNA levels

Of particular interest in the EGF/PDGF PCR array was the DUSP1 gene, which codes for MKP-1 protein. In fact, this array was chosen because it included DUSP1. As previously discussed, MKP-1 activity is up-regulated in response to heparin treatment and other data collected from the lab suggest that MKP-1 mRNA levels would be a good candidate to be regulated by heparin. However, the DUSP1 PCR array sample showed an insignificant fold change (-1.25) relative to untreated control, suggesting that DUSP1 mRNA level is not regulated by heparin. To further investigate and to validate the PCR array data, targeted gene expression analyses were performed for DUSP1 using Qiagen's SYBR green chemistry and RotorGene RT-PCR equipment. Two representative graphs are shown in Figure 6.5. The results consistently suggest that DUSP1 mRNA level is not regulated by heparin, as shown by fold change values which are not significantly different from control nor significantly different among or within treatment groups. Taken together, these data suggest that DUSP1 gene expression is not regulated by heparin and it is likely the case that heparin regulates DUSP1 protein stability as seen with other heparin-sensitive proteins (Fasciano S et al. 2005). Considering previous data collected by other lab members, it appears that continued MKP-1 synthesis and protein stability are required for heparin-induced MKP-1 activity, but increased DUSP1 expression is not required.

6.3.3: Microarray data agrees with PCR Array and targeted RT-PCR analyses of DUSP1, CDKN1B (p27^{kip1}), and CDKN1C (p57^{kip2})

The microarray data obtained from Genome Explorations support the data collected from the PCR arrays and targeted RT-PCR analyses on DUSP1 and CDKN1B. The targeted RT-PCR analyses of CDKN1B consistently resulted in fold change values less than 1.5 fold across 10, 20, and 30 min of heparin treatment, suggesting that CDKN1B gene expression is not regulated by heparin, agreeing with previously published reports (Fasciano S et al. 2005). The C_T values from the microarray for CDKN1B were 11.43 vs. 11.27 (control vs. heparin) suggesting an extremely small fold change value (which is not reported by Genome Explorations due to this fact). The targeted RT-PCR data for DUSP1 is shown in Figure 6.5, which is similar to the data obtained from the microarray (control: 12.95 vs. heparin 13.15), further suggesting that DUSP1 mRNA is not regulated by heparin.

A third gene was investigated to validate the PCR array and microarray data. CDKN1C (p57^{kip1}) was shown to be significantly increased by 2.29 fold in the MAPK PCR array but was not included in the EGF/PDGF PCR array. Therefore, targeted RT-PCR was performed with primers specific for CDKN1C. The results obtained from these studies consistently yielded fold change values less than 1.5 fold, which was considered to be a non-significant fold increase (data not shown). The experiment was carried out as done for DUSP1 (results shown in Figure 6.5) and resulted in the similar non-significant fold change values within experimental groups. The C_T values from the microarray

(control: 8.57 vs. heparin: 8.61) agree with the data collected from the RT-PCR analyses, suggesting that CDKN1C mRNA levels are not regulated by heparin treatment.

It is important to note that there was an experimental difference in the microarray compared to the PCR arrays and RT-PCR analyses. The microarray was performed in proliferative RAOSMCs treated with 200 µg/ml heparin for 24 hr. The PCR arrays were performed in proliferative A7r5s treated with 200 µg/ml heparin for 30 min. In the targeted RT-PCR analyses, A7r5s were treated with the same concentration of heparin for 20 min in cells synchronized by starvation and serum stimulated for times less than 30 min. The experiments were carried out in this way for multiple reasons. First, the PCR arrays and RT-PCR analyses were carried out first, leading me to believe that shorter time points may not be sufficient to see significant gene expression changes, given that very few genes changed. Second, I wanted to keep the PCR arrays and microarray as simple as possible to avoid inclusion of variables that could confound post-hoc data analysis. Third, I switched from the A7r5 cloned rat line to primary RAOSMCs to avoid any issues stemming from using a cloned line for gene expression work.

Regardless of the differences in experimental design, all three techniques yielded similar results. Heparin does not regulate DUSP1, CDKN1B, or CDKN1C mRNA levels. The data from the microarray showed that mRNA levels of these three genes did not significantly change in heparin-treated cells (C_T values: DUSP1 – control: 12.95 vs. heparin: 13.15, CDKN1B – control: 11.43 vs. heparin: 11.27, and CDKN1C – control: 8.57 vs. heparin: 8.61). Taken together, the data suggest that heparin does not regulate the mRNA levels of these genes, but instead could regulate protein stability, protein turnover,

or translation. It is likely that heparin regulates the stability of these transcripts or proteins via a similar mechanism which was shown for p27^{kip1} (CDKN1B) (Fasciano S et al. 2005).

6.3.4: Microarray data suggest heparin up-regulates gene expression

Given the colossal nature of the microarray data, all of the raw data cannot be included in this dissertation. Instead, I've organized the data in a few logical ways. First, I've included flow charts highlighting pathways that were regulated (Figure 6.6 A, B, and C). Second, I've listed all of the pathways that contained at least 2 genes that were significantly regulated (Table 6.1). Lastly, I've listed all genes with a fold change of ≥ 1.5 which have also been identified by Genome Explorations as significant fold change values (Table 6.2). Having the data organized in these ways should provide an overview of heparin-induced gene expression changes at the pathway level and provide detailed analysis of selected individual genes within those pathways. This should provide a broad view of heparin-induced gene expression changes and leave room for discussion of select heparin-sensitive genes.

As shown in Figure 6.6, I've highlighted what Genome Explorations called biological processes (A), molecular functions (B), and cellular components (C) that were regulated by heparin. Only a small subset of the significantly regulated pathways are highlighted within each grouping. Within Biological processes, 10 genes were regulated that are involved in blood circulation, three of which are involved in blood vessel remodeling (Figure 6.6A). The largest grouping of regulated genes was in the cell surface receptor signaling family, in which 29 genes were regulated (Figure 6.6A). Interestingly,

the last group within biological processes contained three genes that were responsive to laminar fluid shear stress, helping to connect my fluid shear stress project with heparin regulation. As shown in Figure 6.6B, a small subset of molecular functions were regulated by heparin and included receptor serine/threonine kinase binding and endopeptidase inhibitor activity. This section seems to suggest that only a small number of peptidase inhibitors were regulated by heparin and this is in fact not true. There were a large number of peptidases and peptidase inhibitors that were significantly regulated by heparin. Lastly, as shown in Figure 6.6C, a small subset of cellular components were regulated and they include proteinaceous extracellular matrix (ECM) components and integrin complexes. Having the data organized in this way highlights three pathways that were significantly regulated by heparin. These three, however, only represent a small fraction of the pathways that were identified as significantly responsive to a 24 hr heparin treatment.

To dig deeper into the data, all signaling pathways/clusters with 2 or more genes that were heparin responsive are listed in Table 6.1. The pathway with the largest number of regulated genes (16) was the integrin family of cell surface interactions. This is followed by a variety of receptor mediated signaling pathways with 12 genes each (S1PI, PDGFR-beta, EGF receptor, and the LKB1-AMPK signaling pathways. These are only four of about 70 or so pathways that were identified as having significant heparin regulated gene expression occurring within their intermediates. There is also a variety of other pathways that are significantly regulated by heparin that bear mentioning. These include EGF receptor internalization and downstream signaling, protein inhibitor up-

regulation, proteoglycan signaling, TGFBR, and cell surface interactions with the vessel wall. This way of analyzing the data goes slightly deeper, still does not get us to specific genes, but suggests that heparin is involved in the regulation of many pathways and genes.

To further explore the microarray data, all genes which exhibited a fold change of ≥ 1.5 are shown in Table 6.2. Genome Explorations uses algorithms to predict fold changes above 1.0 to be significant, so I took it a step further and set the cut-off for significance to be a fold change of 1.5. This however does not imply that these fold changes are biologically significant, nor are they statistically significant. These fold changes appear to be significant within this microarray data set, as defined by Genome Explorations. Performing the analysis in this way provides a list of about 80 genes that are heparin sensitive. Included in this set are four separate serine or cysteine peptidase inhibitors, integrin alpha 7, oxidized low density lipoprotein (lectin-like) receptor 1, and guanylate cyclase 1 soluble beta 3. There were two genes that were most strongly induced by heparin treatment; these were the regulator of G-protein signaling 4 and asporin, fold change of 3.039 and 3.853 respectively.

Also consistent with the data obtained from the PCR arrays, the majority of gene expression altered by heparin was through up-regulation instead of down-regulation. Using ≥ 1.5 fold change as the cut-off, only one gene was significantly down-regulated by heparin treatment for 24 hr. Given the trend of heparin significantly up-regulating genes, the genes that were down-regulated by heparin were omitted from the data set and will not be discussed in this dissertation. It is also true that none of these down-regulated

proteins have established or related signaling pathways which have been linked to heparin signaling. Taken together, the gene expression analysis data suggest that heparin regulates quite a large number of genes mostly through up-regulation and that heparin may also regulate protein stability of certain proteins involved in heparin signaling.

6.4: Discussion

Although the microarray was performed last chronologically in this dissertation, the PCR array data and targeted RT-PCR data can be used to validate the microarray. The MAPK and EGF/PDGF PCR arrays were performed to gather preliminary data to ensure that pursuing heparin-induced gene expression changes were worthwhile. These arrays provided evidence of enough gene regulation to suggest that further analysis was necessary. Although an educated guess was made that the MAPK and EGF/PDGF arrays would produce the largest number of regulated genes, this was in fact not the case. These arrays produced only 8 genes that were significantly altered by a 30 min heparin treatment. However, these arrays did investigate three genes of interest for this dissertation. As mentioned in the results section, these genes were DUSP1 (MKP-1), CDKN1B (p27^{kip1}), and CDKN1C (p57^{kip2}), all of which were good candidates for heparin regulation.

MKP-1 activity has been shown by our lab to be up-regulated by heparin treatment leading to decreased ERK activity and thereby decreased cell proliferation (Blaukovitch CI et al. 2010). Additional unpublished evidence from our lab suggested that MKP-1 gene transcription was occurring in response to heparin treatment, but could

not rule out transcript stability or sequestration. As discussed previously, these unpublished data included the observation that actinomycin D and doxorubicin (chemicals which block transcription) block DUSP1 synthesis and the observation that blocking translation also blocks the heparin-induced MKP-1 increase. These observations along with the fact that MKP-1 has a very short half-life suggest that both transcription and translation are necessary to get the increase in MKP-1 in response to heparin treatment, but do not rule out transcript stability or sequestration.

The collection of MKP-1 data from this dissertation strongly support a model where DUSP1/MKP-1 mRNA is not regulated by heparin. The lack of heparin-induced changes in mRNA levels were consistently shown across three different methods of assaying heparin-induced gene expression changes. The DUSP1/MKP-1 mRNA data collected herein; do not disagree with the unpublished data collected by other lab members, rather suggest that continued basal DUSP1 gene expression and some level of protein stabilization is required for the heparin-induced MKP-1 activity increases.

CDKN1B (p27^{kip1}) was investigated as a gene for potential heparin regulation because it has been documented to be regulated by heparin. Previous reports have shown that heparin regulates p27^{kip1} transcript stability beyond 18 hr of heparin treatment (Fasciano S et al. 2005). However, I initially hypothesized that 18 hr of heparin treatment would be too long and immediate gene changes would be missed. The rationale behind this hypothesis is based on unpublished data showing that heparin-induced decreases in pERK and increases in MKP-1 can be seen as early as 10 min. These observations suggest that the signaling intermediates downstream of heparin react very quickly to

heparin treatment. Therefore, early mRNA level changes induced by heparin were investigated for CDKN1B.

Although built upon sound science, the original hypothesis was not supported. Rather the data indicate that changes in transcription for these genes are not induced by heparin. All three methods of assaying gene expression performed in this dissertation failed to show significant heparin-induced changes in CDKN1B gene expression. Regardless of whether cells were synchronized via starvation, were proliferative, treated with heparin for ≤ 30 min, or treated with heparin for 24 hr, no changes were observed. These findings do not conflict with the published report or the unpublished observations listed above. Rather it supports the case for CDKN1B to be regulated primarily by transcript accessibility over long-term heparin treatment (Fasciano S et al. 2005). The data showing that CDKN1B gene expression is not changed by 30 min or less of heparin treatment, suggests that if CDKN1B is involved in heparin-induced anti-proliferative effects in VSMCs it is through a mechanism enhancing the usage of existing transcript or protein stability.

The preliminary PCR arrays provided a second CDKI of potential interest for heparin regulation, CDKN1C (p57^{kip2}), a member of the same family as CDKN1B (p27^{kip1}), although no published evidence links CDKN1C and heparin signaling. This provided a candidate anti-proliferative gene whose transcription might be quickly increased by short-term heparin treatment, which could help to explain the fast heparin-induced alterations in pERK and MKP-1. Therefore, CDKN1C was selected for further analysis via targeted RT-PCRs. However, this hypothesis was not supported, because the

data collected from the targeted RT-PCRs and the microarray failed to show any heparin-induced changes in CDKN1C mRNA levels. It is possible that the observed differences in CDKN1C gene expression across analysis methods could be attributed to the experimental differences discussed in the results section. However, this is likely not the case, because the PCR arrays were performed on proliferative VSMCs as was the microarray, albeit at different heparin treatment times. If CDKN1C was truly regulated by heparin in proliferative cells, it would have come up by 24 hr of heparin treatment, because the anti-proliferative effects of heparin are sustained for much longer durations than 24 hr. Taken together, the gene expression analyses for CDKN1C suggest that the transcription of this gene is not regulated by heparin.

The microarray data for DUSP1 and CDKN1B agree with the PCR array and targeted RT-PCR data and the microarray data for CDKN1C agree with the RT-PCR data. The CDKN1C PCR array data point was determined to be an outlier and not representative of heparin regulation. These findings strengthen the conclusion that heparin does not significantly regulate these three genes in VSMCs. A current model which is in line with the data suggests that heparin regulates transcript and protein stability to facilitate, at least in part, its anti-proliferative effects in VSMCs. This has been shown to be the case for CDKN1B (Fasciano S et al. 2005) and is likely the case for DUSP1 and CDKN1C. Another possibility is that heparin could regulate transcript usage as well, which could also explain the results showing a lack of heparin-induced mRNA level changes.

The genes from the microarray analysis can be broken into four major categories of cell surface receptor signaling, peptidase activity, integrin complexes and signaling, and responses to fluid shear stress. Of particular interest to this dissertation are the responses to fluid shear stress and the regulation of cell surface receptor signaling. The response to laminar shear stress is interesting because it ties Chapter 3 into this chapter. Chapter 3 dealt with the atheroprotective nature of FSS in the vasculature, establishing a role for cofilin and actin realignment in endothelial barrier maintenance. The microarray identified that gene responses to laminar shear stress were also regulated by heparin, suggesting that the FSS experiments should be completed in the presence and absence of heparin to further determine their combined atheroprotective roles. This idea is being explored by Sara Lynn Nicole Farwell, who is interested in studying cellular responses to heparin and cytokines under physiologically relevant FSS conditions. This is an exciting area to explore, because the two fields have yet to be explored jointly and will undoubtedly yield promising data.

As mentioned, another interesting finding from the microarray was that heparin regulates a large amount of cell surface receptor signaling. The role of heparin in cell surface receptor signaling has been established for many receptors and signaling cascades, but the microarray provided many novel pathways that have not been studied in the context of heparin. As a preamble to this discussion, it is unknown as to whether heparin would exert its effects on these pathways through binding to a receptor altering downstream signaling cascade or if it would be due to growth factor sequestration or receptor binding enhancement. Both models have been demonstrated for various

signaling systems and are extensively documented in the literature (for review see Slee JB, Pugh R, and Lowe-Krentz LJ 2012).

The signaling molecule that is the highest interest to the work done in the lab is guanylate cyclase 1, soluble, beta 3 gene (GUCY1B3) which was up-regulated 1.714 fold by heparin treatment for 24 hr. GUCY1B3 is the beta subunit of soluble guanylate cyclase (sGC) which catalyzes the conversion of GTP to the second messenger cyclic GMP (cGMP), and functions as the main receptor for nitric oxide (NO). It has been shown that heparin signaling in VSMCs depends on cGMP and PKG (Gilotti AC *discovery* 2000 and Chapter 7). The finding that heparin up-regulates GUCY1B3 raises the possibility of a feed forward loop in which heparin increases cGMP to in turn increase PKG, thus strengthening the heparin responses in these cells. These data further support the conclusions drawn in Chapter 7, showing that PKG is involved in heparin signaling. The role of cGMP and PKG in heparin signaling will be discussed further in Chapter 7, however the finding that heparin increased GUCY1B3 is a biologically relevant finding of the microarray, raising the possibility of a feed forward signaling mechanism.

Another interesting finding is that the regulator of G-protein signaling 4 (RGS4) was increased 3.039 fold by heparin treatment for 24 hr in RAOSMCs. RGS4 is a member of a protein family which accelerates GTP hydrolysis by the alpha subunit of heterotrimeric G-proteins, thereby inactivating the G-protein and rapidly switching off GPCR signaling pathways (Gu S et al. 2009). Although not heavily cited in the literature, RGS4 is most well known for its role in endothelial cells where it has been shown that RGS4 over-expression antagonizes vascular endothelial growth factor (VEGF)

stimulation of DNA synthesis, ERK1/2 activation, and p38 MAPK activation, suggesting that RGS4 inhibits cell proliferation, migration, and invasion in endothelial cells (Albig AR and Schiemann WP 2005). While, it was initially thought that RGS4 was not expressed in cultured smooth muscle cells (Wieland T and Mittmann C 2003); it has since been shown to be expressed in VSMCs where it is involved in sphingosine-1-phosphate (S1P) signaling (Hendriks-Balk MC et al. 2008). Although further work is necessary to validate the RGS4 microarray data, it is an exciting possibility for being involved in heparin signaling because RGS4 has been shown to inhibit cell proliferation by antagonizing VEGF-stimulated cell proliferation and ERK activation in endothelial cells. If the same is true in VSMCs in response to heparin, this could provide another downstream target of heparin that leads to decreased cell proliferation by modulating DNA synthesis and ERK activity. Given that RGS4 is regulated by heparin, it is not surprising, that the S1P signaling pathway was a pathway with 12 genes which were regulated by heparin treatment for 24 hr.

Another interesting gene that was regulated by heparin and has interesting physiological implications for atherosclerosis was oxidized low density lipoprotein (lectin-like) receptor 1 (LOX-1), showing a fold change of 1.773 relative to untreated control. LOX-1 is a receptor which belongs to the C-type lectin superfamily that serves as the receptor for oxidized low-density lipoproteins (Mehta JL et al. 2006 and Li DY et al. 2002). LOX-1 has been extensively shown to be up-regulated in advanced atherosclerotic arteries and its inhibition has been associated with attenuation of the atherosclerotic process (Mehta JL et al. 2006 and Li DY et al. 2002). LOX-1 is thought to serve as a

central hub in atherosclerosis serving as the initial player in promoting endothelial cell dysfunction and apoptosis (Ulrich-Merzenich G and Zeitler H 2013, Li DY et al. 2002, and Mehta JL et al. 2006). LOX-1 expression has been shown to be regulated by a variety of factors such as cytokines and shear stress which are involved in atherosclerosis (Mehta JL et al. 2006), further suggesting the central role of LOX-1 in the progression of atherosclerosis. Aside from its known roles in endothelial cells, LOX-1 has also been shown to be involved in the proliferation, migration, and apoptosis of smooth muscle cells as well as other events critical to the pathogenesis of atherosclerosis (reviewed in: Xu S et al. 2012). Because LOX-1 has been linked to the development of atherosclerosis, it is interesting that heparin treatment would cause a moderate fold increase, given that LOX-1 inhibition has been strongly linked to protection against atherosclerosis. Clearly at this point, the mechanism behind heparin-induced LOX-1 expression is unknown, but this presents an exciting gene to explore given its role in atherosclerosis and recent excitement about finding drugs which could potentially inhibit LOX-1.

Not surprisingly, the integrin family was the pathway with the largest number of regulated genes (16 genes total). Of these 16 genes, 3 of them were regulated at a level greater than 1.5 fold, including integrin alpha 4 (1.612), integrin alpha 7 (1.699), and integrin beta-like 1 (2.049). As mentioned previously, two of the major hallmarks of atherosclerosis are vascular smooth muscle cell proliferation and migration to the site of injury. Both of which are strongly inhibited by heparin treatment (reviewed in: Slee JB, Pugh R, and Lowe-Krentz LJ 2012). Therefore it is logical that heparin would up-regulate certain genes that are involved in cell migration, such as the integrin family.

Integrin alpha 4 has been shown to associate with paxillin (Han J et al. 2001) which serves as a docking protein to recruit signaling molecules to focal adhesions (Schaller MD 2001). Paxillin also provides a link between integrins and the actin cytoskeleton, to facilitate cell spreading and motility (Schaller MD 2001). It has also been shown that inhibition of integrin alpha 4 association with paxillin inhibits integrin alpha 4-dependent cell proliferation (Liu S et al. 2002). Integrin beta-like 1 has also been associated with cell adhesion, proliferation, and migration (Humphries JD, Byron A, and Humphries MJ 2006). Lastly, integrin alpha 7 serves as the receptor for laminin in skeletal, heart, and smooth muscle cells and is involved in cell migration through the p130(CAS)/Crk protein complex (Mielenz D et al. 2001). Assuming the increased mRNA of these integrin components would equate to increased protein expression, it is clear that they could be involved in mediating heparin's effects on cell adhesion, proliferation, and migration.

Eluding to the notion that heparin may regulate protein stability and/or degradation, a large number of peptidase inhibitors were upregulated by a 24 hr heparin treatment. The following peptidase inhibitors were upregulated: serine (or cysteine) peptidase inhibitor clade A (1.528), serine (or cysteine) peptidase inhibitor clade B member 2 (1.603), serine (or cysteine) peptidase inhibitor clade A member 3N (1.685), serine (or cysteine) peptidase inhibitor clade B member 7 (1.702), serine (or cysteine) peptidase inhibitor clade A (1.791), and peptidase inhibitor 15 (2.163). Serine (or cysteine) peptidase inhibitors are often referred to as Serpins (Serine Protease Inhibitors) for short. Common Serpins include antithrombin (AT), heparin cofactor II (HCII), anti-trypsin, and protein C inhibitor (PCI) (Rein CM, Desai UR, and Church FC 2011). The

entire Serpin family share poor sequence homology but share a highly conserved core structure that is essential for their function as protease inhibitors, allowing for significant overlapping mechanisms of inhibition (Huntington JA 2011). The activity of most Serpins relies on glycoasminoglycans (GAGs), such as heparin or heparan sulfates, to reach physiological relevant rates of inhibition (Rein CM, Desai UR, and Church FC 2011 and Huntington JA 2011). The GAGs act as a bridge between the Serpin and the protease, allowing for faster complex formation, thereby strengthening the rate of inhibition (Rein CM, Desai UR, and Church FC 2011 and Huntington JA 2011). Perhaps the best characterized example of heparin interacting with a Serpin is AT. Heparin facilitates the interaction of AT with thrombin, inhibiting thrombin and subsequent thrombus formation (Huntington JA 2011). Therefore, it comes as no surprise that heparin treatment increased the mRNA level of various Serpins, due to their essential interaction with GAGs which is virtually required for inhibition of their target.

Lastly, a number of transcription factors were upregulated in response to 24 hr of heparin treatment. Most notably, these include the activating protein-1 (AP-1) transcription factor network, specifically fos-related antigen-1 and 2 (Fra1 and Fra2). AP-1 is an early response heterodimeric transcription factor composed of proteins belonging to the c-Fos, c-Jun, activating transcription factor (ATF), and jun dimerization protein (JDP) families (Karin M, Liu Zg, and Zandi E 1997). AP-1 is involved in cell proliferation, transformation, apoptosis, and inflammation (Shaulian E and Karin M. 2002 and Schonhaler HB, Guinea-Viniegra J, and Wagner EF 2011), suggesting that heparin could alter AP-1-induced gene expression to facilitate long term changes in

vascular smooth muscle cell physiology. Although further work is needed to validate the role of AP-1 in heparin signaling, it is an interesting avenue to explore in the future, because it could be the start of differentiation-related gene expression.

The collection of gene expression analyses performed within this chapter suggest that not only is heparin capable of regulating transcript and protein stability, but also regulating gene expression of a moderate number of genes. Of all genes tested, only 100 or so genes were significantly regulated by heparin, suggesting that heparin's effects are mediated by a small number of signaling molecules and pathways. The pathways represented overlap considerably with a single regulated gene being involved in multiple pathways, serving as cross-talk points between them. Another interesting conclusion that can be drawn from the data is that heparin seems to preferentially up-regulate gene expression rather than down-regulate it. Of the 100 or so genes that are significantly regulated by heparin, approximately 80 of them are up-regulated and only 20 of them are down-regulated, many of which are down-regulated at very small non-significant fold changes. Given the relatively small number of heparin-sensitive genes, there are a number of opportunities for future endeavors into further or understanding of non-traditional heparin signaling in vascular smooth muscle cells.

6.5: Figures

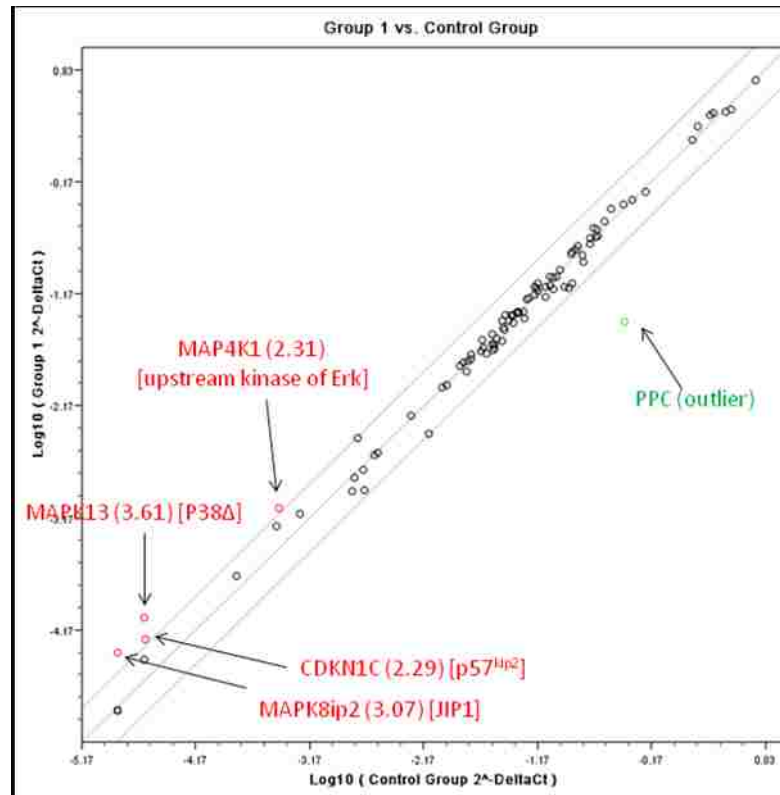


Figure 6.3: MAPK PCR array data highlights
Graph highlighting fold changes that were determined to be significant by SABiosciences analysis software. Gene falling with a range of ± 2 were highlighted in red (fold increase) or green (fold decrease).

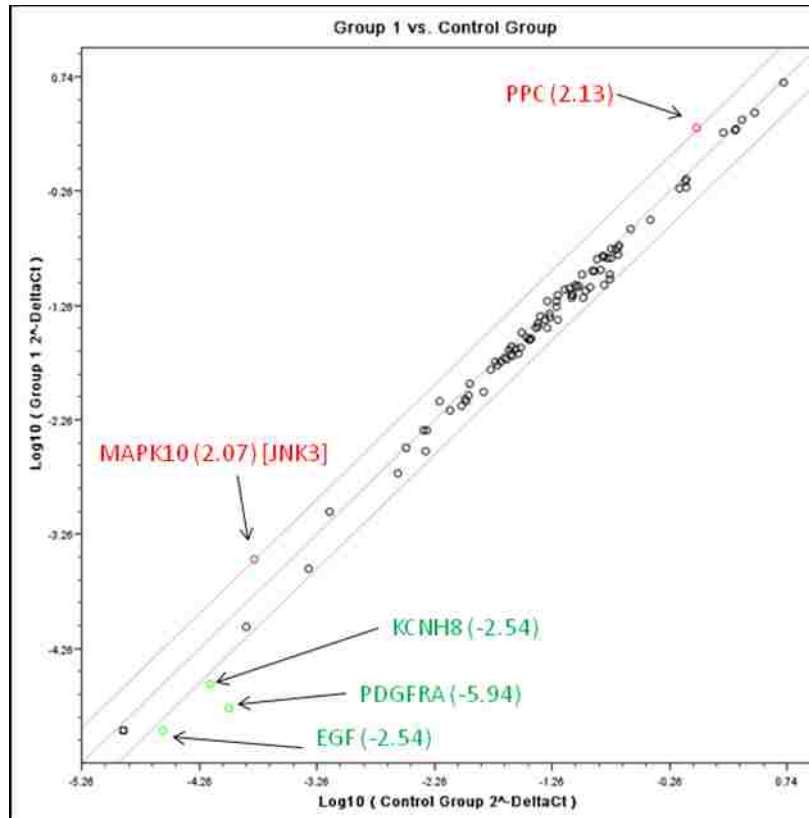


Figure 6.4: EGF/PDGF PCR array data highlights
 Graph highlighting fold changes that were determined to be significant by SABiosciences analysis software. Gene falling with a range of ± 2 were highlighted in red (fold increase) or green (fold decrease).

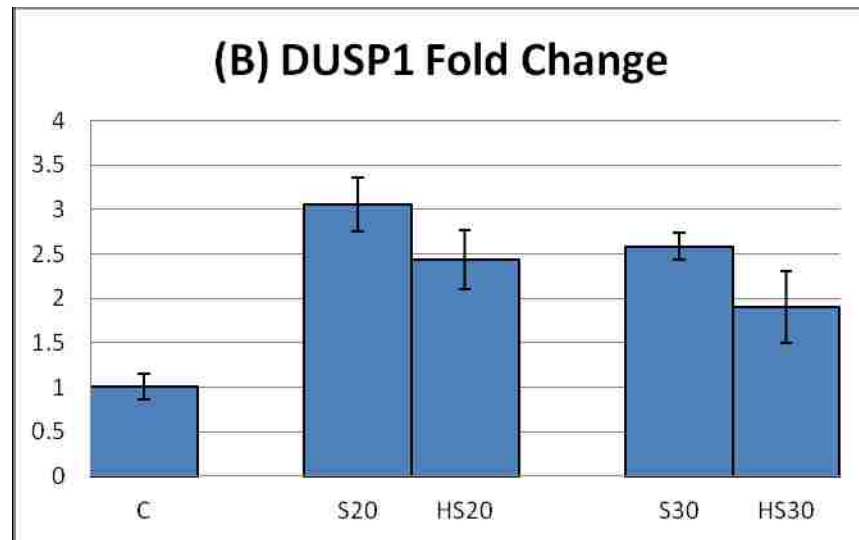
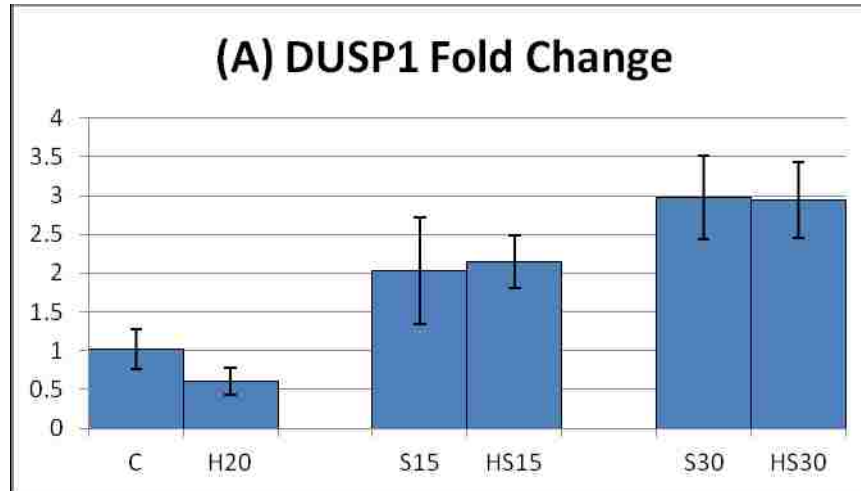


Figure 6.5: Short-term heparin treatment does not alter MKP-1 mRNA levels (A) and (B) show two representative repeats of at least five experiments of targeted MKP-1 gene expression changes induced by heparin. Fold change was calculated relative to GAPH control. (A) Control cells were untreated, H20 was a 20 min heparin treatment without serum, S15 was a 15 min serum treatment, HS15 was a 20 min heparin treatment prior to a 15 min serum treatment, and HS30 was a 20 min heparin treatment prior to a 30 min serum treatment. (B) The same experimental design as (A), but 20 and 30 min serum treatments were used. C = control, H = heparin, S = serum, HS = heparin + serum, # = duration of serum treatment in min.

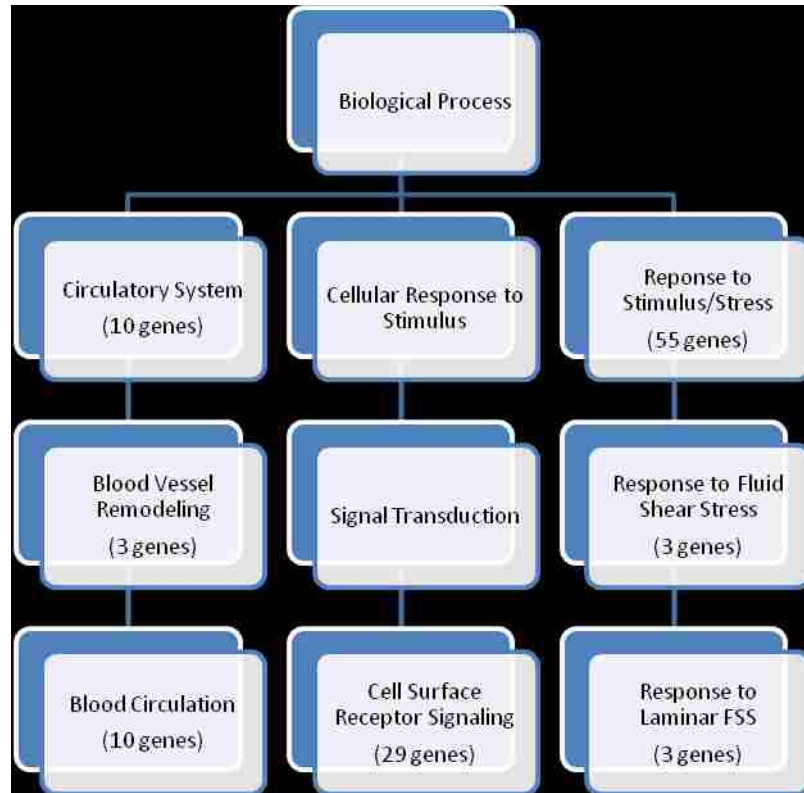
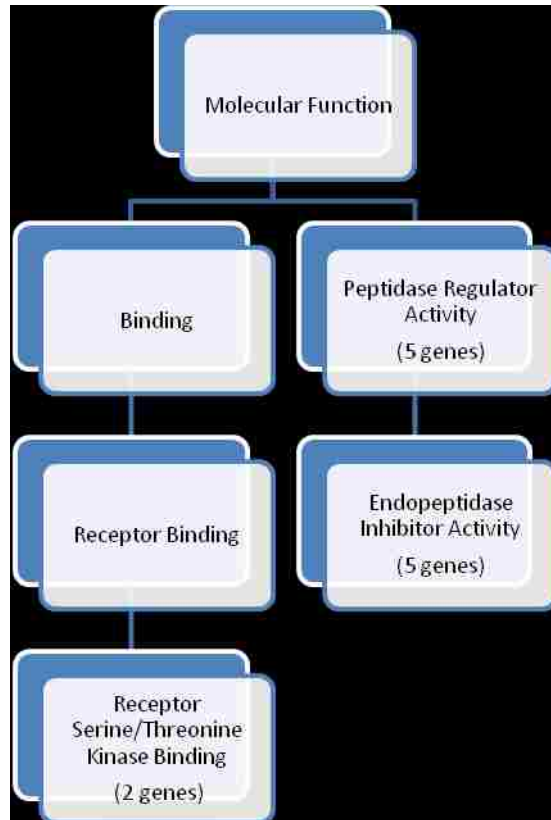
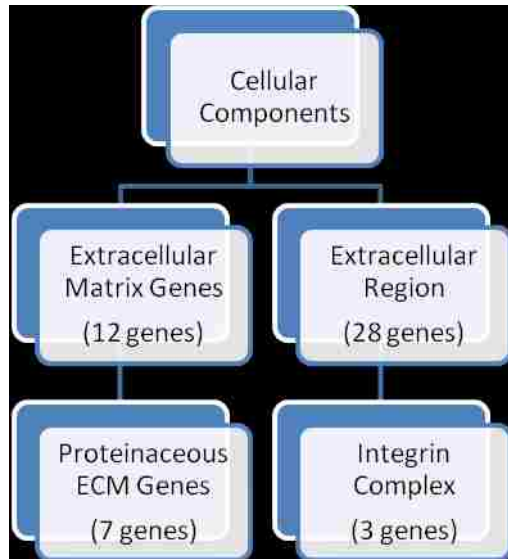


Figure 6.6: Flow chart diagramming pathways with a significant number of heparin regulated genes (either fold increase or fold decrease)
 (A) Flow chart illustrating biological processes with a significant number of heparin regulated genes.



(B) Flow chart illustrating molecular functions with a significant number of heparin regulated genes



(C) Flow chart illustrating cellular components with a significant number of heparin regulated genes.

Pathway	Number of Genes
Integrin family cell surface interactions	16
Beta1 integrin cell surface interactions	16
S1P1 pathway	12
PDGFR-beta signaling pathway	12
EGF receptor (ErbB1) signaling pathway	12
LKB1 signaling events	13
IL3-mediated signaling events	13
Urokinase-type plasminogen activator (uPA) and uPAR-mediated signaling	12
Glypican pathway	13
ErbB1 downstream signaling	12
Thrombin/protease-activated receptor (PAR) pathway	12
Internalization of ErbB1	12
Glypican 1 network	12
Class I PI3K signaling events mediated by Akt	12
Signaling events mediated by VEGFR1 and VEGFR2	12
Signal Transduction	13
Arf6 trafficking events	12
PAR1-mediated thrombin signaling events	12
Nectin adhesion pathway	12
Insulin Pathway	12
Signaling events mediated by Hepatocyte Growth Factor Receptor (c-Met)	12
Plasma membrane estrogen receptor signaling	12
PDGF receptor signaling network	12
IGF1 pathway	12
EGFR-dependent Endothelin signaling events	12
GMCSF-mediated signaling events	12
Arf6 downstream pathway	12
mTOR signaling pathway	12
IFN-gamma pathway	12
Arf6 signaling events	12
Alpha9 beta1 integrin signaling events	13
Signaling events mediated by focal adhesion kinase	12
VEGF and VEGFR signaling network	13
Proteoglycan syndecan-mediated signaling events	13
Syndecan-1-mediated signaling events	12
IL5-mediated signaling events	12
Class I PI3K signaling events	12
Sphingosine 1-phosphate (S1P) pathway	12

Endothelins	12
ErbB receptor signaling network	12
TRAIL signaling pathway	12
A third proteolytic cleavage releases NICD	2
GPCR ligand binding	6
Integrin-linked kinase signaling	8
BMP receptor signaling	5
HIF-1-alpha transcription factor network	3
Class A/1 (Rhodopsin-like receptors)	5
AP-1 transcription factor network	7
Signaling by TGF beta	2
Hypoxic and oxygen homeostasis regulation of HIF-1-alpha	3
Innate Immune System	4
Signaling by Notch	2
Immune System	6
Hemostasis	5
CDC42 signaling events	7
RXR and RAR heterodimerization with other nuclear receptor	2
Regulation of CDC42 activity	7
Signaling by GPCR	7
Alpha4 beta1 integrin signaling events	2
TGFBR	3
Retinoic acid receptors-mediated signaling	2
ALK1 signaling events	4
ALK1 pathway	4
Peptide ligand-binding receptors	3
NOTCH	2
Validated targets of C-MYC transcriptional repression	2
Cell surface interactions at the vascular wall	2
Integrin cell surface interactions	2
Notch signaling pathway	2
Notch-mediated HES/HEY network	2
Signaling events mediated by HDAC Class I	2
G alpha (q) signalling events	2
Validated transcriptional targets of AP1 family members Fra1 and Fra2	2

Table 6.1: Microarray results organized by number of genes regulated by heparin broken down by signaling pathway

Gene Description	Gene Symbol	Fold Change
mannan-binding lectin serine peptidase 1	Masp1	1.505
naked cuticle homolog 2 (Drosophila)	Nkd2	1.506
fibronectin type III domain containing 1	Fndc1	1.507
thioredoxin interacting protein	Txnip	1.509
thyroid hormone receptor beta	Thrb	1.512
transient receptor potential cation channel, subfamily V, member 2	Trpv2	1.516
potassium channel, subfamily K, member 2	Kcnk2	1.516
cysteine dioxygenase, type I	Cdo1	1.516
vasoactive intestinal peptide receptor 2	Vipr2	1.518
similar to leucine zipper protein 2	RGD1563838	1.519
epoxide hydrolase 1, microsomal	Ephx1	1.521
semaphorin 3D	Sema3d	1.521
ciliary neurotrophic factor	Cntf	1.521
guanine deaminase	Gda	1.522
estrogen receptor 1	Esr1	1.526
serine (or cysteine) peptidase inhibitor, clade A	Serpina9	1.528
dystrophia myotonica-protein kinase	Dmpk	1.530
LIM and senescent cell antigen like domains 2	Lims2	1.533
pentraxin related gene	Ptx3	1.534
gastrin releasing peptide receptor	Grpr	1.535
transmembrane protein 204	Tmem204	1.538
signal peptide, CUB domain, EGF-like 3	Scube3	1.538
proprotein convertase subtilisin/kexin type 5	Pcsk5	1.538
LIM and cysteine-rich domains 1	Lmcd1	1.539
sarcoglycan, gamma (dystrophin-associated glycoprotein)	Sgcg	1.554
myozenin 2	Myoz2	1.562
olfactory receptor 325	Olr325	1.568
solute carrier family 35, member F1	Slc35f1	1.585
chemokine (C-C motif) receptor-like 1	Ccr1	1.591
ADAM metallopeptidase with thrombospondin type 1 motif, 5	Adamts5	1.592
inositol polyphosphate-4-phosphatase, type II	Inpp4b	1.594
matrix Gla protein	Mgp	1.595
serine (or cysteine) peptidase inhibitor, clade B, member 2	Serpinb2	1.603
integrin, alpha 4	Itga4	1.612
decorin	Dcn	1.617
5-hydroxytryptamine (serotonin) receptor 1F	Htr1f	1.641
family with sequence similarity 38, member B	Fam38b	1.644

amine oxidase, copper containing 3 (vascular adhesion protein 1)	Aoc3	1.677
serine (or cysteine) peptidase inhibitor, clade A, member 3N	Serpina3n	1.685
microfibrillar-associated protein 4	Mfap4	1.687
chondroitin sulfate N-acetylgalactosaminyltransferase 1	Csgalnact1	1.691
family with sequence similarity 5, member B	Fam5b	1.691
transglutaminase 2, C polypeptide	Tgm2	1.697
integrin, alpha 7	Itga7	1.699
Notch homolog 3 (Drosophila)	Notch3	1.699
presenilin 2	Psen2	1.702
serine (or cysteine) peptidase inhibitor, clade B, member 7	Serpib7	1.713
guanylate cyclase 1, soluble, beta 3	Gucy1b3	1.714
olfactomedin-like 2B	Olfml2b	1.721
transmembrane 7 superfamily member 2	Tm7sf2	1.744
oxidized low density lipoprotein (lectin-like) receptor 1	Olr1	1.773
ceruloplasmin	Cp	1.776
serine (or cysteine) peptidase inhibitor, clade A	Serpina9	1.791
sprouty homolog 1, antagonist of FGF signaling (Drosophila)	Spry1	1.794
similar to transmembrane protein 2	RGD1305254	1.799
selenoprotein P, plasma, 1	Sepp1	1.848
carboxypeptidase X (M14 family), member 2	Cpxm2	1.875
CD180 molecule	Cd180	1.887
bone morphogenetic protein 6	Bmp6	1.889
mast cell protease 1	Mcpt1	1.905
similar to C21ORF7	LOC304131	1.920
WAP four-disulfide core domain 1	Wfdc1	1.922
similar to ABI gene family, member 3 (NESH) binding protein	RGD1562717	1.937
calsequestrin 2 (cardiac muscle)	Casq2	1.979
integrin, beta-like 1	Itgb11	2.049
phospholamban	Pln	2.062
Fraser syndrome 1 homolog (human)	Fras1	2.112
tumor necrosis factor (ligand) superfamily, member 18	Tnfsf18	2.114
peptidase inhibitor 15	Pi15	2.163
elastin	Eln	2.253
fin bud initiation factor homolog (zebrafish)	Fibin	2.296
sodium channel, voltage-gated, type VII, alpha	Scn7a	2.370
slit homolog 3 (Drosophila)	Slit3	2.505
myosin, heavy chain 2, skeletal muscle, adult	Myh2	2.556
aldo-keto reductase family 1, member C14	Akr1c14	2.594

bone morphogenetic protein 3	Bmp3	2.717
myosin, heavy polypeptide 1, skeletal muscle, adult	Myh1	2.742
fibromodulin	Fmod	2.789
osteomodulin	Omd	2.871
regulator of G-protein signaling 4	Rgs4	3.039
asporin	Aspn	3.853

Table 6.2: Microarray results showing genes with a fold change ≥ 1.5

Chapter 7: Heparin responses in vascular smooth muscle cells involve PKG

7.1: Introduction

Following injury to an artery, VSMC migration from the tunica intima into the vessel lumen is a hallmark in the development of atherosclerosis. Heparin is a potential molecule for the short-term treatment of atherosclerosis. It was initially shown that heparin suppresses VSMC growth more than 30 years ago (Clowes AW and Karnovsky MJ 1977); yet the mechanism by which heparin inhibits VSMC proliferation remains unclear. Heparin has been documented to block PKC-dependent c-fos induction and ERK activation in response to a variety of treatments in sub-cultured VSMCs (Castellot JJ et al. 1989, Ottlinger ME, Pukac LA, and Karnovsky MJ 1993). As discussed in detail in Chapters 1 and 6, heparin treatment causes decreased CDK2 activity by stabilizing p27^{kip1} (Fasciano S et al. 2005). Some of the anti-proliferative effects of heparin can be attributed to growth factor sequestration; however, sequestration cannot explain all of the effects of heparin on VSMCs (Reilly CF et al. 1989, Pukac LA et al. 1997, Savage JM et al. 2001, Blaukovitch CI et al. 2010).

VSMCs specifically bind and endocytose heparin (Castellot JJ et al. 1985). This specific binding activity, in combination with heparin's effects on cell signaling pathways, supports a model whereby heparin binds to cell surface proteins and initiates its own signaling pathways. This notion is supported by the fact that monoclonal antibodies which recognize a single heparin-binding cell surface protein specifically inhibit heparin binding to cells *in vitro* and act as agonists of heparin, mimicking both heparin's effects on cell signaling and its anti-proliferative effects on cultured VSMCs (Patton WA et al. 1995, Savage JM et al. 2001, and Blaukovitch CI et al. 2010).

MAPK activity is regulated by the reversible phosphorylation of specific tyrosine and threonine residues, and active ERK accumulation in the nucleus is critical in cell cycle progression through G₁ (Brunet A et al. 1999) where the sustained ERK activity results in Elk-1 phosphorylation (Shin HS et al. 2003). DUSPs play important roles in ERK inactivation, and MKP-1 localizes to the nucleus (Rohan PJ et al. 1993) where it is able to regulate ERK signaling in VSMCs. Loss of active ERK in the nucleus results in decreased Elk-1 activity (Shin HS et al. 2003). Data from our laboratory demonstrate that heparin and anti-heparin receptor antibodies increase MKP-1 protein levels in VSMCs, mediating, at least in part heparin-induced ERK activity decreases (Blaukovitch CI et al. 2010). However, the signaling intermediates between heparin's interaction with its receptor and induction of MKP-1 expression remain unknown. One possibility is suggested by studies of insulin signaling (Begum N et al. 1998 and Jacob A et al. 2002). These studies report the expression of MKP-1 in VSMCs in response to insulin and IGF; where insulin and IGF induce the expression of iNOS, eventually increasing the levels of cGMP in response to the NO activation of sGC. The increase in cGMP levels was shown to be sufficient to induce MKP-1 expression and attenuate ERK activity. Similarly, leptin treatment induces decreased VSMC proliferation, and this depends on iNOS induction (Rodríguez A et al. 2010). As well as in heparin treated cells, p27^{kip1} is induced in response to cGMP rises and PKG activity in VSMCs (Sato J et al. 2000).

Another agent that elevates cGMP in VSMCs is ANF or ANP. Upon ligand binding, the ANP receptor activates an intracellular guanylate cyclase thereby increasing cGMP levels. Both ANP and cGMP have been shown to decrease the proliferation of

VSMCs (Baldini PM et al. 2002 and Tantini B et al. 2005). Increased cGMP induces MKP-1 expression in smooth muscle, mesangial and endothelial cells through PKG (Sugimoto T et al. 1996, Baldini PM et al. 2002, Jacob A et al. 2002, and Furst R et al. 2005). The increased MKP-1 expression decreases ERK activation, and provides a mechanism for the anti-proliferative activity of ANP in VSMC (Sugimoto T et al. 1996, Baldini PM et al. 2002, and Tantini B et al. 2005). ANP treatment, like heparin treatment, induces increases in p27^{kip1} levels (Hannken T et al. 2001).

Heparin and cGMP affect VSMCs similarly. First, both inhibit growth of VSMCs late in the G₁ phase of the cell cycle. Second, the proximity of the endothelium to VSMCs *in vivo* provides a source for both endogenous heparin and cGMP-elevating agents such as NO. Endogenous heparin from endothelial cells could maintain quiescence in VSMCs (Castellot JJ et al. 1981). Third, in reducing VSMC growth, both cGMP and heparin cause an inactivation of ERK due, at least in part, to the induction of MKP-1 (Baldini PM et al. 2002 and Blaukovitch CI et al. 2010). Because of the similarities in the way that heparin, ANP, and NO-induced cGMP increases affect VSMCs, the lab hypothesized that heparin's cellular effects are mediated through the second messenger cGMP target, PKG. Consistent with this idea is evidence that reductions in cGMP signaling occur with neointimal proliferation and vascular dysfunction in late-stage atherosclerosis (Melichar VO et al. 2004). Also consistent with this hypothesis is the fact that expression of constitutively active PKG inhibits VSMC proliferation in response to high glucose (Wang S and Li Y 2009).

Previously collected data from the lab suggest that cGMP mimics heparin and PKG inhibition blocks heparin-induced decreases in VSMC DNA synthesis shown by BrdU incorporation (Gilotti AC diss 2000). The heparin-induced inhibition of DNA synthesis was shown to be dependent on PKG and the role of PKA was ruled out using inhibitors of PKA (Gilotti AC diss 2000). Heparin signaling normally results in decreased ERK activity, but when PKG is inhibited using chemical inhibitors, this affect is significantly decreased (Gilotti AC diss 2000 and Miller EA unpublished data). It was also established that heparin decreases Elk-1 activity along with decreasing ERK activity, and that inhibiting PKG disrupts these decreases (Nimlamool WN unpublished data). Concurrent with the requirement for PKG in mediating heparin signaling, heparin treatment in VSMCs results in increases in cGMP concentration (Gilotti AC diss 2000). As discussed previously, some of the anti-proliferative action of heparin is mediated through MKP-1, which was shown to be dependent upon cGMP and MKP-1 activity (Gilotti AC diss 2000). The missing piece of experimental evidence from this work was definitive evidence showing that reducing PKG levels resulted in altered heparin signaling. To accomplish this, I set out to utilize targeted PKG siRNA and functionally link decreased PKG to decreased heparin sensitivity in A7r5 VSMCs. Taken together with my contribution to the project, we have shown PKG activity is required for heparin-induced decreases in VSMC ERK activity, Elk-1 phosphorylation, and VSMC proliferation. The culmination of this work has been submitted to J. Cell Physiol and is pending their initial review.

7.2: Methods

7.2.1: Cell Culture

A7r5s were cultured as described in Chapter 2.

7.2.2: PKG siRNA Transfection

PKG siRNA transfection was carried out as described Chapter 5 for TMEM184A siRNA.

7.2.3: Heparin Assay in PKG siRNA Transfected Cells

The heparin assay was performed as done in Chapter 5.

7.2.4: Immunofluorescence Staining

Primary antibodies against pERK, PKG α and β (Santa Cruz Biotechnology), and pElk-1 (Cell Signaling, Boston, MA) were used as described in Chapter 2.

7.2.5: Fluorescence Microscopy

Fluorescent microscopy was used to determine whole cell expression levels of PKG, relative knockdown of PKG in siRNA/shRNA-treated cells, and the PDGF/Heparin-induced responses in pERK and pElk-1 levels. Performed as described in Chapter 2.

7.2.6: SDS-PAGE and Western Blotting

Performed as described in Chapter 2.

7.3: Results

Because the timing of PKG inhibitors in these assays was very specific, we confirmed the importance of PKG activity in heparin effects on ERK phosphorylation in cells where PKG levels were significantly decreased through the use of siRNA. Recall

from Chapter 5 that control experiments were carried out with FITC-control siRNA in A7r5s showing that the majority of cells took up the siRNA (Figure 4.10). PKG knockdown efficiency varied between experiments from occasionally greater than 90% knockdown to about 50% decrease in staining in A7r5 cells treated with siRNA compared to scrambled control. Cells allowed to recover in starvation media exhibited insignificant knockdown of PKG (data not shown). Therefore, cells were treated with control siRNA or PKG siRNA and were cultured in regular growth media for 72 hr and then treated with heparin for 20 min followed by PDGF for 15 min. Controls with PDGF or no treatment were compared. The presence of PKG, pERK and pElk-1 was determined by immunofluorescent staining (Figure 7.1A and 7.1B). Despite incomplete knockdown, it is clear that heparin-induced decreases in pERK and pElk-1 staining were very limited in PKG siRNA treated cells compared to cells with scrambled siRNA. Western Blots confirm that heparin treatment does not have much effect on ERK activation in cells where PKG levels have been significantly decreased (Figure 7.1C).

7.4: Discussion

The proliferation of VSMCs in healthy vessels is carefully regulated, and heparin has been shown to block a number of important signaling events in VSMCs (i.e. Ottlinger ME et al. 1993 and Pukac LA et al. 1997). Data showing that antibodies to a heparin receptor mimic the effects of heparin strongly suggesting that heparin is acting through a receptor protein to mediate a portion of its effects (Savage JM et al. 2001). Heparin binding to its receptor protein would presumably trigger an intracellular signal

transduction cascade likely involved in heparin-induced decreases in PDGF-stimulated BrdU incorporation and deactivation of ERK MAPK activity (Savage JM et al. 2001), expression of MKP-1 (Blaukovitch CI et al. 2010), and decreased Elk-1 phosphorylation in VSMCs. In fact, the changes in Elk-1 phosphorylation are consistent with reports that Elk-1 phosphorylation results in changes in gene expression. Obvious mechanisms for heparin-induced PKG-mediated modulation of VSMC proliferation involve phosphorylation of transcription factors (reviewed in Pilz RB and Broderick KE 2005) and reported for Elk-1 (Choi CS et al. 2010). Previous results from the lab coupled to my experimental data provide evidence for the involvement of PKG in downstream events of heparin receptor activation. Heparin has previously been demonstrated to have an anti-proliferative effect on VSMCs in rats and in an endothelial/VSMC co-culture system, but while NO production in the heparin-treated rats played a role in the response; it did not appear to be involved in heparin-induced decreases in VSMC proliferation (Horstman D et al. 2002).

NO is a cell permeable activator of soluble guanylyl cyclase. Treatment of cells with synthetic NO donors or activators of NO synthase causes a rapid increase in intracellular concentrations of cGMP, while particulate guanylyl cyclases often result in limited cGMP increases (Su J et al. 2005). In addition, production of cGMP at the membrane does not produce cGMP increases throughout the cell (Nausch LW et al. 2008), consistent with the idea that robust increases in cGMP may not be necessary for physiological responses. Rather, limited localized signaling might lead to physiological results without significant increases in total cGMP levels due to location specific smaller

increases in cGMP. ANP treatment of VSMCs does limit their proliferation (Baldini PM et al. 2002), and the limited increase in cGMP induced by heparin seems to be an important mechanism by which heparin interaction with the receptor induces changes in VSMC signaling and proliferation.

One possible mechanism whereby heparin could affect VSMCs while inducing modest elevations of cGMP levels is through localization in caveolae. As mentioned previously, caveolae serve as signaling hubs in most cells, especially cells of the vasculature. The expression of caveolin has been reported to be affected by heparin and caveolin expression has been linked to VSMC growth (Peterson TE et al. 1999). Heparin receptor localization to caveolae could also explain other heparin effects which have been shown to be associated with caveolae function (Liu YT, Song L, and Templeton DM 2007). If the heparin receptor is localized in caveolae, binding could result in localized signaling through PKG by activating a NOS protein in VSMC (Cheah LS et al. 2002) or caveolae might modulate PKG activity adjacent to the caveolae. Characterization of TMEM184A as a receptor for heparin supports the notion that the receptor co-localizes with caveolin-1 at membrane patches (Figure 4.4). Signaling through cGMP and PKG is further supported by the fact that TMEM184A also co-localizes with eNOS in vascular cells (Figure 4.5). The functional data presented in Chapter 4, strongly suggest that TMEM184A is a receptor for heparin, demonstrating that at least a subset of the heparin receptor localizes to cav-1-containing caveolae to mediate the proposed signaling events outlined above.

Whatever the mechanism and down-stream signaling from PKG, our data suggest that heparin treatment causes the elevation of cGMP levels and indicate a role for PKG in heparin-induced decreased VSMC proliferation. My contribution to this project specifically demonstrated that PKG knockdown caused reduced heparin sensitivity in VSMCs as assayed by PDGF-induced changes in pERK and pElk-1. When PKG is significantly decreased by siRNA, cells not longer exhibit heparin-induced decreases in PDGF stimulated pERK and pElk-1. The culmination of this work suggests a mechanism whereby heparin binds to this cell surface protein activating a guanylyl cyclase causing a rapid elevation of cGMP, in turn, activating PKG. This idea is supported by 1) the rapid elevation of intracellular cGMP in heparin-treated cells, 2) the sensitivity of the heparin effects to PKG inhibitors, and 3) the sensitivity to partial knock down of PKG protein.

7.5: Figure

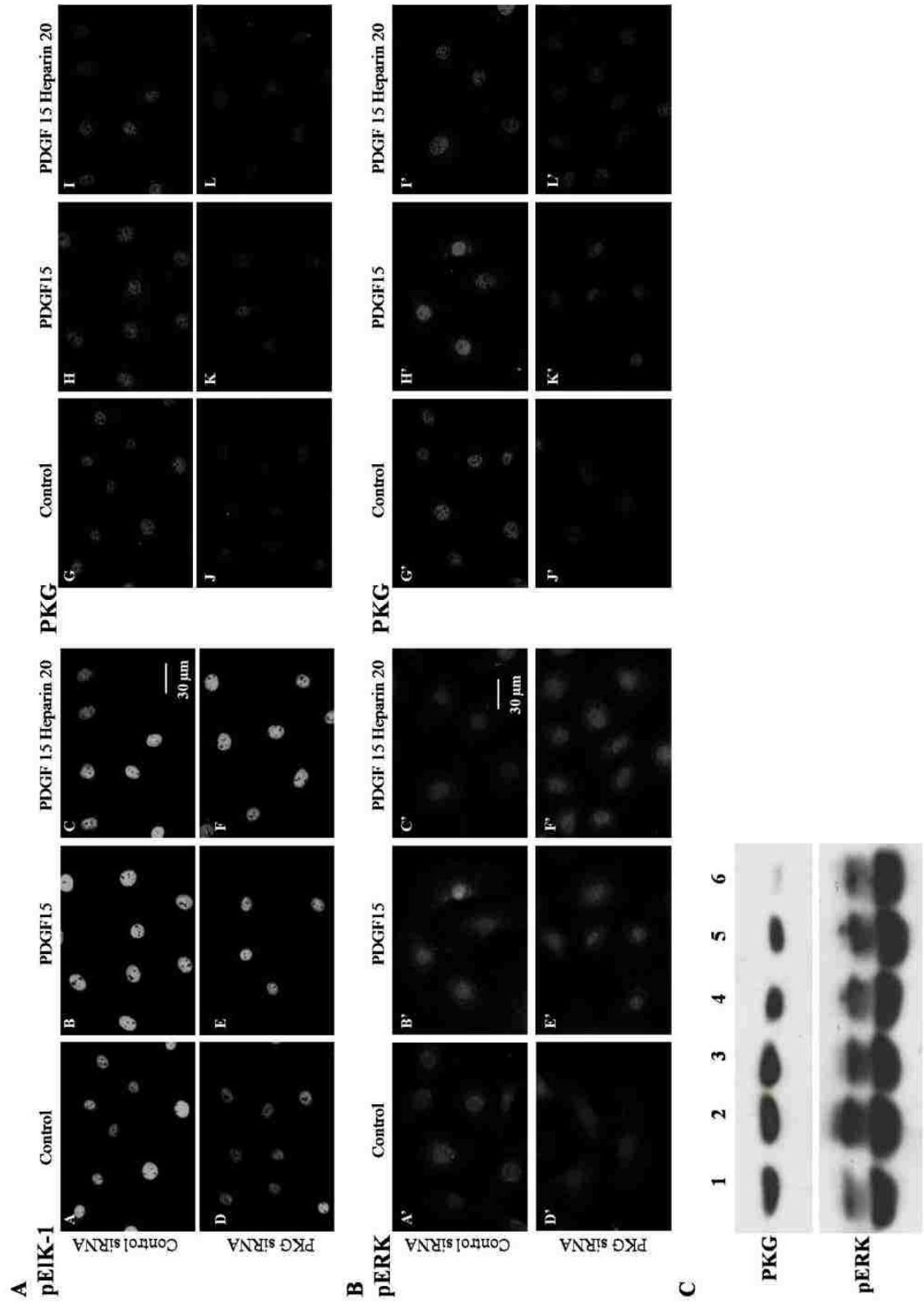


Figure 7.1: Knockdown of PKG decreases heparin effects on ERK activity and pElk

A7r5 cells were electroporated with siRNA designed to knock down PKG in rat cells or scrambled RNA, and the cells were allowed to proliferate in growth media for 72 h with feeding at 24 h. At 72 h, cells were untreated, treated with PDGF for 15 min or heparin for 20 min before PDGF was added for 15 min. Panel (A) illustrates the pElk levels (pictures A-F). Staining for PKG is illustrated in the same cells in pictures G-L. Scrambled siRNA (A,B,C,G,H,I) as compared to PKG siRNA (D,E,F,J,K,L) is shown for cells not stimulated (A,D,G,J), PDGF treated cells (B,E,H,K) and heparin plus PDGF (C,F,I,L). Panel (B) illustrates an experiment where pERK was monitored (A'-F') PKG staining for these cell samples is shown in pictures G'-L'. The treatment pattern is identical to that for panel A. These experiments are representative of two similar experiments each. Panel (C) illustrates Western Blots of A7r5 cells treated to knock down PKG for 72 h as above and analyzed by blotting for pERK and PKG levels. Lanes 1-3 illustrate cells treated with scrambled siRNA and 4-6 represent cells treated with PKG siRNA. Lanes 1 and 4 illustrate cells harvested without further treatment, lanes 2 and 5 cells treated with PDGF for 15 min and lanes 3 and 6 are cells treated with heparin and PDGF as above. Blots were developed using ECL reagents. Images are representative of a least three experiments. Scale bars = 30 μ m.

Chapter 8: Conclusions and future directions

It is clear that cardiovascular diseases, including atherosclerosis and its complications, are the leading causes of death in many societies. The alarming increase in cardiovascular disease-related deaths correlates with the increasing percentage of the population classified as obese. Although cardiovascular disease and obesity are largely preventable through lifestyle modification, no decrease in their occurrence is foreseeable in the near future. Therefore, great interest in science and medicine has been focused on understanding the development of atherosclerosis and on potential mechanisms to slow or reverse the atherosclerotic process.

Atherosclerosis is an inflammatory disease which occurs in response to injury to the arterial wall, resulting in endothelial cell dysfunction, VSMC proliferation, and migration to the site of injury (Ross R 1999 and Rudijanto A 2007). This injury leads to endothelial cell dysfunction causing excessive, chronic inflammation and phenotypic changes in the endothelial cell layer. The endothelium loses its anticoagulant nature becoming pro-coagulant. This pro-coagulant nature causes the release of inflammatory cytokines, platelet activation, and the release of PDGF triggering the surrounding VSMCs to become proliferative (Ross R 1993 and Ross R 1999). Although not completely understood at this time, the inflammatory response is largely mediated by IL-1 β and TNF α (Kishikawa H, Shimokama T, and Watanabe T 1993, Rus HG, Niculescu F, and Vlaicu R 1991, Moyer CF et al. 1991, and Galea J et al. 1996), and the immune response is predominantly mediated by the upregulation of adhesion molecules (i.e. ICAM and VCAM) (Viemann D et al. 2006). This recruitment of macrophages and lymphocytes causes the release of additional inflammatory molecules including

hydrolytic enzymes, cytokines, chemokines, and growth factors leading to more wall damage and the development of a fibrous plaque (Ross R 1993 and Ross R 1999).

Two major hallmarks of atherosclerosis include endothelial cell dysfunction and smooth muscle cell proliferation induced through the uncontrolled inflammatory response. Therefore the goal of this dissertation was to further our understanding of the development of atherosclerosis and potential ways to attenuate this excessive inflammation. These goals included the anti-inflammatory nature of shear stress in the vasculature and the potential use of heparin as a short-term anti-inflammatory treatment or the possibility of activating the heparin signaling pathway without heparin for the long-term treatment of vascular disease. To accomplish these goals, the role of shear stress in maintaining barrier integrity in vascular endothelium was determined to involve cofilin, a cell surface protein was identified as a receptor for heparin, and the signaling pathway from that receptor to MKP-1 was elucidated. Along with identifying this signaling pathway, heparin-induced gene expression changes were investigated in vascular smooth muscle cells. Lastly, it was shown that heparin exerts its anti-inflammatory effect by attenuating TNF α responses in vascular endothelial cells.

It has been well established that shear stress plays a crucial role in maintaining vascular homeostasis and promoting the anti-coagulant and anti-inflammatory (atheroprotective) environment found in healthy vasculature (and reviewed in: Mengistu M, Slee JB, and Lowe-Krentz LJ 2012 and Hahn C and Schwartz MA). Regions of the vasculature that are exposed to laminar shear stress are considered atheroprotective whereas regions exposed to disrupted shear stress are pro-coagulant and pro-

inflammatory (atheroprone). However the exact mechanism underlying how this mechanical stress affects vascular physiology remains unclear. Previous work performed in the lab documented that atheroprotective levels of shear stress induce whole cell, nuclei, and actin microfilament realignment in the direction of shear stress, suggesting that this alignment was in some way beneficial (Mengistu M et al. 2011 and reviewed in: Mengistu M, Slee JB, and Lowe-Krentz LJ 2012). This alignment in the direction of shear stress is also found *in vivo* further supporting the hypothesis that this alignment is in some way atheroprotective (reviewed in: Mengistu M, Slee JB, and Lowe-Krentz LJ 2012). Hamel M et al. (2006) also determined that stress kinase (JNK and p38) activity was required for this shear stress-induced actin realignment, further supporting the observation that active JNK and p38 associate with the actin cytoskeleton.

To further understand the role of shear stress as an anti-inflammatory mediator, I investigated the role that cofilin played in the process of shear stress-induced actin realignment. Cofilin, a prominent actin depolymerizing protein, is involved in regulating actin dynamics by binding actin filaments and facilitating their breakdown. Shear stress was shown to induce p-cofilin localization to the nucleus without significantly altering total cofilin levels in a confluent monolayer of vascular endothelial cells (Slee JB and Lowe-Krentz 2013). The change in cofilin activity and localization were also dependent, in part, upon stress kinases JNK and p38, although they were not directly involved in cofilin phosphorylation (Slee JB and Lowe-Krentz 2013). It has been shown that shear stress induces endothelial barrier tightening, creating an effective barrier in the vascular system (DePaola N et al. 2001 and Seebach J et al. 2000). I have shown that cofilin

activity is required for this shear stress-induced barrier tightening through its regulation of actin realignment (Slee JB and Lowe-Krentz 2013).

Endothelial cells with improperly regulated cofilin fail to exhibit traditional actin realignment ultimately leading to gaps and breaks in cell-cell junctions (Slee JB and Lowe-Krentz 2013). These findings demonstrate that cofilin-mediated actin realignment is necessary for maintaining endothelial barrier integrity during shear stress, which furthers our understanding of how shear stress is atheroprotective. Cofilin in combination with JNK and p38 are activated in response to atheroprotective shear stress to facilitate actin realignment in the direction of shear stress which facilitates cell-cell junction tightening and increased barrier integrity. This is one way in which healthy endothelial cell physiology is promoted in order to prevent “leaky” endothelium which is associated with the development of atherosclerosis by the recruitment of immune cells and the release of inflammatory mediators. Given that this atheroprotective shear stress is not found in all regions of the vascular system, it is important to understand the underlying mechanisms involved in mediating the downstream effects. The results from this work suggest that actin realignment is mis-regulated in atheroprone shear stress regions.

An interesting future aspect to the shear stress work is in the field of implantable devices and stents. In the case of vascular stents, two major problems arise after implantation. Short-term failure can be caused by the inability of endothelial cells to grow on the stent and form the necessary anti-inflammatory layer. Long-term failure is often attributed to failure to endothelialize the stent and calcification of the stent leading to increased inflammatory signaling resulting in plaque formation in the stent (reviewed

in: Mengistu M, Slee JB, and Lowe-Krentz LJ 2012). The findings from my work mimics the implantation of stents. In this system, static cells are exposed to a surge of shear stress, similar to the surge of blood when a stent is implanted. Also understanding how shear stress relates to the atheroprotective nature of the vasculature by promoting a strong endothelial barrier, sheds light onto mechanisms of how to create this atheroprotective physiology in stents. Increasing our knowledge of how cells respond to this initial shear stress could potentially increase vascular stent success. To further explore ways to prevent calcification of vascular stents and promote the development of an atheroprotective stent environment I will be exploring the molecule CD47 in my post-doctoral position at Children's Hospital of Philadelphia. Initial studies show that CD47 greatly reduces calcification and increases long-term success of implantation (Finley MJ et al. 2012).

A second way to potentially combat inflammation in the vascular system is to utilize the molecule heparin. Heparin has been repeatedly shown to possess anti-proliferative and anti-inflammatory qualities that make it an excellent possibility for treatment of vascular disease. However future work aimed at reducing the somewhat severe side effects before it could be used medicinally as a long-term therapy. The anti-proliferative effects of heparin have been linked to the regulation of MAPK cascade intermediates and to regulation of the cell cycle. Both serve to slow cell proliferation, which would be beneficial in atherosclerosis where one of the hallmarks is unwanted VSMC proliferation. The anti-inflammatory nature of heparin is starting to gain traction in the literature and includes the inhibition of complement activation, adhesion

molecules, and NF κ B signaling (reviewed in: Mengistu M, Slee JB, and Lowe-Krentz LJ 2012). In my opinion, one of the best ways to further our understanding of heparin is to identify a protein which serves as a receptor. Evidence from our lab suggests that heparin exerts a portion of its effects through a receptor. Identification of a receptor for heparin opens up many options for harnessing the anti-proliferative and anti-inflammatory qualities of heparin without the side effects associated with long-term heparin treatment. Knowing the receptor would allow for the design of receptor agonists which could, in theory, mimic the effects of heparin in the vasculature.

The data presented herein, combined with previously collected work by Raymond Pugh, strongly suggest that TMEM184A functions as a receptor for heparin. Data supporting this conclusion include mass spectrometry sequence analysis, immunoprecipitation, and siRNA knockdown coupled to functional assays. Along with the data demonstrating a role for TMEM184A as a receptor for heparin, descriptive experiments were performed to further our understanding of TMEM184A. TMEM184A was found to localize to peri-nuclear and membrane regions, where it co-localizes with VAMP, cav-1, and eNOS. A GFP-tagged version of TMEM184A was also used to demonstrate that it co-localizes with Rhodamine-tagged heparin in vascular smooth muscle cells. All of which indirectly support TMEM184A as a receptor for heparin. The functional data showing that TMEM184A knock down decreases heparin's effects on established targets indicates that TMEM184A could be a receptor for heparin.

Although some of the effects of heparin are due to sequestration of growth factor and other signaling molecules, identification of a receptor for heparin provides crucial

information for furthering our understanding of the mechanisms for heparin. We have published evidence and data presented in this dissertation that indicate signaling from a receptor is mediated through cGMP and PKG. Initially, work done by Albert Gilotti suggested that the cGMP/PKG pathway was involved in heparin signaling (Gilotti A diss 2000), which was strengthened by various members of the lab. My contribution to the project showed that specific knock down of PKG reduced heparin's effects on published pathways. Although not definitively investigated in this dissertation, the possible involvement of eNOS in this pathway exists. Not only does eNOS typically play a role in increasing cGMP it was also determined that internalized TMEM184A co-localizes with eNOS in vascular endothelial and smooth muscle cells. The involvement of eNOS in mediating heparin signaling is currently being investigated by members of the lab. Preliminary results suggest that eNOS may be involved in heparin signaling (Swanson K and Li Y unpublished data), although considerable more work is needed to confirm these data.

In separate but related experiments, it was determined that heparin attenuates TNF α -induced inflammation in vascular endothelial cells. Initial work done by Marianne Hamel and Daniela Kanyi showed that heparin treatment decreased TNF α -induced JNK and p38 activity and decreased their target activation (Hamel M diss 2001 and Kanyi D diss 2006). It was determined that these effects were also seen when anti-heparin receptor antibodies were used in place of heparin, indicating that heparin is acting through a receptor. To complete this story, I have shown that TNF α strongly induces actin stress fibers in sub-confluent endothelial cells and that this response is significantly attenuated

by heparin pretreatment. These data suggest that heparin possess anti-inflammatory qualities capable of reversing TNF α inflammation, which is mediated through receptor binding.

To further our understanding of the mechanisms behind heparin, heparin-induced mRNA changes were investigated. The culmination of these studies suggests that heparin regulates a large number of genes that are related to cell proliferation, migration, inflammatory signaling, and GAG-dependent Serpins. Some of the genes that were shown to be significantly altered by heparin treatment were in pathways that I would expect to be regulated by heparin. GUCY1B3 is the gene of highest priority for immediate investigation, because it further supports involvement of cGMP and PKG in heparin signaling. This presents a possible feed forward loop in which the signal initiated by heparin binding to its receptor could be amplified by increasing GUCY1B3 and cell sensitivity to heparin. Another gene upregulated by heparin treatment suitable for immediate investigation includes RGS4, which has been shown to antagonize VEGF stimulation of DNA synthesis, ERK1/2 activation, and p38 MAPK activation. Essentially, RGS4 performs much of the same functions of heparin in vascular cells. A final interesting point worth noting is that heparin preferentially upregulates more genes than it down-regulates. In fact, hardly any down-regulated genes reach a fold change of 1.5, suggesting that heparin does not have many inhibitory roles on gene expression.

The common thread among all of the data in this dissertation is inflammation and proliferation associated with atherosclerosis and ways to prevent them. Shear stress is an important player in maintaining the anti-inflammatory and anti-coagulant atmosphere

necessary for healthy vasculature. Heparin is in a unique position to as an anti-inflammatory and anti-proliferative molecule in the vascular system. To mediate at least a portion of these effects, it seems that heparin binds to TMEM184A (heparin receptor) to facilitate an intracellular signaling cascade. One of those cascades involves signaling through cGMP, PKG, and presumably eNOS in VSMCs. A second of those cascades culminates in JNK and p38 activity to reduce inflammatory signaling in vascular endothelial cells, although the upstream signaling molecules are unknown at this point. Although it cannot be associated with receptor binding, heparin regulates a large number of genes in VSMCs related to proliferation, migration, inflammation, and transcription, suggesting that the study of heparin is only in its infancy.

Chapter 9: References

- Albig AR and Schiemann WP. Identification and characterization of regulator of G protein signaling 4 (RGS4) as a novel inhibitor of tubulogenesis: RGS4 inhibits mitogen-activated protein kinases and vascular endothelial growth factor signaling. *Mol Biol Cell* 2005 Feb;16(2):609-25. Epub 2004 Nov 17.
- Ali S, Hardy LA, and Kirby JA. Transplant immunobiology: a crucial role for heparan sulfate glycosaminoglycans? *Transplantation* 2003;75:1773-1782.
- Almeida E, Ilic D, Han Q, Hauck C, Jin F, Kawakatsu H, Schlaepfer D, and Damsky C. Matrix survival signaling: from fibronectin via focal adhesion kinase to c-Jun NH₂-terminal kinase. *J Cell Biol* 2000;149:741-754.
- An SS, Pennella CM, Gonnabathula A, Chen J, Wang N, Gaestel M, Hassoun PM, Fredberg JJ, and Kayyali US. Hypoxia alters biophysical properties of endothelial cells via p38 MAPK- and Rho kinase-dependent pathways. *Am J Physiol Cell Physiol* 2005; 289(3):C521-30.
- Aplin AE, Howe A, Alahari SK, and Juliano RL. Signal transduction and signal modulation by cell adhesion receptors: the role of integrins, cadherins, immunoglobulin-cell adhesion molecules, and selectins. *Pharmacol Rev* 1998;50:197-263.
- Azuma N, Akasaka N, Kito H, Ikeda M, Gahtan V, Sasajima T, and Sumpio BE. Role of p38 MAP kinase in endothelial cell alignment induced by fluid shear stress. *Am J Physiol Heart Circ Physiol* 2001;280:H189-H197.
- Baldini PM, De Vito P, Fraziano M, Mattioli P, Luly P, and Di Nardo P. Atrial natriuretic

- factor inhibits mitogen-induced growth in aortic smooth muscle cells. *J Cell Physiol* 2002 Oct;193(1):103-9.
- Barakat A and Davies P. Mechanisms of shear stress transmission and transduction in endothelial cells. *Chest* 1998;114:58S-63S.
- Barbee K, Davies P, and Lal R. Shear stress-induced reorganization of the surface topography of living endothelial cells imaged by atomic force microscopy. *Circ Res* 1994;74:163-171.
- Bârză T, Molho P, Tobelem G, Petitou M, and Caen J. Binding and endocytosis of heparin by human endothelial cells in culture. *Biochim Biophys Acta* 1985;845:196-203.
- Bârză T, Van Rijn JL, Petitou M, Molho P, Tobelem G, and Caen JP. Endothelial binding sites for heparin: specificity and role in heparin neutralization. *Biochem J* 1986;238:847-854.
- Basta G, Lazzerini G, Massaro M, Simoncini T, Tanganelli P, Fu C, Kislinger T, Stern DM, Schmidt AM, and De Caterina R. Advanced glycation end products activate endothelium through signal-transduction receptor RAGE: a mechanism for amplification of inflammatory responses. *Circulation* 2002; 105:816-822.
- Begum N, Song Y, Rienzie J, and Ragolia L. Vascular smooth muscle cell growth and insulin regulation of mitogen-activated protein kinase in hypertension. *Am J Physiol* 1998 Jul;275(1 Pt 1):C42-9.
- Bernard O. Lim Kinases, Regulators of Actin Dynamics. *Int J Biochem Cell Biol* 2007;39(6):1071-1076.

- Berstein BW and Bamburg JR. ADF/Cofilin: a functional node in cell biology. *Trends in Cell Biology* 2010;20(4):187-195.
- Best D and Adams IR. Sdmg1 is a component of secretory granules in mouse secretory exocrine tissues. *Dev Dyn* 2009;238:223-231.
- Best D, Sahlender DA, Walther N, Peden AA, and Adams IR. Sdmg1 is a conserved transmembrane protein associated with germ cell sex determination and germline-soma interactions in mice. *Development* 2008;135:1415-1425 doi: 10.1242/dev.019497.
- Birukov KG, Birukova AA, Dudek SM, Verin AD, Crow MT, Zhan X, DePaola N, AND Garcia JGN. Shear stress-mediated cytoskeletal remodelling and cortactin translocation in pulmonary endothelial cells. *Am J Respir CellMolec Biol* 2002; 26:453-464.
- Blaukovitch CI, Pugh R, Gilotti AC, Kanyi D, and Lowe-Krentz LJ. Heparin treatment of vascular smooth muscle cells results in the synthesis of the dual-specificity phosphatase MKP-1. *J Cell Biochem* 2010;110(2):382-91.
- Bogoyevitch MA, Boehm I, Oakley A, Ketterman AJ, and Barr R. Targeting the JNK MAPK cascade for inhibition: basic science and therapeutic potential. *Biochimica et Biophysica Acta* 2004;1697:89-101.
- Bogoyevitch M and Kobe B. Uses for JNK: the many and varied substrates of the c-Jun N-terminal kinases. *Microbiology and Molecular Biology Reviews* 2006;70(4):1061-1095.
- Bonecchi R, Bianchi G, Bordignon PP, D'Ambrosio D, Lang R, Borsatti A, Sozzani S,

- Allavena P, Gray PA, Mantovani A, and Sinigaglia F. Differential expression of chemokine receptors and chemotactic responsiveness of type 1 T helper cells (Th1s) and Th2s. *J Exp Med* 1998;187:129-134.
- Bonifacino JS and Traub LM. Signals for sorting of transmembrane proteins to endosomes and lysosomes. *Annu Rev Biochem* 2003;72:395-447.
- Brunet A, Roux D, Lenormand P, Dowd S, Keyse S, and Pouyssegur J. Nuclear translocation of p42/p44 mitogen-activated protein kinase is required for growth factor-induced gene expression and cell cycle entry. *EMBO J* 1999 Feb 1;18(3):664-74.
- Bucci M, Gratton JP, Rudic RD, Acevedo L, Roviezzo F, Cirino G, and Sessa WC. In vivo delivery of the caveolin-1 scaffolding domain inhibits nitric oxide synthesis and reduces inflammation. *Nat Med* 2000 Dec;6(12):1362-7.
- Busch SJ, Martin GA, Barnhart RL, Mano M, Cardin AD, and Jackson RL. Transrepressor activity of nuclear glycosaminoglycans on Fos and Jun/AP-1 oncoprotein-mediated transcription. *J Cell Biol* 1992 Jan;116(1):31-42.
- Byrne DP, Dart C, and Rigden DJ. Evaluating caveolin interactions: Do proteins interact with the caveolin scaffolding domain through a widespread aromatic residue-rich motif? *PLoS ONE* 2012;7(9) E44879.
- Cain BS, Harken AH, and Meldrum DR. Therapeutic strategies to reduce TNF α mediated cardiac contractile depression following ischemia and reperfusion. *J Mol Cell Cardiol* 1999;31:931-947.
- Cano E and Mahadevan LC. Parallel signal processing among mammalian MAPKs.

- Trends Biochem Sci* 1995;20:117–122.
- Caro CG, Fitz-Gerald JM, and Schroter RC. Arterial wall shear and distribution of early atheroma in man. *Nature* 1969 Sep 13;223(5211):1159-60.
- Castellot JJ, Addonizio ML, Rosenberg R, and Karnovsky MJ. Cultured endothelial cells produce a heparinlike inhibitor of smooth muscle cell growth. *J Cell Biol* 1981 Aug;90(2):372-9.
- Castellot JJ, Beeler DL, Rosenberg RD, and Karnovsky MJ. Structural determinants of the capacity of heparin to inhibit the proliferation of vascular smooth muscle cells. *J Cell Physiol* 1984;120: 315-320.
- Castellot JJ, Pukac LA, Caleb BL, Wright TC Jr, and Karnovsky MJ. Heparin selectively inhibits a protein kinase C-dependent mechanism of cell cycle progression in calf aortic smooth muscle cells. *J Cell Biol* 1989;109: 3147-3155.
- Castellot JJ, Wong K, Herman B, Hoover RL, Albertini DF, Wright TC, Caleb BL, and Karnovsky MJ. Binding and internalization of heparin by vascular smooth muscle cells. *J Cell Physiol* 1985;124:13-20.
- Cheah LS, Gwee M, Das R, Ballard H, Yang YF, Daniel EE, and Kwan CY. Evidence for the existence of a constitutive nitric oxide synthase in vascular smooth muscle. *Clin Exp Pharmacol Physiol* 2002 Aug;29(8):725-7.
- Chen Q and Pollard TD. Actin filament severing by cofilin dismantles actin patches and produces mother filaments for new patches. *Curr Biol* 2013 Jul 8;23(13):1154-62
- Chen YA and Scheller RH. SNARE-mediated membrane fusion. *Nat Rev Mol Cell Bio* 2001;2:98-106.

- Chidlow JH Jr and Sessa WC. Caveolae, caveolins, and cavins: complex control of cellular signaling and inflammation. *Cardiovasc Res* 2010;86:219-225
doi:10.1093/cvr/cvq075.
- Cho J-W, Park K, Kweon G, Jang B-C, Baek WK, Suh M-H, Kim C-W, Lee K-S, and Suh S. Curcumin inhibits the expression of COX-2 in UVB-irradiated human keratinocytes (HaCaT) by inhibiting activation of AP-1: p38 MAP kinase and JNK as potential upstream targets. *Exp Mol Med* 2005;37:186-192.
- Choi C, Sellak H, Brown FM, and Lincoln TM. cGMP-dependent protein kinase and the regulation of vascular smooth muscle cell gene expression: possible involvement of Elk-1 sumoylation. *Am J Physiol Heart Circ Physiol* 2010 Nov;299(5):H1660-70. doi: 10.1152/ajpheart.00677.2010.
- Clarke D, Katoh O, Gibbs RV, Griffiths SD, and Gordon MY. Interaction of interleukin 7 (IL-7) with glycosaminoglycans and its biological relevance. *Cytokine* 1995;7:325-330.
- Clowes AW and Karnovsky MJ. Suppression by heparin of smooth muscle cell proliferation in injured arteries. *Nature* 1997;265: 625-626.
- Conway D and Schwartz MA. Lessons from the endothelial junctional mechanosensory complex. *F1000 Biology Reports* 2012;4:1.
- Côté MC, Lavoie JR, Houle F, Poirier A, Rousseau S, and Huot J. Regulation of vascular endothelial growth factor-induced endothelial cell migration by LIM kinase 1-mediated phosphorylation of annexin-1. *J Biol Chem* 2010;285(11):8013-8021.

- Cramer L, Siebert M, and Mitchinson T. Identification of novel graded polarity actin filament bundles in locomoting heart fibroblasts: implications for the generation of motile force. *J Cell Biol* 1997;136(6):1287-1305.
- Cuadrado A and Nebreda A. Mechanisms and functions of p38 MAPK signalling. *Biochem J* 2010;429:403-417.
- Daum G, Hedin U, Wang Y, Wang T, and Clowes AW. Diverse Effects of Heparin on Mitogen-Activated Protein Kinase-Dependent Signal Transduction in Vascular Smooth Muscle Cells. *Circulation Research* 1997;81:17-23.
- David L, Mallet C, Vailhe B, Lamouille S, Feige J-J, and Bailly S. Activin receptor-like kinase 1 inhibits human microvascular endothelial cell migration: potential roles for JNK and ERK. *J Cell Physiol* 2007;213:484-489.
- Davis RJ. MAPKs: new JNK expands the group. *Trends Biochem Sci* 1994;19:470 – 473.
- Dejana E, Orsenigo F, and Lampugnani MG. The role of adherens junctions and VE-cadherin in the control of vascular permeability. *J Cell Sci* 2008;121:2115-2122.
- DePaola N, Phelps JE, Florez L, Keese CR, Minnear FL, Giaever I, and Vincent P. Electrical impedance of cultured endothelium under fluid flow. *Ann Biomed Eng* 2001;29:648-656.
- Dewey C, Bussolari S, Gimbrone M, Davies P. The dynamic response of vascular endothelial cells to fluid shear stress. *J Biomechanical Eng* 1981; 103:177–185
- Dhillon AS, von Kriegsheim A, Grindlay J, and Koch W. Phosphatase and feedback regulation of Raf-1 signaling. *Cell Cycle* 2007;6:3-7.

- Dickinson RJ and Keyse SM. Diverse physiological functions for dual-specificity MAPK kinase phosphatases. *J Cell Science* 2006;119:4607-4615.
- Dixit VM, Green S, Sarma V, Holzman LB, Wolf FW, O'Rourke K, Ward PA, Prochownik EV, and Marks RM. Tumor necrosis factor-alpha induction of novel gene products in human endothelial cells including a macrophage-specific chemotaxin. *J Biol Chem* 1990 Feb 15;265(5):2973-8.
- Edelberg JM, Conrad HE, and Pizzo SV. Heparin oligosaccharides enhance tissue-type plasminogen activator: A correlation between oligosaccharide length and stimulation of plasminogen activation. *Biochemistry* 1991;30:10999-11003.
- Eyers CE, McNeill H, Knebel A, Morrice N, Arthur SJC, Cuenda A, and Cohen P. The phosphorylation of CapZ-interacting protein (Cap-ZIP) by stress-activated protein kinases triggers its dissociation from CapZ. *Biochem J* 2005;389:127-135.
- Fan J and Watanabe T. Inflammatory reactions in the pathogenesis of atherosclerosis. *J. Atheroscler Thromb* 2003;10:63-71. 203.
- Fasciano S, Patel RC, Handy I, and Patel CV. Regulation of Vascular Smooth Muscle Proliferation by Heparin. *J Biol Chem* 2005;289(16):15682-89.
- Fasshauer D, Eliason WK, Brünger AT, and Jahn R. Identification of a minimal core of the synaptic SNARE complex sufficient for reversible assembly and disassembly. *Biochemistry* 1998;37:10354-10362.
- Finley MJ, Rauova L, Alferiev IS, Weisel JW, Levy RJ, and Stachelek SJ. Diminished adhesion and activation of platelets and neutrophils with CD47 functionalized blood contacting surfaces. *Biomaterial* 2012 Aug;33(24):5803-11.

- Flitney FW, Goldman RD, Skalli O, Mercurious K, and Davies P. Dynamic properties of intermediate filaments in cultured endothelial cells: effects of controlled fluid shear stress. *The Biology of Nitric Oxide* London: Portland. 1996; p. 251.
- Fouty BW, Grimison B, Fagan KA, Le Cras TD, Harral JW, Hoedt-Miller M, Sclafani RA, and Rodman DM. p27^{kip1} Is Important in Modulating Pulmonary Artery Smooth Muscle Cell Proliferation. *Am J Respir Cell Mol Biol* 2001;25:652-658.
- Franke R, Graffe M, Schnittler H, Seiffge D, and Mittermayer C. The induction of human vascular endothelial stress fibers by fluid shear stress. *Nature* 1984;307:648-649.
- Frostegård J, Ulfgren AK, Nyberg P, Hedin U, Swedenborg J, Andersson U, and Hansson GK. Cytokine expression in advanced human atherosclerotic plaques: dominance of proinflammatory (Th1) and macrophage-stimulating cytokines. *Atherosclerosis* 1999;145:33-34.
- Fryer A, Huang YC, Rao G, Jacoby D, Mancilla E, Whorton R, Piantadosi CA, Kennedy T, and Hoidal J. Selective O-Desulfation produces nonanticoagulant heparin that retains pharmacological activity in the lung. *J Pharmacol Exp Ther* 1997;282:208-219.
- Fukai N, Kenagy RD, Chen L, Gao L, Daum G, and Clowes AW. Syndecan-1: an inhibitor of arterial smooth muscle cell growth and intimal hyperplasia. *Arterioscler Thromb Vasc Biol* 2009;29:1356-1362.
- Furman C, Sieminski AL, Kwiatkowski AV, Rubinson DA, Vasile E, Bronson RT, Fässler R, and Gertler FB. Ena/VASP is required for endothelial barrier function in vivo. *J Cell Biol* 2007;179(4):761-775.

- Fürst R, Brueckl C, Kuebler WM, Zahler S, Krötz F, Görlach A, Vollmar AM, and Kiemer AK. Atrial natriuretic peptide induces mitogen-activated protein kinase phosphatase-1 in human endothelial cells via Rac1 and NAD(P)H oxidase/Nox2-activation. *Circ Res* 2005 Jan 7;96(1):43-53. Epub 2004 Nov 29.
- Galbraith CG, Shalak R, Chien S. Shear stress induces spatial reorganization of the endothelial cytoskeleton. *Cell Motility and the Cytoskeleton* 1998;40:314-330
- Galea J, Armstrong J, Gadsdon P, Holden H, Francis SE, Holt CM. Interleukin-1 beta in coronary arteries of patients with ischemic heart disease. *Arterioscler Thromb Vasc Biol* 1996 Aug;16(8):1000-6.
- García-Cardena G, Martasek P, Masters BS, Skidd PM, Couet J, Li S, Lisanti MP, and Sessa WC. Dissecting the interaction between nitric oxide synthase (NOS) and caveolin. Functional significance of the nos caveolin binding domain in vivo. *J Biol Chem* 1997 Oct 10;272(41):25437-40.
- Gilloti AC. Characterization of heparin receptor signal transduction in vascular smooth muscle cells. Diss. Lehigh University. 2000.
- Girard PR and Nerem RM. Shear stress modulates endothelial cell morphology and F-actin organization through the regulation of focal adhesion-associated proteins. *J Cell Physiol* 1995;163:179-193.
- Gitay-Goren H, Soker S, Vlodavsky I, and Neufeld G. The binding of vascular endothelial growth factor to its receptors is dependent on cell surface heparin-like molecules. *J Bio Chem* 1992;267:6093-6098.
- Goldin A, Bechman JA, Schmidt AM, and Creager MA. Advanced glycation end

- products. Sparking the development of diabetic vascular injury. *Circulation* 2006;Aug 8;114(6):597-605.
- Goyal P, Pandey D, Behring A, and Siess W. Inhibition of nuclear import of LIMK2 in endothelial cells by protein kinase C-dependent phosphorylation at Ser-283. *J Biol Chem* 2005;280(30):27569-27577.
- Gu S, Cifelli C, and Wang S, Heximer SP. RGS proteins: identifying new GAPs in the understanding of blood pressure regulation and cardiovascular function. *Clin Sci (Lond)*. 2009 Mar;116(5):391-9. doi: 10.1042/CS20080272.
- Gurniak CB, Perlas E, and Witke W. The actin depolymerizing factor n-cofilin is essential for neuron tube morphogenesis and neural crest cell migration. *Dev Biol* 2005;278:231-241.
- Hahn C and Schwartz MA. Mechanotransduction in vascular physiology and atherogenesis. *Nat Rev Mol Cell Biol* 2009;10(1):53-62.
- Hahn C, Wang C, Orr AW, Coon BG, and Schwartz MA. JNK2 promotes endothelial cell alignment under flow. *PLoS ONE* 2011;6(8):e24338.
- Hamel M. Deactivation and localization of stress-activated protein kinases in wounded vascular endothelial cells. Diss Lehigh University. 2001.
- Hamel M, Kanyi D, Cipolle MD, and Lowe-Krentz LJ. Active stress kinases in proliferating endothelial cells associated with cytoskeletal structures. *Endothelium* 2006;13:157-170.
- Han J, Liu S, Rose DM, Schlaepfer DD, McDonald H, and Ginsberg MH.

- Phosphorylation of the integrin alpha 4 cytoplasmic domain regulates paxillin binding. *J Biol Chem* 2001 Nov 2;276(44):40903-9
- Hannken T, Schroeder R, Stahl RA, and Wolf G. Atrial natriuretic peptide attenuates ANG II-induced hypertrophy of renal tubular cells. *Am J Physiol Renal Physiol* 2001 Jul;281(1):F81-90.
- Hansson GK, Libby, P, Schönbeck, U, and Yan, ZQ. Innate and adaptive immunity in the pathogenesis of atherosclerosis. *Circ Res* 2002;Aug 23;91(4):281-91.
- Hatakeyama M, Imaizumi T, Tamo W, Yamashita K, Yoshida H, Fukuda I, and Satoh K. Heparin inhibits IFN- γ -induced fractalkine/CX3CL1 expression in human endothelial cells. *Inflammation* 2004;28(1):7-13.
- Heidenreich PA et al. Heart Disease and Stroke Statistics – 2009 Update: A Report From the American Heart Association Statistics Committee and Strokes Statistics Subcommittee. *Circulation* 2009;119(3): e21-181.
- Helmke BP, Thakker DB, Goldman RD, and Davies PF. Spatiotemporal analysis of flow-induced intermediate filament displacement in living endothelial cells. *Biophys J* 2001 Jan;80(1):184-94.
- Hendriks-Balk MC, van Loenen PB, Hajji N, Michel MC, Peters SL, and Alewijnse AE. S1P receptor signalling and RGS proteins; expression and function in vascular smooth muscle cells and transfected CHO cells. *Eur J Pharmacol* 2008 Dec 14;600(1-3):1-9. doi: 10.1016/j.ejphar.2008.09.041. Epub 2008 Oct 7.
- Horstman DJ, Fischer LG, Kouretas PC, Hannan RL, and Rich GF. Role of nitric oxide in

- heparin-induced attenuation of hypoxic pulmonary vascular remodeling. *J Appl Physiol* 2002 May;92(5):2012-8.
- Huang TY, DerMardirossian C, and Bokoch GM. Cofilin phosphatases and regulation of actin dynamics. *Curr Opin Cell Biol* 2006;18:26-31.
- Humphries JD, Byron A, and Humphries MJ. Integrin ligands at a glance. *J Cell Sci* 2006;119, 3901-3903.
- Huntington JA. Serpin structure, function and dysfunction. *J Thromb Haemost* 2011 Jul;9 Suppl 1:26-34. doi: 10.1111/j.1538-7836.2011.04360.x.
- Hu S, Chen J, Fabry B, Numaguichi Y, Gouldstone A, Ingber D, Fredberg J, Butler J, Wang N. Intracellular stress tomography reveals stress focusing and structural anisotropy in cytoskeleton of living cells. *Am J Physiol – Cell Physiol* 2003;285:C1082-C1090.
- Iida K, Matsumoto S, and Yahara I. The KKRKK sequence is involved in heat-shock-induced nuclear translocation of the 18-kDa actin-binding protein, cofilin. *Cell Struct Funct* 1992;17:39-46.
- Jacob A, Molkenin JD, Smolenski A, Lohmann SM, and Begum N. Insulin inhibits PDGF-directed VSMC migration via NO/ cGMP increase of MKP-1 and its inactivation of MAPKs. *Am J Physiol Cell Physiol* 2002 Sep;283(3):C704-13.
- Jiang G, Dallas-Yang Q, Liu F, Moller D, and Zhang B. Salicylic acid reverses phorbol 12-myristate-13-acetate (PMA)- and tumor necrosis factor α (TNF α)-induced insulin receptor substrate 1 (IRS1) serine 307 phosphorylation and insulin

- resistance in human embryonic kidney 293 (HEK293) cells. *J Biol Chem* 2003;278:180-186.
- Jo H, Sipos K, Go YM, Law R, Rong J, and McDonald JM. Differential effect of shear stress on extracellular signal-regulated kinase and N-terminal Jun kinase in endothelial cells. G_{i2} - and $G_{b/g}$ -dependent signaling pathways. *J Biol Chem* 1997;272:1395-1401.
- Ju H, Zou R, Venema VJ, and Venema RC. Direct interaction of endothelial nitric-oxide synthase and caveolin-1 inhibits synthase activity. *J Biol Chem*. 1997 Jul 25;272(30):18522-5.
- Kadohama T, Akasaka N, Nishimura K, Hoshino Y, Sasajima T, and Sumpio BE. p38 MAPK activation in endothelial cells is implicated in cell alignment and elongation induced by FSS. *Endothelium* 2006;13: 43-50.
- Kaminska B. MAPK signalling pathways as molecular targets for anti-inflammatory therapy-from molecular mechanisms to therapeutic benefits. *Biochim Biophys Acta* 2005; 1754(1-2):253-62.
- Kanyi D. Cytoskeletal associations of SAPK/MAPK members, and a role for PKG and phosphatases in heparin modulation of inflammation-induced signaling transduction in endothelial cells. Diss. Lehigh University. 2006.
- Karcher H. A three-dimensional viscoelastic model for cell deformation with experimental verification. *Biophys J* 2003;85:3336-3349.
- Karderon D, Richardson WD, Markham AF, and Smith AE. Sequence requirements for nuclear localization of simian virus 40 large-T antigen. *Nature* 1984;311:499-509.

- Karin M, Liu Zg, and Zandi E. AP-1 function and regulation. *Curr Opin Cell Biol* 1997 Apr;9(2):240-6.
- Kassel O, Sancono A, Kratzschmar J, Kreft B, Stassen M, and Cato A. Glucocorticoids inhibit MAP kinase via increased expression and decreased degradation of MKP-1. *EMBO J* 2001;20:7108-7116.
- Kayyali US, Pennella CM, Trujillo C, Villa O, Gaestel M, and Hassoun PM. Cytoskeletal changes in hypoxic pulmonary endothelial cells are dependent on MAPK-activated protein kinase MK2. *J Biol Chem* 2002;277:42596-42602.
- Kazi M, Lundmark K, Religa P, Gouda I, Larm O, Ray A, Swedenborg J, and Hedin U. Inhibition of rat smooth muscle cell adhesion and proliferation by non-anticoagulant heparins. *J Cell Physiol* 2002;193:365-372.
- Keezer SM, Ivie SE, Krutzsch HC, Tandle A, Libutti SK, and Roberts DD. Angiogenesis inhibitors target the endothelial cell cytoskeleton through altered regulation of heat shock protein 27 and cofilin. *Cancer Res* 2003;63:6405-6412.
- Kiemer A, Weber N, Furst R, Bildner N, Kulhanek-Heinze S, and Vollmar A. Inhibition of p38 MAPK activation via induction of MKP-1: atrial natriuretic peptide reduces TNF-alpha-induced actin polymerization and endothelial permeability. *Circ Res* 2002;90:874-881.
- Kinsella MG, Tran PK, Weiser-Evans MC, Reidy M, Majack RA, and Wight TN. Changes in perlecan expression during vascular injury: role in the inhibition of smooth muscle cell proliferation in the late lesion. *Arterioscler Thromb Vasc Biol* 2003;23:608-614.

- Kishikawa H, Shimokama T, and Watanabe T. Localization of T lymphocytes and macrophages expressing IL-1, IL-2 receptor, IL-6 and TNF in human aortic intima. Role of cell-mediated immunity in human atherogenesis. *Virchows Arch A Pathol Anat Histopathol* 1993;423(6):433-42.
- Kobayashi M, Nishita M, Mishima T, Ohashi K, and Mizuno K. MAPKAPK-2-mediated LIM-kinase activation is critical for VEGF-induced actin remodeling and cell migration. *EMBO J* 2006;25(4):713-26.
- Kumar S, Jiang MS, Adams JL, and Lee JC. Pyridinylimidazole compound SB20580 inhibits the activity but not the activation of p38 mitogen-activated protein kinase. *Biochem et Biophysica Res Comm* 1999;263:825-831.
- Kyriakis JM, Banerjee P, Nikolakaki E, Dai T, Rubie EA, Ahmad MF, Avruch J, and Woodgett JR. The stress-activated protein kinase subfamily of c-Jun kinases. *Nature* 1994;369:156 –160.
- Laage R, Rohde J, Brosig B, and Langosch D. A conserved membrane-spanning amino acid motif drives homomeric and supports heteromeric assembly of presynaptic SNARE proteins. *J Biol Chem* 2000;275:17481-17487.
- Lander HM, Tauras JM, Ogiste JS, Hori O, Moss RA, and Schmidt AM. Activation of the receptor for advanced glycation end products triggers a p21(ras)-dependent mitogen activated protein kinase pathway regulated by oxidant stress. *J Biol Chem* 1997;272:17810-17814.
- Langille BL and Adamson SL. Relationship between blood flow direction and endothelial

- cell orientation at arterial branch sites in rabbits and mice. *Circ Res* 1981;48:481-488.
- Lasa M, Abraham S, Boucheron C, Saklatvala J, and Clark AR. Dexamethasone causes sustained expression of mitogen-activated protein kinase (MAPK) phosphatase 1 and phosphatase-mediated inhibition of MAPK p38. *Mol Cell Biol* 2002;22:7802-7811.
- Lazarides E and Burridge K. Alpha-actinin: immunofluorescent localization of a muscle structural protein in nonmuscle cells. *Cell* 1975;6(3):289-298.
- Liao W, Feng L, Zheng J, and Chen DB. Deciphering mechanisms controlling placental artery endothelial cell migration stimulated by endothelial growth factor. *Endocrinology* 2010;151:3432-3444.
- Libby P. Inflammation in atherosclerosis. *Arterioscler Thromb Vasc Biol* 2012 Sep;32(9):2045-51.
- Libby P, Ridker PM, and Maseri A. Inflammation and atherosclerosis. *Circulation* 2002 Mar 5;105(9):1135-43.
- Li DY, Chen HJ, Staples ED, Ozaki K, Annex B, Singh BK, Vermani R, and Mehta JL. Oxidized low-density lipoprotein receptor LOX-1 and apoptosis in human atherosclerotic lesions. *J Cardiovasc Pharmacol Ther* 2002 Jul;7(3):147-53.
- Li S, Kim M, Hu Y-L, Shila J, Schlaepfer DD, Hunter T, Chien S, and Shyy JY-J. Fluid shear stress activation of focal adhesion kinase. Linking to mitogen-activated protein kinases. *J Biol Chem* 1997;272:30455-30462.
- Li S, Chen BP, Azuma N, Hu YL, Wu SZ, Sumpio BE, Shyy JY, and Chien S. Distinct

- roles for the small GTPases Cdc42 and Rho in endothelial responses to shear stress. *J Clin Invest* 1999;103:1141-1150.
- Lindahl U, Kusche-Gullberg M, and Kjellén L. Regulated diversity of heparan sulfate. *J Biol Chem* 1998;273(39):24979-24982.
- Lin MC, Galletta BJ, Sept D, and Cooper JA. Overlapping and distinct functions for cofilin, coronin, and Aip1 in actin dynamics in vivo. *J Cell Sci* 2010;123:1329-1342.
- Lin T, Zeng L, Liu Y, DeFea K, Schwartz MA, Chien S, and Shyy JA. Rho-ROCK-LIMK-Cofilin pathway regulates shear stress activation of sterol regulatory element binding proteins. *Circ Res* 2003;92:1296-1304.
- Liu S, Kiosses WB, Rose DM, Slepak M, Salgia R, Griffin JD, Turner CE, Schwartz MA, and Ginsberg MH. A fragment of paxillin binds the alpha 4 integrin cytoplasmic domain (tail) and selectively inhibits alpha 4-mediated cell migration. *J Biol Chem* 2002 Jun 7;277(23):20887-94.
- Liu YT, Song L, and Templeton DM. Heparin suppresses lipid raft-mediated signaling and ligand-independent EGF receptor activation. *J Cell Physiol* 2007 Apr;211(1):205-12.
- Lortat-Jacob H, Garrone P, Banchereau J, and Grimaud JA. Human interleukin 4 is a glycosaminoglycan-binding protein. *Cytokine* 1997;9:101-105.
- Mach F, Sauty A, Iarossi AS, Sukhova GK, Neote K, Libby P, and Luster AD. Differential expression of three T lymphocyte-activating CXC chemokines in human atheroma-associated cells. *J Clin Invest* 1999;104:1041-1050.

- Malek AM and Izumo S. Mechanism of endothelial cell shape change and cytoskeletal remodeling in response to fluid shear stress. *J Cell Sci* 1996;109:713-726.
- Mamluk R, Gechtman Z, Kutcher ME, Gasiunas N, Gallagher J, and Klagsbrun M. Neuropilin-1 binds vascular endothelial growth factor 165, placenta growth factor-2, and heparin via its b1b2 domain. *J Biol Chem* 2002;277:24818–24825.
- Matsuzaki F, Matsumoto S, Yahara I, Yonezawa N, Nishida E, and Sakai H. Cloning and characterization of porcine brain cofilin cDNA. Cofilin contains the nuclear transport signal sequence. *J Biol Chem* 1988 Aug 15;263(23):11564-8.
- McMullen ME, Bryant PW, Glembotski CC, Vincent PA, and Pumiglia KM. Activation of p38 has opposing effects on the proliferation and migration of endothelial cells. *J Biol Chem* 2005;280:20995-21003.
- Mehta JL, Chen J, Hermonat PL, Romeo F, and Novelli G. Lectin-like, oxidized low-density lipoprotein receptor-1 (LOX-1): a critical player in the development of atherosclerosis and related disorders. *Cardiovasc Res* 2006 Jan;69(1):36-45.
- Melichar VO, Behr-Roussel D, Zabel U, Uttenthal LO, Rodrigo J, Rupin A, Verbeuren TJ, Kumar H S A, and Schmidt HH. Reduced cGMP signaling associated with neointimal proliferation and vascular dysfunction in late-stage atherosclerosis. *PNAS* 2004 Nov 23;101(47):16671-6. Epub 2004 Nov 16.
- Mengistu M, Brotzman H, Ghadiali S, and Lowe-Krentz LJ. Fluid shear stress-induced JNK activity leads to actin remodeling for cell alignment. *J Cell Physiol* 2011;226(1):110-121.
- Mengistu M, Slee JB, and Lowe-Krentz LJ. Stressed Out and Actin Up: stress-activated

- protein kinase regulation of actin remodeling directs endothelial cell morphology and migration. In: Consueles VA and Minas DJ, editors. Actin: Structure, Functions, and Disease. New York: Nova Science Publishers. p 177-205. 2012.
- Michel JB, Feron O, Sacks D, and Michel T. Reciprocal regulation of endothelial nitric-oxide synthase by Ca²⁺-calmodulin and caveolin. *J Biol Chem* 1997 Jun 20;272(25):15583-6.
- Mielenz D, Hapke S, Pöschl E, von Der Mark H, and von Der Mark K. The integrin alpha 7 cytoplasmic domain regulates cell migration, lamellipodia formation, and p130CAS/Crk coupling. *J Biol Chem* 2001 Apr 20;276(16):13417-26.
- Mishra-Gorur K and Castellot JJ. Heparin Rapidly and Selectively Regulates Protein Tyrosine Phosphorylation in Vascular Smooth Muscle Cells. *J Cell Physiol* 1999;178: 205-215.
- Mongiati M, Taylor K, Otto J, Aho S, Uitto J, Whitelock JM, and Iozzo RV. The protein core of the proteoglycan perlecan binds specifically to fibroblast growth factor-7. *J Biol Chem* 2000;275(10):7095-7100.
- Moriyama K, Iida K, and Yahara I. Phosphorylation of Ser-3 of cofilin regulates its essential function on actin. *Genes Cells* 1996 Jan;1(1):73-86.
- Morrison P, Lowe-Krentz LJ. Heparin induces changes in the synthesis of porcine aortic endothelial cell heparan sulfate proteoglycans. *Exp Cell Res* 1989 Oct;184(2):304-15.
- Mott RE, Helmke BP. Mapping the dynamics of shear stress-induced structural changes

- in endothelial cells. *American Journal of Physiology - Cell Physiology* 2007; 293:C1616–C1626.
- Moyer CF, Sajuthi D, Tulli H, and Williams JK . Synthesis of IL-1 alpha and IL-1 beta by arterial cells in atherosclerosis. *Am J Pathol* 1991 Apr;138(4):951-60.
- Mrabat H, Garg HG, and Hales CA. Growth inhibition of bovine pulmonary artery smooth muscle cells following long-term heparin treatment. *J Cell Physiol* 2009;221:603-608.
- Nagaoka R, Abe H, and Obinata T. Site-directed mutagenesis of the phosphorylation site of cofilin: its role in cofilin-actin interaction and cytoplasmic localization. *Cell Motil Cytoskeleton* 1996;35(3):200-9.
- Nagata-Ohashi K, Ohta Y, Goto K, Chiba S, Mori R, Nishita M, Ohashi K, Kousaka K, Iwamatsu A, Niwa R, Uemura T, and Mizuno K. A pathway of neuregulin-induced activation of cofilin-phosphatase slingshot and cofilin in lamellipodia. *J Cell Biol* 2004;165:465-471.
- Napoli C, D'Armiento FP, Mancini FP, Postiglione A, Witztum JL, Palumbo G, and Palinski W. Fatty streak formation occurs in human fetal aortas and is greatly enhanced by maternal hypercholesterolemia. Intimal accumulation of low density lipoprotein and its oxidation precede monocyte recruitment into early atherosclerotic lesions. *J Clin Invest* 1997 Dec 1;100(11):2680-90.
- Nausch LW, Ledoux J, Bonev AD, Nelson MT, and Dostmann WR. Differential patterning of cGMP in vascular smooth muscle cells revealed by single GFP-linked biosensors. *PNAS* 2008 Jan 8;105(1):365-70.

- Nerem RM, Levesque MJ, and Cornhill JF. Vascular endothelial morphology as an indicator of the pattern of blood flow. *J Biomech Eng* 1981;103:172-176.
- Nishida E and Gotoh Y. The MAP kinase cascade is essential for diverse signalling pathways. *Trends Biochem Sci* 1993;18:128 –131.
- Nishida E, Iida K, Yonezawa N, Koyasu S, Yahara I, and Sakai H.
Cofilin is a component of intranuclear and cytoplasmic actin rods induced in cultured cells. *PNAS* 1987;Aug;84(15):5262-6.
- Nishida E, Maekawa S, and Sakai H. Cofilin, a protein in porcine brain that binds to actin filaments and inhibits their interaction with myosin and tropomyosine. *Biochemistry* 1984;23:5307-5313.
- Noria S, Xu F, McCue S, Jones M, Gotlieb AI, and Langille BL. Assembly and reorientation of stress fibers drives morphological changes to endothelial cells exposed to shear stress. *Am J Pathol* 2004;164(4):1211-1223.
- Ogden CL, Carroll MD, Kit BK, and Flegal KM. Prevalence of obesity in the United States, 2009–2010. NCHS data brief, no 82. Hyattsville, MD: National Center for Health Statistics. 2012.
- Ohura N, Yamamoto K, Ichioka S, Sokabe T, Nakatsuka H, and Baba A. Global analysis of shear stress-responsive genes in vascular endothelial cells. *J Atheroscler Thromb* 2003;10:304-313.
- Oktay M, Wary KK, Dans M, Birge RB, and Giancotti FG. Integrin-mediated activation

- of focal adhesion kinase is required for signaling to Jun NH₂-terminal kinase and progression through the G₁ phase of the cell cycle. *J Cell Biol* 1999;145:1461-1469.
- Ono K, Hattori H, Takeshita S, Kurita A, and Ishihara M. Structural features in heparin that interact with VEGF165 and modulate its biological activity, *Glycobiology* 1999;9:705–711.
- Orr AW, Sanders JM, Bevard M, Coleman E, Sarembock IJ, and Schwartz MA. The subendothelial extracellular matrix modulates NF-κB activation by flow: a potential role in atherosclerosis. *J Cell Biol* 2005;169:191-202.
- Osborn EA, Rabodzey A, Dewey Jr CF, and Hartwig JH. Endothelial actin cytoskeleton remodeling during mechanostimulation with fluid shear stress. *Am J Physiol Cell Physiol* 2006;290:C444-52.
- Ottlinger ME, Pukac LA, and Karnovsky MJ. Heparin Inhibits Mitogen-Activated Protein Kinase Activation in Intact Rat Vascular Smooth Muscle Cells. *J Biol Chem* 1993;268:19173-19761.
- Paleolog EM, Delasalle SA, Buurman WA, and Feldmann M. Functional activities of receptors for tumor necrosis factor-α on human vascular endothelial cells. *Blood* 1994 Oct 15;84(8):2578-90.
- Parton RG and Simmons K. The multiple faces of caveolae. *Nat Rev Mol Cell Biol* 2007;8:185-194.
- Patel HH, Murray F, and Insel PA. Caveolae as organizers of pharmacologically relevant signaling transduction molecules. *Annu Rev Pharmacol Toxicol* 2008;48:359-91.

- Patton WA, Granzow CA, Getts LA, Thomas SC, Zotter LM, Gunzel KA, and Lowe-Krentz LJ. Identification of a heparin-binding protein using monoclonal antibodies that block heparin-binding to porcine aortic endothelial cells. *Biochem J* 1995;331:461-469.
- Patton WA. Ladder Sequencing of a Peptide using MALDI-TOF Mass Spectrometry. *Chem Educator* 2004;9:272-275.
- Pederson T. As functional nuclear actin comes into view, is it globular, filamentous, or both? *J Cell Biol* 2008;180:1061-1064.
- Pellegrin S and Mellor H. Actin stress fibers. *J Cell Sci* 2007;120(20):3491-3499
- Penc SF, Pomahac B, Eriksson E, Detmar M, and Gallo RL. Dermatan sulfate activates nuclear factor- κ B and induces endothelial and circulating intercellular adhesion molecule-1. *J Clin Invest* 1999;103:1329-1335.
- Pendleton A, Pope B, Weeds A, and Koffer A. Latrunculin B or ATP depletion induces cofilin-dependent translocation of actin into nuclei of mast cells. *J Biol Chem* 2003;278(16):14394-14400.
- Peterson TE, Kleppe LS, Caplice NM, Pan S, Mueske CS, and Simari RD. The regulation of caveolin expression and localization by serum and heparin in vascular smooth muscle cells. *Biochem Biophys Res Commun* 1999 Nov 30;265(3):722-7.
- Pilz RB and Broderick KE. Role of cyclic GMP in gene regulation. *Front Biosci* 2005 May 1;10:1239-68.
- Pukac LA, Castellot JJ, Wright TC, Caleb BL, and Karnovsky MJ. Heparin Inhibits c-fos

- and c-myc mRNA Expression in Vascular Smooth Muscle Cells. *Cell Regul* 1990;Apr;1(5):435-443.
- Pukac LA, Ottlinger ME, and Karnovsky MJ. Heparin Suppresses Specific Second Messenger Pathways for Proto-oncogene Expression in Rat Vascular Smooth Muscle Cells. *J Biol Chem* 1992;267:3707-3711.
- Pukac LA, Carter JE, Ottlinger ME, and Karnovsky MJ. Mechanisms of Inhibition by Heparin of PDGF Stimulated MAP Kinase Activation in Vascular Smooth Muscle Cells. *J Cell Physiol* 1997;122:69-78.
- Pugh R. Determining How Heparin Interferes with the MAPK/ERK Pathway: An Attempt to Understand the Atherosclerotic Process. Diss. Lehigh University. 2010.
- Ramsden L and Rider CC. Selective and differential binding of interleukin (IL)-1 alpha, IL-1 beta, IL-2 and IL-6 to glycosaminoglycans. *Eur J Immunol* 1992;22:3027-3031.
- Ranjbaran H, Wang Y, Manes TD, Yakimov AO, Akhtar S, Kluger MS, Pober JS, and Tellides G. Heparin displaces interferon- γ -inducible chemokines (IP-10, I-TAC, and Mig) sequestered in the vasculature and inhibits the transendothelial migration and arterial recruitment of T cells. *Circulation* 2006;114:1293-1300.
- Rao NV, Argyle B, Xu X, Reynolds PR, Walenga JM, Prechel M, Prestwich GD, MacArthur RB, Walters BB, Hoidal JR, and Kennedy TP. Low anticoagulant heparin targets multiple sites of inflammation, suppresses heparin-induced

- thrombocytopenia, and inhibits interaction of RAGE with its ligands. *Am J Cell Physiol* 2010;299:C97-C110.
- Rath G, Dessy C, and Feron O. Caveolae, caveolin and control of vascular tone, nitric oxide (NO) and endothelium derived hyperpolarizing factor (EDHF) regulation. *J Phys and Pharmacol* 2009;60(4):105-109.
- Reilly CF, Kindy MS, Brown KE, Rosenberg RD, and Sonenshein GE. Heparin prevents vascular smooth muscle cell progression through the G1 phase of the cell cycle. *J Biol Chem* 1989;264(12):6990-6995.
- Rein CM, Desai UR, and Church FC. Serpin-glycosaminoglycan interactions. *Methods Enzymol* 2011;501:105-37.
- Reinhard J and Scheller RH. SNARES – engines for membrane fusion. *Nat Rev Mol Cell Bio* 2006;7:631-643.
- Rhen T and Cidlowski J. Antiinflammatory action of glucocorticoids - New mechanisms for old drugs. *N Engl J Med* 2005;353:1711-1723.
- Roberts R, Gallagher J, Spooncer E, Allen TD, Bloomfield F, and Dexter TM. Heparan sulphate bound growth factors: a mechanism for stromal cell mediated haemopoiesis. *Nature* 1988;332:376-378.
- Rodríguez A, Gómez-Ambrosi J, Catalán V, Fortuño A, and Frühbeck G. Leptin inhibits the proliferation of vascular smooth muscle cells induced by angiotensin II through nitric oxide-dependent mechanisms. *Mediators Inflamm* 2010;2010:105489.
- Rohan PJ, Davis P, Moskaluk CA, Kearns M, Krutzsch H, Siebenlist U, and Kelly K.

- PAC-1: a mitogen-induced nuclear protein tyrosine phosphatase. *Science* 1993 Mar 19;259(5102):1763-6.
- Ross R. Atherosclerosis: A Defense Mechanism Gone Awry. *AJP* 143(4):987-1002. 1993.
- Ross R. Atherosclerosis – An Inflammatory Disease. *New England J. of Med* 1999;340(2):115-126.
- Rüegg J, Holsboer F, Turck C, and Rein T. Cofilin 1 is revealed as an inhibitor of glucocorticoid receptor by analysis of hormone-resistant cells. *Mol Cell Biol* Nov 2004;24(21):9371-82.
- Ruderman JV. MAP kinase and the activation of quiescent cells. *Curr Opin Cell Biol* 1993;5:207–213.
- Rudijanto A. The Role of Vascular Smooth Muscle Cells on the Pathogenesis of Atherosclerosis. *Acta Med Indones-Indones J Intern Med* 2007;39(2):86-93.
- Rus HG, Niculescu F, and Vlaicu R. Tumor necrosis factor-alpha in human arterial wall with atherosclerosis. *Atherosclerosis* 1991 Aug;89(2-3):247-54.
- Salgame P, Abrams JS, Clayberger C, Goldstein H, Convit J, Modlin RL, and Bloom BR. Differing lymphokine profiles of functional subsets of human CD4 and CD8 T cell clones. *Science* 1991;254:279-282.
- Sato M, Levesque M, and Nerem R. Micropipette aspiration of cultured bovine aortic endothelial cells exposed to shear stress. *Atherosclerosis* 1987;7:276-286.
- Sato J, Nair K, Hiddinga J, Eberhardt NL, Fitzpatrick LA, Katusic ZS, O'Brien T. eNOS

- gene transfer to vascular smooth muscle cells inhibits cell proliferation via upregulation of p27 and p21 and not apoptosis. *Cardiovasc Res* 2000 Sep;47(4):697-706.
- Savage JM, Gilotti AC, Granzow CA, Molina F, and Lowe-Krentz LJ. Antibodies against a heparin receptor slow cell proliferation and decrease MAPK activation in vascular smooth muscle cells. *J Cell Physiol* 2001;187:283-293.
- Schaller MD. Paxillin: a focal adhesion-associated adaptor protein. *Oncogene* 2001 Oct 1;20(44):6459-72.
- Schnittler H. Structural and functional aspects of intercellular junctions in vascular endothelium. *Basic Research in Cardiology* 1998;93:30-39.
- Schnittler H, Schneider S, Raifer H, Luo F, Dietrich P, Just I, Aktories K. Role of actin filaments in endothelial cell-cell adhesion and membrane stability under fluid shear stress. *Eur J Physiol* 2001;42:675-687.
- Schonthaler HB, Guinea-Viniegra J, and Wagner EF. Targeting inflammation by modulating the Jun/AP-1 pathway. *Ann Rheum Dis* 2011 Mar;70 Suppl 1:i109-12. doi:10.1136/ard.2010.140533.
- Seebach J, Dieterich P, Luo F, Schillers H, Vestweber D, Oberleithner H, Gall HJ, and Schnittler HJ. Endothelial barrier function under laminar fluid shear stress. *Lab Invest* 2000;80(12):1819-1831.
- Seeger R and Krebs EG. The MAPK signaling cascade. *FASEB J* 1995;9: 726 –735.
- Shaulian E and Karin M. AP-1 as a regulator of cell life and death. *Nat Cell Biol* 2002 May;4(5):E131-6.

- Shen J and DiCorleto P. ADP stimulates human endothelial cell migration via P2Y1 nucleotide receptor mediated mitogen-activated protein kinase pathways. *Circ Res* 2008; 102:448-456.
- Shih VF, Tsui R, Caldwell A, and Hoffmann A. A single NF κ B system for both canonical and non-canonical signaling. *Cell Res* 2011;21:86-102.
- Shin HS, Lee HJ, Nishida M, Lee MS, Tamura R, Yamashita S, Matsuzawa Y, Lee IK, and Koh GY. Betacellulin and amphiregulin induce upregulation of cyclin D1 and DNA synthesis activity through differential signaling pathways in vascular smooth muscle cells. *Circ Res* 2003;Aug 22;93(4):302-10.
- Siasos G, Tousoulis D, Siasou Z, Stefanadis C, and Papavassiliou AG. Shear Stress, Protein Kinases and Atherosclerosis. *Current Medicinal Chemistry* 2007;14: 1567-1572.
- Singh S, Powell DW, Rane MJ, Millard TH, Trent JO, Pierce WM, Klein JB, Machesky LM, and McLeish KR. Identification of the p16-Arc Subunit of the Arp 2/3 Complex as a Substrate of MAPK-activated Protein Kinase 2 by Proteomic Analysis. *J Biol Chem* 2003;278(38):36410-36417.
- Slee JB and Lowe-Krentz LJ. Actin Realignment and Cofilin Regulation Are Essential for Barrier Integrity During Shear Stress. *J Cell Biochem* 2013;114: 782–795.
- Slee JB, Pugh R, and Lowe-Krentz LJ. Beyond anticoagulation: Roles for heparin in the vasculature. In: Heparin: Properties, Uses, and Side Effects. Editors: DE Piyathilake and Rh Liang. Nova Sciences Publishers Inc. 2012:59-8.
- Soosairajah J, Mairi S, Wiggan O, Sarmiere P, Moussi N, Sarcevic B, Sampath R,

- Bamburg JR, and Bernard O. Interplay between components of a novel LIM kinase-slingshot phosphatase complex regulates cofilin. *EMBO J* 2005;24:473-486.
- Sowa G. Caveolae, caveolins, cavins, and endothelial cell function: new insights. *Front Physiol* 2012;2(120):1-13.doi: 10.3389/fphys.2011.00120.
- Spivak-Kroizman T, Lemmon MA, Dikic I, Ladbury JE, Pinchasi D, Huang J, Jaye M, Crumley G, Schlessinger J, and Lax I. Heparin-induced oligomerization of FGF molecules is responsible for FGF receptor dimerization, activation, and cell proliferation. *Cell* 1994;79:1015–1024.
- Spronk H, van der Voort D, and Ten Cate H. Blood coagulation and the risk of atherothrombosis: a complex relationship. *Thrombosis J* 2004;2:12-21.
- Strydom HC, Chandler AB, Glagov S, Guyton JR, Insull W Jr, Rosenfeld ME, Schaffer SA, Schwartz CJ, Wagner WD, and Wissler RW. A definition of initial, fatty streak, and intermediate lesions of atherosclerosis. A report from the Committee on Vascular Lesions of the Council on Arteriosclerosis, American Heart Association. *Circulation* 1994 May;89(5):2462-78.
- Su J, Scholz PM, and Weiss HR. Differential effects of cGMP produced by soluble and particulate guanylyl cyclase on mouse ventricular myocytes. *Exp Biol Med* 2005 Apr;230(4):242-50.
- Sugimoto T, Haneda M, Togawa M, Isono M, Shikano T, Araki S, Nakagawa T,

- Kashiwagi A, Guan KL, Kikkawa R. Atrial natriuretic peptide induces the expression of MKP-1, a mitogen-activated protein kinase phosphatase, in glomerular mesangial cells. *J Biol Chem* 1996 Jan 5;271(1):544-7.
- Suurna MV, Ashworth SL, Hosford M, Sandoval RM, Wean SE, Shah BM, Bamburg JR, and Molitoris BA. Cofilin mediates ATP depletion-induced endothelial cell actin alterations. *Am J Physiol Renal Physiol* 2006;290:F1398-1407.
- Tantini B, Manes A, Fiumana E, Pignatti C, Guarnieri C, Zannoli R, Branzi A, and Galie N. Antiproliferative effect of sildenafil on human pulmonary artery smooth muscle cells. *Basic Res Cardiol* 2005 Mar;100(2):131-8. Epub 2004 Nov 24.
- Tharakan B, Hellman J, Sawant DA, Tinsley JH, Parrish AR, Hunter FA, Smythe WR, and Childs EW. β -catenin in the regulation of microvascular endothelial cell hyperpermeability. *Shock* 2012;Mar37(3):306-311.
- Thornton TM and Rincon M. Non-Classical p38 MAP Kinase Functions: Cell Cycle Checkpoints and Survival. *Int J Biol Sci* 2009;5(1):44-53.
- Thourani VH, Brar SS, Kennedy TP, Thornton LR, Watts JA, Ronso, RS, Zhao ZQ, Sturrock AL, Hoidal JR, and Vinten-Johansen J. Nonanticoagulant heparin inhibits NF-kappaB activation and attenuates myocardial reperfusion injury. *Am J Physiol Heart Cir Physiol* 2000;48:H2084-H2093.
- Tock J, Van Putten V, Stenmark KR, and Nemenoff RA. Induction of SM-a-actin expression by mechanical strain in adult vascular smooth muscle cells is mediated through activation of JNK and p38 MAP kinase. *Biochem Biophys Res Commun* 2003;301:1116-1121.

- Tran PK, Tran-Lundmark K, Soininen R, Tryggvason, K, Thyberg J, and Hedin U. Increased intimal hyperplasia and smooth muscle cell proliferation in transgenic mice with heparan sulfate-deficient perlecan. *Circ Res* 2004;94:550-558.
- Tzima E, Irani-Tehrani M, Kiosses WB, Dejana E, Schultz DA, Engelhardt B, Cao G, DeLisser H, and Schwartz MA. A mechanosensory complex that mediates the endothelial cell response to fluid shear stress. *Nature* 2005;437:426-431.
- Ulrich-Merzenich G and Zeitler H. The lectin-like oxidized low-density lipoprotein receptor-1 as therapeutic target for atherosclerosis, inflammatory conditions and longevity. *Expert Opin Ther Targets* 2013 Jun 6. [Epub ahead of print]
- Vadiveloo PK, Filonzi EL, Stanton HR, and Hamilton JA. G1 phase arrest of human smooth muscle cells by heparin, IL-4, and cAMP is linked to repression of cyclin D1 and cdk2. *Atherosclerosis* 1997;Aug;133(1):61-69.
- van Besouw NM, Daane CR, Vaessen LM, Mochtar B, Balk AH, and Weimar W. Donor-specific cytokine production by graft-infiltrating lymphocytes induces and maintains graft vascular disease in human cardiac allografts. *Transplantation* 1997;63:1313-1318.
- Viemann D, Goebeler M, Schmid S, Nordhues U, Klimmek K, Sorg C, and Roth J. TNF induces distinct gene expression programs in microvascular and macrovascular human endothelial cells. *J Leukoc Biol* 2006;80:174-185.
- Vincent PA, Xiao K, Buckley KM, and Kowalczyk AP. VE-cadherin: adhesion at arm's length. *Am J Physiol Cell Physiol* 2004;286:C987-97.

- Volin M, Huynh N, Klosowska K, Reyes R, and Woods J. Fractalkine-induced endothelial cell migration requires MAP kinase signaling. *Pathobiology* 2010; 77:7-16.
- Wang J, Fan J, Laschinger C, Arora PD, Kapus A, Seth A, and McCulloch CA. Smooth Muscle Actin Determines Mechanical Force-induced p38 Activation. *J Biol Chem* 2005;280(8):7273-7284.
- Wang K, Ash J, and Singer S. Filamin, a new high-molecular weight protein found in smooth muscle and non-muscle cells. *PNAS* 1975;72(11)4483-4486
- Wang L, Brown JR, Varki A, and Esko JD. Heparin's anti-inflammatory effects require glucosamine 6-O-sulfation and are mediated by blockade of L- and P-selectins. *J Clin Invest* 2001;Jul;110(1):127-136.
- Wang S and Li Y. Expression of constitutively active cGMP-dependent protein kinase inhibits glucose-induced vascular smooth muscle cell proliferation. *Am J Physiol Heart Circ Physiol* 2009 Dec;297(6):H2075-83.
- Webb LM, Ehrengruber MU, Clark-Lewis I, Baggiolini M, and Rot A. Binding to heparan sulfate or heparin enhances neutrophil responses to interleukin 8. *PNAS* 1993;90:7158-7162.
- Weber K and Groeschel-Steward U. Antibody to myosin: the specific visualization of myosine-containing filaments in nonmuscle. *PNAS* 1974;71(11):4561-4564.
- Wechezak A, Viggers R, and Sauvage L. Fibronectin and F-actin redistribution in cultured endothelial cells exposed to shear stress. *Laboratory Investigation* 1985;53(6)639-647.

- Weiler JM, Edens RE, Linhardt RJ, and Kapelanski DP. Heparin and modified heparin inhibit complement activation *in vivo*. *J Immunol* 1992;148:3210–3215.
- Wieland T and Mittmann C. Regulators of G-protein signalling: multifunctional proteins with impact on signaling in the cardiovascular system. *Pharmacol Ther* 2003 Feb;97(2):95-115.
- Won KJ, Park SH, Park T, Lee CK, Lee HM, Choi WS, Kim SJ, Park PJ, Jang HK, Kim SH, and Kim B. Cofilin Phosphorylation mediates proliferation in response to platelet-derived growth factor-BB in rat aortic smooth muscle cells. *J Pharmacol Sci* 2008;108:372-379.
- Xia Y, Makris C, Su B, Li E, Yang J, Nemerow GR, and Karin M. MEK kinase 1 is critically required for c-Jun N-terminal kinase activation by proinflammatory stimuli and growth factor-induced cell migration. *PNAS* 2000;97:5243-5248.
- Xu S, Ogura S, Chen J, Little PJ, Moss J, and Liu P. LOX-1 in atherosclerosis: biological functions and pharmacological modifiers. *Cell Mol Life Sci* 2012 Nov 3. [Epub ahead of print].
- Yalcin HC, Perry SF, and Ghadiali SN. Influence of airway diameter and cell confluence on epithelial cell injury in an in-vitro model of airway reopening. *J Appl Physiol* 2007;103:1796-1807.
- Yamamoto K and Ando J. New molecular mechanisms for cardiovascular disease: Blood flow sensing mechanism in vascular endothelial cells. *J Pharmacol Sci* 2011;116:323-331.
- Yang N and Mizuno K. Nuclear export of LIM-kinase 1, mediated by two leucine-rich

- nuclear export signals within the PDZ domain. *Biochem J* 1999;338:793-798.
- Yoo Y, Ho HJ, Wang C, and Guan JL. Tyrosine phosphorylation of cofilin at Y68 by v-src leads to its degradation through ubiquitin-proteasome pathway. *Oncogene* 2010;14;29(2):263-272.
- Yu L, Quinn DA, Garg HG, and Hales CA. Gene expression of cyclin-dependent kinase inhibitors and effect of heparin on their expression in mice with hypoxia-induced pulmonary hypertension. *Biochem and Biophys* 2006;345:1565-1572.
- Zarubin T and Han J. Activation and Signaling of the p38 MAPK Pathway. *Cell Research* 2005;15(1):11-18.
- Zhang L, Deng M, Parthasarathy R, Wang L, Mongan M, Molkenin JD, Zheng Y, and Xia Y. MEKK1 Transduces Activin Signals in Keratinocytes To Induce Actin Stress Fiber Formation and Migration. *Mol Cell Biol* 2005;25(1):60-65.
- Zhao B, Stavchansky SA, Bowden RA, and Bowman PD. Effect of interleukin-1beta and tumor necrosis factor-alpha on gene expression in human endothelial cells. *Am J Physiol Cell Physiol* 2003;284:C1577-1583.
- Zheng B, Han M, Bernier M, and Wen JK. Nuclear actin and actin-binding proteins in the regulation of transcription and gene expression. *FEBS J* 2009;276:2669-2685.

Chapter 10: Appendices

Appendix I: RNA Isolation and Processing Methods

RNA Isolation

In all cases (RT-PCR analysis, PCR arrays, and microarray) RNA was isolated from 100 mm dishes of A7r5s or RAOSMCs using the Qiagen RNeasy total RNA isolation kit with the optional on-column DNase digestion. Briefly, cells were harvested in 600 μ l of buffer RLT to which 600 μ l of 70% ethanol was added. 700 μ l of this solution was then added to an RNeasy spin column and centrifuged for 15 sec at $\geq 10,000$ rpm. The flow through was discarded and the column was rinsed with 350 μ l of buffer RW1 and centrifuged for 15 sec at $\geq 10,000$ rpm. Following the centrifugation, the on-column DNase digestion was performed by adding 10 μ l of DNase I stock to 70 μ l of buffer RDD and adding this entire solution to the membrane of the RNeasy spin column for 15 mins at room temperature. Following DNase digestion, 350 μ l of buffer RW1 was added to the column and centrifuged for 15 sec at $\geq 10,000$ rpm. The flow-through was discarded and 500 μ l of buffer RPE was added to the column and centrifuged for 15 sec at $\geq 10,000$ rpm. The flow-through was again discarded and 500 μ l of buffer RPE was added to the column and centrifuged for 2 min at $\geq 10,000$ rpm to dry the membrane. The RNeasy spin column was then placed in a new 2 ml collection tube and centrifuged for 1 min at $\geq 10,000$ rpm to eliminate any remaining buffer RPE. The RNeasy spin column was then placed in a 1.5 ml microcentrifuge tube with the cap cut off. To elute RNA, 50 μ l of provided RNase-free water was added direction to the RNeasy spin column membrane for at least 1 min and centrifuged for 1 min at $\geq 10,000$ rpm.

RNA Quality Control

To ensure that high quality total RNA was isolated, a nanodrop measurement was obtained for all RNA samples and an agarose gel was run. For RNA to pass the nanodrop measurement, the sample needed to have an $A_{260/280\text{nm}}$ ratio of $\sim 2.0 \pm 1.5$ and a concentration of ≥ 100 ng/ml. All samples also needed to show intact and robust ribosomal RNA bands on a 1% agarose gel run in 1% TAE buffer. Briefly, samples RNA samples were mixed with loading dye (50:50) and loaded onto the 1% agarose gel. Gels were run for ~ 30 mins at 70 volts, stained using ethidium bromide, and imaged using a photodyne imager with ethidium bromide filter. High quality RNA samples were kept at -20 °C until used for the reverse transcription reaction. For the microarray analysis, additional quality control measures were performed by the company.

Reverse Transcription Protocol

Reverse transcription was carried out using Invitrogen's SuperScript III First-Strand Synthesis Super Mix reagents. According to the manufacturer's instructions, the following were combined in a microcentrifuge tube on ice:

Table A1.1: Reverse Transcription Reaction Step 1

Component	Amount
Up to 5 μg total RNA	n μl
50 mM Oligo dT Primer	1 μl
Annealing Buffer	1 μl
RNase/DNase-Free Water	To 8 μl (if necessary)

Note: Since Oligo dT primers were used, only mRNA was reverse transcribed to cDNA, eliminating any other RNA species from analysis.

The above mixture was incubated in a heat block set to 65 °C for 5 mins and then immediately placed on ice for 1 min and then briefly centrifuged to collect the contents.

The following were then added to the tube on ice:

Table AI.2: Reverse Transcription Reaction Step 2

Component	Amount
2X First-Strand Reaction Mix	10 µl
Superscript III/RNaseOUT Enzyme Mix	2 µl

The sample was then briefly vortexed to mix, centrifuged to collect the contents, and incubated in a heat block set to 50 °C for 50 mins. Following the 50 min incubation, the reaction was terminated by placing the tubes in a heat block set to 85 °C for 5 min. cDNA samples were stored at -20 °C.

RT-PCR Method

Qiagen's RotorGene RT-PCR equipment and kits were used for RT-PCR analysis. The Qiagen RotorGene RT-PCR reaction relies on SYBR green chemistry as a way to quantitate relative levels of cDNA in a reaction mixture. The reaction mixture was set up as follows:

Table AI.3: RT-PCR Reaction Set-up

Component	Volume/Reaction	Final Concentration
2X SYBR Green Master Mix	12.5 µl	1X
10X Quantitect Primer (GAPDH, DUSP1)	2.5 µl	1X
Template cDNA	2 µl (20ng)*	≤ 100 ng/ml
RNase-free Water	8 µl	-----
Total Reaction Volume	25 µl	-----

**For reverse transcription reaction, 200 ng of RNA was converted to cDNA. Resulting solution is 200 ng/ 20 µl which is 10 ng/ml. For RT-PCR reaction, 2 µl of this solution was used to reach a concentration of 20 ng for the reaction.*

The RotorGene was programmed with the following cycling conditions:

Table AI.4: RotorGene Cycling Conditions

Step	Time	Temperature (°C)	Comments
PCR Initial Activation	5 min	95	Activates Polymerase
Two-Step Cycling			
Denaturation	5 sec	95	---
Combined Annealing and Extension	10 sec	60	Perform fluorescence data collection
# of Cycles	40	---	Depends on amount of template cDNA

SABiosciences PCR Array Analysis

SABiosciences RT² Profiler PCR arrays (Qiagen) (Rat MAPK PCR Array and EGF/PDGF PCR Array) were used for PCR Array analysis. Total RNA was isolated from A7r5s and quality was determined as described above. First strand cDNA synthesis was carried out using SABiosciences RT2 First Strand Kit (Qiagen). The reverse transcription reaction was performed as follows. The genomic DNA elimination mixture was prepared in a sterile PCR tube for each sample, according to the following table.

Table AI.5: SABiosciences RT² Genomic DNA Elimination Reaction Mix

Component	Volume/Concentration
Total RNA	25.0 ng to 5.0 µg
GE (5X gDNA elimination buffer)	2.0 µl
diH ₂ O	10 µl

The contents were mixed and briefly centrifuged and incubated for 5 mins at 42 °C.

Following incubation the tubes were chilled on ice for at least 1 min. The RT cocktail was prepared while the tube incubated on ice, according to the following table.

Table AI.6: SABiosciences RT Reaction Mix

Component	1 Reaction (μl)	2 Reactions (μl)	3 Reactions (μl)
BC3 - 5X RT Buffer 3	4	8	16
P2 – Primer and External Control Mix	1	2	4
RE3 – RT Enzyme Mix 3	3	6	12
Water	3	6	12
Final Volume	10	20	30

Once the above two mixes were prepared, 10 μ l of RT Cocktail was added to each 10 μ l Genomic DNA Elimination Mixture. The solutions were mixed gently with a pipettor and incubated for 15 min and then the reaction was immediately terminated by heating to 95 °C for 5 min. 91 μ l of water was added to each 20 μ l cDNA synthesis reaction and mixed well. The cDNA was kept on ice until ready to use or stored at -20 °C overnight.

The PCR Array was carried out using the following mix:

Table AI.7: SABiosciences PCR Reaction Mix

Component	Volume (μl)
RT ² SYBR Green qPCR Mastermix	12.5
ddH ₂ O	10.5
Template cDNA (up to 250 ng)	1.0
Gene-Specific PCR Primer Pair Stock	1.0
Total Volume	25.0

The qPCR reaction was carried out using a two-step cycling program and an **Applied Biosystems 7300 Real-Time PCR System**.

Table AI.8 SABioscience PCR Array Cycling Parameters

Step	Time	Temperature (°C)	Comments
PCR Initial Activation	10 min	95	Activates Polymerase
Two-Step Cycling			
Denaturation	15 sec	95	---
Combined Annealing and Extension	60 sec	60	Perform fluorescence data collection
# of Cycles	40	---	Depends on amount of template cDNA

Data analysis was performed using SABioscience's online program. Raw data are converted to fold change relative to their controls

It is important to note that this methodology was only used for the SABiosciences PCR Arrays. Qiagen RotorGene reagents were used for the targeted RT-PCR analyses.

Appendix II: MAPK PCR Array Genes

Rplp1 H01	Mos G01	Mapk3 F01	Map2k7 E01	Jun D01	Crebbp C01	Cdk4 B01	Araf A01
Hprt1 H02	Myc G02	Mapk6 F02	Map3k1 E02	Kcnh8 D02	Dlk1 C02	Cdk6 B02	Atf2 A02
Rpl13a H03	Nfatc4 G03	Mapk7 F03	Map3k2 E03	Kcnn1 D03	E2f1 C03	Cdkn1a B03	Ccnal A03
Ldha H04	Nras G04	Mapk8 F04	Map3k3 E04	Kras D04	Egfr C04	Cdkn1b B04	Ccna2 A04
Acib H05	Pak1 G05	Mapk8ip1 F05	Map3k4 E05	Ksr1 D05	Egr1 C05	Cdkn1c B05	Ccnb1 A05
RGDC H06	Rac1 G06	Mapk8ip2 F06	Map4k1 E06	Map2k1 D06	Ets1 C06	Cdkn2a B06	Ccnb2 A06
RTC H07	Raf1 G07	Mapk8ip3 F07	Mapk1 E07	Map2k1ip-1 D07	Ets2 C07	Cdkn2b B07	Ccnd1 A07
RTC H08	Rb1 G08	Mapk9 F08	Mapk10 E08	Map2k2 D08	Fos C08	Cdkn2c B08	Ccnd2 A08
RTC H09	Met2c G09	Mapkapk2 F09	Mapk11 E09	Map2k3 D09	Grb2 C09	Cdkn2d B09	Ccnd3 A09
PPC H10	Sfn G10	Max F10	Mapk12 E10	Map2k4 D10	Hras C10	Chuk B10	Ccne1 A10
PPC H11	Smad4 G11	Mknk1 F11	Mapk13 E11	Map2k5 D11	Hspa5 C11	Col1a1 B11	Cdc42 A11
PPC H12	Tp53 G12	Mapkapk5 F12	Mapk14 E12	Map2k6 D12	Hspb1 C12	Creb1 B12	Cdk2 A12

Appendix III: EGF/PDGF PCR Array Genes

Rplp1 H01	Raf1 G01	Pdgfra F01	Mapk1 E01	Hras D01	Egr1 C01	Casp9 B01	Actr2 A01
Hprt1 H02	Rap1a G02	Pdgfrb F02	Mapk10 E02	Ikbkb D02	Eif4e C02	Cblb B02	Akt1 A02
Rpl13a H03	Rasa1 G03	Pdgfra F03	Mapk3 E03	Il2 D03	Eps8 C03	Ccnd1 B03	Akt2 A03
Ldha H04	Rhoa G04	Pdpk1 F04	Mapk8 E04	Jak1 D04	Faslg C04	Chuk B04	Akt3 A04
Acib H05	Rps6ka5 G05	Pik3ca F05	Mapk9 E05	Jun D05	Fn1 C05	Col1a1 B05	Araf A05
RGDC H06	Rps6kb1 G06	Pik3r1 F06	Mknk1 E06	Kcnh8 D06	Fos C06	Creb1 B06	Atf1 A06
RTC H07	Shc1 G07	Pik3r2 F07	Mmp7 E07	Kras D07	Foxo3 C07	Csnk2a1 B07	Atf2 A07
RTC H08	Src G08	Plat F08	Nck2 E08	Lta D08	Gab1 C08	Csnk2b B08	Bad A08
RTC H09	Stat1 G09	Plcg1 F09	Nfatc3 E09	Map2k1 D09	Grb2 C09	Dusp1 B09	Bcar1 A09
PPC H10	Stat3 G10	Ppp2ca F10	Nfkb1 E10	Map2k4 D10	Gsk3a C10	Dusp6 B10	Bcl2 A10
PPC H11	Stat5a G11	Prkca F11	Nras E11	Map2k7 D11	Gsk3b C11	Egf B11	Braf A11
PPC H12	Tp53 G12	Pten F12	Nup62 E12	Map3k2 D12	Hbegf C12	Egfr B12	Casp3 A12

Appendix IV: Microarray Results showing genes with significant fold changes

Gene Description	Gene Symbol	Fold Change (HEP24 vs CON024)
neuritin	Nrn1	0.332
carbonic anhydrase 3	Car3	0.361
calmegin	Clgn	0.400
SMAD family member 9	Smad9	0.421
inhibitor of DNA binding 1	Id1	0.444
solute carrier family 9 (sodium/hydrogen exchanger), member 2	Slc9a2	0.486
inhibitor of DNA binding 2	Id2	0.548
lectin, galactoside-binding, soluble, 3	Lgals3	0.561
Ral GEF with PH domain and SH3 binding motif 2	Ralgps2	0.583
paired related homeobox 2	Prrx2	0.584
microsomal glutathione S-transferase 2	Mgst2	0.591
EGL nine homolog 3 (C. elegans)	Egln3	0.592
purinergic receptor P2Y, G-protein coupled, 1	P2ry1	0.596
small proline-rich protein 1A-like	Sprr1al	0.602
PTPRF interacting protein, binding protein 2 (liprin beta 2)	Ppfbp2	0.611
SMAD family member 6	Smad6	0.612
ATP-binding cassette, sub-family A (ABC1), member 1	Abca1	0.614
neuropilin (NRP) and tolloid (TLL)-like 2	Neto2	0.615
neuropeptide Y	Npy	0.627
serine incorporator 2	Serinc2	0.630
shroom family member 1	Shroom1	0.635
atonal homolog 8 (Drosophila)	Atoh8	0.639
interferon regulatory factor 8	Irf8	0.640
similar to RalA binding protein 1	LOC304239	0.644
olfactory receptor 920	Olr920	0.645
partner and localizer of BRCA2	Palb2	0.650
SMAD family member 7	Smad7	0.656
similar to 4833420G17Rik protein	RGD1306227	0.659
protein phosphatase 2 (formerly 2A), regulatory subunit B, beta isoform	Ppp2r2b	0.664
mannan-binding lectin serine peptidase 1	Masp1	1.505
naked cuticle homolog 2 (Drosophila)	Nkd2	1.506
fibronectin type III domain containing 1	Fndc1	1.507
thioredoxin interacting protein	Txnip	1.509
thyroid hormone receptor beta	Thrb	1.512
transient receptor potential cation channel, subfamily V, member 2	Trpv2	1.516
potassium channel, subfamily K, member 2	Kcnk2	1.516
cysteine dioxygenase, type I	Cdo1	1.516
vasoactive intestinal peptide receptor 2	Vipr2	1.518
similar to leucine zipper protein 2	RGD1563838	1.519
epoxide hydrolase 1, microsomal	Ephx1	1.521
sema domain, immunoglobulin domain (Ig), short basic domain, secreted, (semaphorin) 3D	Sema3d	1.521

ciliary neurotrophic factor	Cntf	1.521
guanine deaminase	Gda	1.522
estrogen receptor 1	Esr1	1.526
serine (or cysteine) peptidase inhibitor, clade A (alpha-1 antiprotease, antitrypsin), member 9	Serpina9	1.528
dystrophin myotonia-protein kinase	Dmpk	1.530
LIM and senescent cell antigen like domains 2	Lims2	1.533
pentraxin related gene	Ptx3	1.534
gastrin releasing peptide receptor	Grpr	1.535
transmembrane protein 204	Tmem204	1.538
signal peptide, CUB domain, EGF-like 3	Scube3	1.538
proprotein convertase subtilisin/kexin type 5	Pcsk5	1.538
LIM and cysteine-rich domains 1	Lmcd1	1.539
sarcoglycan, gamma (dystrophin-associated glycoprotein)	Sgcg	1.554
myozenin 2	Myoz2	1.562
olfactory receptor 325	Olr325	1.568
solute carrier family 35, member F1	Slc35f1	1.585
chemokine (C-C motif) receptor-like 1	Ccr1	1.591
ADAM metalloproteinase with thrombospondin type 1 motif, 5	Adamts5	1.592
inositol polyphosphate-4-phosphatase, type II	Inpp4b	1.594
matrix Gla protein	Mgp	1.595
serine (or cysteine) peptidase inhibitor, clade B, member 2	Serpib2	1.603
integrin, alpha 4	Itga4	1.612
decorin	Dcn	1.617
5-hydroxytryptamine (serotonin) receptor 1F	Htr1f	1.641
family with sequence similarity 38, member B	Fam38b	1.644
amine oxidase, copper containing 3 (vascular adhesion protein 1)	Aoc3	1.677
serine (or cysteine) peptidase inhibitor, clade A, member 3N	Serpina3n	1.685
microfibrillar-associated protein 4	Mfap4	1.687
chondroitin sulfate N-acetylgalactosaminyltransferase 1	Csgalnact1	1.691
family with sequence similarity 5, member B	Fam5b	1.691
transglutaminase 2, C polypeptide	Tgm2	1.697
integrin, alpha 7	Itga7	1.699
Notch homolog 3 (Drosophila)	Notch3	1.699
presenilin 2	Psen2	1.702
serine (or cysteine) peptidase inhibitor, clade B, member 7	Serpib7	1.713
guanylate cyclase 1, soluble, beta 3	Gucy1b3	1.714
olfactomedin-like 2B	Olfml2b	1.721
transmembrane 7 superfamily member 2	Tm7sf2	1.744
oxidized low density lipoprotein (lectin-like) receptor 1	Olr1	1.773
ceruloplasmin	Cp	1.776
serine (or cysteine) peptidase inhibitor, clade A (alpha-1 antiprotease, antitrypsin), member 9	Serpina9	1.791
sprouty homolog 1, antagonist of FGF signaling (Drosophila)	Spry1	1.794
similar to transmembrane protein 2	RGD1305254	1.799
selenoprotein P, plasma, 1	Sepp1	1.848
carboxypeptidase X (M14 family), member 2	Cpxm2	1.875
CD180 molecule	Cd180	1.887

bone morphogenetic protein 6	Bmp6	1.889
mast cell protease 1	Mcpt1	1.905
similar to C21ORF7	LOC304131	1.920
WAP four-disulfide core domain 1	Wfdc1	1.922
similar to ABI gene family, member 3 (NESH) binding protein	RGD1562717	1.937
calsequestrin 2 (cardiac muscle)	Casq2	1.979
integrin, beta-like 1	Itgb11	2.049
phospholamban	Pln	2.062
Fraser syndrome 1 homolog (human)	Fras1	2.112
tumor necrosis factor (ligand) superfamily, member 18	Tnfsf18	2.114
peptidase inhibitor 15	Pi15	2.163
elastin	Eln	2.253
fin bud initiation factor homolog (zebrafish)	Fibin	2.296
sodium channel, voltage-gated, type VII, alpha	Scn7a	2.370
slit homolog 3 (Drosophila)	Slit3	2.505
myosin, heavy chain 2, skeletal muscle, adult	Myh2	2.556
aldo-keto reductase family 1, member C14	Akr1c14	2.594
bone morphogenetic protein 3	Bmp3	2.717
myosin, heavy polypeptide 1, skeletal muscle, adult	Myh1	2.742
fibromodulin	Fmod	2.789
osteomodulin	Omd	2.871
regulator of G-protein signaling 4	Rgs4	3.039
asporin	Aspn	3.853

JOSHUA B. SLEE

Curriculum Vitae

Education

Lehigh University	Bethlehem, PA
<i>Ph.D. Cell and Molecular Biology</i>	2013
Marywood University	Scranton, PA
<i>M.S. Biotechnology</i>	2008
<i>B.S. Biotechnology, chemistry minor</i>	2007

Honors and Awards

1. Nemes Fellow – Lehigh University (Fall 2011)
2. Philip E. Mulry Medal for Excellence in Chemistry – Marywood University (2007)
3. Dean's List recognition for 8 consecutive semesters – Marywood University

Employment & Research Experience

The Children's Hospital of Philadelphia	Start: September 2013	Philadelphia, PA
Stanley Stachelek, Ph.D. and Robert J. Levy, M.D., Ph.D.		
<i>T32 Post Doctoral Fellow</i>		
➤ Joining a team of scientists on an NIH T32 training grant in Molecular Therapeutics for Pediatric Cardiology. My project specifically relates to the use of CD47 as an anti-inflammatory agent in implantable devices and biomaterials.		

Lehigh University	Fall Semester 2008 – August 2013	Bethlehem, PA
Linda Lowe-Krentz, Ph.D.		
<i>Graduate Research Assistant</i>		
➤ Investigated the anti-inflammatory pathways protecting against the development of atherosclerosis. Determined a role for the protein cofilin in mediating shear stress-induced actin realignment and established the importance of proper actin realignment in shear stress-induced vascular endothelium barrier integrity.		
➤ Currently investigating the anti-inflammatory mechanisms of heparin in vascular endothelium using immunofluorescent microscopy. Validating the identity of the heparin receptor as TMEM184A through functional assays utilizing targeted siRNA, fluorescent microscopy, co-immunoprecipitation, and western blotting.		

Lehigh University	Summer 2008	Bethlehem, PA
Howard Hughes Medical Institute BDSI Program (Linda Lowe-Krentz, Ph.D.)		
<i>Graduate Student Advisor</i>		
➤ Responsible for supervising two undergraduate students working in the lab during a two month summer project, culminating in a group presentation and poster to the campus community and an undergraduate student-initiated poster at a national engineering conference presented by one of the undergraduate students.		

Marywood University	Summer 2006 – Spring 2008	Scranton, PA
Kenneth W. Rundell, Ph.D.		
<i>Research Assistant</i>		
➤ Developed a standardized method for exhaled breath condensate collection and analysis, by normalization to sodium and potassium ions. Performed sputum collection and analysis for markers of		

bronchospasm caused through the action of eosinophils. Investigated the effects of auto and truck emission on athletic performance.

- Applied knowledge of biology, chemistry, and biochemistry, developed and performed High Performance Liquid Chromatography (HPLC) methods and analyzed liquid samples via HPLC, spectrometry, nitric oxide analysis, and enzyme immunoassays.

Marywood University

Fall 2005

Scranton, PA

Deborah Hokien, Ph.D.

Research Assistant

- Applied knowledge of biology, developed cell culture techniques, prepared culture media, and utilized aseptic laboratory techniques to culture breast cancer cell lines.

Teaching Experience

Lehigh University

Fall Semester 2012

Bethlehem, PA

Bios 161: Undergraduate Research (Linda Lowe-Krentz, Ph.D.)

Course Leader

- Designed and managed a one credit paper review/discussion course for a sophomore student interested in world health and public policy. Responsible for developing course material and supervising student throughout the semester.

Lehigh University

Fall Semester 2012

Bethlehem, PA

Bios 010: Bioscience in the 21st Century (Vassie Ware, Ph.D.)

Guest Lecturer

- Designed and effectively administered a lecture encompassing cardiovascular diseases and their implications to human health, government policy, and financial concerns.

Lehigh University

Summer Session I 2012

Bethlehem, PA

Bios 041: Cellular and Molecular Biology (Michael Kuchka, Ph.D.)

Guest Lecturer

- Designed and effectively delivered four lectures encompassing cellular respiration (glycolysis, the citric acid cycle, and fermentation) and photosynthesis (light reactions and the Calvin cycle). Created self-assessment quizzes to facilitate increased student involvement in classroom learning. Assisted in exam preparation for this section of the course.

Lehigh University

Fall Semester 2010

Bethlehem, PA

Bios377: Biochemistry Lab (Linda Lowe-Krentz, Ph.D.)

Teaching Assistant

- Responsible for running one section of upper level Biochemistry lab, which meets twice a week. Supervised students to ensure experiments were conducted correctly and that all necessary safety precautions were followed. Assisted students in designing, planning, and completing their own independent experiments.

Lehigh University

Summer Session I 2010

Bethlehem, PA

Bios041: Cellular and Molecular Biology (Michael Kuchka, Ph.D.)

Teaching Assistant

- Responsible for re-grading exams to allow students to earn additional credit towards their final grade. Provided assistance for the primary professor regarding matters other than grading.

Lehigh University

Spring Semester 2010

Bethlehem, PA

Bios041: Cellular and Molecular Biology (Matthias Falk, Ph.D.)

Teaching Assistant

3. **Slee JB**, Lowe-Krentz LJ. (2012). Cofilin regulation of actin realignment is essential for vascular endothelial barrier integrity during shear stress. *Mol Biol Cell* 23, 4663. Abstract No. 251
4. **Slee JB**, Lowe-Krentz LJ. (2011). Phospho-regulation of cofilin is essential for fluid shear stress-mediated actin microfilament realignment. *Mol Biol Cell* 22, 4705. Abstract No. 815
5. **Slee JB**, Lowe-Krentz LJ. (2010) Shear Stress induces cofilin-mediated actin microfilament realignment via the JNK and p38 pathways. *Mol. Biol. Cell* 21 (suppl), Abstract No. 89
6. Maciaszek J, Alejandra S, **Slee JB**, Lowe-Krentz L, and Ghadiali S. Finite element modeling of force transmission in endothelial cells during shear flow. *BMES annual meeting abstract*. 2008.
7. **Slee JB**, Rundell KW. Does Exercise Affect Exhaled Breath Condensate Ion Concentration? *Med. Sci. Sports Exer.* (abstract/national presentation). 40:5, 2008.
8. **Slee JB**, Caviston R, Hollenbach AM, Bulbulian R, Rundell KW. Decreased Lung Function and Altered Nitrate Formation after High Auto/Truck Emission Inhalation during Exercise. *Med. Sci. Sports Exer.* (abstract/national presentation). 37:5, 2007.
9. Hollenbach AM, **Slee JB**, Caviston R, Rundell KW. Exercise while Breathing High Ambient Auto/Truck Emission causes Decreased Lung Function in Non-Asthmatic Subjects. *Med. Sci. Sports Exer.* (abstract/national presentation). 37:5, 2007.
10. **Slee JB**, Hokien D. "The Process of Culturing Breast Cancer Cells." *American Chemical Society Mid-Atlantic Regional Meeting Presentation*. 2006.

Professional Affiliations

1. American Society of Cell Biology
2. American Society for Biochemistry and Molecular Biology
3. New York Academy of Sciences
4. Delta Epsilon Sigma National Honors Society member
5. Kappa Gamma Pi National Catholic Graduate Honors Society member

Service to the Scientific Community

Lehigh University Summer 2013 Bethlehem, PA
Guest Lecturer

Howard Hughes Medical Institute BDSI Summer Program

- Delivered an invited talk entitled: The Anatomy of a Poster: Creating an Effective Scientific Poster Presentation covering how to construct and deliver an effective scientific poster presentation.

Lehigh University Fall 2011 – Spring 2012 Bethlehem, PA
 Dean's Advisory Council (College of Arts and Sciences)
Biological Sciences Representative

- Served as a liaison for the graduate students in the department of biological sciences to voice their concerns and needs to the dean of the College of Arts and Sciences. Provided insight to the council from a scientist's point of view.

Lehigh University Spring 2010 – Spring 2012 Bethlehem, PA
 Biology Organization of Graduate Students (BOGS)

Secretary

- Served as secretary to the graduate student-initiated organization. Duties include taking and preparing meeting minutes, sending emails to all members, assisting with meeting preparations, and facilitating volunteer work to the greater community.

Freedom High School

Spring 2009

Bethlehem, PA

Invited Speaker

- Delivered a lecture covering biology and biotechnology as a field of study and profession to juniors and seniors in high school.

References

Linda J. Lowe-Krentz, Ph.D.
(Research Advisor)
Professor of Biochemistry
Lehigh University
111 Research Drive
Bethlehem, PA 18015
Email: lj10@lehigh.edu
Phone: 610-758-3680

Michael Kuchka, Ph.D.
Associate Professor Molecular Biology
Lehigh University
111 Research Drive
Bethlehem, PA 18015
Email: mrk5@lehigh.edu
Phone: 610-758-3680

Lynne Cassimeris, Ph.D.
Professor Cell Biology
Lehigh University
111 Research Drive
Bethlehem, PA 18015
Email: lc07@lehigh.edu
Phone: 610-758-3680